Roles and regulation of *Saccharomyces cerevisiae* Rho-type GTPases Rho5p and Cdc42p

Robert Annan

Department of Biochemistry
McGill University
Montreal, Quebec, Canada
August, 2008

A thesis submitted to McGill University in partial fulfillment
of the requirements for the degree Doctor of Philosophy

Dedicated to my wife, Ineke,
and my three boys, Gordon, Bruce, and Jack

ABSTRACT

The eukaryotic Rho family of GTPases acts as central regulators of numerous processes, including the polarization of cell morphology, membrane transport, transcription, and MAPK pathway signaling. As GTPases, Rho proteins act as molecular switches that, in the GTP-bound form, transduce upstream signals to a variety of downstream effectors, thereby generating appropriate cellular responses. As central nodes of signaling, they are subject to strict regulation, and the regulation of the GTP-GDP cycle of Rho members has been well characterized. Rho GTPases participate in a variety of pathways, though in many cases the mechanisms are still poorly understood. This study examines the roles and regulation of two Rho GTPases in *Saccharomyces cerevisiae*, Rho5p and Cdc42p. First, we describe the regulation of Rho5p signaling by phosphorylation and ubiquitination, the first instance of post-translational regulation of a yeast Rho-type GTPase. This regulation is mediated by a module involving the Npr1p kinase and its inhibitor Msi1p. We also identify Rgd2p as the RhoGAP for Rho5p *in vivo*, and demonstrate a genetic interaction between *RHO5* and *STE50*: a *STE50* deletion combined with expression of an activated *RHO5* allele results in osmotic sensitivity. Next, we describe a role for Rho5p in the activation of the cAMP-PKA pathway. Expression of an activated allele of *RHO5* generates a number of phenotypes associated with activated cAMP-PKA pathway signaling, and also suppresses the lethality of a strain deleted for two other cAMP-PKA activators, *Δras1 Δras2*. A mechanism by which Rho5p may activate the pathway is suggested by the observed two-hybrid interaction between Rho5p and adenylyl cyclase, Cyr1p. Finally, we investigate Cdc42p-associated signaling by performing a biochemical screen for substrates of the Cdc42p-effector,

Ste20p. The results of this screen were used to generate a computational predictor for Ste20p substrates which exhibits significant overlap with Ste20's genetic and physical interaction neighbourhoods. This approach resulted in the identification of the *in vitro* phosphorylation by Ste20p of two Cdc42p-related proteins, Bni1p and Bud6p. Together these results expand our understanding of yeast GTPases, and suggest further avenues for investigation.

RÉSUMÉ

La famille eucaryote des GTPases Rho agit à titre de régulateur principal de nombreux processus biologiques, incluant la polarisation de la morphologie cellulaire, le transport membranaire, la transcription et la voie de signalisation MAPK. En tant que GTPases, les protéines Rho jouent un rôle de controlleurs moleculaires qui, sous la forme liée au GTP, transmettent les signaux en amont à une variété d'effecteurs en aval, générant ainsi les réponses cellulaires appropriées. Étant des acteurs principaux de la signalisation, les protéines Rho sont sujettes à une régulation précise. La régulation du cycle GTP-GDP par les membres de la famille Rho a été largement caractérisée. Cependant, les GTPases Rho participent à une variété de mécanismes qui, dans plusieurs cas, sont encore aujourd'hui sous-étudiés. Cette étude examine plus particulièrement les rôles et la régulation de deux GTPases Rho chez la levure *Saccharomyces cerevisiae*, Rho5p and Cdc42p. Dans un premier temps, nous décrivons la régulation de la signalisation de Rho5p par la phosphorylation et l'ubiquitination, ceci étant le premier exemple de régulation post-traductionnelle d'une GTPase de type Rho chez la levure. Cette régulation est arbitrée par un module impliquant la kinase Npr1p et son inhibiteur MSi1p. Nous démontrons également une interaction génétique entre *RHO5* et *STE50*. En effet, une délétion au niveau de *STE50* combinée à l'expression d'un allèle activé de *RHO5* résulte en une sensibilité osmotique. De plus, nous identifions Rgd2p comme étant le RhoGAP pour Rho5p *in vivo*. Dans un deuxième temps, nous décrivons un rôle pour Rho5p dans l'activation de la voie cAMP-PKA. L'expression d'un allèle activé de *RHO5* génère de nombreux phénotypes associés à l'activation de la voie de signalisation cAMP-PKA et supprime également la létalité d'une souche portant une délétion pour

deux autres activateurs de cette voie, *Δras1 Δras2*. L'interaction observée entre Rho5p et l'adenylyl cyclase, Cyr1p, par la méthode deux-hybride, suggère un mécanisme par lequel Rho5p pourrait activer la voie cAMP-PKA. Finalement, nous étudions la signalisation associée à Cdc42p en réalisant un criblage biochimique pour identifier les substrats de l'effecteur de Cdc42p, soit Ste20p. Les résultats de ce criblage ont été utilisés pour élaborer un outil de prédiction informatique pour les substrats de Ste20p démontrant un chevauchement significatif avec son réseau d'interactions génétiques et physiques. Cette approche a conduit à l'identification de la phosphorylation *in vitro* par *Ste20p* de deux protéines reliée à Cdc42p, soit Bni1p and Bud6p. Ensemble, ces résultats élargissent notre compréhension des GTPases chez la levure et suggèrent davantage d'autres avenues de recherche.

TABLE OF CONTENTS

LIST OF TABLES AND FIGURES

Chapter 1.

Chapter 2.

Chapter 3

Chapter 4

TABLE OF ABBREVIATIONS

1,3-β-GS	1,3-β-Glucan Synthase
ATP	Adenosine Triphosphate
AU Score	Approximately Unbiased Score
BBD	Bud6-binding Domain
cAMP	Cyclic Adenosine Monophosphate
CDK	Cyclin-Dependent Kinase
cDNA	Complementary DNA
DAD	Dia-autoregulatory Domain
DH	Dbl homology
DNA	Deoxyribonucleic Acid
DRF	Diaphonous-related Protein
EGF	Epidermal Growth Factor
ER	Estrogen Receptor
FH1	Formin-homology 1 Domain
FH2	Formin-homology 2 Domain
FH3	Formin-homology 3 Domain
FRET	Förster Resonance Energy Transfer
GAP	GTPase Activating Protein
GBD	GTPase Binding Domain
GDI	Guanosine Nucleotide Dissociation Inhibitor
GDP	Guanosine Diphosphate
GEF	Guanine Nucleotide Exchange Factor
GIN	Genetic Interactor Neighbourhood
GO	Gene Ontology
GPCR	G-Protein Coupled Receptor
GST	Glutathione-S-Transferase
GTP	Guanosine Triphosphate
HIV	Human Immunodeficiency Virus
HOG	High Osmolarity Glycerol
HOG	High Osmolarity Glycerol
MAP4K	MAPKKK Kinase
MAPK	Mitogen Activated Protein Kinase
MAPKK	MAPK Kinase
MAPKKK	MAPKK Kinase
MAPKKKK	MAPKKK Kinase
MDCK cells	Madin Darby Canine Kidney cells
MEK	MAPK Kinase
MEKK	MAPKK Kinase
MLC	Myosin Light Chain
mRNA	Messenger Ribonucleic Acid
NLS	Nuclear Localization Sequence
PAK	p21-Activated Kinase
PH	Pleckstrin Homology
PIN	Physical Interactor Neighbourhood
PKA	Protein Kinase A
PKC	Protein Kinase C
PKG	Protein Kinase G
RA	Ras-associated
ROC Curve	Receiver-Operator Characteristic Curve
SAM	Sterile Alpha Motif
SD	Synthetic Dextrose
SDS-PAGE	Sodium Dodecyl Sulfate Polyacrylamide Gel Electrophoresis
SH3	Src Homology 3
SLARG	Synthetic Low Ammonium Raffinose Galactose Medium
SRE	Serum Response Element
STRE	Stress Response Element
TCF	Ternary Complex Factor
TOR	Target of Rapamycin
YPD	Growth medium composed of Yeast Extract, Peptone, and Dextrose

Original Contributions to Knowledge

1. A novel genetic interaction between *RHO5* and *STE50* is described wherein an activated *RHO5* allele expressed in a *Δste50* strain results in osmotic lethality. Several suppressors are identified, including *RGD2*, thus confirming that Rgd2p can regulate Rho5p activity *in vivo*, presumably through its RhoGAP activity.

2. Rho5p is regulated by a module involving the kinase Npr1p and its nuclear inhibitor Msi1p. I show that Rho5p is phosphorylated by Npr1p and is ubiquitinated *in vivo* and that this regulation is responsible for the downregulation of signaling by an activated Rho5p. This is the first description of a yeast Rho-GTPase regulated by either phosphorylation or ubiquitination.

3. Rho5p is an activator of cAMP-PKA signaling. Expression of hyperactive alleles of *RHO5* generate a number of phenotypes associated with activated cAMP-PKA pathway, including pseudohyphal growth, invasive growth, and heat shock sensitivity. Activated *RHO5* expression rescues the *Δras1 ras2*^{ts} strain at restrictive temperatures, suggesting it can replace Ras function in activating the pathway. A two-hybrid interaction between Rho5p and adenylyl cyclase is also demonstrated, suggesting a mechanism by which Rho5p may activate the pathway.

4. A biochemical genomics screen of more than 500 yeast proteins in *in vitro* kinase assays with Ste20p kinase identify 14 substrates, and leads to the identification of a novel nuclear role for Ste20p.

5. Data from the biochemical genomics screen is used to generate a computational predictor for the identification of substrates *in silico*. The biochemical predictor employs machine learning techniques to identify multiple motifs which are common amongst Ste20p substrates. The predicted substrate list demonstrates a significant overlap with members of Ste20's genetic and physical neighbourhoods, suggesting the validity of the approach. The approach can be generalized for use with other kinases, including kinases from other organisms.

6. Bni1p and Bud6p are confirmed as *in vitro* substrates of Ste20p, after being predicted as such by the computational predictor. The regions of Bni1p phosphorylation are mapped and are localized in an area involved in auto-regulation and Bud6p-binding. *In vivo* phosphorylation sites are identified on Bud6p, though their function remains to be determined.

Contributions of authors

As permitted under the "Guidelines for Thesis Preparation" provided by the Graduate and Postdoctoral Studies Office, Chapters 2, 3, and 4 of this thesis include manuscripts either published or to be submitted for publication. The contributions of listed authors are listed below:

Chapter 2.

The contents of this chapter have been published:

Annan RB, Wu C, Waller DD, Whiteway M, Thomas DY. (2008). Rho5p is involved in mediating the osmotic stress response in S. cerevisiae and its activity is regulated via Msi1p and Npr1p by phosphorylation and ubiquitination. *Eukaryotic Cell*. **7**(9): 1441-9.

The contributions made by collaborators for this chapter:

Dr. Cunle Wu performed the overlay assay as shown in Figure 2.1A. All other experiments were performed by me. Daniel Waller and Drs. Wu, Whiteway and Thomas provided helpful suggestions and reviewed the manuscript.

Chapter 3.

The contents of this chapter have been submitted for publication:

Annan RB, Wu C, Waller DD, Whiteway M, Thomas DY. (2008). The Rho5p GTPase is a regulator of cAMP-PKA signaling in budding yeast. *Submitted*.

The contributions made by collaborators for this chapter:

All the experiments in this chapter were performed by me. Daniel Waller and Drs. Wu, Whiteway and Thomas provided helpful suggestions and reviewed the manuscript.

Chapter 4.

The contents of this chapter will be submitted for publication:

Annan RB, Lee AY, Iouk TL, Whiteway M, Hallett MT, Thomas DY. (2008). A biochemical genomics screen for substrates of Ste20p kinase reveals a nuclear role for Ste20p and allows for the computational prediction of novel substrates. *Manuscript*.

The contributions made by collaborators for this chapter:

I performed the biochemical genomics screen for *in vitro* phosphorylation by Ste20p, analyzed the results of the predictor and interaction neighbourhood analysis, and performed the verification of Bni1p and Bud6p as Ste20p substrates and mapped their regions of phosphorylation. Anna Lee, Dr. Hallett, Dr. Thomas and I collaborated on the general design of the predictor. Anna Lee was responsible for the bioinformatics, including coding the final version of the predictor, performing statistics to verify the

efficacy of the predictor, and generating figures summarizing the results of the predictor. Dr. Iouk was responsible for the experiments detailing the role for Ste20p in the nucleus contained in figure 4.2. Anna Lee, Dr. Whiteway, Dr. Hallett, and Dr. Thomas edited and reviewed the manuscript.

Acknowledgements

This thesis would not have been possible without the assistance and influence of people too numerous to mention. Thank you to Dr. David Thomas, my supervisor, who showed me what it takes to be an independent and productive scientist, and provided me opportunities to identify and pursue research avenues of my own choosing. I also owe a deep debt of gratitude to Dr. Malcolm Whiteway, who provided supervision and mentorship during my several years working in his lab at the Biotechnology Research Institute (B.R.I.). His enthusiasm for science is infectious and I am grateful for the time and effort he invested in my research. I'd also like to extend a sincere thanks to Dr. Nahum Sonenberg who, as the third member of my advisory committee, gave generously of his time and encouragement. I'd also like to acknowledge my appreciation to the faculty of the Department of Biochemistry who, formally or informally, provided assistance and advice during my program, and provided by example a high standard of scientific achievement. I also extend thanks to the staff of the Department, particularly Maureen Caron, whose tireless work on behalf of the students is universally appreciated.

Thank you to all of the members of the Thomas and Whiteway labs who made the everyday business of doing research an enjoyable pursuit, and provided me with guidance, advice, and encouragement on a daily basis. In particular I'd like to thank my fellow student Dan Waller who shared these years with me, for better and for worse, and whose knowledge and intellect I appreciate and respect. Dr. Cunle Wu patiently and with good humour taught me the techniques of biochemistry and enthusiastically encouraged my work. At McGill, Dr. Gregor Jansen, Jamie Surprenant, and Amelie Fredette gave generously of themselves as members of the yeast research group and as friends. Amelie

also assisted me in the preparation of my thesis by helping me translate the Abstract into French, which I greatly appreciated. I count myself lucky to have been surrounded during my program by good scientists who are also good people.

Of course, science is a collaborative process, and I have been fortunate to have received assistance from many fine sources. In particular, I'd like to thank Anna Lee, Dr. Mike Hallett, and members of his Bioinformatics group for help with Chapter IV of this thesis. Anna worked tirelessly to meet my thesis deadline, which was no doubt less daunting than trying to help me understand naïve Bayes classifiers, and I sincerely appreciate her efforts. I'd also like to thank scientists who assisted my research by providing reagents or through discussion at conferences. I'd also like to acknowledge the support of the Max Stern Foundation and NSERC during my research.

It is impossible to say in a few words how much I have appreciated the support of friends and family. My parents, Barb Kalar and Bruce and Veronica Annan, my siblings Scott Annan, Adrienne Annan, and John Kalar, and my wife's parents, Hazel and Clarence, have provided untold support and encouragement. They have sustained me through difficult times and have shared my successes with equal enthusiasm. A very large thanks also to the community of scientists who have also been dear friends to me at McGill, and have shared my joys and frustrations in equal measure, Alex, Roy, Val, Kyle, Tamiko, and Loc.

My greatest thanks goes to my loving wife, Ineke, and my three boys, Gordon, Bruce, and Jack. It would have been impossible to complete this thesis without the unwavering and committed support of Ineke, whose love and companionship sustain me. Ineke: thank you for your understanding and encouragement. Whether during late nights

in the lab or weekends spent writing, you have been an unwavering supporter and have worked tirelessly to provide a loving and supportive environment for me and the boys. And finally, the three most important results I achieved during my PhD - Gordon, Bruce, and Jack – whose enthusiastic greeting every evening recharged my spirit and showed me what matters most in life isn't what you do but by whom you are loved.

CHAPTER ONE

GENERAL INTRODUCTION

1.1 The Rho GTPase family

1.1.1 Description of Rho GTPase family

Rho-type GTPases are members of the extensive Ras superfamily, whose members act as master regulators of diverse cellular processes. Like other GTPases, they act as molecular switches by cycling between a GTP-bound "active" state and a GDP-bound "inactive" state. In the active state, they bind to effectors and generate a cellular response, which continues until the hydrolysis of GTP to GDP by the GTPase renders it inactive. More than 60 members of the Rho family have been identified in eukaryotes (see (430)).

Rho-family proteins are defined by the presence of a characteristic insert within the GTPase domain, distinguishing them from other members of the Ras superfamily (153, 167, 424, 434). Like Ras, Rho proteins are membrane-associated due to the post-translational modification at their C-terminus by isoprenylation. The Rho family is further subdivided into six subfamilies (Figure 1.1): the RhoA-related subfamily (RhoA, RhoB, and RhoC); the Rac1-related subfamily (Rac1, Rac2, Rac3, and RhoG); the Cdc42-related subfamily (Cdc42 (and a brain-specific splice variant G25K), TC10, TCL, Chp/Wrch-2, and Wrch1); the Rnd subfamily (Rnd1, Rnd2, and RhoE/Rnd3); the RhoBTB subfamily; and the Miro subfamily, whose members are localized to mitochondria and who lack the Rho insert domain. Additionally, there are several Rho proteins which do not obviously belong to any of these families (RhoD, Rif, and TTF/RhoH).

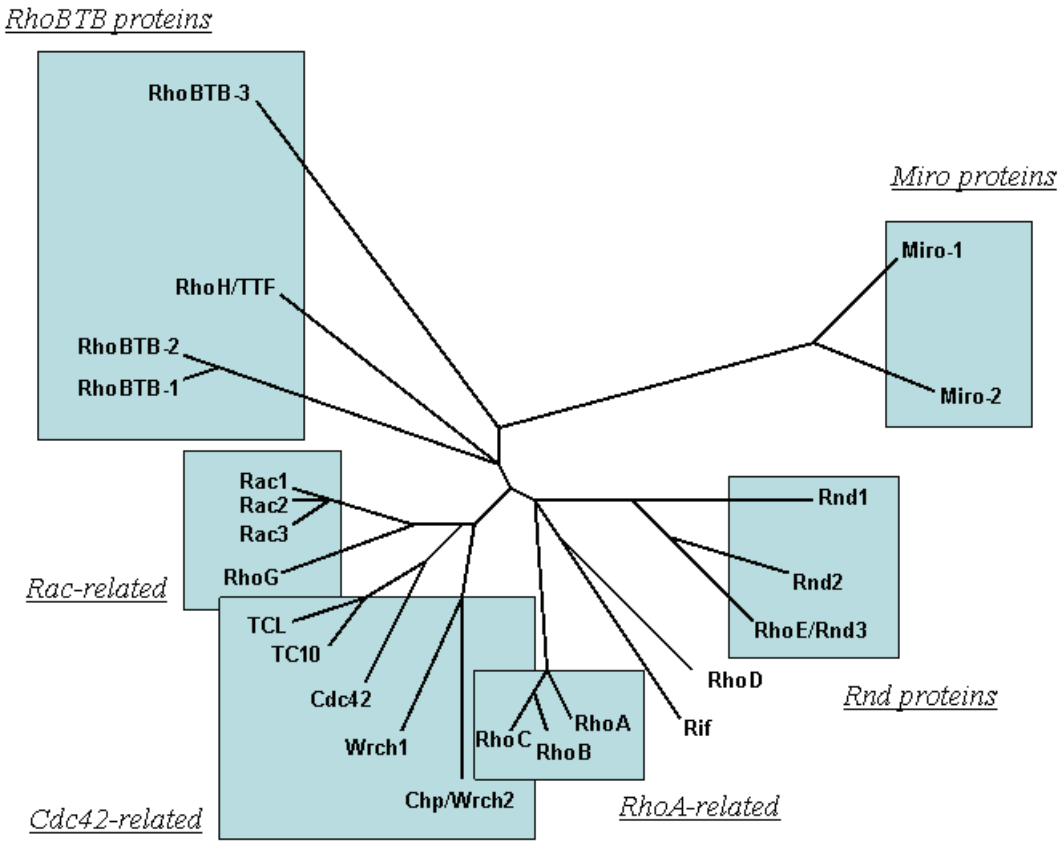

Figure 1.1. The human Rho GTPase family. Dendrogram showing the phylogenetic relationships between the 22 human Rho GTPases, and their subgrouping into six major branches. RhoD and Rif are not clearly associated with any of the major branches. Adapted from (430).

1.1.2 History of the Rho family

The first *Rho* gene was cloned in 1985 from the sea slug *Aplysia* (235). The authors noted that the gene product shared extensive (35%) amino acid similarity with *H-ras*, one of the three members of the Ras GTPase family which had then been identified. They also noted that the gene was evolutionarily conserved in yeast and *Drosophila* and quickly identified three human homologs, *RhoA, RhoB, and RhoC*. The *Ras* genes (*H-Ras, Ki-Ras,* and *N-Ras*) had been identified in the early 1980s as oncogenes mutated in human tumours. Consequently, several researchers quickly began work on the *Rho* genes, thinking that they, too, could be oncogenes. While no Rho family member has been found mutated in human cancer, it is believed that Rho-related signaling probably plays a role in tumour growth and metastasis (see below). Though they were not implicated in cancer, it was soon discovered that Rho proteins were the cellular targets of the *Clostridium botulinum* toxins (7, 451). Continuing work identified additional members of the family, with Rac described at nearly the same time as the identification of *Saccharomyces cerevisiae* Cdc42 and its human homolog (178, 271, 277). The family continued to expand, though Rho, Rac, and Cdc42 remain the most extensively studied members of the family, and quickly became established as a key component of cellular signaling networks

1.2 Functions of Metazoan Rho GTPases

Rho GTPases play numerous roles in metazoan cells, and many excellent reviews are dedicated to describing them (45, 98, 168, 333, 388, 389). In this section, I present a summary of the major roles played by the Rho family in metazoans, focusing first on the

biochemical interactions of Rho GTPases. Next, I place these interactions in context and describe the biological roles played by Rho proteins. Finally, I provide a brief overview of our understanding of the role played by Rho-signaling in cancer.

1.2.1 Biochemical Functions

1.2.1.1 Actin Cytoskeleton Dynamics

Early work sought to determine whether RhoA microinjected into fibroblasts would, like Ras, stimulate DNA synthesis (102). While no effect on DNA synthesis was observed, researchers noticed that the morphology of the Swiss 3T3 cells was dramatically altered and they noted a remarkable increase in actin stress fibers (297). Subsequent work has demonstrated a central role for Rho GTPases in cytoskeletal dynamics involving actin filaments.

Actin filament formation depends on one of two actin polymerization factors common to all eukaryotic cells: the Arp2/3 complex and Formins (for reviews, see (65, 304)). Rac and Cdc42 activate Arp2/3 activity indirectly through members of the Wiskott-Aldrich syndrome protein (WASP) family. Activated Rac/Cdc42 binds to WASP proteins, thereby relieving an intramolecular inhibition and exposing a C-terminal ARP2/3 binding site. The binding of WASP to ARP2/3 activates ARP2/3's core actin nucleation machinery and thereby induces actin filament polymerization. Thus, activated Rac/Cdc42 stimulates the formation of branched actin filaments at the cell periphery, especially in actin-rich lamellipodia and filopodia.

While the Arp2/3 complex is responsible for the nucleation of branched actin cables, the formin family of proteins is responsible for the nucleation and polymerization of unbranched actin filaments (see reviews, above). In mammalian cells, Rho activates diaphanous-related formins (DRF) mDia (mDia1, and possibly mDia2). The binding of activated Rho to mDia1 releases an auto-inhibitory domain, exposing the FH2 (formin-homology 2) domain responsible for actin binding and polymerization. mDia1 also contains a FH1 domain which binds the profilin/actin complex, thus delivering G-actin to the growing barbed end of the filament. DRFs bind a number of additional proteins, such as Src tyrosine kinase, eEF1A, and Dia-interacting protein (DIP, also called AF3p21, SPIN90, WISH), and thus can also act as scaffolds to link Rho signaling to additional associated downstream effectors (423).

1.2.1.2 Microtubule Cytoskeleton Dynamics

The microtubule cytoskeleton participates in the generation of cell polarity and contributes to the distribution of organelles such as the Golgi and the mitotic spindle. Like actin filaments, microtubules exhibit polarity, with a static minus end and a dynamic plus end. The plus end alternates between periods of growth (rescue) and shrinking (catastrophe), resulting in a dynamic instability characteristic of microtubules. Cdc42/Rac promotes the elongation of microtubules through the inactivation of the plus-end destabilizing protein Op18/stathmin via phosphorylation by the kinase Pak1, a member of the Cdc42/Rac-activated p-21 activated kinase (PAK) family, whose members are primary effectors for Cdc42/Rac (78).

In addition to encouraging their elongation, Rho GTPases also promote the interaction of the plus-ends of microtubules with proteins at the cell cortex, a process called plus-end capture. For example, the microtubule plus-end interaction protein CLIP-170 also binds to the Rac/Cdc42 effector IQGAP at the leading edge of migrating cells (53). Expression of constitutively activated Rac/Cdc42 results in increased association between CLIP-170 and IQGAP. Microtubule association with the cell cortex is also promoted by the association of the plus-end binding protein EB1 with the adenomatous polyposis coli (APC) tumour suppressor protein (15). In migrating astrocytes, this association is mediated by Cdc42 through the Par6/atypical protein kinase Cζ (aPKC) complex (97). Interestingly, both EB1 and APC also bind to IQGAP, and both are involved in the maintenance of CLIP-170 at the cell surface, suggesting a sophisticated coordination of microtubule-cortex dynamics (428). Thus, Rho family members Rac and Cdc42 regulate cytoskeletal microtubule dynamics.

1.2.1.3 Regulation of Gene Expression

The promoters of many genes encoding components of the cytoskeleton contain the serum response element (SRE). The SRE binds to two transcription factors: the ternary complex factor (TCF); and the serum response factor (SRF). The TCF is activated via the ERK, JNK/SAPK, and p38/Mpk2/RK MAPK pathways, whereas the SRF is not activated by these pathways, but by processes which are still poorly understood (see (48)). Both transcription factors can be activated by Rho, Rac, and Cdc42 in both MAP kinase cascade-dependent and –independent processes. First, Rac1 and Cdc42, but not RhoA activate the JNK/SAPK and p38/Mpk2/RK MAP kinase cascades (71, 109, 261,

419). Expression of constitutively activated alleles of Rac1 and Cdc42 resulted in activation of the both pathways whereas expression of dominant-negative alleles of Rac1 or Cdc42 blocked activation of the pathways. The ability of Rac1 and Cdc42 to activate TCF-dependent expression via the ERK pathway is less clear (71, 109, 261). Second, all three of RhoA, Rac1, and Cdc42 can activate transcription via SRF independently of MAPK signaling (Hill, Wynne et al. 1995; Urich, Senften et al. 1997). RhoA was shown to be required for the activation of SRF-mediated transcription. While the details of the mechanism remain unclear, it has been suggested that activation occurs via the RhoA effector mDia, which may act as a scaffold for assembling a signaling complex for SRF activation (124). Thus, through activation of signaling networks, including MAPK cascades, Rho GTPases affect gene transcription for SRE-containing genes, including many which code for proteins also involved in cytoskeletal dynamics.

1.2.1.4 Regulation of Enzymatic Activities

Another means by which Rho-family proteins influence cellular processes is by direct regulation of enzymatic activities through direct associations with relevant proteins. For instance, Rho, Rac, and Cdc42 can all participate in lipid metabolism through associations with PI4P 5-kinase, PI3 kinase, DAG kinase, and phospholipase C (PLC), among others (see (168)). Rac has also been implicated in the generation of reactive oxygen species (ROS) due to its association with p67phox, a component of the NADPH oxidase complex found in phagocytic cells (84). The large number of effectors for the Rho family suggests that more examples remain to be identified.

1.2.2 Biological functions

The functions of Rho family proteins are coordinated into broader biological processes. Often, different Rho GTPases play individual roles in the same pathway, or a single Rho GTPase may play multiple roles in a single pathway or process. Below, I discuss the biochemical functions of Rho GTPases in a broader biological context, and describe the roles of Rho GTPases in the regulation of three biological processes: morphogenesis, motility, and the cell cycle.

1.2.2.1 Morphogenesis

Mammalian cells adopt a variety of cell shapes which are intimately tied to cellular function. From simple epithelial cells to highly-elongated neurons, Rho GTPases help coordinate the generation of the relevant cell morphology.

In *Caenorhabditis elegans*, Cdc42 participates in the establishment of the anterior/posterior axis within the zygote through the asymmetric partitioning of six *par* genes (PAR1-6) and an atypical protein kinase C (aPKCζ) (176, 225, 317). Disruption of Cdc42 results in the delocalization of these polarity factors and a resultant loss of polarity in the zygote. These factors are conserved throughout the animal kingdom where they participate in polarity establishment in numerous contexts, including *Xenopus* oocytes and *Drosophila* neuroblasts (286, 439).

Cells in epithelial tissue demonstrate an asymmetrical cell shape related to their varied functions. Epithelial cell proteins are asymmetrically distributed between the apical and basolateral membranes. The division of the cell membrane into distinct subcompartments is possible due to the polarized distribution of tight junctions and

adherens junctions, the polarized delivery of secretory vesicles, in addition to the polarization of the cytoskeleton. For instance, tight junctions are required for the generation of epithelial cell polarity, as tight junctions serve to restrict plasma membrane components to either the apical or basolateral membranes The Par6-atypical PKC complex, with Par3, is required for the formation of this cell-cell junction, and is probably activated by Cdc42, as in *C. elegans* (176). Rho GTPase activity is also involved in the establishment of adherens junctions, as inhibition of Rho prevents adherens junction formation. Cdc42 and Rac may also be involved in the establishment or maintenance of adherens junctions, as cadherin-mediated formation of adherens junctions results in their activation and their recruitment to the sites of formation (158, 285). Rho involvement in the regulation of cell-cell contacts is assumed to involve remodeling of the actin cytoskeleton, though actin-independent processes have also been proposed (98).

Rho-type GTPases are involved in numerous other morphological processes in various cell types. In MDCK cells, expression of a dominant negative Cdc42 results in the inhibition of transport of vesicular cargo vesicles to basolateral surfaces, leading to a depolarization of these membranes (201). In neurons, highly polarized neurite outgrowth is promoted by Cdc42 and Rac, and is inhibited by Rho (197, 356). This observation is similar to what is observed in migrating cells (see below), where Rac/Cdc42 promote membrane outgrowth at the leading edge, whereas Rho activity promotes retraction at the trailing edge, through differential effects on actin-myosin dynamics

1.2.2.2 Motility

Cell migration is an essential feature of metazoan development, and is required to maintain the integrity of tissues and to perform specialized cell tasks. Generally, cellular motility is achieved through actin filament polymerization and microtubule elongation at the leading edge coupled with actin-myosin filament contraction at the rear of the cell. Rac stimulates actin polymerization in lamellipodia at the leading edge through activation of the Arp2/3 complex. Fluorescence resonance energy transfer (FRET) has demonstrated that Rac-GTP levels are highest at the leading edge of a migrating cell, though some Rac-GTP is also observed at the contractile rear of cells, suggesting that Rac may be playing distinct roles at different ends of the cell (114).

Rho acts at the trailing edge of the cell to coordinate the contractile forces required for the cell body and peripheral membrane to follow the leading edge. Through its effector, Rho kinase (ROCK), Rho mediates the phosphorylation of myosin light chain (MLC), resulting in the activation of myosin and thereby generating the contractile forces required to move the cell forward (335, 411). ROCK also seems to act at the lateral edges of cells to prevent the formation of new integrin adhesion complexes (442). Rho thereby promotes trailing-edge retraction and disrupts cell-cell contacts to allow the Rac- and Cdc42-associated lamellipodia to move cells forward.

Cell motility also requires the polarization of the microtubule cytoskeleton. Cdc42 at the front of migrating cells leads to the localized activation of the complex involving Par6/aPKC. In lamellipodia, this activation results in the inactivation of the protein kinase GSK3, which promotes the association of APC with microtubule plus-ends, as previously described (97). It has also been suggested that the activated Par6/aPKC complex

promotes the association of the cortex-bound Dlg polarity protein and microtubule-bound APC (168).

Cdc42 also helps to link the assembly of polarity components, including Rac and Arp2/3 with external cues. Cdc42 is essential for the chemotactic migration of a macrophage cell in a chemical gradient: when Cdc42 is inhibited, cells still move but do so in a random fashion (9). Furthermore, when cell migration by fibroblasts is induced by scratching a monolayer, Cdc42 is required to restrict Rac-dependent actin polymerization to the leading edge of migrating cells (51). The mechanism by which the signal transduction occurs remains to be elucidated, but it is clear that Cdc42 is an important factor in linking external cues with the internal polarization of the cell.

1.2.2.3 Cell Cycle

Rho GTPases also contribute to the regulation of cell cycle progression, in both cytoskeleton-dependent and –independent ways. During M phase, Rho GTPases are central to the organization of the actin cytoskeleton and microtubules involved in partitioning chromosomes. During prophase and metaphase, microtubules emanating from two centrosomes are responsible for the proper alignment of chromosomes. Astral microtubules interact with the cell cortex to align the mitotic spindle in an axis perpendicular to the future cytokinesis plane. The proper positioning of the centrosomes has been shown to depend on actin-myosin filaments under the control of ROCK, though the mechanism remains unclear (347). Astral microtubules are also responsible for the asymmetric distribution of the centrosomes in cell divisions where mother and daughter cells differ in size and specification (*e.g.* in development or stem cells). This process

seems to involve the Par proteins and the atypical PKCζ kinase (205, 296, 370). As mentioned, a complex containing these proteins is a target for Cdc42 activation; indeed, Cdc42 has been shown to be essential for asymmetric cell division (126). Cdc42 and its effector mDia3 are also involved in the attachment of spindle microtubules to the kinetochore. Inhibition of Cdc42 or depletion of mDia3 results in misattachment of chromosomes to microtubules and consequent mitotic arrest (454). Finally, Rho GTPases also play a central role in cytokinesis, where they localize to the cleavage furrow with their effectors ROCK, Citron kinase, and mDia (see (122)). Inhibition of either Rho or Cdc42 prevents the assembly of the contractile ring (87); however, overexpression of either Rho or Cdc42 also blocks cytokinesis, suggesting that cycling between active and inactive forms may be required for function (98). Phosphorylation of MLC at Thr18 and Thr19 drives contraction of the actin filament ring, and the phosphorylation state of these two residues may be influenced by both ROCK and Citron kinase (255). While the details remain to be elucidated, it is clear that Rho and Cdc42 participate in the formation and constriction of the actin-myosin ring.

Rho proteins also influence the cell cycle by cytoskeleton-independent means. Inhibition of Rho, Rac, and Cdc42 blocks cell cycle progression at G1 in a variety of cell types (288, 451). All three can also promote entry into G1 and progression into S phase when expressed in quiescent fibroblasts. While the mechanisms remain to be identified, Rho seems to both inhibit the cyclin/CDK inhibitor $p21^{Waf1/Cip1}$, and to induce G1 phase cyclin D1 expression through the activation of ERK MAP kinase (289, 429). Rac is essential for cyclin D1 expression during G1 in endothelial cells, though this effect seems to be mediated by translation of mRNA rather than gene transcription (259).

1.2.3 Roles of Rho GTPases in Cancer

Given that Rho was first cloned as a Ras homologue, many researchers suspected it, too, may act as an oncogene. Ras is found mutated in nearly 30% of all cancers (35, 365), suggesting the same might be true for Rho proteins. Given its central role in numerous processes central to tumour formation and progression (cell cycle control, cell motility, polarization, etc.), it is perhaps especially surprising that no oncogenic mutations have been found in Rho proteins. Only a single genetic rearrangement of a Rho gene has been associated with cancer: RhoH (also known as TTF) was found rearranged in non-Hodgkin's lymphoma, multiple myeloma, and diffuse large cell lymphomas (295, 309). Apparently, activation or inactivation of the Rho proteins is not favourable for the initiation or progression of tumour cells.

Nonetheless, Rho signaling has been widely implicated in cancer, as demonstrated in numerous studies *in vivo* and *in vitro* using cell lines, primary tumours, and mouse models (for review, see (93)). Rho proteins are aberrantly expressed in a number of cancers and cancer-derived cell lines, with overexpression and downregulation in some instances associated with prognosis and development. For instance, RhoA overexpression has been observed in a wide variety of cancers, including those of the breast, colon, lung, stomach, bladder, and testicle as well as in head and neck squamous cell carcinoma (93). An *in vitro* study has shown that overexpression of RhoA leads to an increase in invasion of tumour cells due to its localization to the plasma membrane, where it activates ROCK and actin-myosin (457). Mutations or alterations in Rho protein expression levels have also been positively correlated with human renal-cell and prostate

carcinomas as well as with breast cell tumour progression (summarized in (93)). Changes in protein expression levels in human tumours have also been observed for GDIs and GAPs.

More often, mutations are found in Rho regulators, resulting in deregulated Rho signaling which can result in tumour initiation and progression. For example, mutations in the Rac-specific GEF Tiam1 lead to an increase in Ras-induced invasiveness in epithelial skin tumours (159, 240). In most instances, the molecular mechanism by which Rho regulators may influence Rho signaling in tumours is unclear. Furthermore, the degree of specificity of many Rho regulators remains unknown, and so conclusions drawn must remain tentative. However, the requirement of Rho GTPase signaling for Ras proteins to induce oncogenic transformation and the altered protein expression levels of Rho proteins and their regulators suggest that Rho signaling and cancer is biologically relevant (318, 319, 467).

1.3 Rho GTPases in *Saccharomyces cerevisiae*

Budding yeast has proven to be a valuable model organism for investigating the roles of Rho-type GTPases. Yeast genetics provided the first results linking *CDC42* to cell polarity (4), and has since provided a powerful tool for investigating Cdc42-related pathways. For instance, soon after the Dbl oncogene was identified, it was observed that it shared a region of homology with the *S. cerevisiae* protein Cdc24 (344). While the function of Dbl was unknown, previous work had determined that Cdc24 interacts genetically with Cdc42 (21). Subsequent work demonstrated that the homologous region of Cdc24 and Dbl (the DH, or Dbl homology, domain) could catalyze GDP-GTP

exchange on Cdc42 (140). DH domains have since been identified in a wide array of eukaryotic organisms, where they exhibit different specificities for various Rho proteins.

Of course, Rho-related signaling networks in yeast are often simplified compared to higher eukaryotes, where the Rho family and many of its signaling networks have undergone extensive evolutionary expansion. For instance, only one RhoGDI has been identified in yeast, and its deletion does not produce any detectable phenotype (196). Nonetheless, the yeast Rho family of proteins is involved in diverse processes analogous to those observed in metazoans: generation of cell polarity, cell cycle dynamics and cytokinesis, and the activation of MAPK signaling networks, among others. As in metazoans, they promote physiological responses both directly through the activation of relevant proteins and indirectly through the activation of signaling cascades. Whereas the metazoan Rho family has expanded considerably, the yeast Rho-family comprises six members, Cdc42 and Rho1 through Rho5.

1.3.1 Cdc42

CDC42 was first identified in *S. cerevisiae*, in a temperature-sensitive mutant strain carrying a mutation, *cdc42-1*, which prevented bud formation at 37C, but which continued to grow in cell volume and size (4). DNA replication continued, but actin cables were delocalized and cell surface components were deposited uniformly around the cell, suggesting that Cdc42p played a role in the cell polarization. Subsequent work has shown that Cdc42 plays a central role in establishing cell polarity in all eukaryotic organisms, including yeast. Notably, the advantages of yeast genetics have allowed the

S. cerevisiae has proven an invaluable resource for studying cell polarity, which underlies yeast morphology and cell division (for reviews, see (237, 312)). Yeast cells exhibit polarity in three contexts in particular. First, during vegetative growth, budding yeast grow isotropically until they reach a critical size and then they polarize growth to a particular site on the cell cortex where they form a bud. The actin cytoskeleton polarizes along the mother-bud axis and new cell wall components, among other cellular components, are selectively directed into the growing bud. Second, when haploid yeast cells are exposed to pheromones secreted by haploid yeast of the opposite mating type, they form polarized mating projections called shmoos, which are oriented towards the highest extracellular concentration of pheromone and which are capable of mediating cell-cell fusion as part of yeast mating. Third and finally, under conditions of nutrient deprivation, yeast can undergo a morphological switch from ellipsoidal bipolar budding to an elongated unipolar morphology: pseudohyphal growth (or invasive growth in haploids). In all cases, Cdc42 acts as a central regulator of the machinery involved in polarizing the cell.

1.3.1.1 Activation of Cdc42p at the plasma membrane

The key event in Cdc42-initiated polarized growth is its recruitment to the plasma membrane, where Cdc42p can interact with scaffolds and effectors to initiate remodeling of the actin cytoskeleton. The membrane association of Cdc42 is essential for polarized growth, as *cdc42* mutants lacking the geranylgeranyl membrane anchor or Δ*cdc43*

mutants, which lack the geranylgeranyl transferase, exhibit the same phenotype as temperature-sensitive mutants of *cdc42* grown at restrictive temperatures, which exhibit delocalized actin patches before arresting as large unbudded cells (4, 466). The activation of Cdc42 at the appropriate site of polarized growth depends on its GEF Cdc24 (274). During vegetative growth, Cdc24p is sequestered in the nucleus with Far1p until the Cdc28p-Cln2p-dependent degradation of Far1p in late G1 (275). Cdc24 then relocalizes to the presumptive bud site where it binds to the bud site protein Rsr1p/Bud1p and polarity scaffolding protein Bem1p (375). During mating, activation of the mating MAPK cascade results in the recruitment of Far1p to the shmoo site, where it interacts with the Gβγ-subunits, resulting in the accumulation of Cdc24p at sites of polarized growth (275). In both cases, Cdc42p activation is restricted until an internal or external signal results in its co-localization with its GEF, Cdc24.

1.3.1.2 Assembly of the Septin Ring and Polarization of the Actin Cytoskeleton

An early step of all three modes of polarized growth is the establishment of a septin ring at the interface between the mother cell and site of polarized growth (121). Cdc42p is a direct activator of septin self-assembly, independent of the actin cytoskeleton (52, 119). The septin ring acts as a scaffold for the recruitment of many actin-cytoskeleton related proteins, among them the Cdc42p effector Iqg1p, the yeast homologue of IqGAP (292). Cdc42p also interacts at these sites with its effector kinases, the PAKs Ste20p and Cla4p, which interact with a variety of polarity proteins including septins, Cdc24p, and Bni1p (see (237)). Ste20p also phosphorylates the type I myosins Myo3p and Myo5p, which are required for proper cytoskeletal organization (446).

Cdc42p also interacts directly with the formin Bni1p and is required for its proper localization at sites of polarized growth (99, 293). Bni1p is bound by Cdc42p and is phosphorylated in a Ste20p-dependent fashion, though it remains unclear whether these interactions affect Bni1 activity directly (123). Cdc42p also interacts with many proteins through its effectors Gic1 and Gic2, which serve as adaptors to link Cdc42p to many proteins involved in polarized growth, including Bni1p, Bud6p, and Spa2p, all members of the polarisome: a protein complex involved in actin filament formation (173, 293). Cdc42p also participates in the recruitment of an Arp2/3 activating comprising Bee1p/Las17p (the orthologue of WASp) and Vrp1p (215). Both directly, and through its effectors the PAKs and Gic proteins, Cdc42p thus coordinates the machinery involved in the formation of actin cables at sites of polarized growth.

1.3.1.3 Polarized Secretion and Cell Cycle Progression

Polarized growth requires the targeted delivery of secretory vesicles to sites of polarized growth, and Cdc42p plays a key role in the regulation of this process (2). Cdc42p binds to Sec3p, which serves as a cortical landmark for polarized exocytosis (461) Additionally, *CDC42* interacts genetically with *MSB2* and *MSB4*, whose protein products depend on Cdc42p for their localization (26). Msb2p and Msb4p regulate the Rab-type GTPase Sec4p, a regulator of exocytosis (394).

Paradoxically, in addition to promoting bud emergence and polarized growth, Cdc42p also participates in preventing subsequent rounds of bud emergence and in the switch from apical to isotropic growth in the bud. Studies with *cdc42* mutants demonstrated that hyperactivated alleles of *CDC42* result in a multibudded phenotype,

with consecutive formation of small, incompletely formed buds (53, 330). Thus, it is the level of Cdc42p activity which determines the frequency of budding. Expression of an allele with another mutation in *CDC42 (cdc42V44A*) results in highly elongated buds indicative of a delay in the apical/isotropic switch (331). These cells also exhibited multiple nuclei, suggesting a defect in the G2/M morphogenic checkpoint. While the mechanism remains to be elucidated, Cdc42V44Ap is defective in binding to Cla4p and the Gic proteins, but retains the binding to Ste20p, Bni1p, and Igq1p. Thus, as in metazoans, Cdc42p participates in the regulation of polarized secretion and cell cycle progression.

1.3.1.4 Activation of MAPK signaling

In addition to the direct regulation of effectors which direct cell polarity, Cdc42p influences cell polarity through its role as an activator of numerous MAPK signaling pathways in yeast (Figure 1.2). MAPK signaling cascades are involved in regulating the responses to mating pheromones, high-osmolarity, and pseudohyphal growth conditions. These pathways are all activated by the Cdc42p effector Ste20p, which acts as a MAPKKK kinase (also MEKKK, MAPKKKK, or MAP4K) (77). Cdc42p is required for signaling through the pseudohyphal pathway and through the Sho1p branch of the HOG pathway, where it acts upstream of Ste20p (269, 321, 393). Cdc42p's role in the mating pheromone pathway is less clear. Early studies indicated that Cdc42 acted upstream of Ste20p to activate the pathway (379, 462), though studies with Ste20p lacking the Cdc42p-binding domain suggested that Cdc42p binding was dispensable for Ste20p signaling in polarized morphogenesis (213, 302). More recent results have indicated that

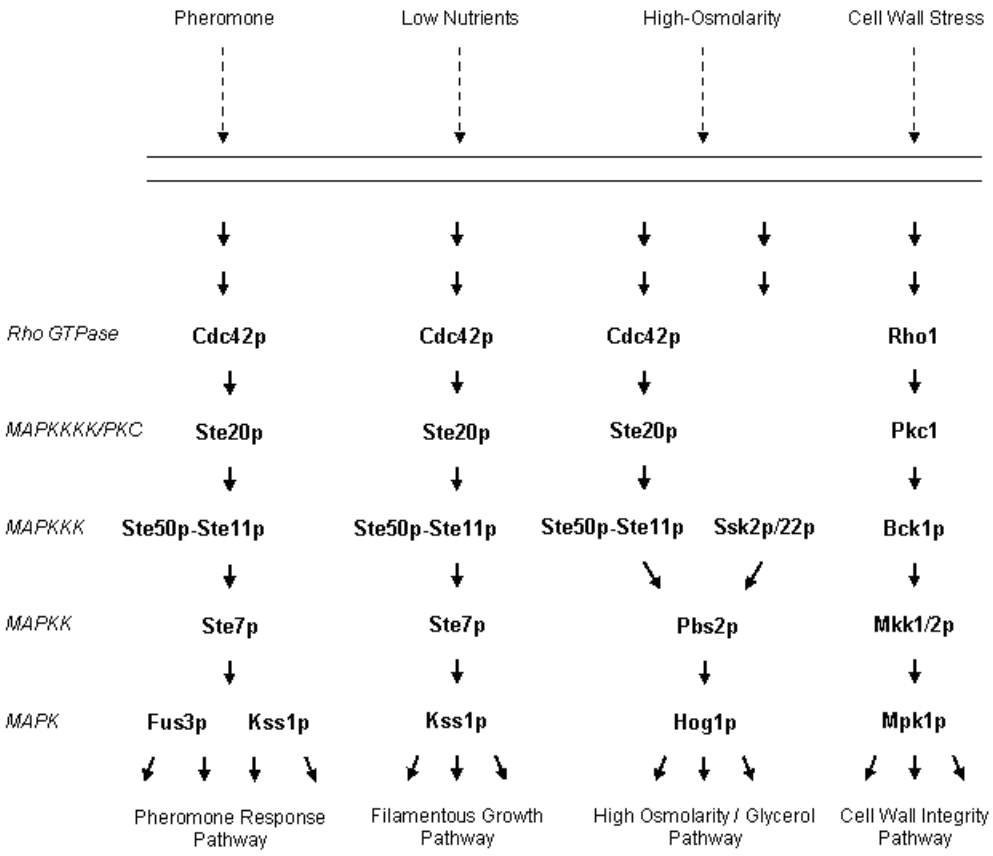

Figure 1.2. Schematic representation of the major MAPK signaling pathways in *S. cerevisiae*. Extracellular signals are detected by cell membrane sensors or receptors and are transduced through receptor-associated intracellular signaling molecules (not shown). These signals generally result in the activation of a Rho family member and associated kinase (Ste20p or PKC). PKC is not generally considered a MAPKKK given its involvement in only one pathway. The kinases of the various MAPK pathways are defined at left, and only the core kinase components involved in MAPK pathway signaling are depicted, with the exception of the Ste50p adapter protein required for Ste11p activity. Adapted from (58).

the deletion constructs employed in these studies resulted in constitutive activation of Ste20, and again suggest that Cdc42p is required for efficient induction of the pheromone signaling pathway by full-length Ste20p (13, 207, 270). Activation of these pathways results in the initiation of a transcriptional response, the promotion of morphogenetic programs and other physiological responses to effect the appropriate response. Cdc42p plays a central role in the activation of these programs and coordinates their activation with direct regulation of factors involved in polarized morphogenesis.

1.3.2 Rho1

1.3.2.1 1,3-β-glucan synthesis

Rho1p was the first Rho-type GTPase to be characterized in yeast, along with its homologue Rho2p (236). This work identified *RHO1* as an essential gene, and revealed that it functioned independently of Ras-related cAMP-dependent signaling, suggesting that Rho proteins act in a biochemically distinct pathway from Ras. The first suggestion of a role for Rho1p came from the observation that the activity of 1,3-β-glucan synthase required the presence of a small GTPase *in vitro* (264), which was subsequently identified as Rho1p (89, 256, 316). 1,3-β-glucan is the main structural component of the yeast cell wall, and is synthesized by the plasma membrane-associated 1,3-β-glucan synthase (1,3-β-GS). *FKS1* and *GSC2* encode the catalytic subunits of the 1,3-β-GS. Rho1 was identified as the regulatory subunit of this enzyme based on a number of observations. First, expression of a hyperactive *RHO1* allele results in GTP-independent 1,3-β-GS activity. Second, expression of a temperature-sensitive allele of *rho1* results in reduced 1,3-β-GS activity at elevated temperatures. Third, Rho1p co-fractionates with

Fks1p, they co-localize in the cell, and they bind to each other *in vivo*. These observations led to the early identification of Rho1p as a subunit of 1,3-β-glucan synthase.

1.3.2.2 PKC pathway

Rho1p also plays a separate role as an activator of the PKC pathway (Figure 1.2). The yeast protein kinase C (PKC) regulates a MAP kinase cascade involving a MEKK (Bck1p), two redundant MEKs (Mkk1/2p), and a MAPK (Slt2p) (for review, see (58)). This pathway is also called the cell integrity pathway, as mutants in this pathway exhibit cell wall defects which often result in lysis, especially at high temperatures. Early studies of complementation of *rho1* mutants demonstrated that RhoA could partially complement *rho1* deletions, though cell lysis was still observed at elevated temperatures (315). A suppressor of this defect was isolated and was identified as an activated allele of *PKC1*, and it was shown that Rho1p and Pkc1p interact in the same pathway (278) and that Rho1p is an activator of Pkc1p signaling (184). The participation of Rho1p in PKC-pathway regulation is distinct from its role as a subunit of 1,3-β-glucan synthase, as mutations in *RHO1* have been identified which are distinct to each role (353).

1.3.2.3 Polarized growth and cell cycle dynamics

Rho1p also participates in the regulation of polarized growth and cell cycle progression in a PKC-independent pathway. Early work demonstrated that a temperature sensitive allele of *rho1*, *rho1-104(D72N; C164Y)*, arrested growth at the nonpermissive temperature in G1, prior to the repolarization of the actin cytoskeleton during bud development (452). Further work demonstrated that temperature-sensitive alleles

exhibited a number of polarization defects, including polarized distribution of actin to presumptive bud sites, failed localization of Cdc42p and Spa2p, and the formation of shmoos (88). These were demonstrated to be independent of Rho1p's roles as a regulator of both PKC signaling and 1,3-β-glucan synthesis. Rho1p also directs the assembly of the actin ring at sites of cytokinesis in a process regulated by the polo-like kinase Cdc5p (409, 456). Rho1p's role in the polarization of the actin cytoskeleton is possibly explained through its ability to bind and activate the yeast formin, Bni1p (85, 293, 409).

Rho1p has also been implicated in cell cycle progression through its association with cell-cycle checkpoints at both the G1/S and G2/M boundaries (190). Two sets of *rho1* mutants were identified: one group had defects in the G2/M checkpoint which resulted in early entry into mitosis, whereas the other had defects in G1/S which resulted in the formation of buds by abnormally small mother cells. This latter group also exhibited an early accumulation of cyclin Cln2p levels, which have previously been shown to be regulated by Rho1p in a PKC-independent pathway (263).

As with metazoans, Rho1p participates in polarized secretion through regulation of the exocyst, a protein complex which coordinates the docking of exocytic vesicles with the plasma membrane. Several *rho1* alleles were found in a screen for mutants defective in the localization of exocyst components, though the localization defect was shown to be independent of the actin cytoskeleton (131). Rho1p interacts directly with Sec3p, which acts as a spatial landmark for sites of polarized secretion (105). Cdc42p also interacts with Sec3p, and it has been proposed that the two Rho GTPases may interact with Sec3p at different stages of the cell cycle (460).

1.3.3 Rho2

RHO2 was identified at the same time as *RHO1*, but was found to be unessential for growth (236). Rho2p does not seem to participate in most Rho1p-related processes, including activation of the PKC pathway, cell-cycle checkpoints, or Bni1p-induced filament formation in buds (85, 139). Rho2p is, however, proposed to be involved in the regulation of actin cortical patch assembly, based on the identification of *RHO2* as a suppressor of profilin-deficient (*Δpfy1*) cells (113). *Δpfy1* mutants are viable, but exhibit aberrant actin dynamics, with cortical actin patches visible in the mother cell at all stages of the cell cycle. This results in continual isotropic growth with a number of associated phenotypic defects (134). *RHO2* was one of several multicopy suppressors identified which could correct the phenotypic defects of the *Δpfy1* mutant, suggesting that it participates in the control of actin patch assembly. The other suppressors require the presence of Rho2p, as they did not suppress a synthetic *Δpfy1 Δrho2* defect, leading researchers to speculate that Rho2p acts as a central regulator of the repolarization of actin patches.

1.3.4 Rho3 and Rho4

RHO3 and *RHO4* were identified together in 1992 (253). Deletion of *RHO3* causes a severe growth delay and an increase in cell death. When combined with a *RHO4* deletion (*Δrho3 Δrho4*), cells are inviable, suggesting that they share a common function. These Rho GTPases play a contributing role in establishing polarized growth, as the loss of *rho3* or the combination of *rho3* and *rho4* mutations result in depolarized actin and isotropic growth, whereas expression of a constitutively active allele of *RHO3*

(*RHO3*^{D119A}) results in hyperpolarization of growth (164). The contribution of Rho3p and Rho4p in cell polarization may be best seen in bud formation, as mutant strains with *rho3* and *rho4* mutations exhibit defects in bud formation (253). These defects are suppressed by overexpression of *CDC42* and the gene encoding the polarity-related protein Bem1p in a process that involves the Bem1p-binding partners Boi1p and Boi2p (252). Like *Δrho3 Δrho4* mutants, *Δboi1 Δboi2* mutants arrest as depolarized cells with defects in bud formation. This defect is suppressed by overexpression of either *RHO3* or *RHO4*. Thus, it seems that Rho3p and Rho4p share a common polarizing function with Cdc42p in a Bem1p-Boi1/2p dependent manner. This common role is independent of other Cdc42p functions, as overexpression of *RHO3* or *RHO4* exacerbates the defects of cells with mutations in Cdc42-related signaling (*e.g. cdc24-4* or *cdc42-1*) (22). Indeed, it seems the essential role for Rho3p and Rho4p is to activate the Bni1p formin and its homologue Bnr1p, since expression of activated alleles of either bypasses the need for the Rho proteins (85).

Like Cdc42p and Rho1p, Rho3p seems to play a role in the targeting of secretory vesicles. First, *SEC4* was identified as a high-copy suppressor of *rho3* mutations (164). Sec4p is a rab-type GTPase that acts as a regulator of exocytosis and resides on secretory vesicles located at sites of polarized exocytosis (280). Additionally, *RHO3* exhibits a number of other genetic interactions with various secretory pathway components, including *SEC8*, *SEC15*, and *SEC9* (39, 280). Rho3p also binds directly to two proteins directly involved in vesicle transport, Myo2p, the myosin which ferries cargo vesicles along actin cables; and exocyst component Exo70p (135, 340). Overexpression of *RHO3* resulted in mislocalization of both Myo2p and Exo70p, and resulted in an abnormal

morphology. Furthermore, Rho3p colocalizes with Exo70 at sites of polarized growth. Through their involvement in actin dynamics and exocytosis, Rho3p and Rho4p participate in the regulation of actin-cable-based vesicular transport (312).

1.3.5 Rho5

Rho5p was the last Rho-family member to be identified in yeast, and remains perhaps the most poorly characterized It was found based on its similarity (62%) to Cdc42p, with whom it shares an identical effector region (113). Rho5p was initially characterized as a regulator of the PKC cell integrity pathway based on the phenotypic analysis of the *RHO5* deletion, which is resistant to drugs such as Calcofluor white and caffeine (364). In this study, epistasis experiments placed Rho5p downstream of Slt2p, though the upstream activators of Rho5p and its downstream effectors in this pathway remain to be identified.

More recently, it was shown that Rho5p is necessary for H_2O_2-induced cell death (380). Upon exposure to reactive oxygen species, yeast cells undergo apoptosis-like cell death (238). Deletion of *RHO5* results in a resistance to cell death, whereas expression of the constitutively activated mutant *RHO5Q91H* exhibited an increased sensitivity to H_2O_2 and concomitant increase in cell death. Rho5p-GTP interacts with the thioredoxin reductase Trr1p in the vacuole after exposure to H_2O_2, and the increase in Trr1p levels after H_2O_2 treatment depend on *RHO5*. Thus, it seems that under conditions of oxidative stress, Rho5p participates in the apoptosis-like response through Trr1p.

Though many details remain to be uncovered, the study of yeast Rho GTPases has provided valuable insight into the details of this family, especially their involvement in polarized growth, exocytosis, cell cycle dynamics, and MAPK signaling. In addition to the identification of their roles and effectors, the study of yeast Rho GTPases has provided a wealth of information about their modes of regulation, as summarized below.

1.4 Regulation of Rho GTPases

As key mediators of essential cellular processes, Rho GTPases are subject to extensive regulation. Notwithstanding the relatively simple GTP-GDP "switch" that governs Rho activity, the combined effects of numerous switch regulators allows for rapid and sophisticated regulation of the GTP-GDP cycle. More recently, an appreciation has been developing for regulation of Rho signaling that does not impinge on the GTP-GDP cycle, but rather on Rho proteins themselves. These regulatory methods include differential isoprenylation, subcellular localization, gene expression, phosphorylation, and Rho protein degradation. This section provides an overview of the main regulators of the GTP-GDP cycle, and then focuses on the non-canonical modes of Rho regulation outlined above.

1.4.1 GTP-GDP cycle

Like all members of the Ras superfamily, Rho proteins cycle between an active GTP-bound conformation and an inactive GDP-bound conformation (Figure 1.3). In the GTP-bound form, they interact with downstream effector proteins and thereby instigate

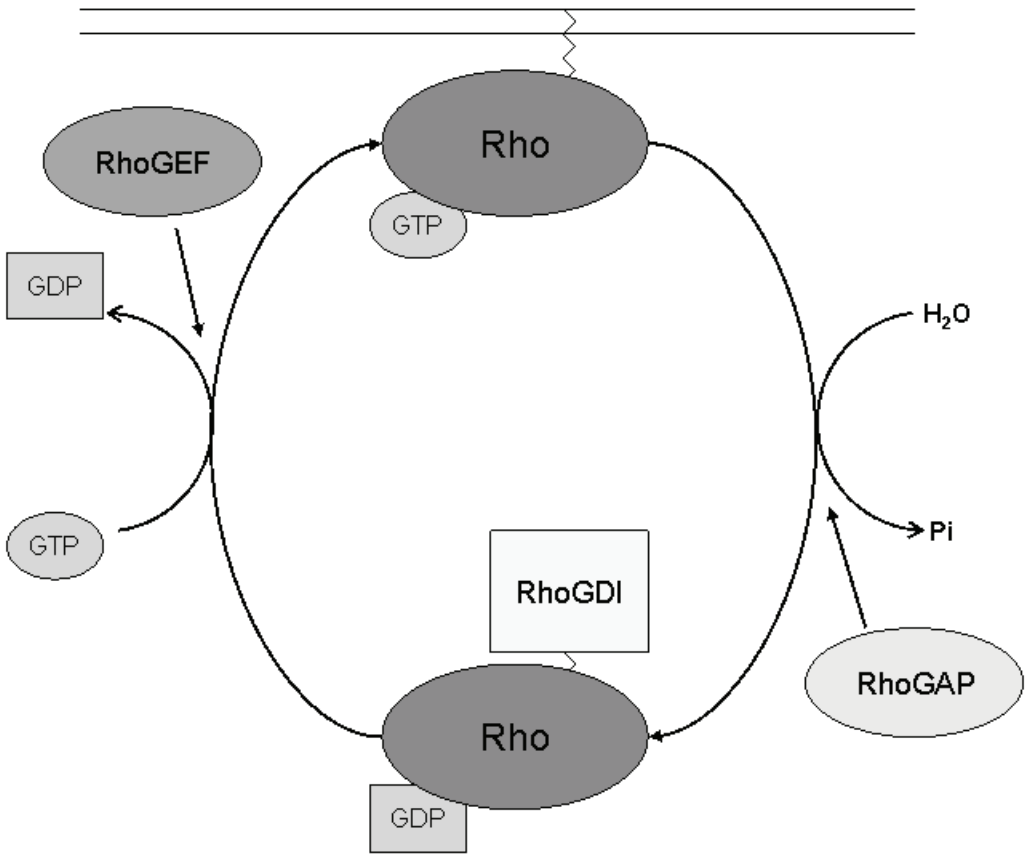

Figure 1.3. The Rho GTPase cycle. Inactivated Rho (GDP-Rho) is often sequestered in the cytosol through the association of its isoprenyl group with a GDI. Relevant upstream signals result in the dissociation of Rho from GDI and its relocalization to membranes where it is anchored by the isoprenyl group. Activation at cell membranes is achieved through the exchange of GDP for GTP, a process catalyzed by specific Rho GEFs. Attenuation of signaling is achieved through the hydrolysis of GTP due to intrinsic Rho GTPase activity with the assistance of RhoGAPs. GDI, guanine nucleotide dissociation inhibitor; GEF, guanine nucleotide exchange factor; GAP, GTPase activating protein.

cellular responses. GTP hydrolysis results in a changed Rho conformation, and an attenuation of the signal. GTP-binding by Rho proteins is facilitated through the exchange of GDP for GTP by guanine nucleotide exchange factors (GEFs), which thereby promote the activity of Rho GTPase signaling. The hydrolysis of GTP to GDP is due to intrinsic Rho GTPase activity, which can be promoted through the activity of GTPase activating proteins (GAPs). Rho signaling, therefore, is largely regulated by the opposing effects of GEFs and GAPs. Additionally, the Rho GTPase cycle is regulated by guanine nucleotide dissociation inhibitors (GDIs), which inhibit both the exchange of GTP for GDP and the hydrolysis of GTP, thus preserving the Rho protein in a steady state. Most regulation of Rho GTPase signaling occurs through the coordinated regulation of GAPs, GEFs, and GDIs (for review, see (98)).

1.4.1.1 Guanine Nucleotide Exchange Factors (GEFs)

The prototypical RhoGEF is the human oncogene Dbl, which was shown to share a region of homology with the *S. cerevisiae* Cdc24p protein involved in cell polarity and budding (344). Subsequent work showed that Dbl could act as a GEF for human Cdc42 (140). Dbl and Cdc24p were thus the founding members of a family of GEFs which are defined by the characteristic Dbl-homology (DH) domain. The DH domain is responsible for catalyzing the exchange of GDP for GTP by catalyzing nucleotide-free intermediates of Rho proteins, which are then loaded preferentially with GTP due to the higher concentrations of intracellular GTP (433). Adjacent to the DH domain, RhoGEFs contain a pleckstrin homology (PH) domain, which is thought to promote the association of GEFs with the plasma membrane (273, 355). Outside these domains, RhoGEFs exhibit

significant sequence divergence, and exhibit many additional domains which contribute to the variety of cellular tasks performed by family members. To date, the family comprises at least 69 members in humans (for reviews see (348, 361).

GEFs are frequently targets of signaling inputs, since they are largely responsible for converting RhoGTPases to the active state. RhoGEFs receive signals from a multitude of upstream regulators, and they are subject to a variety of regulatory mechanisms, including N-terminal truncation, phosphorylation, and subcellular sequestration (348). Furthermore, the variety of protein domains among GEFs means they often act as signaling scaffolds, bringing together signaling partners with localized activation of associated Rho GTPases. While no general paradigm exists for RhoGEF regulation, the extensively studied yeast GEF Cdc24 illustrates many of the general principles involved (for review, see (130)).

1.4.1.1.1 The Yeast GEF: Cdc24

Cdc24p is one of six yeast Rho GEFs, and is believed to be the sole RhoGEF for Cdc42p (177). It is largely responsible for directing Cdc42p signaling to the appropriate pathways. As described above, Cdc24p is sequestered in the nucleus through its association with Far1p (275, 375, 407). In response to intrinsic cell-cycle signals through Cdc28p-Cln2p signaling or extrinsic signals, for instance pheromone signaling through the seven-transmembrane mating pheromone receptor and its associated heterotrimeric G-protein subunits $G_{\beta\gamma}$, Cdc24p is rapidly exported from the nucleus to the plasma membrane. At bud emergence, the cyclin dependent kinase (CDK)-cyclin complex Cdc28p-Cln2p phosphorylates Far1p, leading to its destruction and the consequent

release of Cdc24p from the nucleus (147, 275, 375). Cdc24p binds to the small GTPase Rsr1p/Bud1p at the bud site, and this interaction has been proposed to activate Cdc24p by relieving Cdc24p autoinhibition (130). During mating, inhibition of Cdc28p-Cln2p allows the nuclear export of the Far1p-Cdc24p complex (29, 30), which then relocalizes to sites of mating projections, where Far1p interacts with the $G_{\beta\gamma}$ subunits thereby delivering Cdc24p to the appropriate sites for polarized growth (47). Thus, Cdc42p-signaling is restricted to areas of polarized growth through the highly regulated subcellular localization of its activating GEF, Cdc24p.

Whether in budding or mating, Cdc24p is stabilized at the membrane where it acts to recruit polarization factors. In addition to activating Cdc42p, Cdc24p recruits the scaffold protein Bem1p which also binds to Cdc42p, thus creating a positive feedback loop which sustains localized polarized growth (46, 376, 450). Bem1 also recruits other key factors to promote polarized growth, resulting in a Cdc42p-Cdc24p-associated polarized growth complex. Bem1p also recruits the Cdc42-effector Cla4p, which phosphorylates Cdc24p. This phosphorylation results in the dissociation of Cdc24p from Bem1p, thereby ending polarized growth (129). Thus, Cdc24p is a key component in a large macromolecular complex to promote polarized growth, and its changed subcellular localization or phosphorylation are the key steps in regulating Cdc42p-dependent polarized growth.

1.4.1.2 GTPase-Activating Proteins (GAPs)

The RhoGAP family is defined by the presence of a characteristic domain of roughly 150 amino acids which is shared among the roughly 80 family members

identified in humans (for review, see (265)). RhoGAPs greatly outnumber their Rho substrates, suggesting that they may play specialized roles and thus individually influence Rho activity in response to specific inputs. Indeed, GAPs exhibit a wide specificity in their interactions with Rho proteins, with some family members exhibiting GAP activity for a wide range of Rho proteins, while others are restricted to a single substrate. RhoGAPs have been identified as key regulators of Rho signaling activity in neuronal morphogenesis, cell growth and differentiation, endocytosis, and tumourogenesis.

Like GEFs, GAPs represent a common target of regulation for mediating Rho-related signaling. For example, p190 RhoGAP activity is regulated by phosphorylation through the opposing effects of Src tyrosine kinase and low molecular weight protein-tyrosine phosphatase (LMW-PTP). Phosphorylation by Src activates p190, resulting in the inactivation of Rho GTPase and the concomitant disruption of actin stress fibers, and focal adhesions (42, 144, 345). De-phosphorylation by LMW-PTP inactivates p190. Interestingly, LMW-PTP is also a substrate for Src, and its phosphatase activity is stimulated by phosphorylation, suggesting a highly-tuned coordination of signaling which impinges on p190 RhoGAP function. RhoGAPs have also been shown to be regulated by phospholipid binding through specific lipid-binding domains and through protein-protein interactions (49, 174).

1.4.1.2.1 Yeast RhoGAPs

The *S. cerevisiae* genome encodes nine RhoGAP proteins (396), which exhibit a varying degree of substrate specificity for the six yeast Rho GTPases. Interestingly, the GTPase hydrolysis by Rho1 and Cdc42 are both activated by five or six RhoGAPs,

whereas the other Rho proteins are downregulated by only one or two (see (350)). *RHO1* and *CDC42* are both essential for yeast cell survival, and have been implicated in numerous processes and pathways; the association of so many RhoGAPs underscores the number of roles played by these Rho proteins. Like their mammalian counterparts, yeast RhoGAPs are important targets of regulation. Phosphorylation of the Cdc42p-GAPs Bem2p and Bem3p by Cdc28p-Cln2p at bud emergence results in their inactivation, and prevents early attenuation of Cdc42p signaling (193). Furthermore, the yeast RhoGAPs Bem2p, Bem3p, Lrg1p, Rgd2p, and Sac7p all display PEST motifs within their sequences, suggesting that they may be targets for ubiquitin-mediated proteolysis (350).

1.4.1.3 Guanine Nucleotide Dissociation Inhibitors (GDIs)

GDIs have a diverse set of functions, including the extraction of Rho GTPases from membranes with a consequent change to cytosolic localization and the ability to inhibit both guanine nucleotide exchange and GTP hydrolysis, probably by sterically maintaining the Rho protein in either the GDP- or GTP- bound state (see (31, 35)). The RhoGDI family is much smaller than the other Rho regulators, with only three members so far identified in humans: ubiquitously expressed RhoGDIa; B- and T-lymphocyte specific Ly/D4-GDI or RhoGDIb; and RhoGDI-3 or –g, which is preferentially expressed in brain, pancreas, lung, kidney, and testis (287). RhoGDI was isolated as a protein which preferentially associated with GDP-bound RhoA and RhoB, and thereby inhibited dissociation of GDP (110, 417). Subsequent work demonstrated that RhoGDI could bind Cdc42 and Rac in addition to Rho, in either the GDP or GTP bound conformations (1, 68, 141, 219). A key role for GDIs is to bind and solubilize inactive Rho proteins,

maintaining them in the cytosol and sequestering them from membrane-associated activators and effectors, then releasing them into the membrane upon activation, though the mechanisms involved remain unclear (390, 391). The function of RhoGDIs *in vivo* remains unclear, though mouse knockouts of RhoGDIa (ARHGDIA) leads to age-independent renal failure and death (408). The disruption of the single yeast GDI isoform, *RDI1*, results in no discernable phenotype, though Rdi1p colocalizes with Cdc42p at sites of polarized growth and overexpression of Rdi1p results in loss of Cdc42p from membranes (251, 332).

Though the biological functions of GDIs remain elusive, several mechanisms of RhoGDI regulation have been identified. Phosphorylation of RhoGDIs has been implicated in both stabilizing interactions between Rho and RhoGDI (37, 418) and in destabilizing them (81, 258, 310), depending on cellular context. Protein-protein interactions can also destabilize the interaction between RhoGDIs and Rho proteins. For instance, binding by ERM (ezrin/radixin/moesin) proteins to RhoGDIa results in the displacement of Rho, Rac, and Cdc42 proteins from membranes (390). Finally, certain phospholipids have been shown in cell-free assays to promote the dissociation between GDI and Rho proteins, including arachidonic acid, phosphatidic acid, and PtdIns(4,5)P_2 (103, 455). Given that the function of many Rho GTPases require specific phospholipid environments (171), it is not surprising that GDIs might be regulated in this fashion.

1.4.2 Isoprenylation and Subcellular Localization

While extensive work has illuminated the regulation of Rho signaling via GEFs, GAPs, and GDIs, less is known about the direct regulation of Rho proteins. One method

by which Rho-protein signaling is regulated is through subcellular localization based on differential post-translational isoprenylation or other sequence features.

The activity of Rho proteins is absolutely dependent on their proper associations with the appropriate membranes. Membrane-association is achieved due to the isoprenylation of a tetrapeptide 'CAAX' box at the C-terminus of nearly all Rho GTPases. The majority of Rho proteins are modified at this C-terminal cysteine by the addition of a 20-carbon geranylgeranyl isoprenoid, though some are modified by the 15-carbon farnesyl isoprenoid (116, 378). Despite the different hydrophobic qualities of the two isoprenoid modifications, they do not seem to influence the localization of Rho GTPases (8, 182, 260, 384). One exception is the growth-promoting Rho protein, RhoB: RhoB appears to be mostly farnesylated (RhoB-F) *in vivo*, though a subset of RhoB is also geranygeranylated (RhoB-GG). This differential isoprenylation specifies the intracellular localization of the RhoB isoforms, with RhoB-GG localizing to multivesicular late endosomes, whereas RhoB-F localizes to the plasma membrane (432). Treatment with farnesyl-transferase inhibitors results in an increase in RhoB-GG and a decrease in RhoB-F with a concomitant inhibition of cell growth. Furthermore, RhoB-GG accumulation is associated with increased apoptosis and antineoplasiticity in human carcinoma cells (91, 228).

Though the differential isoprenylation of the CAAX box cysteine does not affect the function of most Rho GTPases, a second C-terminal modification is required for the proper localization of most family members. Some family members are modified by an additional palmitate group immediately upstream of the CAAX box. For instance, Wrch-1, a Cdc42-related member of the Rho family which can promote anchorage-independent

transformation, is modified by palmitate at a cysteine residue adjacent to the CAAX box, resulting in a localization pattern distinct from Cdc42 (24). Removal of the palmitoylation site results in mislocalization of Wrch1 and loss of transforming ability. Inhibition of palmitoylation with pharmacological inhibitors also results in the mislocalization of RhoB and Cdc42-family member TC10 to the ER and Golgi in place of the plasma membrane and endosomes (260). Differential isoprenylation can also disrupt interactions between Rho GTPases and GDIs, which are involved in the regulation of activity and localization of Rho family members, as mentioned. For example, a palmitoylation site inserted into RhoA abrogated binding by GDIα (260). The importance of C-terminal isoprenylation for proper Rho localization is exploited by pathogenic *Yersinia enterocolitica*, whose YopT cytotoxin cleaves the C-terminus of RhoA, removing the CAAX box (469). This redistributes RhoA from the plasma membrane to the cytosol and prevents its association with GDIs, resulting in a depolarization of the cytoskeleton and disappearance of adhesion complexes (5). In macrophages, this results in a loss of chemotaxis and an inability to form phagocytic cups involved in the uptake of the pathogen.

Subcellular localization of RhoGTPases is also determined through other C-terminal sequence features. Members of the Rac subfamily of proteins contain a polybasic sequence upstream of the CAAX box, and small differences in the composition of this sequence account for the differential subcellular localization of family members (104, 311). For instance, Rac1 targeting depends on a polybasic region upstream of the CAAX box which interacts with its GEF, the SH3 domain-containing protein β-Pix (p21-activating kinase [PAK]-interacting exchange factor) (397). This interaction is necessary

and sufficient for the proper localization of Rac1 to membrane ruffles and focal adhesions, and is dependent on the PAK family member Pak1. In other cases, the mechanisms of Rac1 localization remain to be determined, but the protein-protein interactions involved present a likely target for regulation.

1.4.3 Gene Expression

While the mRNA and protein concentrations of the 'classical' Rho proteins (RhoA, Rac1, and Cdc42) are relatively stable, most Rho family members exhibit cell-type specific and or stimulus-dependent expression. Many Rho proteins exhibit tissue-specific expression: for instance Rac3 is expressed in the neurons of ganglia and the central nervous system (34). Presumably, these Rho proteins perform specialized roles in these cells. For instance, Rac2 is expressed primarily in hematopoetic cells, where it aids specifically in the production of oxygen radicals in host defense mechanisms (338).

In addition to tissue-specific expression Rho family members may be differentially expressed during the cell cycle or in response to external stimuli. As an example, RhoG and RhoB exhibit cell-cycle dependent expression patterns, which peak in G1 and S phases, respectively (421, 458). RhoB expression is also induced by growth factors in PC12 and HeLa cells, and its protein product is degraded rapidly. While the functions of these proteins remain unknown, their expression pattern and the short protein half-life of RhoB suggests the need for tight regulation of their activity (214). Interestingly, the Rnd1 and Rnd2 Rho family members exhibit no GTPase activity and are thus constitutively activated: perhaps not surprisingly, their expression seems to be tightly regulated (138, 166, 210, 229).

1.4.4 Phosphorylation and Ubiquitination

Phosphorylation and ubiquitin-mediated proteolysis form the basis of signal transduction pathways across eukaryotes. Surprisingly, then, these types of post-translational modifications have not been widely reported among Rho-type GTPases. Certainly, there are many examples of the phosphorylation and degradation of GEFs and GAPs, some of which are mentioned above. Direct phosphorylation or degradation of Rho-type GTPases, however, is less commonly observed.

1.4.4.1 Phosphorylation

RhoA is phosphorylated on Ser188 *in vitro* and *in vivo* by the kinases PKA and PKG (208, 358). This phosphorylation inhibits RhoA activity, but does not affect intrinsic GTPase activity, or RhoA binding to GEFs or GAPs (94). Phosphorylation does enhance the interaction with GDI and enhances the ability of GDI to extract it from the membrane, as well as reduces GTP loading by RhoA (94, 107). Phosphomimetic mutants (RhoA(S188E)) expressed in NIH 3T3 cells exhibited reduced cell spreading whereas the RhoA(S188A) mutants were resistant to conditions which cause actin stress fiber disassembly (94). In vascular smooth muscle cells, RhoA phosphorylation is linked to ubiquitination as phosphorylation is reported to antagonize ubiquitin-mediated proteolysis and stabilize RhoA signaling, again through an increased association with RhoGDI (343).

Phosphorylation of Cdc42 by Src kinase is also reported to enhance its association with a GDI (415). This phosphorylation is reported to occur in response to EGF stimulation, resulting in the GDI-dependent relocalization of Cdc42.

RhoE is phosphorylated *in vitro* and *in vivo* by ROCK I, a serine/threonine kinase involved in actomyosin contractility (335). ROCK phosphorylates RhoE on Ser11 upon stimulation with platelet-derived growth factor resulting in its relocalization from the plasma membrane to the cytosol. Additionally, phosphorylation increases RhoE stability and correlates with its activity in disrupting stress fiber formation and Ras-dependent transformation. Recently, RhoB was shown to be phosphorylated by CK1 *in vitro* and in HeLa cells, and this phosphorylation was linked to RhoB activation and an increase in epidermal growth factor (EGF) receptor stability (403). Finally, Rac1 has been shown to be an *in vitro* substrate of Akt kinase, and the phosphorylation of Ser71 results in a decrease in GTP binding and GTPase activity, though the biological consequences remain to be determined (204).

1.4.4.2 Ubiquitination

Regulation by ubiquitin-mediated proteolysis is even less well characterized among Rho GTPases. The best characterized example occurs in migrating fibroblasts, where ubiquitin-mediated proteolysis of RhoA occurs at the leading edge, resulting in the spatial restriction of activated RhoA to the trailing edge (425). Active Cdc42 at the leading edge recruits the Smurf1 E3 ligase via the Par6/aPKCζ complex. Smurf1 interacts with RhoA directly, resulting in its ubiquitination, and leading to its proteasomal degradation (424). The candidate tumour suppressor RhoBTB2 is also a substrate for

ubiquitin-mediated proteolysis (435) While no function has been ascribed to this atypical Rho-type GTPase, it binds to the ubiquitin-ligase scaffold Cul3 and is a substrate for a Cul3-containing ubiquitin ligase complex. Furthermore, a RhoBTB2 missense mutant isolated from a breast cancer cell line neither binds Cul3 nor is a substrate for ubiquitination. Ubiquitin- and proteasome-independent partial cleavage also plays a role in the regulation of Rho proteins. For instance, proteolytic cleavage of Cdc42 by caspases following the activation of the Fas receptor contributes to Fas-dependent apoptosis (414).

1.4.4.2.1 Proteolytic Regulation of Rho Signaling by *E. coli* Toxin

An interesting example of the regulation of Rho proteins by post-translational modifications occurs through the effects of cytotoxic necrotizing factor-1 (CNF1), a classical protein toxin found in roughly 30% of uropathogenic strains of *Escherichia coli* (100). After CNF1 has been internalized and relocalized into the cytosol, it catalyzes the deamidation of a catalytic glutamine to glutamic acid in RhoA, Rac1, and Cdc42 (106, 221, 362). This impairs the GTPase activity of these proteins, rendering them hyperactive. Counterintuitively, the deamidation also increases the susceptibility of Rac1 to ubiquitin/proteasome-mediated degradation (86, 220). Some authors suggest that this mechanism of increasing Rac activity while also increasing Rac inactivation (by degradation) results in a lowering of the activation threshold of Rho proteins by the toxin (86). Also, this dual mechanism allows a balance between increased pathogen internalization into host cells and epithelium spreading due to activated Rho and a dampening of the host's Rho-dependent inflammatory response (86, 272).

1.5 PAK family kinases: primary effectors of Rho-type signaling

To date more than seventy Rho GTPase effectors have been identified, and it is beyond the scope of this introduction to discuss them in depth. (for reviews, see (27, 45)) Many Rho family effectors have been described above in the context of their cellular roles. In this section, I examine the Cdc42/Rac effector p21-activated kinase (PAK) and its yeast homologue Ste20p in greater depth. PAKs are possibly the most-studied Rho family effectors, and yet many questions remain about their various roles and downstream effectors.

1.5.1 Metazoan PAK-like kinases

The original mammalian PAK, called $p65^{PAK}$, was identified in an overlay assay as a rat brain protein that interacted with GTP-Cdc42 and GTP-Rac1, but not GTP-RhoA (246). The selective interaction with the GTP-bound form of Cdc42 and Rac1 suggested that $p65^{PAK}$ could act as an effector of these GTPases. This study also showed that $p65^{PAK}$ kinase activity was stimulated by this, proving that Rho proteins activated effectors much the same way as other small G proteins. The family has since expanded considerably, with as many as 30 PAK and PAK-related kinases identified in humans, though many of these are subdivided into a germinal-centre kinase (GCK) subfamily, whose members do not bind Rho family members (367). The PAK subfamily comprises six members: Pak1 through Pak6. These are further divided into two groups. Group I PAKs are similar structurally but are expressed in different tissues: Pak1 is expressed in brain, muscle, and spleen, Pak2 is ubiquitously expressed, and Pak3 is expressed only in the brain. Group II PAKs are less well studied, and share greater similarity with each other than with Group I

PAKs: Pak4 is expressed in testis and prostate tissue, Pak5 is expressed, like Pak3, in the brain, and Pak6 is ubiquitously expressed (for review, see (169)). Pak isoforms bind and are activated by Cdc42 and Rac subfamily members, but not by Rho subfamily members (32).

All PAKs comprise a similar C-terminal kinase domain and a GTPase binding domain (GBD), also called a p21-binding domain (PBD), responsible for binding to Cdc42 or Rac (44, 246). The most strictly conserved region of the GBD is the Cdc42/Rac interactive binding (CRIB) motif (401), whose presence is required but not sufficient for effective binding of PAKs to Cdc42/Rac. X-ray crystallography reveals that PAK exists as a homodimer in solution and *in vivo* (218). This structural study, combined with biochemical and genetic data, supports a model where binding by Cdc42 inhibits PAK homodimerization and results in a PAK conformation with a catalytically-competent active site (for more detailed review, see (32)). Cdc42/Rac binding thus activates PAKs and allows them to transduce the signal to relevant pathways or physiological targets. Though PAKs have been implicated in numerous cellular processes, their primary roles involve the regulation of actin dynamics and the Cdc42/Rac-dependent activation of MAPK signaling pathways.

1.5.1.1 Actin Cytoskeleton Dynamics

Early work involving Pak showed that it relocalized from the cytosol to actin structures at the cell cortex at sites of polarized growth (82). Microinjection of activated Pak1 into Swiss 3T3 cells induces a rapid formation of lamellipodia, filopodia, and membrane ruffles, similar to the effect when Cdc42 is microinjected (277, 367).

Furthermore, expression of activated forms of Pak1 results in the disassembly of actin stress fibers and focal adhesion complexes, which have been shown to accompany the Cdc42-dependent actin structures at the cell cortex (245, 367). The precise role of Pak1 in these processes remains unclear, however, as Rac1 and Cdc42 mutants defective in Pak-binding still form lamellipodia and filopodia, suggesting that additional effectors are involved, or that Pak1 does not require Cdc42/Rac binding to effect cytoskeletal changes (181, 206). Furthermore, there seem to be some cytoskeletal roles of Pak1 which are kinase-independent (108).

Though the precise roles played by PAK in cytoskeletal dynamics remain to be elucidated, several cytoskeleton-related substrates of PAKs have been identified. Nonmuscle myosins are regulated through phosphorylation on their light chain by myosin light chain kinase (MLCK), which allows the actin-dependent activation of the myosin ATPase (385). Pak1 phosphorylates MLCK, inhibiting its activity and reducing MLC phosphorylation (354). This results in a decrease in cell spreading in BHK-21 and HeLa cells. There have also been reports that Pak2 may regulate cytoskeletal dynamics through the direct phosphorylation of MLC (64). PAKs also seem to be capable of phosphorylating the heavy chains of class I and II myosins, and myosin VI, as well as caldesmon, desmin, Merlin, stathmin/Op18, and Filamin A, though the effects of these phosphorylations remain largely uncharacterized (see (32)). Nonetheless, PAKs are major regulators of cytoskeleton dynamics, and represent an important link between Cdc42/Rac and the morphological machinery.

1.5.1.2 MAPK signaling

PAKs are also involved in the activation of MAPK pathways and represent a major link between Cdc42/Rac activation and MAPK signaling. As mentioned above, Rho GTPases can activate the JNK, p38, and ERK MAPK kinases. PAK members have been implicated in mediating this activation in each pathway, through the phosphorylation of different targets. An early paper described the Cdc42p-dependent Pak3 activation of the JNK/SAPK pathway (16). An activated allele of Pak1 ($Pak1^{L107F}$) also resulted in the activation of JNK/SAPK signaling, possibly through the adaptor protein, Nck (33, 234). The role of Pak1 in activation of this pathway is complicated by the report that Pak1 phosphorylation of MEKK1 on Ser67 inhibits the association of MEKK1 with JNK, inhibiting signaling through the pathway (112). This suggests that Pak involvement in Cdc42-mediated activation of JNK/SAPK signaling is under sophisticated control.

PAKs have also been implicated in activation of the p38 and ERK MAPK pathways. Expression of activated Pak1 stimulates p38 activity whereas expression of a dominant negative allele of PAK1 suppresses Cdc42/Rac-induced p38 activity (459), and Pak1 is necessary for Cdc42-mediated activation of p38 in response to hyperosmotic stress (54). Pak1 also phosphorylates MEK1 serine on serine 298, and this phosphorylation is required for the stimulation of the ERK pathway by Rho proteins (57, 234). Expression of an interfering Pak1 mutant blocks Rho-dependent activation of ERK. Interestingly, phosphorylation of MEK1 by Pak1 assists binding of MEK1 and Raf-1, suggesting a coordination of Rho-mediated and Ras-mediated activation of the pathway (70). Pak3 phosphorylates Raf-1 directly *in vitro* and *in vivo* on Ser338, and that this

phosphorylation is required for Ras-dependent activation of the pathway through Raf-1 (109, 191). Thus, PAK members participate in the direct regulation of MAPK pathways and act in the convergent regulation of signaling by Rho and Ras through the ERK pathway.

1.5.1.3 Other substrates and the association of PAKs with disease

In total, roughly 30 substrates of PAKs have been identified (32). These implicate PAKs in apoptosis through the phosphorylation of Bad and histone H2B (63, 72, 366), control of estrogen-receptor (ER) signaling through direct phosphorylation of the ER (426), and coordination of Ras and Rho-signaling through the phosphorylation of Raf-1 (191). PAK family members have also been implicated in an increasing number of cancers (for a recent review of the role of PAKs in cancer, see (202)). Other PAK substrates, like the HIV protein Nef, point to a role for PAK in other diseases (74, 412). While increasing numbers of substrates have been identified for PAKs, the biology of PAKs remains incomplete. For many substrates, the consequences of the interaction are poorly characterized. More commonly, PAKs can be associated with processes and pathways but the substrates have not been identified.

1.5.2 A Yeast PAK: Ste20p

The yeast Ste20p kinase is the founding member of the PAK family. *STE20* was discovered in a genetic screen for suppressors of the mating defect of strains deleted for the G_β subunit, *STE4* (211, 322). Two homologues have since been identified in yeast: *SKM1* and *CLA4*. Skm1p is largely uncharacterized, though overexpression analysis

suggests it may play a role in morphogenesis (248). Cla4p and Ste20p share an uncharacterized essential function, as a *Δste20 Δcla4* mutant is inviable (76). Like Ste20p, Cla4p binds Cdc42p and is involved in budding and polarized growth (76, 92, 156). It was soon discovered that Cla4p played an essential role in the termination of the polarized growth of a nascent bud and the switch to isotropic bud growth. As mentioned above, Cla4p participates in this switch through the phosphorylation of Cdc24p, resulting in its disassociation with Bem1p and the termination of polarized growth (36, 129). Cla4p also plays a key role in the proper assembly of the septin ring (156, 183, 331, 363, 420), mitotic exit (66, 153, 369), and in linking Cdc42p to phosphoinositide signaling (434). Though participation in many of these pathways is common to the two PAKs, Ste20p and Cla4p often play distinct roles in the pathways.

1.5.2.1 Ste20p kinase in MAPK signaling

Ste20p is the most extensively-studied Rho effector in yeast, and much is known about its roles and regulation. Yeast genetics has identified roles for Ste20p in numerous pathways and processes, though the mechanisms involved remain largely unknown due to the few Ste20p substrates thus far identified. The earliest reports of Ste20p function were based on yeast genetics and involve its role as an activator of the mating pheromone response pathway. Subsequent work revealed that Ste20p, like mammalian PAKs, activates several yeast MAPK pathways, leading to suggestions it be considered a MAPKKK kinase (MAPKKKK, MAP4K) (Figure 1.2).

STE20 was initially identified as a suppressor of the *Δste4* mating defect (211). *Δste20* cells fail in cell cycle arrest in response to pheromone, fail to form shmoos, and

fail to activate pheromone mating factor Fus1p (211, 322). Epistasis analysis in these early reports placed Ste20p after $G_{\beta\gamma}$, but before the components of the mating MAPK cascade, including the MAPKKK Ste11. Ste20p phosphorylates Ste11 *in vitro* and is required for the activation of Ste11 *in vivo* (90, 447). This work established Ste20p as the prototypical MAP4K, a role which seems to have been broadly conserved throughout evolution (77).

Ste20p's role as a MAP4K seems to involve Cdc42p binding, though this has been controversial, as mentioned above. What is clear is that upon pheromone stimulation, Ste20p associates with Ste4p through a short C-terminal motif (217). The MEKK Ste11 is also associated with Ste4, through the scaffold Ste5 (165). Thus, Ste20p is brought in proximity to Ste11p, and the signal can be propagated through the mating MAPK cascade.

Ste20p's role as a MAP4K is not limited to activation of the mating pheromone response pathway, as it was soon shown that Ste20p was involved in the activation of other MAPK pathways in yeast (see (133)). In the pseudohyphal growth pathway, Ste20p transduces a signal from Ras2p through Cdc42p to Ste11 and the other components of the MAPK cascade (268, 269). Ste20p is also involved in activation of the Sho1p-branch of the high-osmolarity glycerol (HOG) pathway, one of two partially redundant branches which converge on the MEK Pbs2p (239). This branch of the pathway also employs the MEKK Ste11, and is activated by Cdc42p-bound Ste20p (321). It has been proposed that Cdc42p brings Ste20p to the plasma membrane where it can activate Ste11p, which is associated with the plasma membrane via Ste50p and Opy2p in response to osmotic

stress (443). Ste20p, thus plays an important role in the activation of MAPK cascades in yeast.

1.5.2.2 Morphogenesis

Ste20p plays several roles in yeast apart from activating MAPK cascades, including in morphogenesis, where it serves as a major effector of Cdc42p. Physiological substrates of Ste20p include the type I myosins Myo3p and Myo5p (446). The phosphorylation of these myosins is essential for their activity, but is not the shared essential function of Ste20p and Cla4p. Instead, their phosphorylation is activating, as in the other myosins mentioned above, and is required for proper budding. Ste20p is also involved in Cdc42-dependent actin cytoskeleton organization and polarized morphogenesis through its association with Bem1 (217, 438). Inactivation of Ste20p does not result in a decrease of actin cables, but does result in a depolarization of the cortical actin cytoskeleton (156). Ste20p has also been implicated in the activation of the Cdc42-effector Bni1, the formin responsible for the polymerization of actin cables at sites of polarized growth (123). Ste20p's role as a central Cdc42p effector is confirmed by the observation that the morphological defects of a *cdc42-1* mutant are rescued by the overexpression of *STE20* (92).

1.5.2.3 Other Functions of Ste20p

Ste20p has been implicated in a variety of other processes, though its roles in these processes are not as well understood. Ste20p has been implicated in the control of mitotic exit with Cdc42p and Cdc24p, in a pathway which is parallel to one involving

Cdc42p, Cla4p and Lte1p, though the pathway and substrate(s) have not been identified (66, 153). Ste20p also phosphorylates histone Htb2 on serine 10 during hydrogen peroxide-induced apoptosis in a process involving the translocation of Ste20p from the cytoplasm into the nucleus (6). More recent work using the split-ubiquitin system has identified a number of proteins involved in sterol synthesis which bind to Ste20p, though the relationship between the two remains unclear (402). Ste20p is involved in myriad cellular processes, though the details of the pathways involved remain largely to be elucidated. While some substrates of Ste20p have been identified, many remain to be uncovered. By uncovering the details of Ste20p-related signaling pathways, and by determining which of them require Cdc42p-binding by Ste20p, a greater understanding will be achieved of Cdc42p signaling pathways in yeast.

1.6 Objectives and Perspective

Rho GTPases are molecular switches that act as fundamental regulators of myriad cellular processes. Despite this, many questions remain about their cellular roles and regulation. For my thesis projects, I have focused on investigating the roles and regulation of the yeast family member Rho5p and the downstream targets of Cdc42p signaling through its Ste20p effector. In Chapter II, I describe the direct regulation of Rho5p by phosphorylation and ubiquitination involving the kinase Npr1p and its antagonist Msi1p. This is the first instance of regulation by post-translational modification of a yeast Rho-type GTPase. In Chapter III, I identify a novel role for Rho5p in the activation of the cAMP-PKA pathway, possibly through a direct interaction with adenylate cyclase. In Chapter IV, I employ a proteomic approach to the identification of novel substrates of Ste20p kinase. A large-scale biochemical genomics screen for Ste20p substrates led to the creation of a bioinformatic predictor of substrates in the proteome. Finally, in Chapter V, I discuss the significance of my results in the context of Rho signaling in yeast specifically and across eukaryotes in general.

CHAPTER TWO

Rho5p is involved in mediating the osmotic stress response in *S. cerevisiae* and its activity is regulated via Msi1p and Npr1p by phosphorylation and ubiquitination.

2.1 Connecting Text

Rho family proteins act as molecular switches whose activation results in wide-ranging cellular responses. As such, their GTPase cycle is tightly regulated by an array of GEFs, GAPs, and GDIs. These regulators have been extensively characterized, and numerous examples exist of their post-translational regulation as a means of controlling Rho GTPase signaling. Less well characterized is the post-translational regulation of Rho GTPases, especially by phosphorylation or ubiquitin-mediated proteolysis. Despite the widespread occurrence of these regulatory modifications in cellular signaling pathways, no example has heretofore been identified in yeast. Chapter II describes a screen to identify the function of the largely uncharacterized Rho5p. This screen revealed that Rho5p is subject to regulation by both phosphorylation and ubiquitination, and that this regulation is mediated by a module involving the Npr1p kinase and its inhibitor Msi1p. This chapter also includes a description of a genetic interaction between *RHO5* and the osmotic stress response, suggesting a novel function for Rho5p.

2.2 Abstract

Small GTPases of the Rho family act as molecular switches, and modulating the GTP-bound state of Rho proteins is a well-characterized means of regulating their signaling activity *in vivo.* In contrast, regulation of Rho-type GTPases by post-translational modifications is poorly understood. Here we present evidence of control of the *Saccharomyces cerevisiae* Rho-type GTPase Rho5p by phosphorylation and ubiquitination. Rho5p binds to Ste50p, and the expression of the activated $RHO5^{Q91H}$ allele in a *Δste50* strain is lethal under conditions of osmotic stress. An overexpression screen identified *RGD2* and *MSI1* as high-copy suppressors of the osmotic sensitivity of this lethality. Rgd2p had been identified as a possible Rho5p-GAP based on an *in vitro* assay; this result supports its function as a regulator of Rho5p activity *in vivo*. *MSI1* has previously been identified as a suppressor of hyperactive Ras/cAMP signaling, where it antagonizes Npr1p kinase activity and promotes ubiquitination. Here we show that Msi1p also acts via Npr1p to suppress activated Rho5p signaling. Rho5p is ubiquitinated and its expression is lethal in a strain that is compromised for proteasome activity. These data identify Rho5p as a target of Msi1p/Npr1p regulation and describe a regulatory circuit involving phosphorylation and ubiquitination.

2.3 Introduction

In *Saccharomyces cerevisiae*, hyperosmotic stress conditions induce a series of signaling events resulting in rapid physiological adaptation. Primary among the signaling responses is the activation of the high-osmolarity glycerol (HOG) pathway (154, 282). Two non-redundant membrane-associated proteins, Sln1p and Sho1p, regulate the activation of this pathway. These proteins activate signaling via separate MAPKKKs, Ssk2p or Ssk22p on the Sln1p branch and Ste11p on the Sho1p branch, but converge on the MAPKK Pbs2p. Pbs2p then activates the MAPK Hog1p, with a resultant efflux of water from the cell and an increased production and accumulation of intracellular glycerol. The adaptor protein Ste50p is essential for the activation of the Sho1p-branch of this pathway. Ste50p binds to the MAPKKK Ste11p through their respective SAM (sterile-alpha motif) domains (172, 307, 444). Besides the N-terminal SAM domain, Ste50p also possesses a RA (Ras-associated) domain (323); RA-domains have been identified in proteins throughout eukaryotic evolution, where they are involved in binding members of the Ras-superfamily, including Rho family members (305). Ste50p's RA-domain binds to the C-terminus of the integral membrane protein Opy2p during HOG signaling, thereby tethering the Ste50p-Ste11p module to the membrane (443). In contrast, during pseudohyphal development, the Ste50p-RA domain has been proposed to bind the Rho-type GTPase Cdc42p, resulting in the localization of Ste50p and Ste11p to the membrane, where Ste11p can be activated by Cdc42p-associated Ste20p (413).

Rho family GTPases are involved in a variety of cellular processes. Rho proteins are known principally for their involvement in controlling cell morphology via actin cytoskeleton dynamics, but they have also been implicated in the control of cell polarity,

membrane transport dynamics, transcription factor activity, and cellular signaling (for a review, see (98)). The budding yeast genome codes for six members of the Rho family of GTPases: *CDC42* and *RHO1-5*. The essential Cdc42p protein is involved in bud site assembly, polarized growth, and cytokinesis (178). Furthermore, Cdc42p is involved in activating MAPK signaling cascades via its effector Ste20p in response to osmotic stress, mating pheromones, and nutrient deprivation (207, 246, 302, 379, 462). The other yeast Rho-family members are less well characterized: Rho1p is an essential protein involved in cell wall synthesis, cell polarity, and regulation of protein kinase C (PKC) signaling (184, 236); Rho2p function is partially redundant with Rho1p (242); Rho3p and Rho4p share an uncharacterized essential function and are involved in establishing cell polarity and exocytosis (3, 253); Rho5p has been implicated in cell-wall integrity signaling (364) and in mediating the oxidative stress response (380).

Like all GTPases, Rho family members cycle between “active” and “inactive” states by binding to GTP or GDP, respectively, and binding to effectors and inducing a cellular response according to their nucleotide-bound state. Intrinsic GTPase activity results in the hydrolysis of GTP to GDP and the conversion of the GTPase to the inactive state. The Rho GTPase is reactivated when GDP is exchanged for GTP. This switch mechanism is tightly regulated by a set of Rho-binding proteins, the Guanine-nucleotide Exchange Factors (GEFs), which catalyze the exchange of GDP for GTP and thus result in their activation (140, 192). GTPase-Activating Proteins (GAPs) perform the opposite function, stimulating the rate of intrinsic GTPase hydrolysis and catalyzing the conversion of the GTPase to its inactive, GDP-bound form (115, 142). A third class of regulators, Guanine nucleotide Dissociation Inhibitors (GDIs), inhibits GDP dissociation,

thereby maintaining Rho GTPases in the inactive state (110, 196). These Rho-associated elements provide targets for signaling networks and allow regulation of Rho-GTPase activity.

Phosphorylation and ubiquitin-mediated proteolysis are well-characterized methods of regulating signaling activity. These post-translational modifications can modulate signaling activity by determining the relative activity, localization, stability, and interactions of the target substrate. Phosphorylation constitutes a major source of cellular regulation; the protein kinase complement of the human genome is estimated to contain over 500 kinases and approximately 30% of cellular proteins are phosphorylated (69, 244). The reversible phosphorylation and dephosphorylation of a protein allows for sophisticated regulatory control involving one or many inputs and finely tuned outputs (for review, see (69)). Conversely, ubiquitin-mediated proteolysis constitutes an irreversible step in many signaling pathways, and is thus a major regulatory mechanism (for review, see (148)). Regulated destruction of components of signal transduction pathways is observed, for instance in the NFκB pathway (59). Often, phosphorylation and ubiquitination are coordinated. Many proteins regulated by ubiquitin-mediated proteolysis contain characteristic PEST sequences. For instance, cyclin-dependent kinase (CDK) phosphorylation of residues within G1 cyclin PEST sequences specifies the protein's recognition and ubiquitination, with subsequent processing by the proteasome (209, 436, 440, 449). This coordination of signaling output via phosphorylation with targeted destruction of signaling components illustrates a way in which post-translational modifications result in sophisticated modulations of cellular physiology.

Despite their prevalence in signaling networks, there have been few reports of post-translational modifications of small Rho-type GTPases. In human natural killer cells, RhoA is phosphorylated by protein kinase A (PKA), resulting in the translocation of membrane-associated RhoA towards the cytosol (208). Phosphorylated RhoA is thereby separated from its effectors and its signaling is terminated independently of GTP/GDP cycling. In fibroblasts, RhoA associates with the E3 ubiquitin ligase Smurf1 in lamellipodia and filopodia and is targeted for destruction (425). This prevents RhoA signaling during dynamic membrane movements at the leading edge of migrating cells. An atypical Rho-type GTPase, RhoBTB2, is ubiquitinated by a Cul3-based ubiquitin ligase complex, and a missense mutation which is not recognized by the ubiquitin-proteasome system has been identified in a lung cancer cell line (435). In yeast, no experimental evidence exists for the phosphorylation or ubiquitination of Rho-type GTPases.

In this study, the yeast Rho-type GTPase Rho5p is shown to interact with Ste50p to regulate the response to osmotic stress. We have identified several means of regulating its activity. First, Rgd2p's purported role as RhoGAP for Rho5p is confirmed *in vivo*. Second, Rho5p is regulated by a module involving Msi1p, phosphorylation by Npr1p, and ubiquitin-mediated proteolysis. We have identified the phosphorylation and ubiquitination of Rho5p, and have linked these post-translational modifications to its regulation *in vivo*.

2.4 Results

2.4.1 Rho5p binds to the RA-domain of Ste50p

Ste50p is involved in the activation of the high-osmolarity glycerol (HOG) MAP kinase pathway in response to hyperosmotic shock. In this pathway, Ste50p is responsible for delivering Ste11p to the plasma membrane (413, 443). We have previously shown that the C-terminal RA-domain of Ste50p is required for Ste50p function in both the pheromone-response and HOG pathways (443, 444). In an attempt to establish which small GTPase(s) could bind to the RA-domain of Ste50p, we performed an *in vitro* resin-binding assay between Ste50p and yeast Ras and Rho type small GTPases. GTPases were expressed as GST fusion proteins in yeast and were purified on glutathione Sepharose beads according to standard procedures (447). Purified yeast GTPases were then incubated with bacterially expressed and purified 8xHIS-tagged Ste50p. The glutathione Sepharose beads were washed extensively, the bound proteins were resolved by SDS-PAGE, transferred onto a nitrocellulose membrane, then revealed by Western blotting using anti-HIS-tag antibodies and appropriate secondary antibodies followed by chemiluminescence. As shown in Figure 2.1A, Ste50p selectively binds to Rho5p and Rhb1p, and weakly to Rho2p and Rho3p. Given the role of Rho GTPases in Ste50p-associated processes, we focused on the interaction between Ste50p and Rho5p.

2.4.2 Expression of $RHO5^{Q91H}$ *in* Δste50 *results in a growth defect and is osmotically lethal*

To determine the biological relevance of the physical interaction between Ste50p and Rho5p, we asked whether there is a role for Rho5p in resistance to hyperosmotic

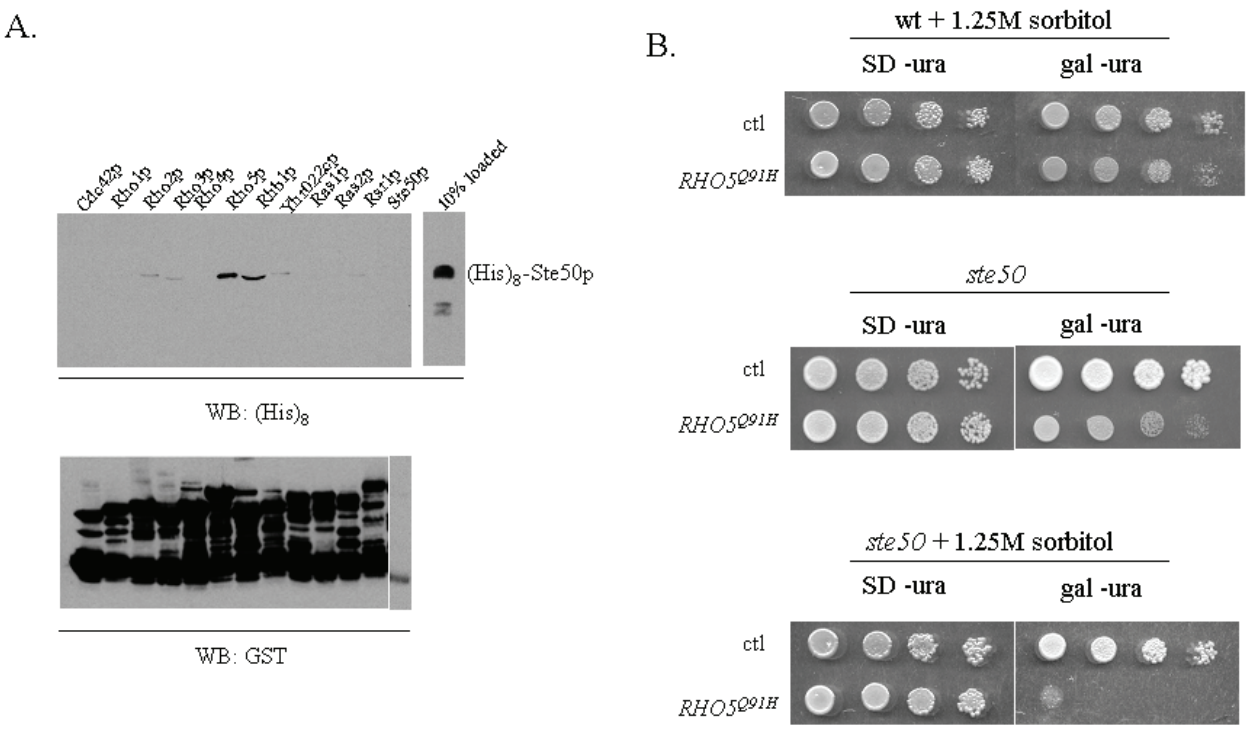

Figure 2.1. Rho5 and Ste50 interact physically and genetically. (A) GST-fusion constructs of yeast Ras-superfamily GTPases were incubated with bacterially-expressed His(8)-tagged Ste50p and were then purified with glutathione sepharose. Bound proteins were separated by SDS-PAGE and the fraction of Ste50p associated with the membrane-bound GTPases was detected with antibodies to His(8); (B) yeast cells transformed with hyperactive *RHO5*^{Q91H} were tested for their ability to grow in hyperosmotic conditions (1.25M sorbitol) in the presence (wt) and absence (*Δste50*) of endogenous Ste50p. (SD –ura) synthetic dextrose uracil drop-out media; (gal –ura) selective media with galactose as the carbon source.

stress. The *RHO5*^{Q91H} allele exchanges the glutamine at position 91 in loop 4 for histidine, creating an activated protein with reduced intrinsic GTPase activity (364). This mutant protein was overexpressed from the *GAL10* promoter in a *ste50* deletion strain (YCW1321). This strain was tested on hyperosmotic media which induced the HOG pathway and on isoosmotic media which permits normal vegetative growth. On osmotically neutral media, the transformants exhibited only a mild growth defect compared to wild-type (Figure 2.1B, middle panel). However, when grown on hyperosmotic media (1.25M sorbitol) under inducing conditions, the *Δste50 RHO5*^{Q91H} strain died (Figure 2.1B, lower panel). Expression of *RHO5*^{Q91H} in a wild-type strain generated no detectable defects in either isoosmotic (data not shown) or hyperosmotic conditions (Figure 2.1B, upper panel). Thus, it appears that Rho5p plays a role in the cellular response to hyperosmotic stress in a Ste50p-dependent manner.

2.4.3 Isolation of high-copy suppressors of RHO5^{Q91H} Δste50 *osmotic sensitivity*

To define the basis of the osmotic sensitivity of the Δ*ste50 RHO5*^{Q91H} strain, we conducted a suppressor screen using the inability to grow under hyperosmotic conditions as a condition for selection. The strain was transformed with a yeast genomic library constructed in the multicopy vector YEp213 and plated onto osmotically neutral SD –ura –leu plates and then replica plated to media selecting for osmotic resistance. Roughly 15,000 colonies were screened.

This approach identified 37 colonies that suppressed the osmotic sensitivity of the Δ*ste50 RHO5*^{Q91H} strain. Plasmids were isolated from these colonies, retested, and confirmed positives were sequenced. We isolated seven genes: *RGD2*(4 times)*, MSI1*(4

times), *PGM1*(1 time), *PGM2*(2 times), *ATX1*(1 time), *GAL80* (4 times), and *URA3* (2 inserts; 20 times). *ATX1* encodes a metallochaperone involved in iron absorption (226). *GAL80* encodes a transcriptional regulator involved in the inhibition of expression of galactose-response genes (222). It presumably suppresses the osmotic sensitivity of the strain by downregulating the expression of the $RHO5^{Q91H}$ from the *GAL10* promoter. Expression of *URA3* on the YEp213 library plasmid presumably allows rescue via the loss of the *URA3*-marked $RHO5^{Q91H}$ plasmid. Both isoforms of phosphoglucomutase (*PGM1* and *PGM2*) act as suppressors. Interestingly, phosphoglucomutase and *MSI1* have both previously been identified as suppressors of hyperactive Ras pathway mutants (161, 351), suggesting a connection between Ras signaling and Rho5p activity. Based on their potential involvement in direct regulation of Rho5p activity, *RGD2* and *MSI1* were chosen for further examination.

2.4.4 Rgd2p acts as a high-copy suppressor of activated Rho5p

RGD2 was identified as a suppressor of the synthetic osmotic sensitivity of the Δ*ste50* $RHO5^{Q91H}$ strain in four isolates (Figure 2.2). Rgd2p was predicted to be a Rho-GAP based on the identification of sequences with similarity to Rho-GAP domains (350). This same study confirmed that Rgd2p stimulated the GTPase activity of Rho5p and Cdc42p in an *in vitro* assay. The $RHO5^{Q91H}$ allele contains a mutation that is analogous to the mutation of glutamine to histidine at position 61 in human p21 Ras, which reduces intrinsic GTP hydrolysis (200, 364). The over-expression of its cognate GAP is predicted to down-regulate the activity of the activated $RHO5^{Q91H}$ allele *in vivo (117).* Rgd2p could

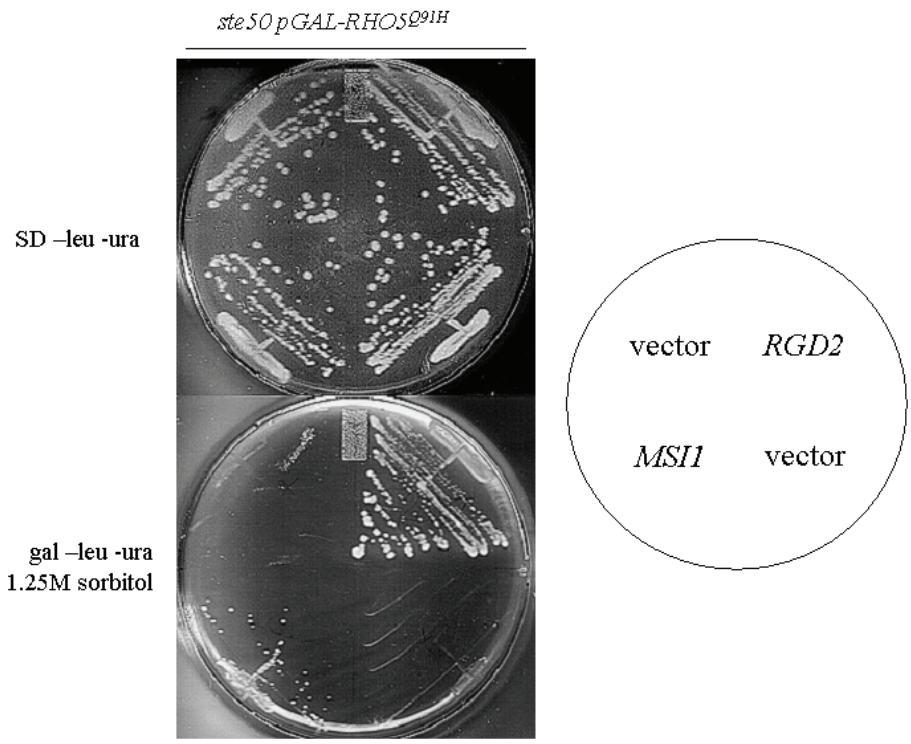

Figure 2.2. A high-copy library screen identifies *RGD2* and *MSI1* as suppressors of the osmotic sensitivity of *Δste50* p*GAL- RHO5*^{Q91H}. (SD –leu –ura) synthetic dextrose leucine and uracil drop-out media; (gal –leu –ura) leucine and uracil drop-out media with galactose as the carbon source.

suppress the synthetic osmotic sensitivity of this strain by stimulating the GTPase activity of *RHO5*^{Q91H}, and thus Rgd2p is *in vivo* likely functioning as a GAP for Rho5p.

2.4.5. MSI1 *suppression of* RHO5^{Q91H} Δste50 *growth defect may involve Npr1p*

MSI1 was identified as a suppressor in four isolates (Figure 2.2). *MSI1* (Multicopy Suppressor of Δ*ira1*) has previously been identified as a suppressor of hyperactive Ras signaling, potentially through its ability to sequester and inhibit the kinase Npr1p (179, 351), because the deletion of *NPR1* was shown to mimic the effect of *MSI1* overexpression (179). To determine if *MSI1* suppression of Δ*ste50 RHO5*^{Q91H} osmotic sensitivity occurs via the same mechanism, we generated a Δ*ste50* Δ*npr1* strain, which we then transformed with the *RHO5*^{Q91H} plasmid. As expected, the deletion of *NPR1* rescued the growth defect of the Δ*ste50 RHO5*^{Q91H} (Figure 2.3A). Microscopic analysis of cells supports the plate phenotypes (Figure 2.3B). In iso-osmotic conditions, expression of *RHO5*^{Q91H} in a variety of strain backgrounds results in mild morphological defects. A wild-type strain overexpressing *RHO5*^{Q91H} exhibits mild morphological defects, including mildly elongated buds and occasional multibudded cells, whereas *Δste50* and *Δste50 Δnpr1* cells exhibit wild-type morphologies, despite the slow growth exhibited by the *Δste50 RHO5*^{Q91H} strain (Figure 2.3A). Osmotic stress, however, results in more severe phenotypes. The wild-type strain expressing *RHO5*^{Q91H} exhibits severely elongated cells. The *Δste50 RHO5*^{Q91H} strain exhibits a variety of aberrant cell morphologies, including large, round, misshapen cells and widespread cell lysis. However, combining the *Δnpr1* and *Δste50* mutations rescues the aberrant morphology

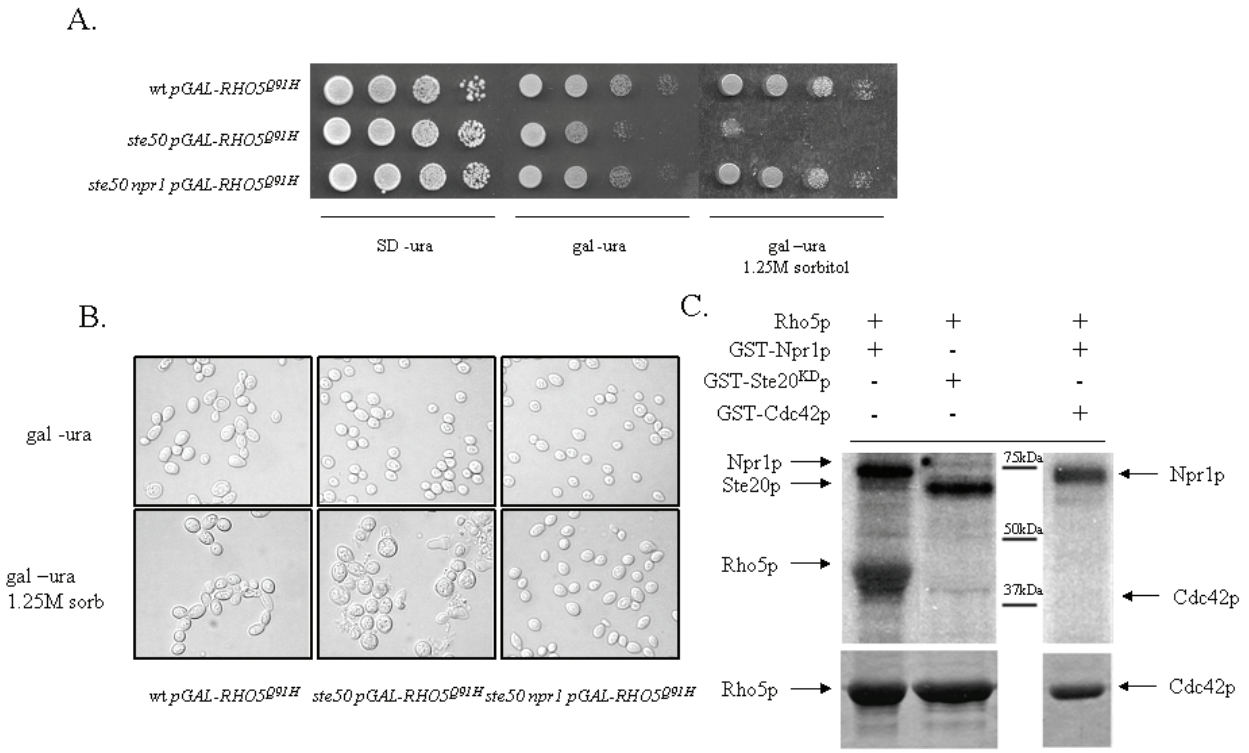

Figure 2.3. *MSI1* suppression of *Δste50 RHO5*^{Q91H} osmotic sensitivity may involve Npr1p phosphorylation. (A) Serial dilutions of relevant genotypes under osmotically neutral non-inducing (SD –ura), neutral inducing (gal –ura), and hyperosmotic inducing (gal –ura 1.25M sorbitol) conditions; (B) the morphology of yeast cells with relevant genotypes (as indicated at bottom of the figure) in neutral (gal –ura) and hyperosmotic (gal –ura 1.25M sorbitol) conditions; (C) the *in vitro* phosphorylation of Rho5p by Npr1p. Relevant proteins were resuspended in the combinations indicated in a buffered solution containing relevant divalent cofactors and [γ-^{32}P]- ATP followed by 30min incubation at 30℃. Radiolabeled proteins were separated by SDS-PAGE and subsequently visualized by autoradiography (upper panels). Loading controls of Rho5p and Cdc42p are indicated by Coomassie staining (lower panels).

Npr1p is a protein kinase whose activity influences the stability of its substrates by promoting or antagonizing ubiquitin-mediated proteolysis (360, 386). We therefore investigated if Rho5p can act as a substrate for Npr1p phosphorylation by using an *in vitro* kinase assay. As can be seen (Figure 2.3C), Rho5p is effectively labeled *in vitro* by GST-Npr1p (lane 1), but not by an unrelated kinase, Ste20p (lane 2). Specificity towards the phosphorylation of Rho5p is demonstrated by the inability of GST-Npr1p to phosphorylate the closely related Rho GTPase, Cdc42p (lane 3). Autophosphorylation of both Npr1p and Ste20p are also observed. This demonstrates that *in vitro*, GST-Rho5p is a substrate of Npr1p.

2.4.6 Rho5p is ubiquitinated and its overexpression is lethal in a strain with a compromised proteasome

Since Npr1p kinase activity has been shown to antagonize ubiquitin-mediated proteolysis, it is possible that the Msi1p/Npr1p regulatory module is moderating Rho5p signaling via this mechanism. We therefore examined whether Rho5p is a substrate for ubiquitination. The WCG4-11 strain carries the *pre1-1* mutation, and results in a temperature sensitive allele of *PRE1*, which codes for a core component of the 26S proteasome (146). This mutation is lethal in strains grown at 37℃, but viable at the semi-permissive temperature of 30℃, where it accumulates ubiquitin-protein conjugates

We then probed the blot with anti-ubiquitin antibodies (Figure 2. 4A). Interestingly, the main GST-Rho5p bands test positive for ubiquitination, suggesting that the majority of GST-Rho5p is ubiquitinated. The estimated molecular weight indicates mono-ubiquitination. Mono-ubiquitination has been identified as a common method of post-translational modification involved in diverse cellular processes, such as membrane trafficking and histone function (149). There is no evidence of the faint smear beneath the primary band, as seen when probed with α-GST antibodies, suggesting the phosphorylated form of Rho5p may correspond with mono-ubiquitination. Furthermore, there is no evidence of the low molecular weight GST-Rho5p breakdown product as seen with α-GST probes, which implies that the processing of GST-Rho5p involves the processing of the ubiquitin-conjugated region of the molecule. In the *pre1-1* strain, we observed a series of higher molecular weight species suggestive of a poly-ubiquitination "ladder". This was not observed in the wild-type strain, suggesting that the *pre1-1* strain

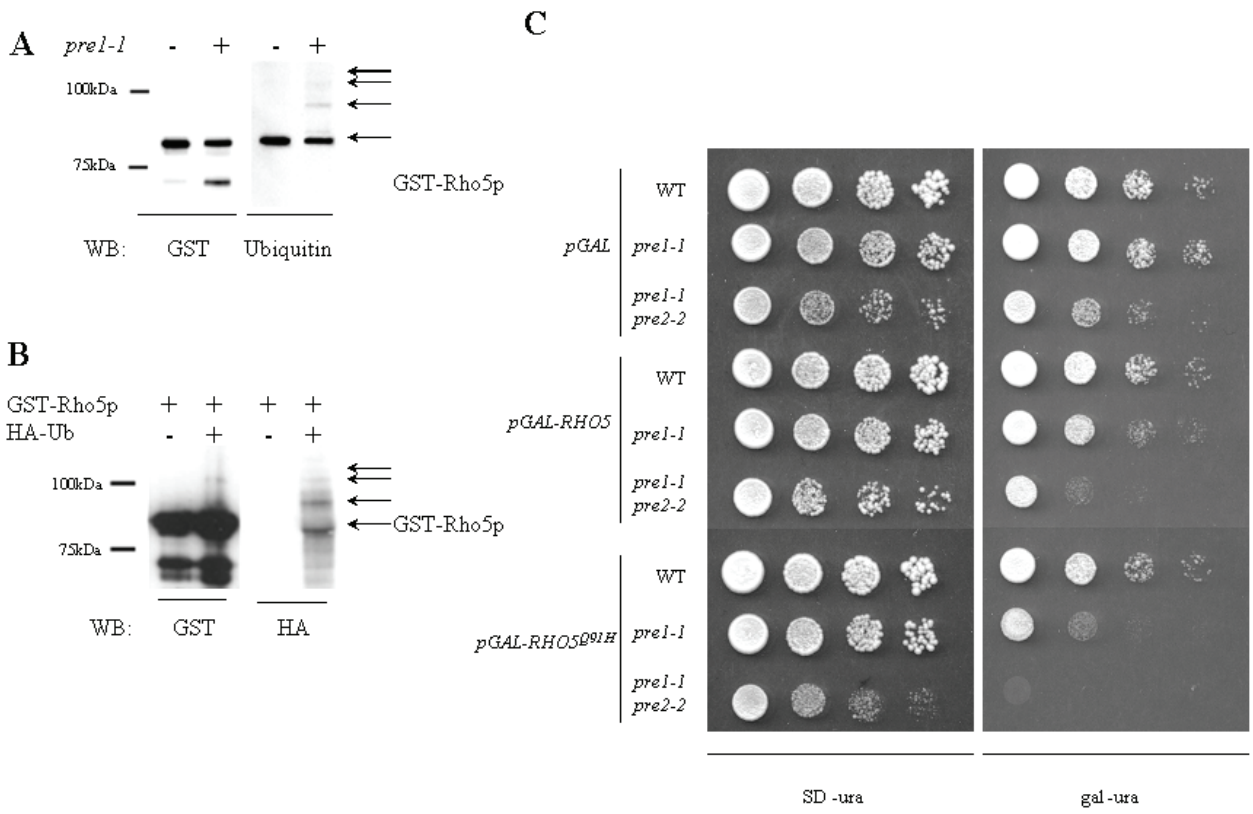

Figure 2.4. Rho5p is ubiquitinated. (A) GST-Rho5p purified from congenic wild-type (wt) and proteasome-impaired (*pre1-1*) strains was assayed for ubiquitination by probing with the anti-ubiquitin antibody. The levels of GST-Rho5p were monitored by the anti-GST antibody. (B) GST-Rho5p was expressed singly or in combination with HA-tagged ubiquitin and was subsequently purified and separated by SDS-PAGE. The presence of HA-ubiquitin was assayed by an anti-ubiquitin antibody. (C) Impaired proteasome function impairs growth of *Rho5*-expressing strains. Vectors containing wild type *RHO5* (p*GAL-RHO5*) and activated *rho5* (p*GAL-RHO5*^{Q91H}) were transformed in strains compromised for proteasome function due to one (*pre1-1*) or two (*pre1-1 pre2-2*) mutations to core components of the 26S proteasome. A congenic wild-type (wt) strain and empty vector (p*GAL*) are included as controls.

grown at semi-permissive temperature is accumulating the poly-ubiquitin-GST-Rho5p conjugates, as predicted. Thus, it seems that GST-Rho5p is mono- and poly-ubiquitinated, though the poly-ubiquitination is only detectable in the proteasome-deficient strain.

To confirm this, we co-expressed GST-Rho5p with an HA-ubiquitin fusion protein in W303 cells. HA-tagged ubiquitin is efficiently utilized by the ubiquitination machinery and has been shown to recapitulate ubiquitination patterns of wild-type ubiquitin, though the HA-ubiquitin-protein conjugates are inefficiently processed by the proteasome (95). In this case, we purified GST-Rho5p and tested for the presence of HA-ubiquitin by probing Western blots with anti-HA probes. As can be seen in Figure 2.4B, GST-Rho5p reacts strongly with anti-HA antibodies when purified from cells co-expressing HA-tagged ubiquitin. Again, we see the presence of a characteristic poly-ubiquitin ladder, as well as the presence of mono-ubiquitinated protein. We also observe lower molecular weight species when blotted for HA-ubiquitin, which we ascribe to processing by the proteasome. This would explain why these species are not observed in the proteasome-compromised *pre1-1* strain in Figure 2.4A. Thus, based on these observations, we conclude that GST-Rho5p is mono-ubiquitinated, and exhibits poly-ubiquitination in strains inhibited for proteasome activity.

In order to assay the importance of Rho5p ubiquitination *in vivo*, we over-expressed *RHO5* alleles in strains compromised for proteasome activity. The strains WCG4, WCG4-11a, and WCG4-11/22a are congenic, with the latter two containing mutations (*pre1-1* or *pre1-1 pre2-2*, respectively) in components of the 20S subunit of the 26S proteasome (145, 146). These strains are inviable at the restrictive temperature of

37°C, but are viable when grown at lower temperatures (30°C). We reasoned that the inability to regulate Rho5p activity by ubiquitin-mediated proteolysis may result in an observable growth defect. We thus expressed wild-type *RHO5* and the activated $RHO5^{Q91H}$ in the appropriate strains and incubated at 30°C for three days. Proteasome-inhibited strains over-expressing wild-type *RHO5* were noticeably impaired for growth, as compared to the wild-type strain and to a plasmid control (Figure 2.4C). The expression of the activated $RHO5^{Q91H}$ allele severely impaired growth in the *pre1-1* strain, and was lethal in the more compromised *pre1-1 pre2-2* strain (Figure 2.4C). The expression of the activated allele in the congenic wild-type strains had no noticeable defect, which suggests that an active proteasome is required to fully insulate the cells from the effects of overexpression of *RHO5* alleles. Furthermore, the increased severity of the phenotype associated with the activated allele of *RHO5* suggests that this is not a general overexpression defect, but is associated with increased Rho5p activity. Thus, we conclude that Rho5p is subject to poly-ubiquitination and subsequent 26S proteasome-mediated proteolysis, and this is an important element of its regulation.

2.5 Discussion

Our investigation of the function of *Saccharomyces cerevisiae* Rho-family member Rho5p has shown that it plays a role in the osmotic shock response, and its activity is regulated by phosphorylation and ubiquitination. Rho5p binds the RA domain of Ste50p, and an activated allele of *RHO5* exhibits a synthetic osmotic growth defect with a *Δste50* mutation. A screen for suppressors of this defect revealed two distinct means of regulating Rho5p activity; overexpression of its purported RhoGAP, Rgd2p, and a module involving phosphorylation and ubiquitin-mediated proteolysis controlled by the nuclear factor, Msi1p. We have described a yeast Rho-type GTPase regulated by phosphorylation and ubiquitination, suggesting the possibility that other Rho-type GTPases may be similarly regulated.

Rho5p binds to Ste50p, and a potential role for Rho5p in regulation of osmotic stress response is suggested by the synthetic osmotic sensitivity of a Δ*ste50 RHO5*^{Q91H} mutant. We have previously shown that the association between the RA-domain of Ste50p and the C-terminus of Opy2p results in the membrane localization of both Ste50p and its SAM-domain-associated partner Ste11p under conditions of osmotic stress (443). The binding of Rho5p to Ste50p suggests another possible interaction and role for Ste50p in coordinating the osmotic stress response. One explanation is that Rho5p may act as a direct negative regulator of HOG pathway signaling, and the combination of increased Rho5p-dependent inhibition with reduced pathway activation due to the *Δste50* mutation results in a synthetic osmotic lethality. A second explanation is that the synthetic effects are indirect, due to the interactions of distinct and separate pathways. Other yeast signaling pathways have exhibited synthetic interactions with HOG pathway mutants. For

example, increased signaling by cAMP/PKA pathway results in increased osmotic sensitivity (150, 279). Also, it has been suggested that the cell integrity and HOG pathways cooperate in the same process (154). If Rho5p is involved in moderating signaling through a separate pathway that exhibits synthetic growth defects with osmotic signaling, then the combination of increased Rho5p signaling and decreased HOG signaling may result in a synthetic osmotic lethality.

A screen for suppressors of this synthetic osmotic defect revealed different means of regulating Rho5p signaling activity. One suppressor, Rgd2p, had previously been suggested as a possible Rho5p RhoGAP based on *in vitro* studies (350). Here we confirm its ability *in vivo* to downregulate Rho5p signaling. It is likely that Rgd2p is not the only RhoGAP for Rho5p; if it were, a *Δrgd2* mutation should mimic the activated $RHO5^{Q91H}$ allele, yet a *Δste50 Δrgd2* strain does not display the synthetic osmotic sensitivity defect characteristic of *Δste50* $RHO5^{Q91H}$ (data not shown). Thus, other RhoGAPs may exist that can stimulate Rho5p GTPase hydrolysis.

The suppressor screen also identified *MSI1*, thus suggesting a regulatory mechanism involving Npr1p phosphorylation and ubiquitin-mediated proteolysis. Npr1p is a kinase that stabilizes several membrane proteins by moderating ubiquitination and subsequent proteasomal degradation (360, 386). Phosphorylation by Npr1p affects the ubiquitination and subsequent processing by the proteasome, thereby stabilizing some substrates such as Gap1p (230, 386) while destabilizing others, such as Tat2p (360). In the suppression of Ras signaling, Npr1p phosphorylation was found to act antagonistically to the ubiquitin-proteasome system (179). We found that Npr1p seems to be similarly involved in the suppression of Rho5p signaling, as a *Δnpr1* mutation

suppresses the hyperosmotic sensitivity of *Δste50 RHO5*^{Q91H}. Rho5p is an efficient *in vitro* substrate for Npr1p phosphorylation; while *in vitro* assays do not necessarily confirm a physiological role for phosphorylation *in vivo*, this result suggests that Rho5p can serve as a substrate for Npr1p. These results suggest that, as in the case of Ras signaling suppression, Msi1p, via Npr1p, suppresses the *Δste50 RHO5*^{Q91H} synthetic osmotic sensitivity via phosphorylation and subsequent ubiquitin-mediated proteolysis of Rho5^{Q91H}p.

In agreement with the model of Msi1p/Npr1p suppression of Rho5p signaling via phosphorylation and subsequent ubiquitin-mediated proteolysis, we found that Rho5p is ubiquitinated *in vivo*. A strain compromised for proteasome activity accumulated a characteristic high-molecular ladder of GST-Rho5p species which were detected with antibodies against ubiquitin. Furthermore, GST-Rho5p purified from a strain co-expressing HA-ubiquitin accumulated high-molecular weight species which were detected with antibodies against the HA tag. These results support the model that Rho5p is ubiquitinated and may be regulated by ubiquitin-mediated proteolysis. We hypothesized that overexpression of Rho5p in a strain compromised for proteasome function may generate a growth defect, and that this defect may be increased upon expression of the activated allele in the same strain. Indeed, expression of wild-type Rho5p in *pre1-1* or *pre1-1 pre2-2* temperature-sensitive strains caused mild growth defects at a semi-permissive temperature. Expression of the activated allele in these backgrounds resulted in more pronounced growth defects. In support of the model of ubiquitin-mediated proteolytic regulation of Rho5p signaling, efficient proteolysis is required to mitigate the effects of Rho5p overexpression. It remains to be determined

under what conditions Rho5p ubiquitination occurs: whether this modification is constitutive, cell-cycle regulated, or occurs in response to conditions of stress.

Rho5p phosphorylation and ubiquitination may be coordinated. This suggestion is supported by the presence of a canonical PEST sequence in Rho5p. PEST sequences are characteristic of many short-lived proteins targeted for proteasome-mediated turnover (341); Rho5p is the only yeast Rho-type GTPase to possess a PEST sequence (350). These regions are often sites of regulated phosphorylation; this provides a signal for ubiquitination, thus allowing signaling networks to efficiently regulate stability of candidate proteins. This is classically observed in the case of G1 cyclins, whose PEST-sequence phosphorylation by their cognate CDKs results in their targeted destruction (209, 436, 440, 449). This regulatory element is observed in numerous other systems in yeast, including membrane proteins (247, 349).

While the function of Rho5p in the osmotic stress response remains elusive, several lines of evidence suggest that it may play a role in mediating signaling by the Ras/cAMP pathway. Three of the suppressors of *Δste50 RHO5*^{Q91H} signaling (*MSI1*, *PGM1*, and *PGM2*) have been previously identified as suppressors of hyperactive Ras pathway mutants (161, 351). Furthermore, cells with a hyperactive Ras pathway are more sensitive to osmotic stress (150, 279). The target of Msi1p/Npr1p mediated suppression of Ras signaling was not identified in previous work (179, 351); Rho5p thus represents a potential target for Msi1p/Npr1p regulation of Ras signaling as the first yeast Rho-type GTPase to be regulated by phosphorylation and ubiquitination.

2.6 Acknowledgements

We gratefully thank Dr. W. Heinemeyer for strains, Drs. J.J. Heinisch and M. Hochstrasser for plasmids, Dr. E. Phizicky for the GST- tagged yeast genomic library and Dr. T. Chow for the YEp213 yeast genomic library. R.A. was the recipient of a NSERC graduate student fellowship. This work was supported by the NRC and grants from the NCIC and CIHR to M.W. and D.Y.T.

This work is NRC publication 49561

2.7 Materials and methods

Materials

Restriction endonucleases and DNA-modifying enzymes were obtained from New England Biolabs and GE Healthcare. The enhanced chemiluminescence (ECL) assay system, protease inhibitor tablets, and reduced glutathione were obtained from Roche. Nitrocellulose membranes were purchased from Bio-Rad. Anti-His polyclonal antibody, anti-ubiquitin mouse antibody, and horseradish peroxidase conjugated secondary antibodies were purchased from Santa Cruz Biotechnology; anti-HA polyclonal antibody was purchased from Open Biosystems; the antibody against GST was described previously (444). Glutathione Sepharose 4B beads and Prescission Protease were purchased from GE Healthcare. Radioisotopes were purchased from GE Health care and Perkin Elmer and film for autoradiography was BioMax MS from Kodak. The Quickchange Site-Directed Mutagenesis kit was purchased from Stratagene. Acid-washed glass beads (450-600um), protease inhibitors, sorbitol, and trypsin were purchased from Sigma.

Construction of plasmids

The His-*tagged STE50* construct is described previously (443). GST-*tagged NPR1* was obtained from the GST-ORF library purchased from Invitrogen. Other GST-tagged constructs were obtained from a genomic collection kindly provided by Eric M. Phizicky (University of Rochester) (250).

The Rho5p overexpression plasmids, p*GAL-RHO5* and p*GAL- RHO5*^{Q91H}, and their parent plasmid (p*GAL*) were provided by Jurgen J. Heinisch (Universitat

Osnabruck) (364). HA-tagged ubiquitin plasmid and its untagged parent were obtained from M. Hochstrasser (Yale) (152).

The *pGEX-RHO5* plasmid was constructed by amplifying the full sequence of Rho5 minus the C-terminal four amino acids of the membrane-localizing CAAX box (nt 1-984) from the vector p*GAL-RHO5* (364)) with the oligos 5'-GAGAGAATTCATGAGGTCTATTAAATGTGTGATAA-3' and 5'-GAGAGTCGACTTACTTTGACTTCTTTTTCTTCTTGTC-3', where the underlined nucleotides are *Eco*RI and *Sal*I sites, respectively. The resultant PCR product was inserted into the vector pGEX-6P-1 by cutting both with *Eco*RI and *Sal*I followed by ligation. The resultant plasmid, *pGEX-RHO5*, was confirmed by sequencing.

Yeast strains and manipulations

Yeast media, culture conditions, and manipulations were as described (346). Transformation of yeast with plasmid DNA was achieved with lithium acetate and standard protocols (346). The yeast deletion strain collection was purchased from ATCC.

Viability assays of yeast cells were performed by performing tenfold serial dilutions of mid-logarithmic phase cultures onto selective plates. Plates were incubated for three days at 30℃.

High-copy library screening for suppressors

The strain YCW1321 (*Δste50::Nat*^{R}) expressing *RHO5*^{Q91H} was transformed with a genomic library constructed in the YEp213 vector (67) Roughly 15,000 transformants were recovered on synthetic dextrose plates lacking uracil and leucine. These were first

replica plated to rich media plates and then re-replicated to selection plates containing 2% galactose as a carbon source and 1.25M sorbitol. Clones which were able to grow on the hyperosmotic media after four days were considered positives.

Preparation of GST fusion or His-tagged proteins

Expression of GST-fusion proteins in *S. cerevisiae* strains BY4741 or W303 was induced by addition of 0.4mM $CuSO_4$ for 3h with *CUP1* promoter-driven expression or with 4% galactose for 5 h with *GAL1*-driven expression. Preparation of total cell extracts and isolation of GST-fusion proteins by binding to glutathione sepharose beads was performed as described previously (444). Eluted proteins were washed with storage buffer and concentrated with Centricon 30 filters before storage at -80℃.

Purification of His-tagged Ste50p was as previously described (443).

Expression of *pGEX-RHO5* was in *E. coli* strain BL21, which was induced with 0.4mM IPTG for three hours. Fusion proteins were obtained essentially as described (383), with the modification that the proteins were eluted by cleavage of the GST tag with PreScission Protease (GE Healthcare).

Protein Kinase Assays

Kinase assays were as described (447). Approximately 1.0μg of Rho5p or GST-Cdc42p substrates in solution were resuspended in kinase buffer supplemented with 1μM ATP and 1μl [γ-^{32}P]-ATP (4,500 Ci/mmol, 10 Ci/μl) and 0.5μg GST-Npr1p or GST-Ste20p where appropriate. Reaction mixtures were incubated for 30 minutes and then

boiled for 5minutes after the addition of Laemmli buffer. Samples were separated by SDS-PAGE, dried, and visualized by autoradiography.

Photomicroscopy

Cells were grown in the conditions indicated and viewed with a microscope (Nikon Eclipse E800) equipped with Nomarski optics. Microscopic photographs were acquired with a 100x objective and a Nikon DXM1200 camera and ACT-1 version 2.10 software (Nikon).

CHAPTER THREE

The Rho5p GTPase is a regulator of cAMP-PKA signaling in budding yeast

3.1 Connecting Text

The identification of *MSI1* as a suppressor of a hyperactive *RHO5* allele suggested a link between Rho5p and the cAMP-PKA pathway. *MSI1* was initially identified in a screen for suppressors of hyperactive *RAS* mutants, and was shown to downregulate cAMP-PKA signaling via its association with Npr1p, though the target for this regulation was not identified. The $RHO5^{Q91H}$ suppressor screen also identified two other hyperactive *RAS* suppressors, *PGM1* and *PGM2*, which led to speculation that hyperactive Rho5p may activate the cAMP-PKA pathway. A study was published around that time that demonstrated that, like $RHO5^{Q91H}$ expression, an activated cAMP-PKA pathway exhibited a synthetic osmotic sensitivity with *Δste50* (306). Chapter III thus describes a novel role for Rho5p as an activator of cAMP-PKA signaling.

3.2 Abstract

Rho-family GTPases are central regulators of diverse eukaryotic signaling networks. In *Saccharomyces cerevisiae*, six Rho family members (Cdc42p and Rho1-5p) are involved in controlling key elements of polarized growth, budding, morphogenesis, cytoskeleton dynamics, and secretion. The Rho5p GTPase has been implicated in several signaling pathways, including regulation of cell wall integrity, and control of the high-osmolarity glycerol and oxidative stress responses. Rho5p is also an important regulator of cAMP-PKA signaling. Expression of a hyperactive allele of *RHO5* results in a variety of phenotypes associated with cAMP-PKA pathway activation: pseudohyphal growth in diploid strains and invasive growth in haploids, heat-shock sensitivity and defects in glycogen accumulation. There are also synthetic genetic defects upon co-expression of activated Rho5p and Ras2p, suggesting that both GTPases are involved in the coordination of cAMP-PKA signaling. Intriguingly, overexpression of activated Rho5p rescues the lethality of the Ras defective mutant *Δras1 Δras2*^{ts} at the restrictive temperature, confirming that activated Rho5 signaling is sufficient to activate cAMP-PKA signaling in the absence of Ras proteins. Finally, Rho5p can bind to the RA domain of adenylyl cyclase (Cyr1p), suggesting a possible mechanism for activation.

3.3 Introduction

In *Saccharomyces cerevisiae*, signaling by the cyclic adenosine monophosphate-Protein Kinase A (cAMP-PKA) pathway is a key regulator of cell growth, metabolism, and response to stress (for reviews see (41, 392, 400)). In response to both growth signals (particularly the presence of glucose or related fermentable sugars) and stress signals (nitrogen starvation), cAMP-PKA pathway signaling modulates concentrations of intracellular cAMP through the opposing effects of adenylyl cyclase (Cyr1p) and phosphodiesterases (Pde1p and Pde2p). Increased levels of intracellular cAMP result in the activation of protein kinase A (Tpk1-3) by release from its inhibitor, Bcy1p (404, 405). Activated PKA transduces the cAMP signal to a number of targets and maintains the cell's readiness for continued growth, inhibiting the transition to stationary phase. Activated PKA also suppresses the activity of the stress-response transcription factors Msn2p and Msn4p, which bind the stress response element (STRE) associated with a large number of stress-related genes (96, 125, 249). Activated PKA also activates the Flo8p transcription factor (294), which links cAMP/PKA signaling to morphological changes.

When diploid cells are grown under conditions of nitrogen starvation, cAMP/PKA signaling mediates a dimorphic transition to an elongated, multi-branched morphology referred to as pseudohyphal growth (118, 294, 387). Haploids do not exhibit pseudohyphal growth but exhibit the related phenotype of invasive growth, whereby yeast cells invade solid media (75, 339, 387). It has also been suggested that this signaling also links nutrient availability to the cell cycle machinery (398). For instance,

inactivating mutations of this pathway cause cells to arrest growth and enter permanently into the stationary phase (G0) (41, 254). Conversely, activated cAMP/PKA mutants fail to accumulate glycogen and trehalose and do not enter stationary phase, but continue proliferating (406). Thus, the cAMP/PKA pathway is considered a central mediator of the nutrient response and corresponding morphological and cell cycle responses.

cAMP/PKA signaling is mediated by a number of upstream components. Prominent among these are small GTPases and their regulators. Ras small G-proteins (Ras1p and Ras2p) were identified early as regulators of adenylyl cyclase (406). Like other small GTPases, Ras cycles between an active GTP-bound form and an inactive GDP-bound form. In response to external signals, the guanine nucleotide exchange factor (GEF) Cdc25p stimulates Ras activity by promoting its exchange of GDP for GTP (136). Ras proteins are negatively regulated through the activity of the GTPase-activating proteins (GAPs) Ira1p and Ira2p, which stimulate the intrinsic GTPase activity of Ras. A separate pathway also signals through adenylyl cyclase in response to extracellular glucose. A G-protein coupled receptor (GPCR), Gpr1p, is thought to act as a glucose sensor (199, 232). Gpr1p signals through a heterotrimeric G-protein alpha subunit (Gα), Gpa2p, to adenylyl cyclase. Recently, the signaling of these two branches in response to glucose levels were shown to be largely redundant (427).

Small GTPases of the Rho family are involved in regulating numerous pathways in yeast. For example, the Rho-family GTPase Cdc42p cooperates with Ras signaling in the pseudohyphal response by activating the pseudohyphal growth MAPK pathway (269). The roles of remaining yeast Rho family members (Rho1-5p) are not as well understood. Rho5p was initially characterized as a regulator of the cell integrity pathway

(364). A *rho5* deletion was shown to result in an increased signaling by the protein kinase C (PKC)-dependent MAPK pathway and an increased resistance to drugs such as caffeine and Calcofluor white, though some observations led the authors to speculate that Rho5p must serve additional functions (364). Rho5p has also been shown to be necessary for apoptotic-like cell death upon exposure to hydrogen peroxide (H_2O_2) (380). Strains expressing a constitutively active allele of *RHO5* were shown to accumulate reactive oxygen species and exhibit an increase in cell death upon H_2O_2 treatment. Recently, it has been shown that Rho5p is regulated post-translationally by phosphorylation and ubiquitination, which is novel among yeast Rho-type GTPases (12). This work demonstrated that the post-translational regulation of Rho5p is mediated by a module involving the antagonistic effects of Msi1p and Npr1p. This module was first identified in the regulation of cAMP-PKA signaling, though the target of Msi1p-Npr1p regulation of cAMP-PKA signaling was not identified (179). Interestingly, a screen for suppressors of hyperactivated Rho5p signaling resulted in the identification of several genes that had also been identified as suppressors of hyperactivated Ras/cAMP-PKA signaling (12). Given the shared suppressors between hyperactivated Rho5p and cAMP-PKA signaling and the fact that the target of Msi1p-Npr1p regulation of cAMP-PKA signaling remained unidentified, we asked whether Rho5p could participate in cAMP-PKA signaling.

Here, we report that Rho5p is a regulator of cAMP-PKA signaling. Activated alleles of Rho5p exhibit a variety of phenotypes associated with cAMP-PKA signaling, including pseudohyphal and invasive growth. Rho5p and Ras exhibit synthetic phenotypes and activated Rho5p can rescue the synthetic lethality of a *ras1 ras2* mutant.

A mechanism for Rho5p activation is suggested by the observed two-hybrid interaction between Rho5p and the Ras-associated (RA) domain of adenylyl cyclase (Cyr1p). Our data support a role for Rho5p in the regulation of cAMP-PKA signaling and identify Rho5p as the target of Msi1p-Npr1p regulation of this pathway.

3.4 Results

3.4.1 Expression of an activated allele of RHO5 *results in haploid phenotypes of an activated Ras/cAMP pathway*

To test whether Rho5p participates in regulation of cAMP-PKA pathway activity, we first examined whether expression of Rho5p would result in relevant haploid phenotypes. Haploid cells with a constitutively activated cAMP-PKA pathway exhibit a characteristic invasion of agar in nutrient-rich conditions (387). We thus examined a strain expressing constitutively activated alleles of *RHO5* (*RHO5*^{Q91H}) and *RAS2* (*RAS2*^{G19V}). These alleles are analogous to the oncogenic mutations at codons 61 and 12 of human *ras* genes H-*ras* and N-*ras,* respectively (35, 257, 364); they encode proteins that are compromised for GTPase activity, and so are rendered hyperactive. To assay invasive growth, cells were grown on solid media for one week, and then non-embedded cells removed by a stream of water (339) . As shown in Figure 3.1A, the expression of the activated *RHO5* allele resulted in a strong invasive growth phenotype. Expression of *RAS2*^{G19V} resulted in a lower degree of invasion whereas wild-type cells exhibited no invasion.

Hyperactivated cAMP-PKA pathway mutants also exhibit decreased accumulation of intracellular glycogen (50, 437). Intracellular cAMP levels due to cAMP-PKA pathway signaling are inversely correlated with glycogen levels, which are easily detected by exposing yeast cells to iodine vapours (62). We thus expressed the hyperactivated alleles *RHO5*^{Q91H} and *RAS2*^{G19V}, and assayed the resultant strains for glycogen levels. Cells were grown for five days on YPD and were subsequently exposed to iodine vapours. As seen in Figure 3.1B, wild-type cells stain darkly, indicative of

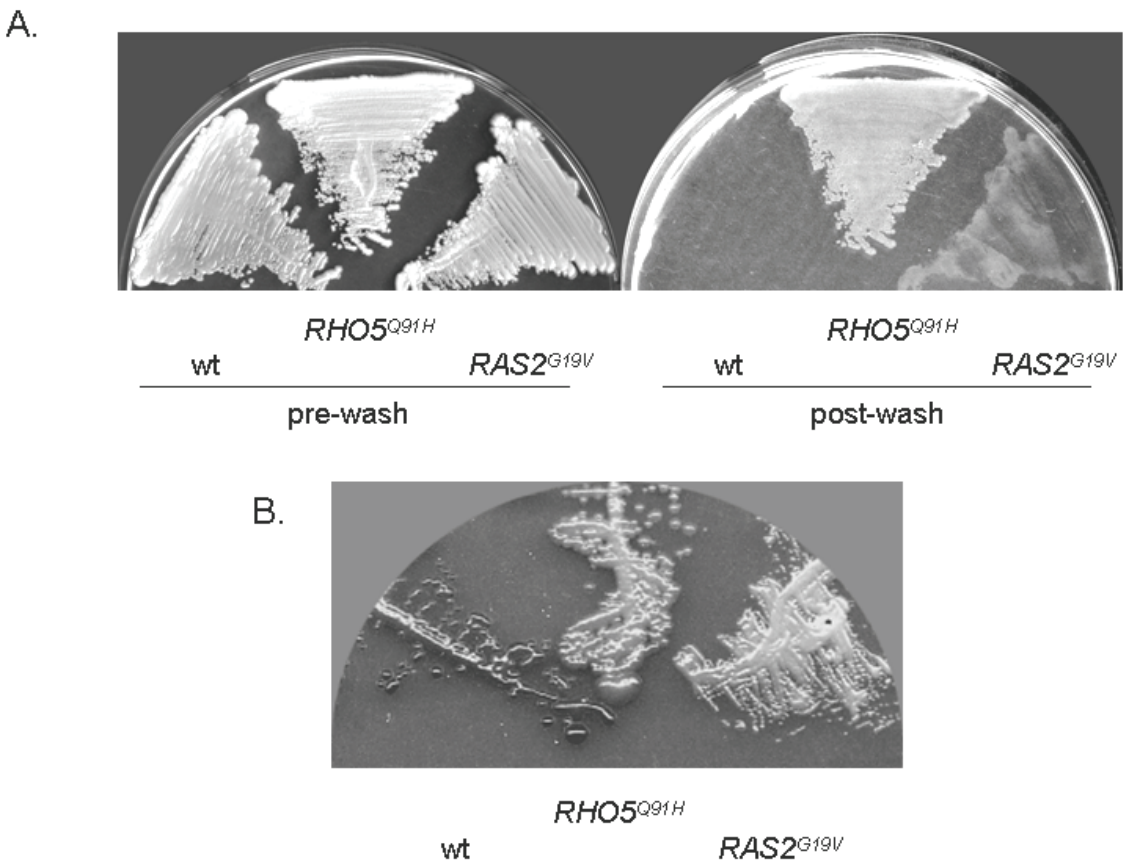

Figure 3.1. Haploid phenotypes of activated *RHO5*^{Q91H} suggest activated cAMP-PKA pathway signaling. (A) Invasive growth of haploid strains expressing plasmids. The haploid BY4741 strain expressing a control plasmid (pGAL) or the *RHO5*^{Q91H} or the *RAS2*^{G19V} plasmids were patched on YPD and were treated as described in Materials and Methods. The plate was photographed before (pre-wash) and after (post-wash) washing the cells off the plate surface with a stream of distilled water. (B) Iodine staining measures glycogen accumulation. Plasmid-expressing strains, as above, were grown on YPD for four days, then were exposed to iodine vapours for several minutes and photographed. Dark staining indicates an elevated concentration of intracellular glycogen.

increased levels of intracellular glycogen. In contrast, both *RHO5*^{Q91H} and *RAS2*^{G19V} stain much more lightly, suggesting a defect in glycogen accumulation. Thus, the expression of an activated allele of *RHO5* in haploid cells results in phenotypes associated with a hyperactive cAMP-PKA pathway.

3.4.2 Expression of an activated allele of RHO5 *results in pseudohyphal growth*

Diploid pseudohyphal growth is mediated via Ras through partially redundant signaling through the cAMP-PKA and *CDC42*/MAPK pathways (269). We thus asked whether *RHO5* expression influenced diploid pseudohyphal growth. Relevant strains were streaked onto solid media containing raffinose and galactose and with low concentrations of nitrogen to induce the formation of pseudohyphae. After thirty-six hours growth, colonies were visualized microscopically. As seen in Figure 3.2, cells expressing the plasmid control form rounded, compact colonies characteristic of normal vegetative growth. Closer examination of the colony edge revealed few pseudohyphal projections at the periphery of the colonies. Expression of *RHO5*^{Q91H}, on the other hand, results in hyperfilamentous growth associated with activated cAMP-PKA signaling. These colonies are smaller and less dense, with long thin projections of cells extending beyond the centre of the colony. An examination of the colony's edge at a higher magnification reveals elongated chains of cells with unipolar budding characteristic of pseudohyphal growth. This morphology is shared with the cells expressing the activated *RAS2*^{G19V}. Interestingly, the colonies expressing *RAS2*^{G19V} form larger and denser colonies than those expressing *RHO5*^{Q91H}. These colonies nonetheless form pseudohyphal projections at the edges of colonies, as clearly demonstrated in Figure 3.2.

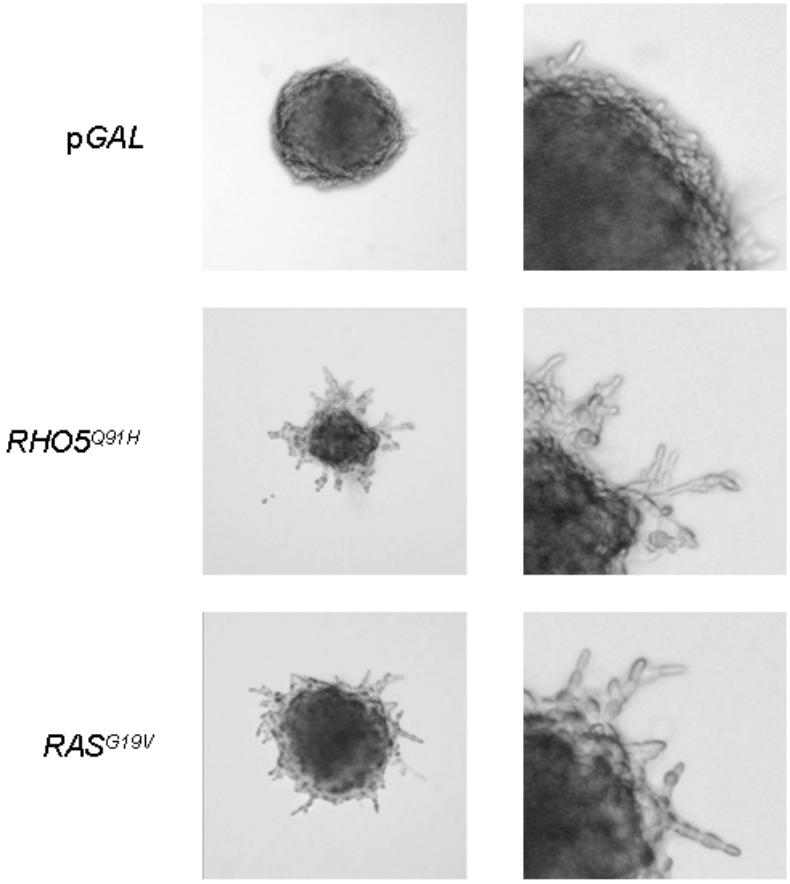

Figure 3.2. Diploid cells expressing *RHO5*^{Q91H} exhibit pseudohyphal growth on low-ammonium media. Diploid CGX31 cells expressing indicated plasmids were streaked onto low-ammonium SLARG plates and were grown for 36 hours. Representative colonies were photographed at lower magnification (400x) to illustrate the colony morphology. The edges of these colonies were then photographed at higher magnification (600x) to more clearly illustrate the pseudohyphal projections protruding beyond the body of the colony in the *RHO5*^{Q91H} - and *RAS2*^{G19V}-expressing strains.

Thus, expression of *RHO5*^{Q91H} results in increased pseudohyphal growth which is characteristic of activated cAMP-PKA signaling.

3.4.3 RHO5 *and* RAS2 *exhibit synthetic growth defects*

Given the ability of Rho5p expression to produce phenotypes associated with cAMP-PKA signaling, we asked whether co-expression of activated alleles of *RHO5* and *RAS2* would produce a synthetic growth defect. Synthetic lethal interactions are said to occur when the combination of two mutations results in compromised viability, despite the viability of each mutant alone (281). Synthetic lethal interactions often occur between genes acting in the same pathway or in different pathways if one pathway can buffer a mutation in the other (143, 410). Relevant strains were grown to mid-log phase and were then transferred in ten-fold dilutions to plates with either glucose or galactose as a carbon source. Hyperactive Ras-pathway mutants exhibit a mild growth defect when grown on galactose as the sole carbon source (161), and both *RHO5*^{Q91H} and *RAS2*^{G19V} exhibit slower growth on galactose (Figure 3.3A). Co-expression of *RAS2*^{G19V} and *RHO5*^{Q91H} results in a synthetic phenotype with the resultant cells exhibiting poor viability when grown on galactose. This synthetic growth defect suggests that Rho5p and Ras2p may be acting in the same pathway.

Given the genetic relationship between *RAS2*^{G19V} and *RHO5*^{Q91H}, we next asked whether *RHO5* was necessary for *RAS*-dependent activation of cAMP-PKA signaling. We thus expressed the *RAS2*^{G19V} allele in a *Δrho5* strain and assayed for growth on galactose. As seen in Figure 3.3A, deletion of *RHO5* did not suppress the galactose growth

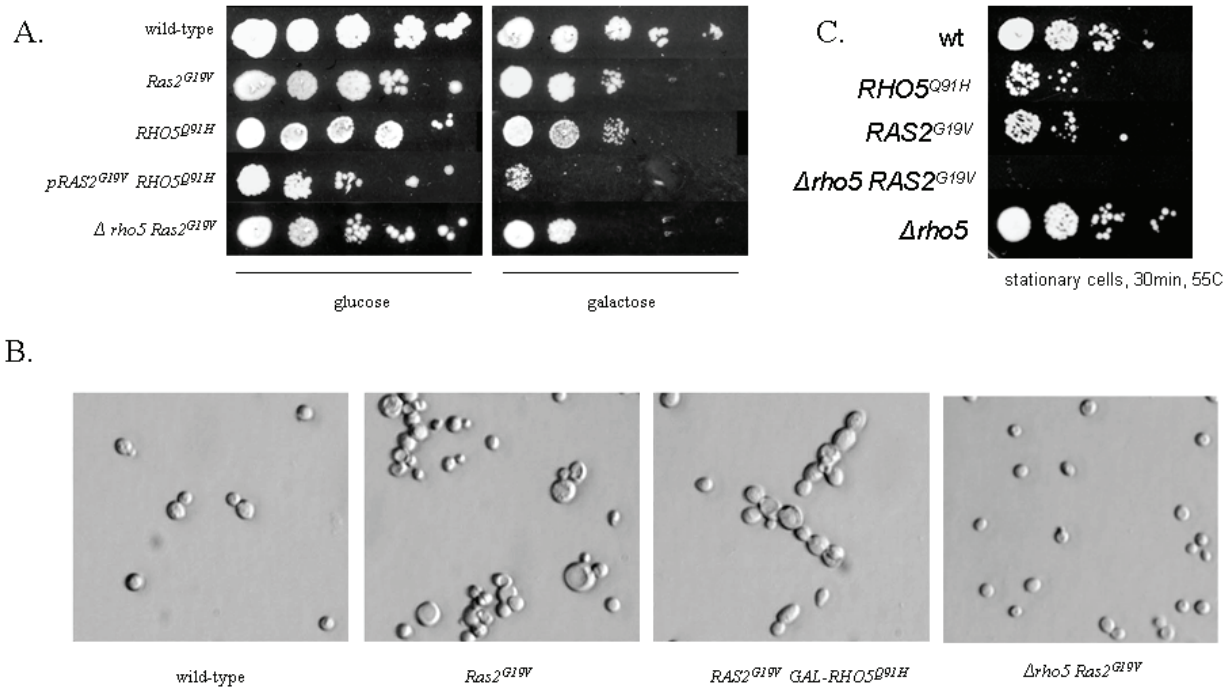

Figure 3.3. *RHO5* and *RAS2* exhibit synthetic genetic effects. (A) ten-fold serial-dilutions of wild-type or isogenic *Δrho5* strains expressing indicated plasmids were assayed for growth on media with glucose or galactose as the carbon source, as indicated; (B) the morphology of yeast cells with relevant genotypes, as indicated at the bottom of the figure; (C) indicated strains were grown to stationary phase and were subjected to a heat-shock of 55C for 30 minutes. Serial dilutions were then prepared and plated onto YPD plates and incubated for three days.

defect associated with *RAS2*^{G19V} expression. Thus, it seems that *RHO5* is able to activate cAMP-PKA signaling, but is not necessary for *RAS*-dependent activation of the pathway.

In order to better characterize the effect of Rho5p on *RAS2*^{G19V} signaling, we examined the relevant strains microscopically. Cells expressing *RAS2*^{G19V}on galactose exhibited pleiotropic morphologies, including large cells characteristic of an activated cAMP-PKA pathway (Figure 3.3B and (19, 262)). In accordance with the observations of the dilution series, expression of *RHO5*^{Q91H} in *RAS2*^{G19V}-expressing strains exacerbated the morphological defects of *RAS2*^{G19V} expression. There were fewer enlarged round cells and a preponderance of chains of cells similar to those observed when haploid cells undergo invasive growth (339). These chains of cells undergo few rounds of cell division, resulting in the poor growth observed. Next, we examined the *Δrho5 RAS2*^{G19V} cells. Interestingly, these cells exhibited none of the morphological defects observed upon *RAS2*^{G19V} expression in wild-type cells when expressed alone or in combination with *RHO5*^{Q91H}. Instead, these cells were like wild-type, though smaller. Furthermore, there were few budded cells visible, in accordance with the growth defect observed in the dilution series. Deletion of *RHO5* rescued the morphological defects linked to *RAS2*^{G19V} expression, further suggesting that Rho5p is associated with *RAS2* signaling. Thus, both by growth rate and microscopically, a synthetic effect is observed between *RHO5* and *RAS2*.

We next analyzed the genetic interaction between *RHO5* and *RAS2* by means of a heat shock assay. Upon entering stationary phase, yeast cells become resistant to stresses, including transient exposure to increased temperatures, a condition referred to as heat shock (431). As mentioned above in regards to the defect in glycogen accumulation,

activated cAMP-PKA pathway mutants exhibit a defect in the entry to stationary phase. Cells with constitutively-active cAMP-PKA pathways thus show a characteristic sensitivity to heat shock (377). We thus investigated whether expression of *RHO5*^{Q91H} would affect quiescent (G0) cells' resistance to heat shock. Relevant strains were grown for 36h until they reached saturation in either 2% glucose or 4% galactose. Cells were then transferred to a 55C water bath for 30min, and then plated as a series of ten-fold dilutions on pre-warmed plates and were allowed to recover on rich media. As seen in Figure 3.3C, cells expressing *RHO5*^{Q91H} are sensitive to heat shock, as are those with activated cAMP-PKA pathways due to the expression of *RAS2*^{G19V}. Thus, the expression of an activated allele of *RHO5* in haploid cells results in another phenotype associated with a hyperactive cAMP-PKA pathway.

Given the unexpected genetic interaction observed between *Δrho5* and activated *RAS2* in galactose-dependent growth, we also investigated the heat shock sensitivity of a *Δrho5* strain expressing *RAS2*^{G19V}. As observed in Figure 3.3B, a *Δrho5* strain exhibited a resistance to heat shock similar to wild-type cells. Intriguingly, however, an increased sensitivity to heat shock was observed when *RAS2*^{G19V} was expressed in the *Δrho5* compared to wild-type. Thus, as with growth on galactose, a genetic interaction is observed between *Δrho5* and *RAS2*^{G19V}.

3.4.4 Expression of RHO5^{Q91H} *rescues* Δras1 ras2^{ts}

S. cerevisiae expresses two Ras isoforms, Ras1p and Ras2p, which share an essential function in vegetatively growing cells (185). We reasoned that if Rho5p is capable of activating cAMP-PKA signaling independent of Ras, then expression of

Rho5p alleles may suppress the synthetic lethality of a *Δras1 ras2^{ts}* mutant. Accordingly, we expressed both wild type and activated Rho5p in the *Δras1 ras2^{ts}* strain (TTM3-4B) (308) at both semi-permissive (30C) and restrictive (37C) temperatures. At semi-permissive temperature, the *Δras1 ras2*^{ts} strain is viable when grown on glucose, but exhibits poor growth on galactose. Galactose-induced expression of the activated *RHO5*^{Q91H} allele rescued the temperature sensitivity of the *Δras1 ras2^{ts}* strain at both semi-permissive and restrictive temperature (Figure 3.4). At 37C, the *Δras1 ras2^{ts}* strain is inviable, though microcolonies are observed. These suggest the appearance of spontaneous mutants capable of suppressing the *Δras1 ras2^{ts}* lethality. We also observe some mild suppression by *RHO5^{Q91H}* under these non-inducing conditions. Expression of wild-type *RHO5* did not suppress the growth defect at either temperature. Thus, the expression of an activated allele of Rho5p is sufficient to rescue the vegetative growth defect of *Δras1 ras2^{ts}* strain, suggesting its ability to maintain pathway activation in the absence of *RAS* genes.

3.4.5 Rho5p and Cyr1p interact in a two-hybrid assay

Ras-association (RA) domains are associated with binding to small GTPases of the Ras-superfamily, including Rho family members (305). We previously identified an interaction between Rho5p and Ste50p, which contains a RA-domain (12). Adenylyl cyclase also possesses a RA-domain which binds to Ras2p *in vitro* and is required for Ras2p activation *in vivo* (189). Given the similarity between the Ras2p and Rho5p effector domains, we speculated that Rho5p may exert its effect on the Ras pathway through binding to the Cyr1p RA-domain. Employing the yeast two-hybrid

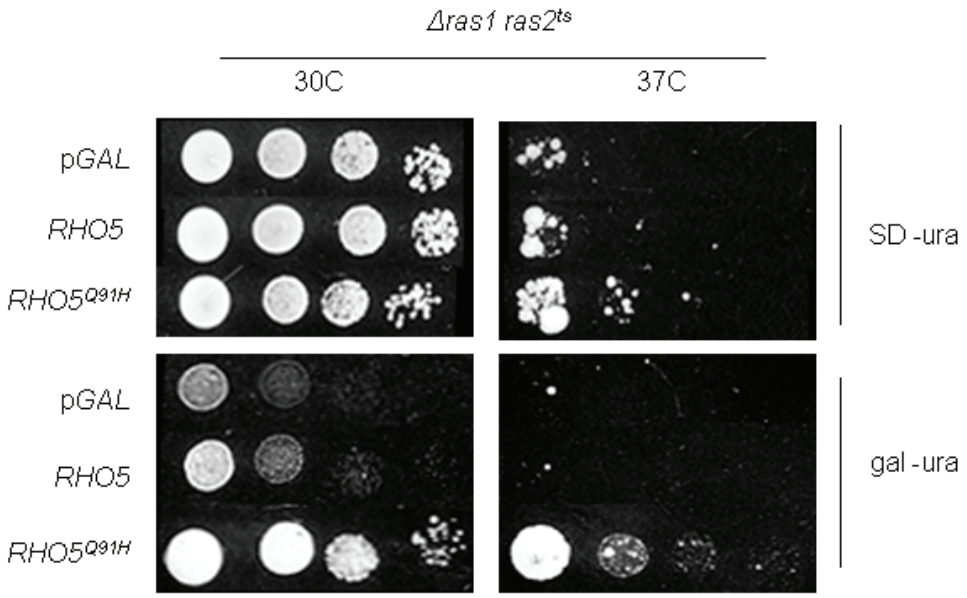

Figure 3.4. Expression of *RHO5*^{Q91H} rescues the synthetic lethality of Δ*ras1 ras2*^{ts} at the restrictive temperature. The Δ*ras1 ras2*^{ts} strain was transformed with plasmids as indicated and was assayed for growth at permissive temperature (30C) and restrictive temperature (37C) on non-inducing media (SD –ura) and on inducing media (gal –ura). (SD –ura) synthetic dextrose uracil drop-out media; (gal –ura) selective media with galactose as the carbon source.

system, we assayed a fragment of Cyr1p (a.a. 640-925) containing the RA-domain fused to the Gal4 activation domain (Gal4-Cyr1p-RA) for its ability to bind to full-length, wild-type Rho5p fused to the LexA DNA-binding domain (LexA-Rho5p). As seen in Figure 3.5, the strain co-expressing Rho5p and Cyr1p grew on the plate lacking histidine whereas strains expressing vector controls grew poorly. This suggests that Rho5p and adenylyl cyclase interact *in vivo*, and indicate a potential mechanism for Rho5p activation of cAMP-PKA pathway signaling.

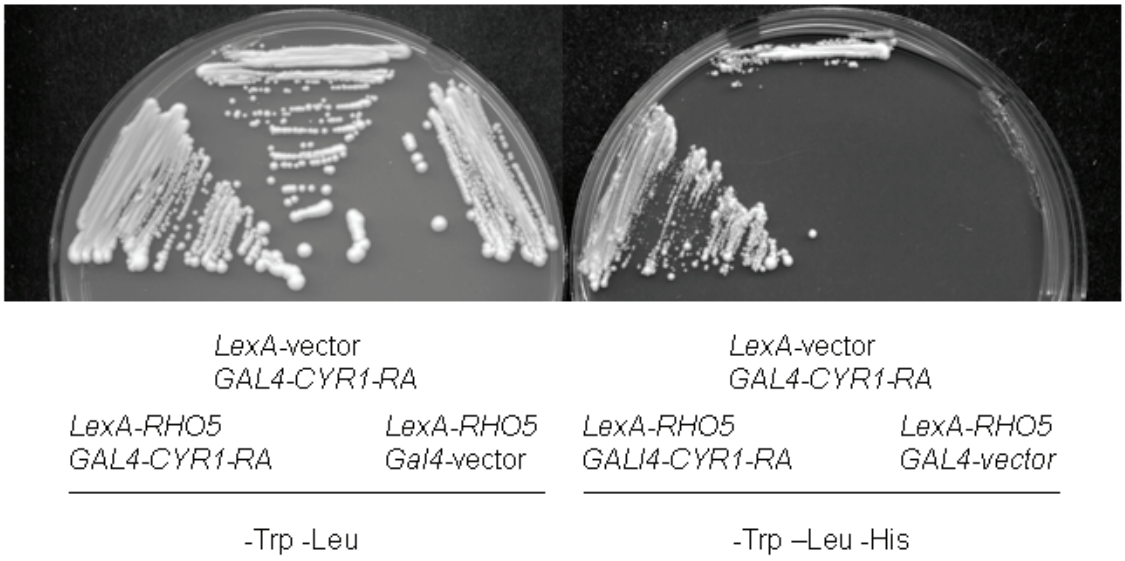

Figure 3.5. Two-hybrid analysis suggests a physical interaction between Rho5p and the RA-domain of adenylyl cyclase (Cyr1p). Co-expression of a fusion protein of the LexA DNA-binding domain and Rho5p (LexA-Rho5p) with a fusion protein of the Gal4 activation domain and the RA-domain of Cyr1p (a.a. 640-925) (Gal4-Cyr1p-RA) allows growth on media lacking histidine. Co-expression of either fusion protein with either the LexA domain or the Gal4 domain alone does not allow growth on histidine. (-Trp –Leu) synthetic dextrose tryptophan and leucine drop-out media; (-Trp –Leu –His) synthetic dextrose tryptophan, leucine, and histidine drop-out media.

3.5 Discussion

In yeast, the cAMP-PKA pathway plays a major role in the regulation of metabolism, cell growth, and stress tolerance. Extensive research has clarified the general architecture of this signaling network. Here, we describe the Rho5 GTPase as a novel regulator of cAMP-PKA signaling in budding yeast. Previously, we showed that Rho5p participates with Ste50p in the yeast response to osmotic stress (12). A screen for suppressors of the osmosensitivity of a *Δste50* strain expressing an activated allele of *RHO5* (*RHO5*^{Q91H}) identified several known suppressors of hyperactive Ras/cAMP pathway mutations: *MSI1, PGM1,* and *PGM2* (161, 351). Furthermore, the osmosensitive phenotype of the *Δste50 rho5*^{Q91H} strain is paralleled by the *Δste50 Δpde2* strain, in which the Ras/cAMP pathway is activated (306), suggesting that there may be a synthetic lethal relationship between *ste50* and cAMP-PKA pathway activation. This led us to speculate that Rho5p may serve as a regulator of cAMP-PKA signaling.

Expression of activated alleles of Rho5p results in phenotypes associated with activated cAMP-PKA signaling including haploid invasive growth, defects in glycogen storage, and diploid pseudohyphal growth. Rho5p's effect on cAMP-PKA pathway function is not redundant with Ras signaling, as *RHO5*^{Q91H} and *RAS2*^{G19V} exhibit synthetic effects in growth and morphology. Nonetheless, expression of an activated allele of Rho5p is sufficient to suppress the lethality of a *Δras1 Δras2* mutant, suggesting that it is able to partially replace Ras function in vegetative growth. Although the details of the mechanism remain to be elucidated, this study establishes a role of Rho5p in the regulation of the cAMP-PKA pathway.

Like Ras2p, Rho5p may exert its regulation of cAMP-PKA signaling via a direct interaction with adenylate cyclase (Cyr1p). Here, we have demonstrated that Rho5p interacts with the Ras-associated (RA) domain of Cyr1p in a two-hybrid assay. Cyr1p is one of two proteins in the yeast proteome with a predicted RA-domain. The other is Ste50p, which also interacts with Rho5p (12). The RA-domain of Cyr1p is required for activation of Cyr1p activity *in vivo* and has been shown to also interact with Ras2p (189). The Ras2p effector domain responsible for Cyr1p-binding is highly conserved among Ras-family GTPases, including Rho-GTPases, and the critical residues are absolutely conserved in Rho5p. Interestingly, Ras2p did not bind to Ste50p in our earlier work; indeed, interactions between Ste50p and Rho-family GTPases exhibited selectivity despite the high degree of sequence similarity among the effector loops of the GTPases. Thus, there must exist other identifying features that confer binding specificity, perhaps located in the long C-terminal loop unique to Rho5p among Rho-type GTPases, but also present in Ras1p and Ras2p.

Rho5p's role in cAMP-PKA signaling is complicated by observations involving expression of $RAS2^{G19V}$ in a *Δrho5* strain. Were Rho5p strictly acting as an activator of cAMP-PKA signaling, the deletion of *RHO5* would be expected to have no effect on the expression of activated *RAS2*. However, these cells exhibit unexpected phenotypes. On the one hand, deletion of *RHO5* reverts $RAS2^{G19V}$ -expressing cells to a wild-type-like morphology, though the growth rate remains compromised. This appears to suggest that Rho5p is required for $Ras2^{G19V}$'s effects on cell morphology. When the *Δrho5* $RAS2^{G19V}$ cells are subjected to heat shock, however, an increase in sensitivity is observed, despite the resistance of the *Δrho5* strain alone. Deletion of *RHO5* thus also exhibits synthetic

phenotypes with *RAS2*, but these phenotypes are not simply explained by Rho5's role as an activator of cAMP-PKA signaling. While GTP-bound Rho5p, as represented by the $RHO5^{Q91H}$ allele, appears to activate cAMP-PKA signaling, Rho5p bound to GDP or cycling between GTP and GDP may play roles in regulating other pathways, resulting in the phenotypes observed with the $\Delta rho5\ RAS2^{G19V}$ strain. It is possible that Rho5p's involvement in multiple pathways may contribute to these phenotypes.

This study describes a role for Rho5p in the regulation of cAMP-PKA signaling. Previous work has also described roles for Rho5p in the regulation of the PKC-cell wall integrity pathway, oxidative stress response, and adaptation to osmotic stress (12, 364, 380). Certainly, Rho-type GTPases often participate in the coordination and regulation of distinct signaling pathways (98), which may account for the diverse roles ascribed to Rho5p. Certainly, the pathways associated with Rho5p function are extensively coordinated with cross-talk observed between each (10, 203).

Indeed, Rho5p's involvement in multiple pathways makes sense of some previous observations. Epistasis experiments which attempted to identify the position of Rho5p regulation of the PKC pathway resulted in some contradictory results, especially regarding the temperature sensitivity of both *Δrho5 Δbck1* and *Δrho5 Δbem2* mutant strains and the caffeine sensitivity of a *Δrho5 Δslt2* double mutant, which are not explained by the suggested role for Rho5p as a regulator of PKC signaling (364). These observations may be explained by a *Δrho5*-dependent reduction in cAMP-PKA signaling, which itself results in sensitivity to elevated temperature and caffeine concentration (151, 203). Indeed, the authors speculate that these results may be explained by Rho5p involvement in the regulation of a parallel pathway.

The role played by Rho5p in separate pathways is complicated by the cross-talk between signaling networks. Activated cAMP-PKA pathway signaling results in several shared phenotypes with PKC pathway mutants. For instance, *Δpde2* mutants exhibit defects in cell wall maintenance and a differential expression of cell wall genes (180). Also, both Ras2p and Pkc1p have been implicated in the depolarization and repolarization of the actin cytoskeleton upon exposure to elevated temperatures, as has Rho5p (80, 151, 364). Thus, signaling through the PKC and cAMP pathways is integrated and coordinated and the definitive assignment of regulatory elements to simply one pathway or the other is difficult and possibly incorrect.

A similar ambiguity exists in Rho5p's involvement in the osmotic stress response. We have previously shown a genetic interaction between *STE50* and *RHO5* in osmotic stress sensitivity (12). The ability of Rho5p and Ste50p to physically associate *in vitro* suggests a direct role for Rho5p in HOG pathway regulation. However, activated PKA-cAMP pathway mutants also exhibit phenotypes associated with osmotic stress sensitivity as well as changes in gene expression associated with adaptation to osmostress (150, 279). Furthermore, the osmotic sensitivity of a *Δste50 Δpde2* mutant indicates a synthetic genetic interaction between the HOG and cAMP-PKA pathways (306). Thus, it remains unclear whether the osmotic sensitivity of the $RHO5^{Q91H}$ *Δste50* mutant is due to Rho5p's role in cAMP-PKA pathway activation or a separable role in Ste50p-related HOG-pathway signaling. Indeed, it is possible that Rho5p may play both roles, and thus represent a potential point of crosstalk between the two pathways.

A recent report of Rho5p involvement in oxidant-induced cell death is also consistent with a role for Rho5p in cAMP-PKA signaling. Indeed, links between cAMP-

PKA signaling and oxidative stress have been described. A decrease in cAMP signaling due to overexpression of the high-affinity cAMP phosphodiesterase *PDE2* reduces oxidative stress sensitivity (56, 127). Thus, the synthetic relationship between activated cAMP-PKA signaling and oxidative stress response may be explained by the physical association of Rho5p and Trr1p under conditions of oxidative stress (380).

This study identifies a role for Rho5p in the regulation of cAMP-PKA signaling. The physical association of Rho5p with the RA-domain of adenylyl cyclase presents a potential mechanism of this regulation. It remains to be determined how Rho5p's role in cAMP-PKA signaling is coordinated with its roles in other signaling networks. Certainly, its controlled relocalization between subcellular compartments (380) and its regulation by post-translational modifications (12), suggest that Rho5p signaling activity is under sophisticated control. Likewise, the identification of Rho5p as a cAMP-PKA signaling regulator reveals the extensive control exerted on signaling through this pathway. Given its role as a central regulator of cell growth, it is not surprising that its activity is mediated by numerous regulators with roles in other pathways. Indeed, it remains a fundamental challenge to understand and describe the regulated coordination of multiple intracellular signaling pathways in response to environmental cues in order to generate highly-tuned physiological responses.

3.6 Acknowledgements

We gratefully thank Dr. Tamara Michaeli for the TTM3-4B strain and Drs. P.K. Herman, J.J. Heinisch, and T. Kataoka for plasmids. R.A. was the recipient of a NSERC graduate student fellowship. This work was supported by the NRC and grants from the NCIC and CIHR to M.W. and D.Y.T.

3.7 Materials and Methods

Materials

The Rho5p plasmids, p*GAL-Rho5* and p*GAL- RHO5*^{Q91H}, and their parent plasmid (p*GAL*) were obtained from Jurgen J. Heinisch (Universitat Osnabruck) (364). The *RAS2*^{G19V} (pPHY453) plasmid was kindly provided by Paul K. Herman (Ohio State University) (160). Restriction endonucleases and DNA-modifying enzymes were obtained from New England Biolabs and GE Healthcare. Oligonucleotides were obtained from Invitrogen. Iodine was obtained from Sigma-Aldrich.

Yeast strains and manipulations

Yeast media, culture conditions, and manipulations were as described (346). Synthetic low-ammonium raffinose-galactose (SLARG) medium contains 50μM ammonium sulfate, 2% raffinose, 0.5% galactose, 2% thrice-washed agar, and 0.17% yeast nitrogen base minus amino acids minus ammonium sulfate, as described (118, 231). Transformation of yeast with plasmid DNA was achieved with lithium acetate and standard protocols (346). The yeast deletion strain collection was purchased from ATCC. The yeast strains used in this work were BY4741 and related strains, except where indicated.

Pseudohyphal growth was assayed by transforming the CGX31 diploid strain with relevant plasmids, followed by streaking transformants on SLARG media. The plates were incubated at 30C for thirty-six hours. Representative colonies were photographed at magnifications which allowed the survey of whole colonies (400x) or individual cells at colony peripheries (600x).

Viability assays of yeast cells were performed by performing tenfold serial dilutions of mid-logarithmic phase cultures onto selective plates. Plates were incubated for three days at 30℃.

In the case of the heat-shock assay, strains were grown for 36 hours until they had saturated the growth media, as measured spectrophotometrically. These were then placed in a 55C water bath for 30 minutes, removed, and ten-fold serial dilutions were prepared in pre-warmed (30C) rich media before being spotted onto pre-warmed (30C) YPD plates for recovery. These plates were incubated for three days and were then photographed.

Plasmid construction and two-hybrid analysis

The *GAL4-CYR1-RA* plasmid was constructed by amplifying the sequence of *CYR1* between nucleotides 1921-2775 from the vector *GST-CYR1*(640-925) (kindly provided by Dr. T Kataoka (Kobe University) (189)) with the oligos 5'-GAGAGAATTCCCAGATGGTGCCCAGAGT-3' and 5'-GAGAGTCGACTTATGGGTAGTGCATGAACTTG-3', where the underlined nucleotides are *Eco*RI and *Sal*I sites, respectively. The resultant PCR product was inserted into the vector pGAD424 by cutting both PCR product and vector with *Eco*RI and *Sal*I followed by ligation, all following standard procedures. The resultant plasmid, *GAL4-CYR1-RA*, was verified by sequencing.

The *LexA-RHO5* plasmid was constructed by amplifying the full sequence of Rho5 minus the C-terminal four amino acids of the membrane-localizing CAAX box (nt 1-984) from the vector p*GAL-RHO5* (364)) with the oligos 5'-GAGAGAATTCATGAGGTCTATTAAATGTGTGATAA-3' and 5'-

GAGAGTCGACTTACTTTGACTTCTTTTTCTTCTTGTC-3', where the underlined nucleotides are *Eco*RI and *Sal*I sites, respectively. The resultant PCR product was inserted into the vector pBTM116 by cutting both with *Eco*RI and *Sal*I followed by ligation. The resultant plasmid, *LexA-RHO5*, was confirmed by sequencing.

The L40 two-hybrid strain (155) was co-transformed with the LexA and Gal4 fusion constructs. Additionally, each fusion construct was co-transformed with the unmodified partner plasmid in order to assay for autoactivation. Transformants were selected on –Leu –Trp synthetic agar plates. These were then tested for growth on –His –Leu –Trp synthetic agar plates by incubation at 30C for three days.

Invasive Growth Assay and Iodine Staining

Invasive growth was essentially as described (339). Patches were incubated at 30C for three days and at room temperature for two days. The plate was photographed using a scanner before washing. A gentle stream of distilled water was then applied to the plate and was applied evenly across the plate in an attempt to remove all the cells from the surface. The agar was not rubbed directly. The plate was allowed to dry briefly, and was subsequently rephotographed.

A qualitative measure of glycogen content was obtained by the iodine staining method (62). Strains were patched onto YPD plates and were grown at 30C for four days. The plates were then exposed to vapours from iodine crystals (Sigma-Aldrich) for three minutes. The plates were removed from the vapours and photographed.

Photomicroscopy

Cells were grown in the conditions indicated and viewed with a microscope (Nikon Eclipse E800) equipped with Nomarski optics. Microscopic photographs were acquired using a 40x, 60x, or 100x objective, as indicated, with a Nikon DXM1200 camera and ACT-1 version 2.10 software (Nikon).

CHAPTER FOUR

A biochemical genomics screen for substrates of Ste20p kinase reveals a nuclear role for Ste20p and allows for the computational prediction of novel substrates

4.1 Connecting Text

While Rho5p represents a largely uncharacterized yeast RhoGTPase, Cdc42p has been extensively studied in yeast, and its participation in many pathways and processes has been described (177). Nonetheless, the downstream components of Cdc42p-related signaling networks remain incompletely characterized. To further understand Cdc42p function in yeast, we performed a biochemical genomics screen for substrates of the Cdc42p-effector Ste20p. Ste20p is the founding member of the PAK family of kinases, and has been implicated in Cdc42p regulation of MAPK signaling and actin cytoskeleton dynamics. The Ste20p screen allowed the creation of a computational predictor of Ste20p substrates across the yeast proteome. By combining the results of the biochemical screen with genetic and physical interaction data, we identified a number of candidate substrates for Ste20p phosphorylation *in vivo*. Many of these are involved in Cdc42p-related processes, and exhibit genetic and physical interactions with Cdc42p. These include the polarisome components Bni1p and Bud6p, whose proper function *in vivo* depends on Cdc42p, and which were shown to be true *in vitro* substrates of Ste20p, suggesting a mechanism by which Cdc42p may activate the polarisome.

4.2 Abstract

Ste20p kinase plays central roles in the activation of several yeast MAPK pathways and participates in the control of actin-based cytoskeletal dynamics. Despite its importance, few of its physiological substrates have been identified. To address this, we have performed a biochemical genomics screen for *in vitro* substrates of Ste20p involving over 500 purified yeast proteins. Fourteen substrates were phosphorylated, including several involved in ribosomal biogenesis. We confirmed the nuclear localization of Ste20p during the cell cycle in a process mediated by a bipartite nuclear localization sequence (NLS), and observed that expression of ΔNLS-Ste20p in *Δste20* cells results in a defect in ribosomal biogenesis. We then employed the data from our screen to generate a computational predictor of Ste20p substrates that we applied to the remainder of the proteome. The predictor employs multiple motifs to reflect the fact that kinase-substrate specificity is often mediated by additional binding events at sites distal to the phosphorylation site. These motifs were selected based on enrichment in the set of verified substrates, favouring those that are functionally important as estimated by conservation across yeast species. The predictor identifies 754 proteins (11.3% of the proteome) as high-probability (≥ 0.9) *in vitro* substrates of Ste20p. Statistical validation estimates threefold predictive improvement (7.9% positive predictive value vs. 2.6% background), despite the lack of a single dominant consensus sequence for Ste20p phosphorylation. Moreover, this predictive improvement is comparable to that of dominant consensus sequences that have been found for other kinases. The predicted substrate set exhibits significant overlap with regions of the genetic and physical interaction networks surrounding Ste20p, suggesting that some of the predicted substrates

represent likely Ste20p substrates *in vivo*. We validated this approach to identifying kinase substrates by confirming the *in vitro* phosphorylation of polarisome components Bni1p and Bud6p.

4.3 Introduction

Protein phosphorylation is the central post-translational modification used in signal transduction. It is essential to myriad cellular processes including growth, division, metabolism, motility, adaptation, transformation, organelle and membrane trafficking, immunity, and memory (243, 244). Underscoring the importance of protein phosphorylation, eukaryotic organisms dedicate roughly 2% of their genes to encode protein kinases, and roughly one-third of all intracellular proteins may be phosphorylated on at least one residue (69, 137, 468). Given the large number of possible substrates for each of the many protein kinases, it is not surprising that the identification of kinase-substrate relationships remains a daunting challenge.

Most of our knowledge of kinase-substrate relationships has been gained by approaches that detect *in vitro* phosphorylation. The traditional approach assayed individual candidate substrates with individual kinases. More recently, researchers have devised large-scale screens to discover larger sets of substrates. These techniques use active, purified kinases and radiolabeled ATP to perform screens against cell lysates or libraries of peptides. Researchers have assayed cellular protein populations *in vitro* by subfractionation of cell lysates before the addition of an exogenous purified kinase, or have employed an ATP analogue specific to the kinase of interest, which has been engineered to use the analogue (194, 372, 373, 416). Both these approaches reduce contamination by cellular kinases and ATPases, but require the identification of radiolabeled substrates by mass spectrometry and may miss low abundance cellular proteins. These challenges have led other researchers to dispense with cell lysates and instead screen purified peptides as potential substrates. One approach involved *in vitro*

phosphorylation of a phage display library immobilized on nitrocellulose membrane with a kinase and [γ-^{32}P]-ATP. The phage which encode substrates of the kinase are detected by autoradiography and the peptide is identified by sequencing the cDNA insert (111). Researchers have also employed protein chip technology to screen collections of proteins *in vitro* in high throughput. In one case, researchers screened 119 of 122 budding yeast kinases against a set of 17 proteins to characterize the substrate characteristics of each kinase (465). More recently, the same group printed 4,400 yeast proteins on the chip and performed *in vitro* kinase assays with 82 yeast kinases (313). This comprehensive approach identified many novel *in vitro* kinase-substrate relationships for further investigation.

In place of identifying substrates directly, some researchers have reasoned that it may be possible to identify kinase-specific consensus sequences associated with phosphorylation. Resultant studies describe directed *in vitro* approaches to assign consensus sequences to individual kinases (40, 188, 299). Consensus sequences were often difficult to assign, as many kinases exhibit a high degree of flexibility in the active site (328). Furthermore, where consensus sequences could be assigned, they often lacked sufficient information for the unambiguous identification of the physiologically relevant kinase. For instance, the consensus sequences for CDK and Src family kinases were determined, but these sequences were too similar to allow for the assignment of phosphorylation sites to one or the other family of the kinases (241). Indeed, it has been recognized that sequence features independent of the phosphorylation site are often crucial for a substrate to be phosphorylated, including binding of the substrate to the regulatory domain of the kinase, binding of kinase and substrate to the same scaffold

protein, or co-localization in the cell of kinase and substrate due to independent interactions (reviewed in (25, 101, 195, 300, 463)). Moreover, it has been recognized that kinases often bind substrates at a second site, distal to the active site, and that these docking interactions are largely responsible for kinase-substrate specificity (327).

While these *in vitro* approaches succeed in identifying which proteins are capable of serving as substrates for particular kinases, they do not ensure that such phosphorylations occur *in vivo*. In order to assay the *in vivo* relevance of kinase-substrate interactions, two main approaches have been employed. Phosphoproteomics involves the use of mass spectrometry to perform large-scale profiles of cellular phosphoproteins (reviewed in (233, 266)). A recent study identified 2285 nonredundant phosphorylation sites across 985 yeast proteins (224). It is also possible to examine the phosphoproteome in relation to specific or dynamic physiological conditions. For example, a quantitative analysis of the phosphoproteins involved in the yeast pheromone signaling pathway was performed by stable isotope labeling by amino acids in cell culture (SILAC) (128). This resulted in the quantification of 139 peptides that were differentially phosphorylated in response to mating pheromone. While approaches like these have the advantage of *in vivo* relevance, they do not permit the unambiguous identification of which kinase(s) are responsible for the observed phosphorylations, relying instead on subsequent *in vitro* testing of candidate kinases.

A second set of approaches to determining the *in vivo* relevance of phosphorylation sites involves the application of bioinformatics to biological or biochemical datasets. These large datasets have been used to train neural networks to predict phosphorylation sites on proteins without reference to individual kinases (28).

Other approaches have employed consensus site sequences for scanning candidate substrates to determine whether they are likely to be phosphorylated by a particular kinase (163, 283, 314, 448). As described above, the variability of phosphorylation sites for many kinases limits this approach, resulting in the application of machine learning techniques to increase the sophistication of consensus site scanning (162, 368, 441). The structures of kinase active sites have also been used to predict likely consensus sequences of substrates, which are then used to predict likely phosphorylations (357). While these approaches have proven to be useful for predicting potential phosphorylation sites for kinases with stringent consensus motifs, their usefulness is compromised when applied to kinases that are more promiscuous. One way of addressing this is to consider global characteristics of potential substrates. For instance, it was recently shown that modeling clusters of Cdk consensus motifs within protein sequences enriches the Cdk predictions with true substrates considerably (55). Finally, these motif-based predictions can be given *in vivo* relevance by combining them with cellular context, as in the NetworKIN methodology (227). Despite these significant advances, assigning kinase-substrate relationships remains a fundamental challenge.

The *Saccharomyces cerevisiae* Ste20p kinase is the founding member of a large family of kinases found in the genomes of all eukaryotes (for reviews see (32) and (77). Ste20p was first described as an activator of the yeast pheromone response MAPK cascade, where it served to transduce the signal from the G-protein βγ-subunits to the MEKK, Ste11p (211, 212, 322, 447). Subsequent work elaborated on the role of Ste20p as a MEKKK upstream of the three-part MAPK mating pheromone pathway, and also confirmed the same role for Ste20p in activating the MAPKs responsible for the

pseudohyphal growth and high-osmolarity glycerol (HOG) response (269, 321). Ste20p was shown to be activated and membrane-localized by binding to GTP-associated Cdc42p (13, 207, 213, 302), and to be regulated in part by phosphorylation by Cln1p- and Cln2p-Cdc28p cyclin-dependent protein kinases (284, 445). In addition to its role in the activation of MAPK cascades, Ste20p has been shown to be involved in the regulation of other physiological processes, such as actin cytoskeleton organization and polarized morphogenesis (92, 156, 217), mitotic exit (66), and hydrogen-peroxide induced apoptosis (6). Furthermore, Ste20p shares an undefined essential role with its homolog Cla4p, as *Δste20 Δcla4* mutants are not viable (76). Despite the breadth of knowledge about Ste20p's cellular roles, few Ste20p substrates have been identified. In addition to its phosphorylation of Ste11p in the activation of MAPK pathways (447), Ste20p promotes actin polarization by phosphorylating type I myosins Myo3p and Myo5p (216, 446), phosphorylates Cdc10p, albeit less efficiently than Cla4p (420), and phosphorylates the histone H2B in the apoptotic response (6). It is thus evident that physiologically relevant substrates of Ste20p remain to be identified.

To gain further insight into targets for Ste20p signaling, we performed a biochemical genomics screen of ~540 yeast proteins to identify *in vitro* targets for Ste20p phosphorylation, resulting in the identification of fourteen substrates. A novel role for Ste20p was suggested by the observation that many substrates are nuclear proteins involved in ribosomal biogenesis. We confirmed the nuclear localization of Ste20p under normal physiological conditions, and detected a defect in ribosomal production in strains expressing a *ste20* mutant defective in nuclear localization. We then used the data derived from the kinase screen to build a computational predictor of Ste20p substrates. Tests

estimate that the substrate rate (*i.e.* percentage of true substrates among predicted substrates) of the predictor is threefold the background rate from the biochemical screen. The predictor was applied to the proteome, resulting in 754 (11.3%) proteins predicted as Ste20p substrates with high probability (≥ 0.9). We provided physiological context by cross-referencing this list against regions of the genetic and physical interaction networks that surround Ste20p. Upon doing so, we selected three predicted substrates are part of the polarisome, and demonstrate that Bni1p and Bud6p are *in vitro* substrates of Ste20p kinase.

4.4 Results

4.4.1 A biochemical genomics screen identifies in vitro *substrates of Ste20p kinase*

We designed a screen for Ste20p substrates that employs a biochemical genomics approach for the identification of enzymatic activity (Figure 4.1A). We screened 539 yeast proteins, roughly ten percent of the yeast proteome, all of which are designated as essential genes (according to the Yeast Proteome Database, (298)). Individual clones expressing GST-fusion constructs under the control of the inducible *GAL1* promoter (464) of each of the designated proteins were grown under non-inducing conditions until mid-log phase. These were then combined in pools of eight, induced for three hours by the addition of galactose, and were immobilized on glutathione Sepharose beads. The combined pools of purified proteins bound to beads were incubated in each of two solutions: a solution containing the kinase domain of Ste20p, expressed and purified from *E. coli*, with necessary cofactors and γ-[P^{32}]-ATP, and a control solution lacking Ste20p kinase. After thirty minutes, the samples were boiled in sample loading buffer and separated by SDS-PAGE, with subsequent visualization of phosphorylation by autoradiography (Figure 4.1B). Where phosphorylation was observed, stepwise deconvolution confirmed the phosphorylation and identified the phosphorylated proteins.

Among the 539 proteins screened, fourteen (2.6%) were reproducible *in vitro* substrates of Ste20p (Table 4.1). In order to determine the specificity of the phosphorylation, we tested these substrates against a closely related member of the Ste20 kinase family, Cla4p. As depicted in Table 4.1, Ste20p exhibits a degree of specificity, as several substrates phosphorylated by Ste20p were not phosphorylated by Cla4p. There are, however several substrates phosphorylated by both kinases. This is expected as

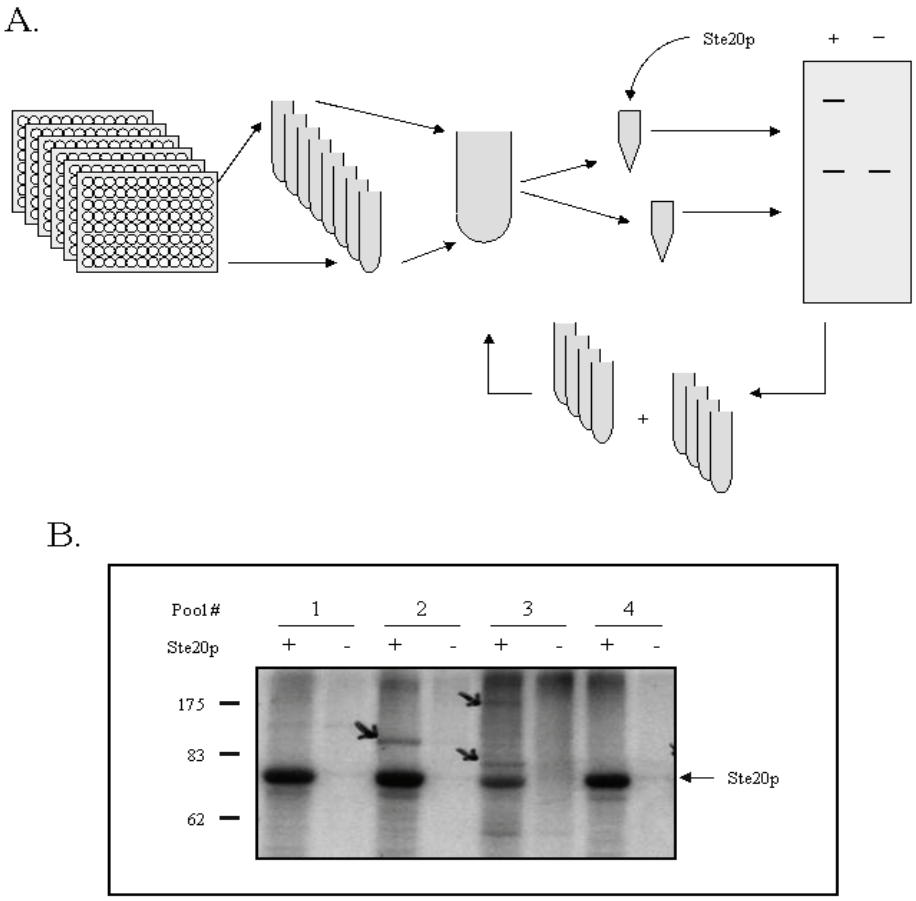

Figure 4.1. The methodology of the biochemical screen. (A) Graphical representation of the screen design. Five-hundred and forty-four yeast strains were inoculated and gown overnight, reinoculated, and combined for induction. Proteins were then purified and immobilized on glutathione-sepharose beads. Batches of purified proteins were split in two aliquots with one receiving recombinant Ste20p kinase and the other serving as a negative control (not shown). Pools containing substrates, visualized by gel electrophoresis and autoradiography were identified visually. The process was repeated with each positive pool being split into two batches for purification and assay until individual proteins were identified, (B) A representative autoradiogram revealing pools which were scored as positive for Ste2op phosphorylation (pools 2 and 3) and pools which were scored as negative (pools 1 and 4).

Table 4.1. Hits from the *in vitro* screen for Ste20p substrates.
*Indicates whether the gene product is phosphorylated by the kinase of the column.

Gene	Ste20p*	Cla4p*	Function/Process	Predictor Score
ALY2	Y	Y	Interacts with CDK Pcl7p, unknown function	1.00
BMS1	Y	N	GTPase involved in ribosome biogenesis	1.00
CDC3	Y	Y	Septin	1.00
COG4	Y	Y	Member of the Golgi complex involved in transport	0.99
PEM1	Y	N	Phosphoacetyl-glucosamine mutase	0.99
RAD53	Y	Y	DNA damage checkpoint kinase	1.00
RPT5	Y	Y	26S proteasome regulatory subunit	1.00
RSC6	Y	N	Component of the RSC chromatin remodeling complex	0.28
RSC8	Y	Y	Component of the RSC chromatin remodeling complex	0.03
SGV1	Y	Y	Nuclear cyclin-dependent kinase	1.00
SPB1	Y	Y	Methyltransferase involved in ribosome biogenesis	1.00
SPT16	Y	Y	Component of FACT complex involved in transcription elongation	0.03
UTP5	Y	Y	Member of the SSU processome involved in ribosome biogenesis	0.03
UTP7	Y	N	Member of the SSU processome involved in ribosome biogenesis	1.00

Ste20p and Cla4p are known to share an uncharacterized essential function in yeast, suggesting they may share common targets (76).

4.4.2 Ste20p localizes to the nucleus and may act in ribosomal biogenesis

A cursory examination revealed that many of the Ste20p substrates are nuclear proteins and that several were involved in ribosomal biogenesis. Mammalian PAKs are often localized to nuclei (63, 223, 453). A nuclear role for Ste20p has been identified in the apoptosis-like response of yeast to oxidative stress (6). The presence of so many nuclear substrates led us to investigate whether Ste20p has a role in the nucleus in vegetatively growing cells as well.

As seen in Figure 4.2, Ste20p is partially localized to the nucleus. First, we examined cells microscopically. Cells were grown for two days on agar plates supplemented with rich media, and were assayed by immunofluorescence for the localization of endogenous Ste20p. As seen in Figure 4.2A, a fraction of Ste20p localizes to the nucleus, as evidenced by the colocalization with the nuclear stain, DAPI. In particular, Ste20p enrichment was observed in the nuclei of quiescent, G0 cells and budding cells passing through the G1 phase of the cell cycle. We next assayed for the presence of Ste20p in the nucleus by subcellular fractionation. Cytosolic and crude nuclear fractions were separated by differential centrifugation and Ste20p content was assayed by immunoblotting (Figure 4.2B). Nup53p was used as a marker for nuclear enrichment, and confirmed an enrichment of a nuclear protein in the nuclear fraction. As seen in Figure 4.2B, a sizeable portion of the cellular Ste20p fraction is localized to

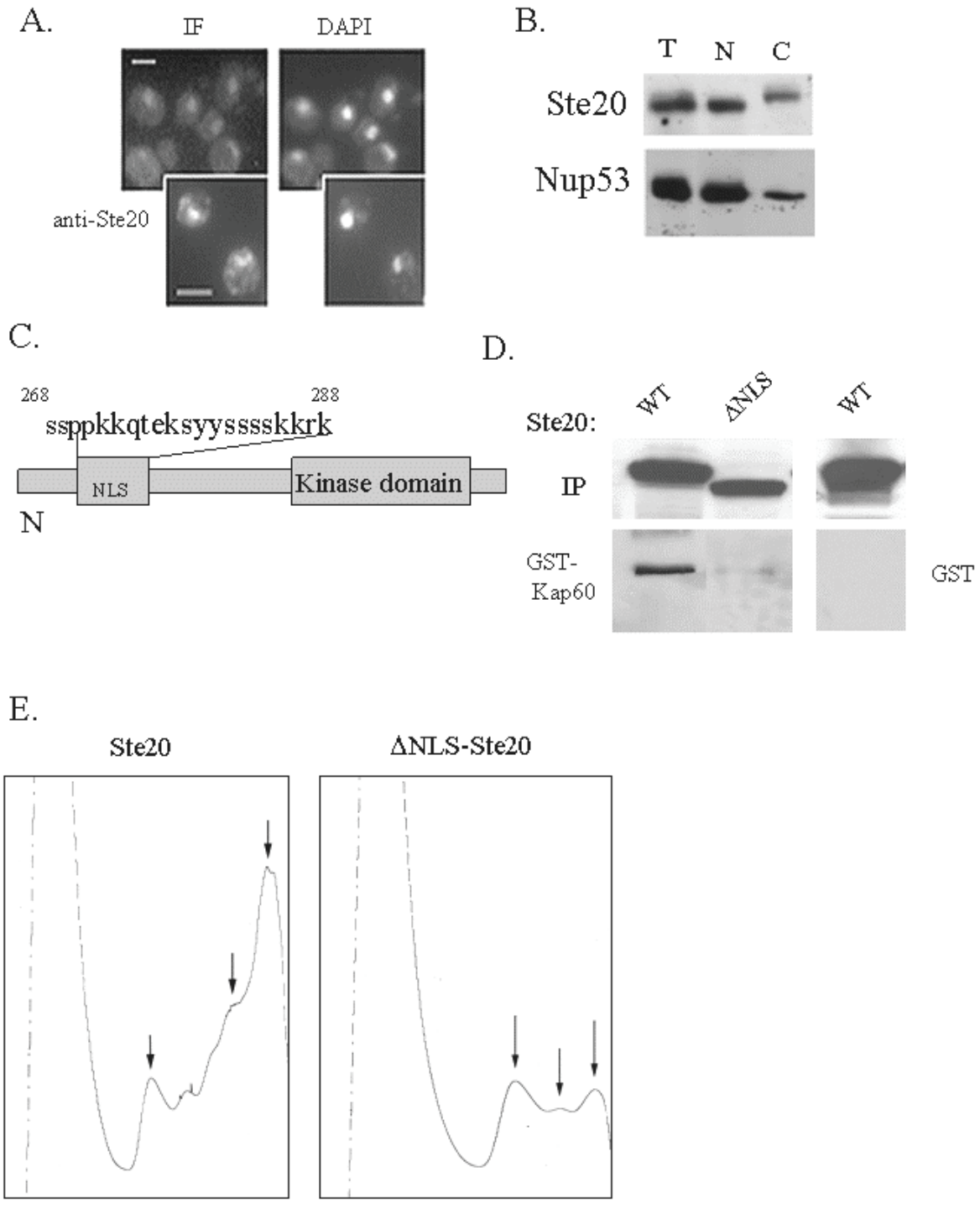
A.
IF
DAPI
anti-Ste20
B.
T
N
C
Ste20
Nup53
C.
268
288
ssppkkqteksyyssssskkrk
NLS
Kinase domain
N
D.
Ste20:
WT
ΔNLS
WT
IP
GST-
Kap60
GST
E.
Ste20
ΔNLS-Ste20

Figure 4.2. A fraction of Ste20p localizes to the nucleus where it participates in ribosomal biogenesis. (A) Ste20p is localized to the nucleus in round and small-budded cells where it colocalizes with the nuclear stain DAPI, (B) Ste20p colocalizes with the nuclear marker Nup53p in crude nuclear lysates. Cytosolic and crude nuclear fractions were prepared by differential centrifugation and separated by SDS-PAGE. Ste20p and Nup53p were detected by Western immunoblotting (C) Ste20p contains a bipartite nuclear localization sequence (NLS). Characteristic lysine-rich sequences are in bold, (D) Ste20p binds the karyopherin Kap60p. Ste20p or ΔNLS-Ste20p was immunoprecipitated from lysates expressing either GST-Kap60 or GST and the interactions were detected by Western immunoblotting, (E) Δste20 cells expressing ΔNLS-Ste20p exhibit a decrease in 60S and 80S ribosomal species. Ribosomal species from logarithmic Δste20 strains expressing either STE20 or ΔNLS-ste20 were separated on 7-to-47% sucrose gradients and detected by their UV absorbance at 254 nm. The position of the 40S, 60S, and 80S species are indicated by arrows (from left to right, respectively).

nuclei. Interestingly, when the fractions are investigated by SDS-PAGE, a mobility shift is observed between the nuclear and cytosolic species of Ste20p, suggesting a link between post-translational modification and subcellular localization.

Investigation of the primary sequence of Ste20p revealed the presence of a putative lysine-rich bipartite nuclear localization sequence (NLS) between residues 268-288 (Figure 4.2C). This type of NLS is predicted to bind the karyopherin alpha homolog Kap60/Srp1 (reviewed by (20)). We have confirmed this interaction by co-immunoprecipitation of Ste20p from GST-Kap60-expressing cell extracts (Figure 4.2D) and Ste20p lacking the NLS (Ste20ΔNLS, Δ269-289) did not bind Kap60. This suggests that nuclear import of Ste20p may be mediated by Kap60, whose binding depends on the NLS.

Since Ste20p appears to phosphorylate several proteins involved in ribosomal biogenesis, we next investigated whether *ste20* mutants exhibit any concomitant defects in the production of ribosomes. We compared ribosomal profiles of extracts from strains expressing either wild-type Ste20p or Ste20ΔNLS (Figure 4.2E). We found that the Ste20ΔNLS-expressing strain exhibited a decrease in the amount of free 60S ribosomal subunits and a drastic decrease in the levels of fully assembled 80S ribosomes. Levels of 40S subunits were unchanged between the strains. Thus, it seems that Ste20p plays a role in the processing of the large ribosomal subunit, and its exclusion from the nucleus results in a decrease in levels of large ribosomal subunits and complete ribosomes.

4.4.3 A bioinformatics approach to the identification of Ste20p substrates

Given the wealth of data generated by the biochemical genomic screen, we reasoned that it may be possible to identify characteristic sequence features enriched within the *in vitro* substrates of Ste20p relative to the screened set as a whole. The identification of such features would allow us to predict Ste20p substrates within the remainder of the yeast proteome. Several studies have previously attempted to describe consensus sequences among substrates that could be used as signature motifs to identify kinase-substrate relationships. These studies have employed techniques such as phage display and peptide microarrays (111, 464, 465). In general, unambiguous consensus sequences were difficult to assign. Instead of limiting our search to consensus sequences at phosphorylation sites, we reasoned that other sequence features may exist that, alone or in combination, act as indicators of Ste20p phosphorylation. These may include features such as docking sites distal to the site of phosphorylation or other sites of post-translational modification. To build a predictor of Ste20p substrates, we used a bioinformatics approach that searches for a small set of motifs that have high predictive accuracy. These motifs were then integrated to form a naïve Bayes predictive tool.

To identify sequence features characteristic of Ste20p substrates, we augmented our set of 14 *in vitro* substrates identified by our Ste20p screen with five substrates from the literature which had not been included in our screen (Htb2p, Myo5p, Myo3p, Ste11p, and Cdc10p (6, 420, 446, 447)) to form the positive training set. We first scanned the protein sequence of each substrate for short fragments where at least half of the residues (in each six amino-acid window) are predicted to be exposed, according to ACCpro 4.0 (60) (see Material and Methods). This procedure identifies fragments that are potentially

accessible for phosphorylation, binding, or other functionally relevant processes. We applied a pattern-matching algorithm, Teiresias (337), to these isolated fragments in order to exhaustively identify in the substrate set short motifs with at least three literal (*i.e.* non-wildcard) residues. Motifs that were present in fragments of at least five different substrates were subsequently checked against the set of proteins from our screen that were not phosphorylated by Ste20p (the negative set). Thereby, we derived a selectivity ratio for each motif and it is defined as the frequency of the motif within the substrate set divided by its frequency within the negative set; motifs with high-selectivity ratios (>1) are overrepresented in the substrate set versus the negative set.

However, to further focus our search for non-random motifs, we weighted each motif occurrence with the expectation that more heavily weighted subsequences are more functionally important. To achieve this, each occurrence was assigned a weight based on the frequency with which it is conserved among *Saccharomyces* species (Figure 4.3).

We focused on motifs that showed at least tenfold enrichment in the substrates versus the negative set (*i.e.* selectivity ratio ≥ 10). These 23 motifs (Table 4.2) were integrated into a naïve Bayes classifier such that occurrences of any of the motifs within a given amino acid sequence contribute to the belief that the sequence encodes a Ste20p substrate. Essentially, the classifier is a predictor that takes any peptide/protein sequence and returns the posterior probability that it represents a Ste20p substrate. We experimented with different parameter values and found that our final choices balance the trade-off between motifs that are overly general leading to more false positives, and motifs that are overly specific to our training data and are thus prone to false negatives (data not shown).

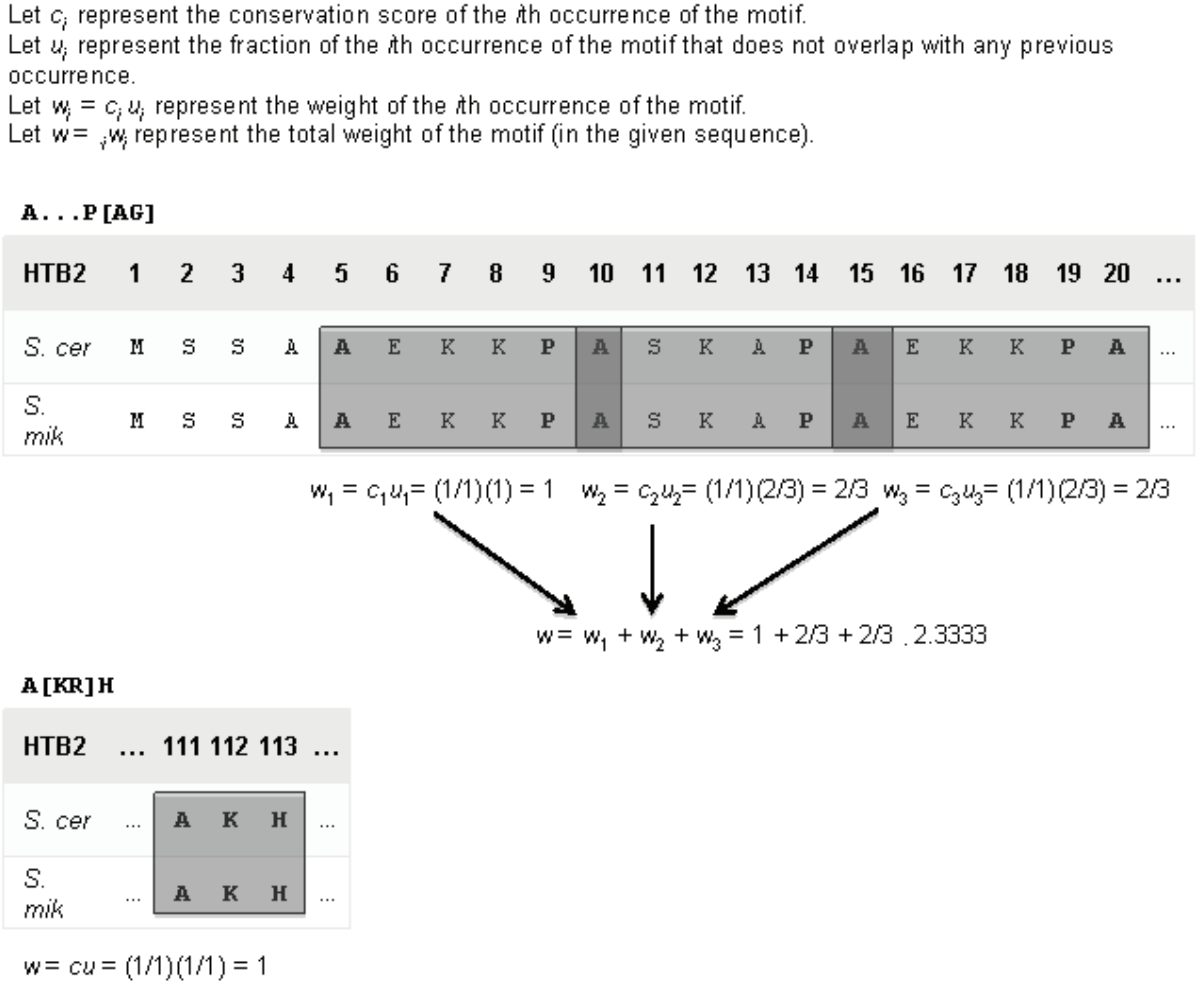

Figure 4.3. Example for computing the weight (*w*) of a motif in a given protein sequence. The sequence for Htb2p has occurrences of two different motifs used by the predictor: A…P[AG] and A[KR]H. The first motif occurs three times in the sequence, moreover, the occurrences overlap. The weight incorporates the conservation of the motif occurrences in other *Saccharomyces* species. Htb2p has an identified orthologue in only one other species in this genus: *S. mikatae*. Abbreviations: *S. cer* = *S. cerevisiae; S. mik* = *S. mikatae*.

Table 4.2. The motifs that comprise the predictor of Ste20p substrates.
*The number of proteins in the positive/negative training set that contain ≥1 occurrence of the motif.

Motif	No. Positive Proteins*	No. Negative Proteins*	Selectivity Ratio
K.H.V	6	13	17.18
KG..R	7	16	16.56
H[AG]..R	5	11	15.92
[ST]V.H	6	15	15.55
A...PG	5	16	13.64
AQR	5	23	13.58
[KR]...HR	5	13	13.04
K..HS	5	20	12.65
N.[KR]..H	10	24	12.29
P.G.Q	5	14	11.86
Q.DP	5	21	11.86
A..PP	6	17	11.85
E.C..[KR]	5	11	11.22
PG...S	7	24	11.05
G.NF	5	14	11.02
PT..Y	6	16	10.86
I..T.H	5	12	10.84
R.S..H	5	18	10.76
A[KR]H	5	16	10.67
G.K.P	5	15	10.32
A...P[AG]	7	35	10.29
K[AG]..R	8	38	10.27
RDA	5	22	10.23

The accuracy of the predictor was tested *in silico* via a modified version of leave-one-out cross-validation (see Materials and Methods). The tests suggest a false positive rate of 11% and a false negative rate of 74% if a protein is predicted as a substrate when its posterior probability (*i.e.* prediction score) is ≥ 0.9 (Supplementary Figure 4.1). Moreover, the frequency with which we expect to identify true substrates among a set of predictions is 8% (*i.e.* the positive predictive value). This is roughly a threefold enrichment over the frequency we observed from experimentally screening the initial selection of proteins in this study, and a fivefold enrichment over the frequency observed for an *in vitro* screen from a previous study (464).

4.4.4 Application of the predictor to the yeast proteome

Using the optimal parameter settings described above, we applied the predictor to the yeast proteome (6696 proteins considered) so that every yeast protein was ascribed a posterior probability that it is an *in vitro* substrate of Ste20p (Supplementary Table 4.1s). In total, 474 proteins (7.1% of proteome) were assigned a probability greater than 0.99, 753 proteins (11.3%) greater than 0.9, and 5050 proteins (75.4%) below 0.05 (Supplementary Table 4.1s). Amongst the substrates identified in the initial screen, ten were scored with probabilities above 0.99 and three were scored below 0.05 (Table 4.1). Amongst the published substrates of Ste20, Ste11, Myo3, and Myo5 were all assigned a probability of 1.0, Cdc10 was assigned a probability of 0.86, and the histone Htb2 was assigned a score of 0.035, perhaps reflecting the distinctive biochemical nature of histones.

4.4.5 Annotations of predicted substrates are consistent with characteristics of Ste20p

We analyzed the predicted Ste20p substrates by using the annotations made available by the Gene Ontology (GO) Consortium (14). GO slims are broad ontologies which allow the assignment of yeast proteins into general categories of cellular components, biological processes, and molecular functions. The significantly overrepresented categories (adjusted $p \leq 0.05$) amongst the predicted substrates (score ≥ 0.9) are shown in Figure 4.4 and Supplementary Tables 4.2s-4.4s. Encouragingly, the cellular components and biological processes that are overrepresented confirm the established role of Ste20p in budding and morphogenesis at sites of polarized growth, including the bud tip. The overrepresentation of cell cortex, plasma membrane, and cytoskeleton categories is also not surprising given what is known about Ste20p biology. Furthermore, the role of Ste20p as a component of several signaling cascades is reflected in the overrepresentation of predicted substrates that are annotated with the molecular function of protein kinase activity. Thus, analysis of the predicted substrate set with GO annotations supports the biological relevance of our predictor.

GO analysis may also reveal novel aspects of Ste20p biology. For instance, nuclear substrates are overrepresented in the predicted substrate set, confirming our observation based on the substrates identified in the initial screen and suggesting that Ste20p may play additional unidentified roles in the nucleus. The analysis also points to a potential role for Ste20p in vesicle-mediated transport; a possible role for Ste20p in this process is supported by the observation that the human Ste20p-related kinase Pak1p plays a role in regulating vesicular-based transport in human fibroblasts (83). Likewise, a role for Ste20p in carbohydrate metabolic processes is supported by the observation that

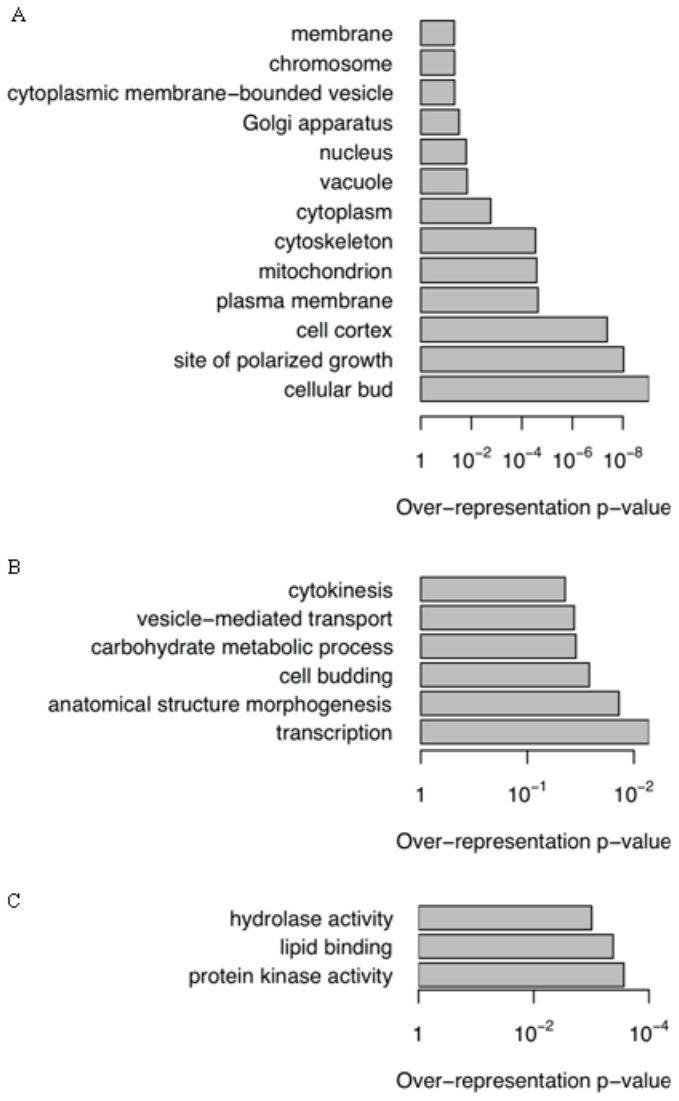

Figure 4.4. Significantly over-represented (adjusted $p \leq 0.05$) GO slim (A) cellular components, (B) biological processes and (C) molecular functions among the predicted Ste20p substrates (score ≥ 0.9).

Pak1p phosphorylates and activates phosphoglucomutase-1 (PGM) (132). Thus, GO analysis of the predicted substrate set points to potential roles for Ste20p in biological processes.

4.4.6 Genetic and physical networks suggest in vivo *relevance of predicted substrates*

Another means of evaluating the *in vivo* relevance of the predicted Ste20p substrates is to determine commonalities between our dataset and datasets that connect genes/proteins to Ste20p in different ways. To this end, we reasoned that, since a kinase and a given substrate act in the same pathways, genes that genetically interact with *STE20* may also interact with *in vivo* substrates of Ste20p. The interaction neighbourhood of every gene in the genetic network was tested for significant overlap with the set of predicted Ste20p substrates (Figure 4.5A). Indeed, the *STE20* genetic interactor neighbourhoods (GINs) tend to overlap more significantly (*i.e.* they have lower p-values) with the predicted substrates compared to the neighbourhoods of the other genes in the network (Figure 4.5B). *STE20* has 42 published genetic interactors and five of the corresponding neighbourhoods were found to have significant overlap with the predicted substrates (adjusted $p \leq 0.05$, (Supplementary Table 4.5s). However, the genetic interaction network has not been completely delineated to date. We investigated whether the significant overlaps were due to *STE20* interactors being examined more frequently than other genes in screens, but determined that *STE20* GINs tend to have more significant overlap even after correcting for frequent study (see Methods). Thus, the regions surrounding *STE20* in the genetic network suggest that the list of predicted *in vitro* Ste20p substrates exhibits physiological relevance.

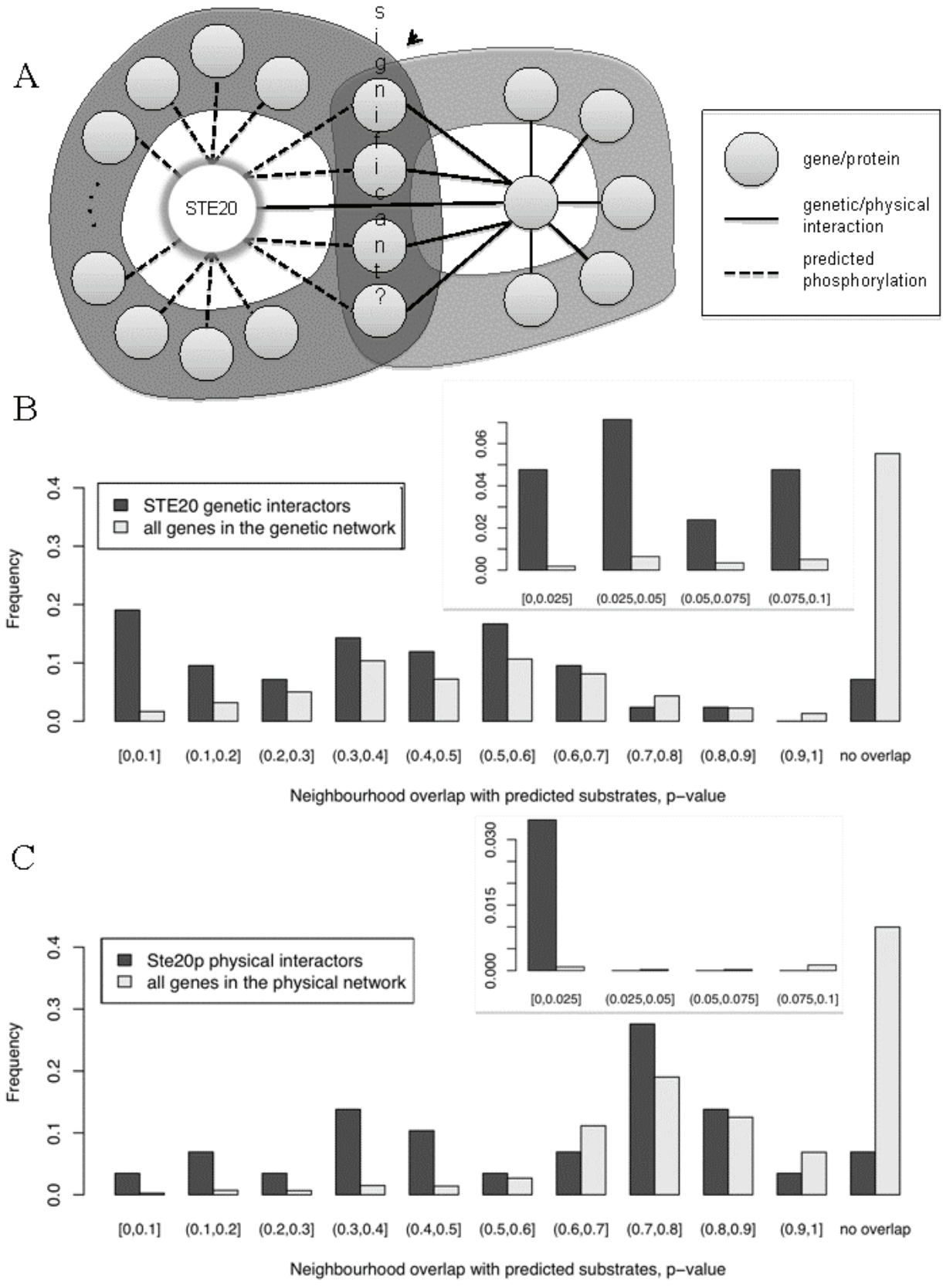
A
STE20
significant?
gene/protein
genetic/physical interaction
predicted phosphorylation
B
STE20 genetic interactors
all genes in the genetic network
Frequency
0.0
0.1
0.2
0.3
0.4
0.00
0.02
0.04
0.06
[0,0.025]
(0.025,0.05]
(0.05,0.075]
(0.075,0.1]
[0,0.1]
(0.1,0.2]
(0.2,0.3]
(0.3,0.4]
(0.4,0.5]
(0.5,0.6]
(0.6,0.7]
(0.7,0.8]
(0.8,0.9]
(0.9,1]
no overlap
Neighbourhood overlap with predicted substrates, p−value
C
Ste20p physical interactors
all genes in the physical network
Frequency
0.0
0.1
0.2
0.3
0.4
0.000
0.015
0.030
[0,0.025]
(0.025,0.05]
(0.05,0.075]
(0.075,0.1]
[0,0.1]
(0.1,0.2]
(0.2,0.3]
(0.3,0.4]
(0.4,0.5]
(0.5,0.6]
(0.6,0.7]
(0.7,0.8]
(0.8,0.9]
(0.9,1]
no overlap
Neighbourhood overlap with predicted substrates, p−value

Figure 4.5. Inferring the biological relevance of Ste20p predicted substrates (score ≥ 0.9) via neighbourhood analysis. (A) Depiction of the test for the statistical significance of the overlap between the predicted substrates and the interaction neighbourhood of a given gene/protein. Here the given gene is known to interact with STE20. (B) Neighbourhood analysis in the context of the genetic network. Comparing the distributions of adjusted p-values shows that the predicted substrates tend to overlap more significantly with the neighbourhoods of STE20 interactors versus those of all genes in the network. (C) Neighbourhood analysis in the context of the physical network. A similar trend is apparent here however the p-values are less extreme for Ste20p physical interactors. Insets for (B) and (C) depict the distributions at higher resolution where $p \leq 0.1$.

We next asked whether an analogous approach based on physical interactions would provide additional support for the predicted substrates. In this case, we reasoned that proteins which form physical interactions with Ste20p binding partners (*i.e.* proteins in the neighbourhoods of Ste20p physical interactors) are more likely to be accessible as substrates for Ste20p given that kinases and their cognate substrates often assemble in macromolecular complexes. The *Saccharomyces* Genome Database (371) contains 96 published protein-protein interactions for Ste20p, though to avoid redundancy, physical interactions identified in a recent high-throughput study were excluded ((313), see Discussion). The remaining 29 physical interactions include, for example, the scaffold proteins for Ste20p-related signaling complexes such as Bem1p and Cdc24p.

Although only one of the 29 Ste20p physical interactor neighbourhoods (PINs) that significantly overlaps the set of predicted substrates (adjusted $p \leq 0.05$, Supplementary Table 4.6s), the 29 PINs tend to have lower overlap p-values than the neighbourhoods of the other proteins in the network (Figure 4.5C). In fact, as in the context of genetic interactions, the neighbourhoods of the majority of proteins do not overlap with the set of predicted substrates at all, whereas 27 out of the 29 Ste20p PINs do.

The significance of the overlap observed between the predicted substrate set and the physical network surrounding Ste20p also suggests a biological relevance to the predictions. By utilizing the data derived from the different approaches, it should be possible to generate more directed models for experimental validation.

We also employed GIN and PIN analysis to investigate the known false negatives and false positives generated by the predictor. First, five of the 19 known Ste20p

Table 4.3. The number of *STE20* Genetic Interactor Neighbourhoods (GINs) and Ste20p Physical Interactor Neighbourhoods (PINs) in which each Ste20p substrate appears. See the blue part of Figure 4.5A for an illustration of an interactor neighbourhood.

Gene	Predictor Score	No. Overlapping *STE20* GINs (out of 42)	No. Overlapping Ste20p PINs (out of 29)
ALY2	1.00	1	1
BMS1	1.00	0	0
CDC3	1.00	0	1
MYO3	1.00	1	1
MYO5	1.00	2	1
RAD53	1.00	3	1
RPT5	1.00	0	0
SGV1	1.00	1	1
SPB1	1.00	0	0
STE11	1.00	12	1
UTP7	1.00	0	1
COG4	0.99	0	0
PCM1	0.99	1	0
CDC10	0.86	2	0
RSC6	0.28	3	0
HTB2	0.03	0	1
RSC8	0.03	1	0
SPT16	0.03	0	3
UTP5	0.03	0	0

substrates from our initial screen or the literature were poorly scored ($p < 0.3$) by the predictor (Table 4.3). Four of these are members of the GINs or PINs of Ste20, suggesting that they retain *in vivo* relevance yet they do not possess the sequence features used by the predictor to characterize Ste20p substrates. These thus represent likely *in vivo* false negatives of the predictor. Second, among the set of proteins which were not phosphorylated in our screen 34 proteins were predicted as Ste20p substrates (Table 4.4). We found that these proteins tend to be found in significantly more of *STE20* GINs compared to all the proteins from the negative set ($p = 3.17\times10^{-5}$, Wilcoxon rank sum test). These proteins therefore represent likely false negatives of the *in vitro* screen yet correctly predicted substrates. Thus, neighbourhood analysis allows for the re-evaluation of the biochemical data and a deeper evaluation of the predicted substrates.

In order to better characterize the physiological relevance of the neighbourhood approach, we clustered the genetic and physical interactors of Ste20 with respect to the predicted substrates in their neighbourhoods (Figures 4.6 and 4.7, respectively). In other words, *STE20* interactors with many common predicted substrates in their respective neighbourhoods are more likely to be clustered together than those with few. Figure 4.6 shows the clustering of the genetic interactors of *STE20*. One large cluster ($p = 0.06$, Figure 4.6B) includes genes that code for proteins involved in cell-cycle progression and polarized growth such as *CDC28*, *SWE1, CLA4*, *CDC42*, and *RAS2*. Moreover, most of the genes in this cluster interact with a set of predicted substrates that also include polarity- and cell-cycle-associated genes such as *CDC5*, *LTE1*, *AXL2*, and *MSB1* (Figure 4.6A, see Supplementary Figure 4.2 for the significance of the predicted substrate

Table 4.4. STE20 genetic neighbourhood analysis suggests that several predicted substrates (score ≥ 0.9) from the negative set may represent false negatives. There are 34 negative set proteins that are predicted as substrates and some are present in the neighbourhoods of STE20 genetic interactors (*i.e.* a table entry is 1 if the predicted substrate of the column is present in the genetic neighbourhood of the gene of the row, 0 otherwise). In general, the negative proteins predicted as substrates are present in more neighbourhoods compared to all proteins in the negative set ($p \cong 3.17\times10^{-5}$, Wilcoxon rank sum test). See the blue part of Figure 4.5A for an illustration of an interactor neighbourhood.

	Negative set proteins with score >=0.9																																
STE20 genetic interactor	MYO2	SEC27	SPC110	TRZ1	RPN2	RPT2	YIL091C	CDC2	MHP1	MCM2	CDC7	TRS31	ARP5	IQG1	MSS4	SRP68	SEC23	SMC4	DNA2	POL2	TOP2	SPT6	RFC1	ERB1	CDC9	CBF2	CDC27	KOG1	KAR1	VTC4	YHR020W	CYR1	STE5	MPS3
SSK1	0	0	0	0	0	0	0	0	0	0	0	0	0	0	0	0	0	0	0	0	0	0	0	0	0	0	0	0	0	0	0	0	1
SIC1	0	0	0	0	0	0	0	0	0	0	0	0	0	0	0	0	0	0	0	0	0	0	0	0	0	0	0	0	0	0	0	0	1
CDC42	0	0	0	0	0	0	0	0	0	0	0	0	0	0	0	0	0	0	0	0	0	0	0	0	0	0	0	0	0	0	0	0	1
STE11	0	0	0	0	0	0	0	0	0	0	0	0	0	0	0	0	0	0	0	0	0	0	0	0	0	0	0	0	0	0	0	0	1
TEM1	0	0	0	0	0	0	0	0	0	0	0	0	0	0	0	0	0	0	0	0	0	0	0	0	0	0	0	0	0	0	1	1	0	0
BUB2	0	0	0	0	0	0	0	0	0	0	0	0	0	0	0	0	0	0	0	0	0	0	0	0	0	0	0	0	0	0	1	0	0	0
SEC14	0	0	0	0	0	0	0	0	0	0	0	0	0	0	0	0	0	0	0	0	0	0	0	0	0	0	0	0	0	0	1	0	0	0
TAF9	0	0	0	0	0	0	0	0	0	0	0	0	0	0	0	0	0	0	0	0	0	0	0	0	0	0	0	0	0	0	1	0	0	0
RAS2	0	0	0	0	0	0	0	0	0	0	0	0	0	0	0	0	0	0	0	0	0	0	0	0	0	0	0	0	0	0	1	0	0	0
CLA4	0	0	0	0	0	0	0	0	0	0	0	0	0	0	0	0	0	0	0	0	0	0	0	0	0	0	0	0	0	1	0	0	0	0
SKM1	0	0	0	0	0	0	0	0	0	0	0	0	0	0	0	0	0	0	0	0	0	0	0	0	0	0	0	0	0	1	0	0	0	0
SLG1	0	0	0	0	0	0	0	0	0	0	0	0	0	0	0	0	0	0	0	0	0	1	0	0	0	0	0	0	0	1	0	0	0	0
WHI2	0	0	0	0	0	0	0	0	0	0	0	0	0	0	0	0	0	0	0	0	0	0	0	0	0	0	0	0	0	1	1	0	0	0
RGA1	0	0	0	0	0	0	0	0	0	0	0	0	0	0	0	0	0	0	0	0	0	0	0	0	0	0	0	1	1	0	0	0	0	0
STE4	0	0	0	0	0	0	0	0	0	0	0	0	0	0	0	0	0	0	0	0	0	0	0	0	0	0	1	0	0	0	0	0	0	0
KIN4	0	0	0	0	0	0	0	0	0	0	0	0	0	0	0	0	0	0	0	0	0	0	0	0	0	0	1	0	1	0	0	0	0	0
BEM3	0	0	0	0	0	0	0	0	0	0	0	0	0	0	0	0	0	0	1	1	1	0	0	0	0	0	0	0	0	0	0	0	0	1
KES1	0	0	0	0	0	0	0	0	0	0	0	0	0	0	0	0	0	0	0	0	0	1	1	1	0	0	0	0	0	0	0	0	0	0
HSP82	0	0	0	0	0	0	0	0	0	0	0	0	0	0	0	0	0	0	0	0	0	0	0	0	0	0	0	0	0	0	0	0	1	0
CLB2	0	0	0	0	0	0	0	0	0	0	0	0	0	0	0	0	0	0	0	0	0	0	0	0	1	1	0	0	0	0	0	0	0	0
Total	**0**	**0**	**0**	**0**	**0**	**0**	**0**	**0**	**0**	**0**	**0**	**0**	**0**	**0**	**0**	**0**	**0**	**0**	**1**	**1**	**1**	**2**	**1**	**1**	**1**	**1**	**2**	**1**	**2**	**4**	**6**	**1**	**1**	**5**

Figure 4.6A


Predicted substrate
Genetic interactor of STE20
CDC5
LTE1
BNI1
SPA2
BUD6
AXL2
MSB1
SSD1
SKG6
CYC8
Predicted substrate
PMI40
NCP1
SSK1
AKR1
OCH1
STE5
STE4
SPO12
TEM1
PUP3
KIN4
GIC2
GIC1
UBA4
URM1
STE12
STE11
BEM1
RGA1
BEM3
SEC14
KES1
HSL7
TAF9
RGA2
SHO1
CDC28
SLG1
CDC34
SWE1
CLA4
LTE1
BUB2
CLB2
CDC42
HSP82
WHI2
SIC1
RAS2
Genetic interactor of STE20

Figure 4.6B

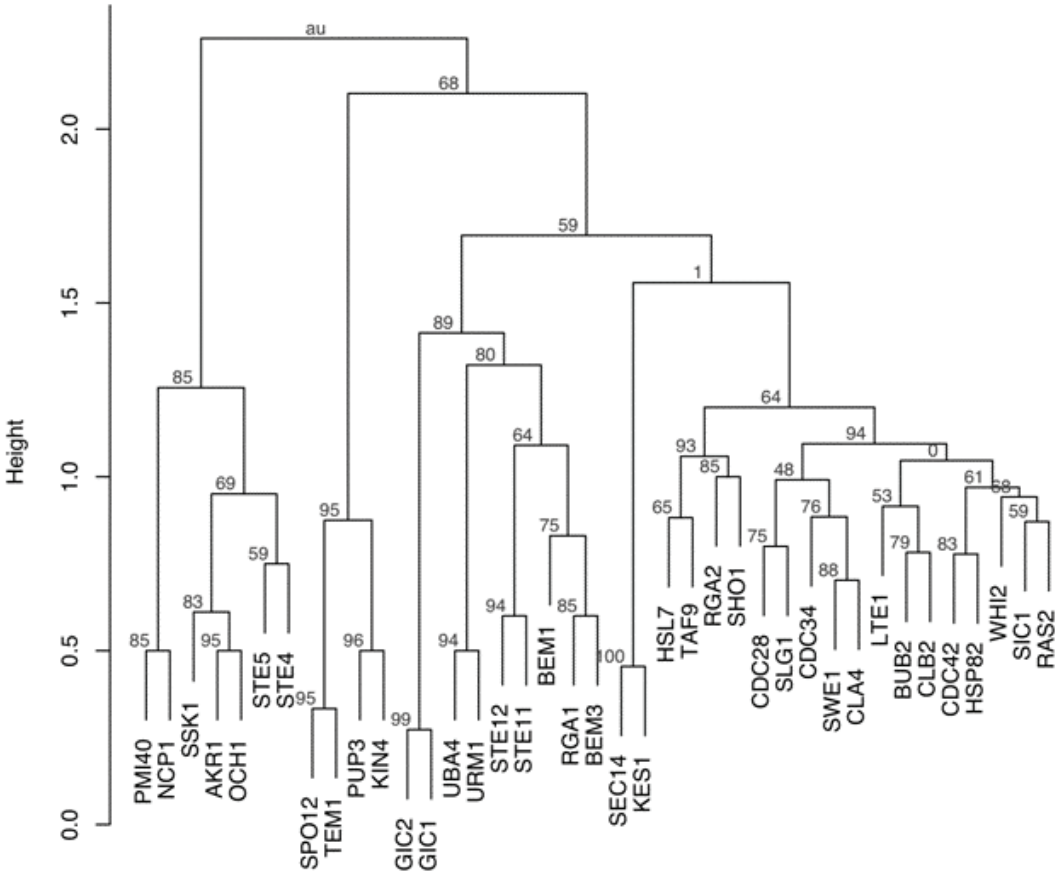

Figure 4.6. Clustering profiles of overlap between the predicted substrates (score ≥ 0.9) and the STE20 Genetic Interactor Neighbourhoods (GINs) identified predicted substrates involved with polarized growth. (A) Depiction of overlap profiles where a filled in cell indicates the presence of a predicted substrate in a GIN. A cluster of predicted substrate profiles is shown at higher resolution. SPA2 and BNI1 form a significant subcluster (p = 0.03, Supplementary Figure 4.2) and they are involved with polarized growth. (B) Dendrogram of the STE20 genetic interactors clustered by their GIN overlap profiles as in (A). Each branch point is labeled with an Approximately Unbiased (AU) score (see Materials and Methods) such that a score ≥ 95 corresponds to a p-value ≤ 0.05 indicating the significance of the cluster.

Figure 4.7A

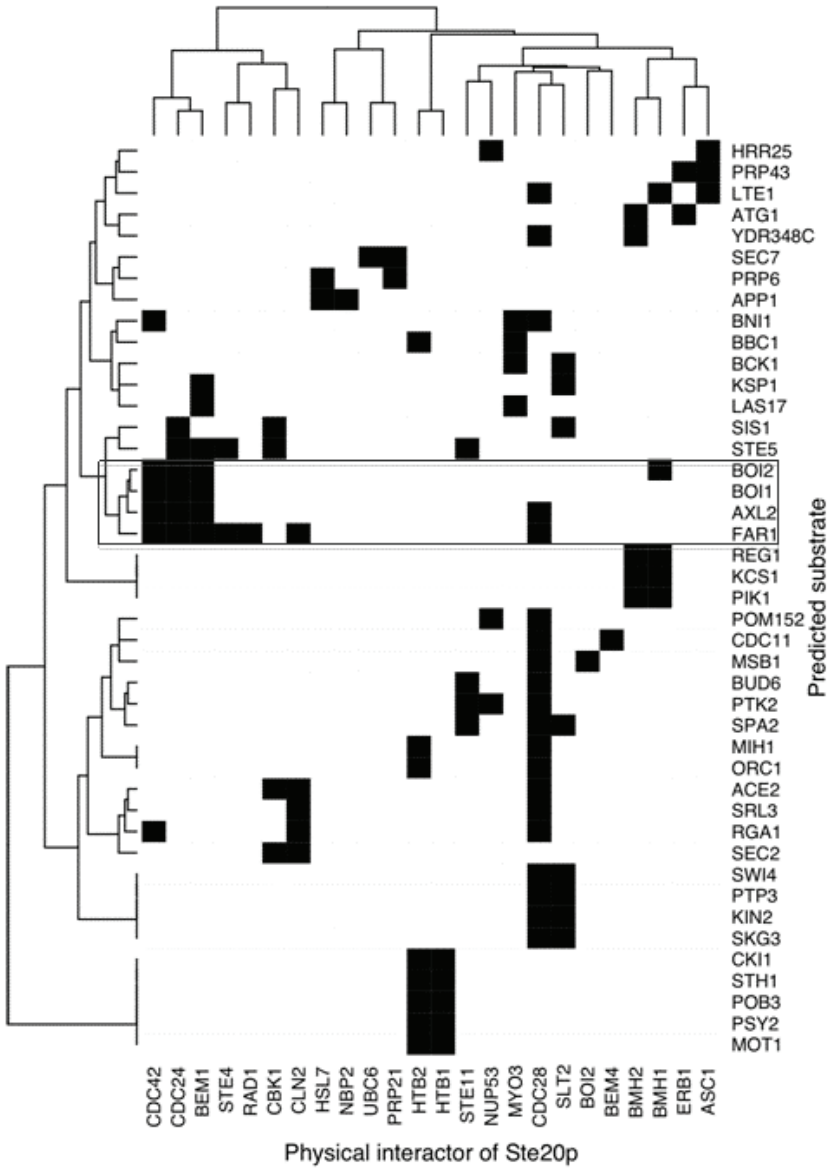
HRR25
PRP43
LTE1
ATG1
YDR348C
SEC7
PRP6
APP1
BNI1
BBC1
BCK1
KSP1
LAS17
SIS1
STE5
BOI2
BOI1
AXL2
FAR1
REG1
KCS1
PIK1
POM152
CDC11
MSB1
BUD6
PTK2
SPA2
MIH1
ORC1
ACE2
SRL3
RGA1
SEC2
SWI4
PTP3
KIN2
SKG3
CKI1
STH1
POB3
PSY2
MOT1
Predicted substrate
CDC42
CDC24
BEM1
STE4
RAD1
CBK1
CLN2
HSL7
NBP2
UBC6
PRP21
HTB2
HTB1
STE11
NUP53
MYO3
CDC28
SLT2
BOI2
BEM4
BMH2
BMH1
ERB1
ASC1
Physical interactor of Ste20p

Figure 4.7B

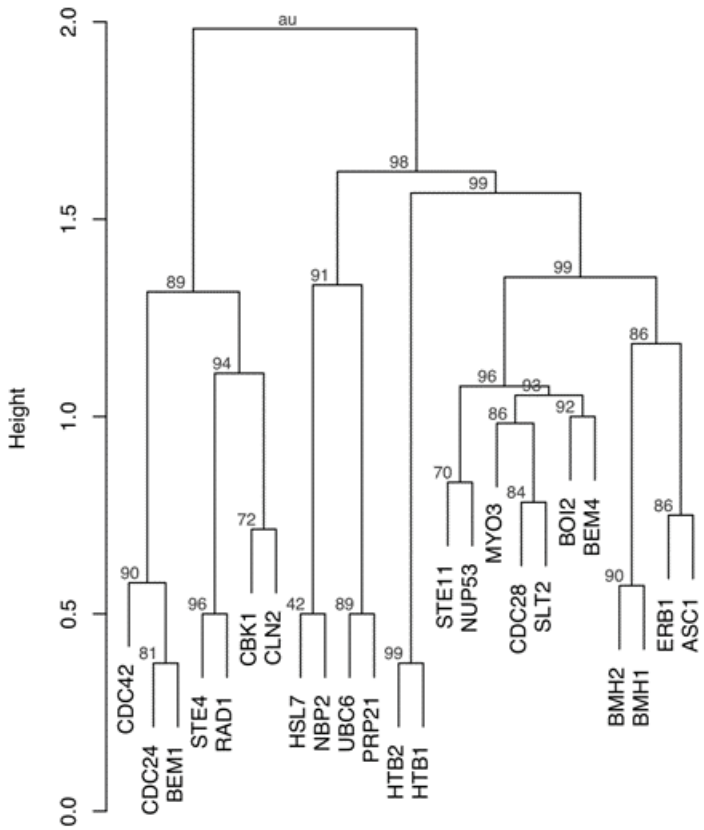

Figure 4.7. Clustering profiles of overlap between the predicted substrates (score ≥ 0.9) and the Ste20p Physical Interactor Neighbourhoods (PINs) identified predicted substrates implicated in polarized growth. (A) Depiction of overlap profiles where a filled in cell indicates the presence of a predicted substrate in a PIN. Several predicted substrates implicated in polarized growth are clustered together ($p = 0.06$, Supplementary Figure 4.3). Highlighted is a subcluster of predicted substrates that are present in the PINs of Ste20p physical interactors that are also involved with polarity (Cdc42p, Cdc24p, Bem1p). (B) Dendrogram of the Ste20p physical interactors clustered by their PIN overlap profiles as in (A). Each branch point is labeled with an Approximately Unbiased (AU) score (see Materials and Methods) such that a score ≥ 95 corresponds to a p-value ≤ 0.05 indicating the significance of the cluster.

clusters). Also included in this list are three of the four components of the polarisome (*BNI1*, *SPA2*, and *BUD6*), whose activation has been linked genetically to *STE20*.

Cluster analysis of the Ste20p PINs also results in the clustering of proteins related to polarized growth (Figure 4.7). Cdc42p, its GEF Cdc24p, and the scaffold Bem1p cluster together and overlap with a significant cluster of predicted substrates (p = 0.06, Supplementary Figure 4.3) that includes the polarity proteins Boi1p and Boi2p, suggesting that these may serve as physiologically relevant substrates of Ste20p. Polarisome components Bud6p and Spa2p cluster together with the kinase Ptk2p, though Bni1p is clustered with another set of actin-associated proteins including Bbc1p and Las17p. Thus, by combining the predicted biochemical relationships between Ste20p kinase and potential substrates with the known relationships of genetic and physical interactors of *STE20*, it becomes possible to identify potentially novel roles for Ste20p phosphorylation *in vivo*.

4.4.7 Polarisome components Bud6p and Bni1p are in vitro *substrates of Ste20p*

We sought to validate our approach to identifying Ste20p substrates by employing the tools described to investigate an aspect of Ste20p biology. Namely, Ste20p participates with Cdc42p in the establishment of polarized growth at directed sites in response to intrinsic budding cues and extrinsic signals such as mating pheromones or altered nutrient conditions (177). Ste20p has been linked in these processes to a 12S macromolecular complex called the polarisome, which has been suggested to promote polarized growth and morphogenesis (123, 312, 374). The polarisome comprises the formin Bni1p, its actin-binding partner Bud6p, the scaffold protein Spa2, and a coiled-

coil protein Pea2p. Like Ste20p, all the polarisome components exhibit synthetic lethality with *Δcla4* (123). While Ste20p has been implicated in the activation of the polarisome, and Bni1p phosphorylation has been shown to depend on Ste20p *in vivo*, the mechanistic details have remained unclear.

Examination of the set of predicted Ste20p substrates revealed that three of the four polarisome components (Bni1p, Bud6p, and Spa2p) were predicted with high probability (>0.98) to be Ste20p substrates (Supplementary Table 4.1s). Furthermore, these three were also identified numerous times when cross-referenced against *STE20* GINs and PINs; *BNI1* is a member of 16 neighbourhoods, *SPA2* is a member of 15, and *BUD6* is a member of 10. Given their high predictor scores and their representation in relevant neighbourhoods, Bni1p, Spa2p, and Bud6p represent strong candidates as *de facto* Ste20p substrates.

We thus verified the predictions by performing *in vitro* kinase assays with the polarisome proteins to determine whether they could serve as substrates of Ste20p. The substrates were expressed and purified as GST-fusion proteins in yeast, as described above. They were then incubated with a recombinant Ste20p kinase domain for 30 minutes with relevant cofactors and γ-[P^{32}]-ATP before being separated by SDS-PAGE and visualized by autoradiography. As shown in Figure 4.8, Bni1p and Bud6p are both phosphorylated by Ste20p *in vitro*. Neither Spa2p nor Pea2p were phosphorylated by Ste20p (data not shown). Thus, for both Bni1p and Bud6p, the predicted ability to be phosphorylated *in vitro* by Ste20p was confirmed experimentally.

In an effort to gain greater insight into possible consequences of Ste20p phosphorylation, we endeavoured to identify phosphorylation sites in each of Bni1p and

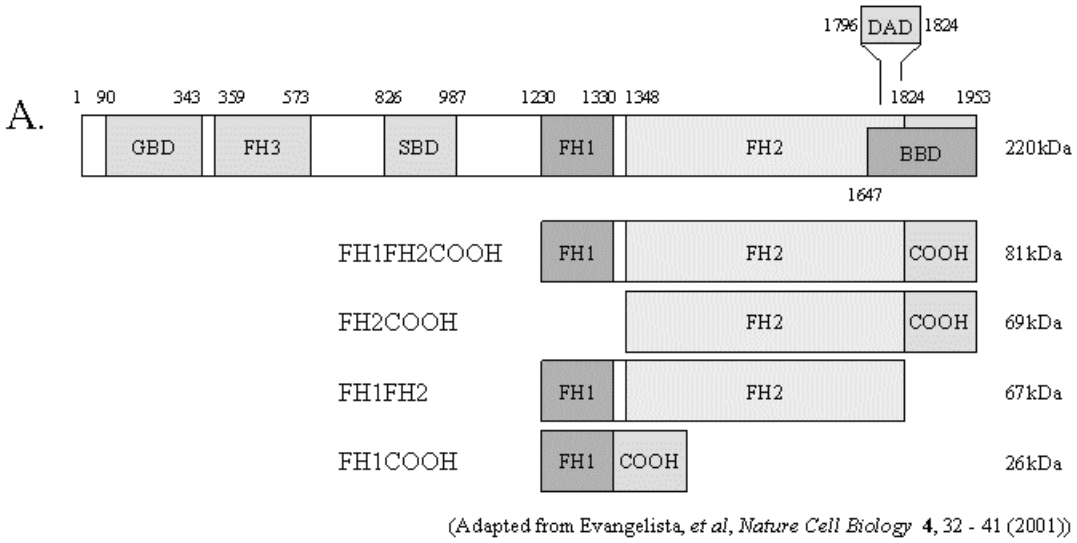

(Adapted from Evangelista, *et al*, *Nature Cell Biology* **4**, 32 - 41 (2001))

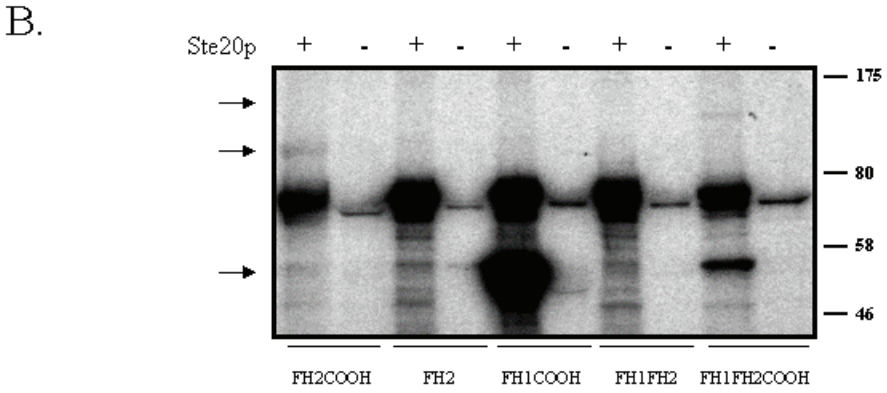

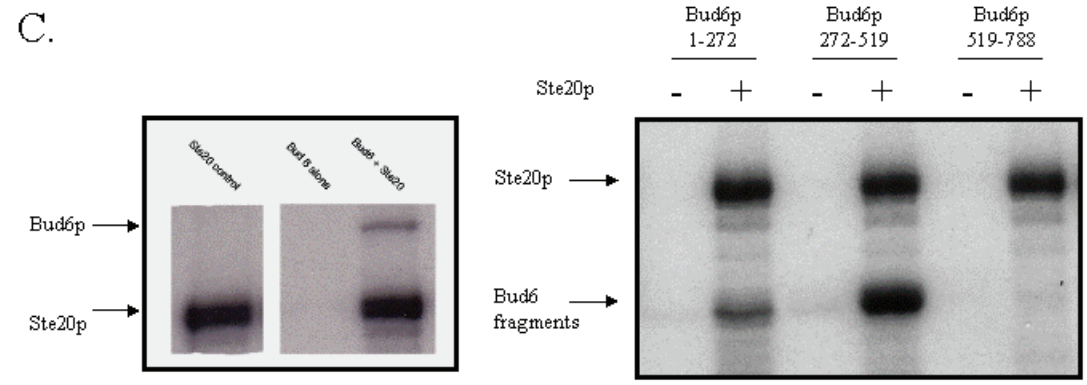

Figure 4.8. Bni1p and Bud6p are phosphorylated by Ste20p *in vitro*. (A) A schematic representation of the functional regions of Bni1p. These are the Formin-Homology domains (FH1, FH2, and FH3), GTPase binding domain (GBD), Spa2p-binding domain (SBD), Dia-autoregulatory domain (DAD), and Bud6p-binding domain. The region C-terminal to the FH2 domain, which contains part of the BBD, is referred to as the COOH region in the text, (B) Ste20p only phosphorylates Bni1p constructs containing the COOH region. Constructs composed of different combinations of the FH1 and FH2 domains and the COOH region were purified and equal concentrations of each were assayed by *in vitro* kinase assays with Ste20p and γ-[P^{32}]-ATP, then visualized by SDS-PAGE and autoradiography. The three constructs containing the COOH regions are phosphorylated (with position of the labeled peptides in their respective lanes indicated by arrows at left), whereas the constructs without the COOH region are not, (C) Ste20p phosphorylates the central region of Bud6. In the left panel, full length Bud6p is phosphorylated by Ste20p. In the right panel, the middle fragment of Bud6p exhibits strong evidence of phosphorylation and the N-terminal fragment exhibits weak evidence of phosphorylation. No signal is detected for the C-terminal fragment.

Bud6p. Bni1p is a large (220kDa) protein, which has previously been shown to be a phosphoprotein *in vivo* whose phosphorylation is reduced in a *Δste20* mutant (123). It comprises a N-terminal Cdc42p binding domain and three C-terminal domains characteristic of the formin-family of proteins and which, together, constitute the actin-assembly machinery. These C-terminal domains are the Formin-homology 1 and 2 (FH1 and FH2) domains and a C-terminal tail region (COOH) which includes the Bud6-binding domain (BBD) and a *cis*-inhibitory Dia-autoregulatory domain (DAD) (Figure 4.8A). Given the functional importance of the C-terminal domains, we expressed subclones composed of the FH1, FH2, and COOH domains as GST-fusion proteins and repeated the *in vitro* Ste20p kinase assays as described, above. As seen in Figure 4.8B, phosphorylation is observed in the constructs containing the COOH region, but is not observed in constructs in which it is absent. Thus, Ste20p phosphorylation *in vitro* occurs within the region of Bni1p responsible for binding Bud6p. It has been previously shown that expression of a *bni1* construct lacking this BBD region is unable to rescue the synthetic lethality of a *Δbni1 Δcla4* mutant, and exhibits a terminal phenotype similar to that of *Δste20 Δcla4* mutants (123). The phenotypic similarity between strains lacking the region of Bni1p phosphorylated by Ste20p and those lacking Ste20p altogether suggests that phosphorylation of this region occurs *in vivo* and is required in the absence of *Δcla4*.

Next, we investigated the *in vitro* phosphorylation of Bud6p. As shown in Figure 4.8C, Bud6p is effectively phosphorylated *in vitro* by Ste20p, as predicted. While the domain organization of Bud6p is not as well-defined as for Bni1p, it has been determined that the C-terminal region (519-788aa) is involved in dimerization as well as binding

Bni1p and actin whereas the N-terminal region (1-166) is required for proper Bud6p localization (175). We thus subcloned Bud6p to determine which regions may be phosphorylated by Ste20p *in vitro*. As seen in Figure 4.8C, a faint phosphorylation is observed in the N-terminal fragment, a stronger signal is observed in the uncharacterized middle region, and no phosphorylation is observed in the region involved in dimerization or binding to actin and Bni1p. Thus, while Ste20p phosphorylates Bni1p on the region responsible for Bud6p binding, the reverse is not true.

We employed mass spectrometry to identify *in vivo* phosphorylation sites for Bud6p. Unlike Bni1p, whose large size made it difficult to purify as a full-length protein, we expressed and purified a TAP-tagged fusion protein of Bud6p in yeast cells according to standard procedures (336). We separated the purified protein by SDS-PAGE, excised the relevant band from the gel and performed in-gel tryptic digestion. Prepared samples were then separated by LC-MS/MS qTOF and analyzed by MASCOT software (301). We identified i*n vivo* phosphorylation on two residues: serine 327 and serine 342. These two residues are found in the middle fragment, which had been phosphorylated by Ste20p *in vitro* (Figure 4.8C). Thus, Bud6p is a phosphoprotein *in vivo* and the phosphorylation on residues Ser327 and Ser342 correlate with the Ste20p phosphorylation of the same region *in vitro*. Given that the region of Bni1p which is phosphorylated by Ste20p is required for viability in the absence of *CLA4*, we asked whether the same is true for Bud6p. Expression of a *bud6* construct with the region containing both phosphorylation sites deleted ($bud6^{\Delta 272\text{-}411}$) retains the ability to rescue the lethality of a *Δbud6 Δcla4* strain and results in morphology similar to a *Δcla4* mutant (d.n.s.). While the *in vivo* relevance of Bud6p remains to be determined, the use of the Ste20p substrate predictor

has suggested that direct phosphorylation of polarisome proteins occurs by Ste20p *in vitro*, and presents opportunities for directed investigation of the mechanism of activation

4.5 Discussion

This work details a biochemical genomic screen for *in vitro* substrates of the *S. cerevisiae* Ste20p kinase, and the subsequent generation of a computational predictor for the identification of high-probability substrates within the rest of the proteome. The initial screen of roughly 540 proteins identified 14 substrates. The observation that several substrates are nuclear proteins involved in ribosomal biogenesis led us to confirm a nuclear localization for Ste20p in vegetatively growing cells where it may participate in this process. The substrate predictor employed the positive and negative datasets from our screen to identify amino acid motifs that are overrepresented in Ste20p substrates versus the negative set. These motifs were not restricted to potential Ste20p phosphorylation consensus sequences, so they likely include motifs that describe other substrate identifying features as well, such as docking sites. The predictor was applied to the yeast proteome, resulting in 753 proteins being predicted with high posterior probability (> 0.9) to be Ste20p substrates. GO analysis revealed that the overrepresented localizations, biological processes, and molecular functions amongst the predicted substrates are consistent with what is known about Ste20p and they also suggest novel roles for the kinase. We then provided additional biological context by cross-referencing the predicted substrates against the *STE20* genetic and physical interactor neighbourhoods. In doing so, polarisome components were highlighted as predicted substrates with contextual support for *in vivo* phosphorylation by Ste20p. That is, Bni1p, Bud6p, and Spa2p are predicted substrates that are present in many of the *STE20* genetic interactor neighbourhoods and interestingly, they are present in many of *same* neighbourhoods (Figure 4.6A). Finally, we validated the approach to identifying Ste20p

substrates by testing these three polarisome components. Both Bni1p and Bud6p were shown to be phosphorylated by Ste20p *in vitro*. Ste20p phosphorylation was mapped to a region of Bni1p which is associated with *STE20* genetically, and which binds to Bud6. *In vivo* phosphorylation sites were identified on Bud6p, but the physiological relevance of these sites remains unclear.

Mammalian members of the Ste20p-kinase family, also referred to as the PAK (p21-activated kinase) family, have been shown to localize to nuclei and participate in nuclear events, most notably during programmed cell death (63). With the induction of apoptosis, Mst1 (mammalian sterile twenty) kinase is cleaved by caspase 3, and is then relocalized to the nucleus, where it phosphorylates histone H2B at residue S14. PAK2 is a pro-apoptotic kinase whose cleavage by caspases removes a regulatory region and exposes a nuclear localization signal (170). This results in the production of an activated PAK2 p34 isoform that is quickly transported to the nucleus where it promotes apoptosis. It has also been previously shown that yeast Ste20p is translocated to the nucleus as a precursor to H_2O_2-induced cell death (6), though this nuclear translocation event is assumed to be pathological. Additionally, mammalian PAK kinases have been implicated in numerous nuclear events apart from apoptosis, including transcription and mediating tamoxifen resistance in breast cancer cells (157, 325, 326, 381) To date, no nuclear role has been identified for Ste20p in yeast under normal growth conditions.

Here, we identify a nuclear role for Ste20p in cells under non-pathological conditions in the regulation of ribosomal biogenesis. Several proteins involved in this process were identified in the initial Ste20p screen. We thus examined *ste20* mutants compromised for nuclear localization to evaluate whether Ste20p participates in this

process. *ste20*Δ*NLS*-expressing cells exhibited decreased levels of both 60S ribosomal subunits and 80S mature ribosomes. Surprisingly, *Δste20* cells exhibited no such defect (d.n.s.), suggesting that in its absence, another kinase may be able to compensate for the loss of Ste20p function, but that this compensation is blocked by the presence of cytosolic Ste20p. Thus, Ste20p nuclear activity seems to be required for proper ribosome biogenesis. It is possible that phosphorylation of one or more of the *in vitro* substrates is required as a regulatory step in ribosome assembly. Indeed, a strain expressing an impaired allele of *SPB1*, one of the substrates identified in our screen, exhibits a decrease in 60S ribosomal subunits similar to *ste20*Δ*NLS* (303). The link between Ste20p and ribosome assembly is further strengthened by the observation that the *S. pombe* PAK inhibitor Skb16p and its *S. cerevisiae* homolog Mak11p associate with pre-ribosomes and are involved in 60S subunit biogenesis (359). The observation that the nuclear pool of Ste20p is greatest during G1 suggests that Ste20p localization may be cell-cycle coordinated. Previous work has shown that Ste20p is phosphorylated by Cln2p-Cdc28p in a cell-cycle dependent manner, suggesting that the two may be linked (445). This suggestion is further supported by the observation that the nuclear and cytosolic pools of Ste20p exhibit a mobility shift by SDS-PAGE. CDK inhibition has been shown to affect ribosome biogenesis at several key points in the cell cycle (382). Thus, it is possible that Ste20p may provide a cell-cycle-dependent link between Cln-Cdc28p and ribosomal biogenesis.

Given the wealth of data generated by the *in vitro* screen for Ste20p substrates, we reasoned that it may be possible to identify characteristic sequence features of Ste20p substrates. Consensus phosphorylation sites alone are generally insufficient for the

identification of kinase substrates. Secondary features such as docking sites for the regulatory domain of the relevant kinase, or binding sites to common scaffolding proteins have also been described as essential features for effective kinase-substrate interactions (25, 300). We reasoned that while no individual sequence feature may be sufficient to identify Ste20p substrates, the combination of relevant motifs may allow for substrate prediction with a higher degree of accuracy. Our predictor identified 23 motifs enriched among the substrate set versus the negative set which we then employed in a naïve Bayes classifier to assign posterior probabilities to each member of the proteome. The statistical cross-validation estimates a threefold predictive improvement (7.9% positive predictive value) over the background rate (2.6%) we identified in our initial screen.

An *in vitro* screening approach to the identification of kinase substrates by employing protein microarrays has been performed by Mike Snyder and colleagues (313). This significant study screened 2/3 (87 of 122) of the yeast kinases against roughly 2/3 (~4400 of ~6700) of yeast proteins, and has thus provided the most complete picture yet of the yeast phosphorylome to date. Their work identified 70 substrates for Ste20p. Eleven of these were tested in our screen, of which four were identified as substrates, demonstrating a 36% recovery of chip-identified substrates in our screen. Of our 14 substrates, four were common to both screens, four were not printed on the chip or were not phosphorylated by any kinases (*i.e.* potentially unphosphorylatable on the microarray), and six were phosphorylated by at least one other kinase but not Ste20p, suggesting a 40% overlap with our study. Thus, though the two approaches result in some variability, the 35-40% overlap in substrates is generally in keeping with observed differences between related high-throughput assays and with the observation that

different approaches to physical, genetic, and biochemical interactions complement each other (422).

The technical challenges of protein purification and *in vitro* kinase assays mean that a complete screen of all kinases against all substrates remains impractical. This is especially true if we wish to identify substrates of kinases in higher eukaryotes, whose proteomes are too large for complete screening. Thus, bioinformatics approaches to predict high-probability substrates have been suggested, usually centered around consensus sequence identification. The Snyder group employed a pattern-searching algorithm to identify potential consensus motifs for each of the tested kinases. They succeeded in identifying motifs for 11 of the 87 kinases tested, suggesting that these 11 represent the subset of kinases with strict phosphorylation site sequence requirements (313). The motifs of a few kinases, when used to scan the whole proteome, allow for large predictive improvements over the substrate discovery rates from the microarray assay; notably for Ark1p (15.8-fold), Rim11p (7.4-fold), and PKA (5.7-fold). The other kinases for which consensus motifs were identified exhibit a roughly twofold predictive improvement. Yet for most of the kinases they screened, including Ste20p, there were presumably no consensus sequences identified with significant enrichment above background.

Our approach was not limited to the identification of phosphorylation site consensus sequences, but rather considered the global sequence characteristics of substrates and allowed for the combination of different, possibly independent motifs. The resulting predictor exhibited a threefold enrichment in substrate discovery above that of the *in vitro* screen (7.9% vs. 2.6%). This improvement compares favourably with the

predictive capabilities of consensus motifs that have been identified for predicting substrates of other kinases. Our substrate enrichment is made more impressive when it is noted that our predictor was based on a screen of only 544 proteins compared with the roughly 4,400 proteins screened by the protein microarray. Furthermore, this approach predicts true substrates of Ste20p kinase despite its lack of a single distinguishing phosphorylation site consensus sequence (32).

Several of the motifs employed by our predictor contain serines or threonines and thus represent candidate consensus sequences for Ste20p phosphorylation sites. Indeed, there are two motifs wherein a serine residue is accompanied by an upstream basic residue and this pattern has been associated with PAK phosphorylation sites (329). Nonetheless, it is the combinatorial usage of several motifs that improves the strength of the predictor. It remains to be determined how the other motifs participate in specifying Ste20p phosphorylation, whether via *cis* effects through a docking interaction with Ste20p, or *trans* effects through binding to a Ste20p-associated scaffold such as Bem1p, Ste5p, or Far1p.

While the predictor remains a tool for identifying a biochemical relationship between a kinase and its potential substrates, GO analysis reveals that the predicted substrate set overlaps significantly with a number of gene sets associated with Ste20p-related processes and localizations. The observed overlaps hint at the *in vivo* relevance of the predicted substrates. This is not altogether surprising since our motif selection process favoured motifs that have functional importance in the cell, measured by conservation across *Saccharomyces* species. Thus, though the predictor is based on primary sequence

and biochemistry, the evolutionary conservation of selective motifs seems to result in biological relevance.

Biological relevance of the predicted substrates was also evaluated using the regions of the genetic and physical interaction networks surrounding Ste20p. Combining genetic and physical interaction data with biochemical data has been shown to be an effective means of evaluating and assigning biological relevance to observed phosphorylation. For instance, the NetworKin methodology employs both types of data, with others, in an effort to assign the thousands of *in vivo* phosphorylation sites to the roughly 500 human kinases (227). In that framework, genetic and physical interactions are used to evaluate possible kinase-substrate relationships. Here, we employ a similar approach to evaluate substrates that have been predicted computationally. We concentrate on using yeast genetic and physical interaction data from primary experimental evidence and high-throughput synthetic lethal and two-hybrid screens, as these provide broad but reliable datasets. The analysis focused on genes/proteins that at most two steps away from *STE20* in the genetic and physical interaction networks, reasoning that these are the most likely to represent strong candidates for biologically relevant associations with the kinase. Genetic interactions often involve pairs of genes operating in redundant or related pathways (291). Given that most phosphorylation events link a kinase and its substrate in a particular pathway or event, we reasoned that the genetic interactions of a kinase and its substrate should therefore exhibit some degree of overlap. Indeed, *STE20* GINs tend to overlap more significantly with the Ste20p predicted substrate set compared to the neighbourhoods of other genes in the network. This trend suggests that the predicted substrates are functionally linked to *STE20* and thus may act in the same pathway as

Ste20p. They therefore represent candidates for *in vivo* phosphorylation by Ste20p. Similar reasoning is employed with regards to physical interactions, except that it exploits the tendency of kinases and substrates to function in multimeric complexes where they bind to common proteins. This is observed, for instance, in MAPK signaling in yeast, where scaffold proteins bind kinases and their respective substrates (267). Analogously, Ste20p PINs tend to overlap more significantly with the predicted substrate set compared to other neighbourhoods. This observation further supports the validity of our approach to predicting Ste20p substrates.

The GIN and PIN analyses may also be able to buffer the effects of false negatives and false positives of both the biochemical genomics screen and the computational predictor. As mentioned above, several of the substrates identified in the screen were scored poorly by the predictor. Interaction neighbourhood analysis suggests that some of these substrates, notably Rsc6p and Spt16p, may yet be biologically relevant, given their membership in three *STE20* GINs and PINs, respectively. Likewise, potential false negatives from the screen, that is proteins that were not found to be phosphorylated but were assigned high scores by the predictor, were re-evaluated in the context of *STE20* GINs. These proteins were found to be members of significantly more *STE20* GINs than the rest of the negative set. This suggests that a subset of these may represent false negatives from the screen. Thus, the evaluation of the predicted substrates using genetic and physical interaction networks provides both biological context and a potentially more sophisticated analysis of the biochemical and computational data.

The goal of any large-scale screen or bioinformatics analysis is to generate novel biological hypotheses. We thus examined the data which came out of the screen to

identify potentially novel functions for Ste20p. Among the predicted substrates were three of four polarisome complex members. All three exhibited significant overlap with Ste20p interactor neighbourhoods. The polarisome comprises Bni1p, Bud6p, Spa2p, and Pea2p, which form a 12S complex associated with sites of polarized growth. Previous work has implicated Ste20p in the activation of the polarisome and has shown that Bni1p is a phosphoprotein whose phosphorylation is reduced in a *ste20* mutant (123). Here, we confirmed that Bni1p is an effective substrate for Ste20p *in vitro*. Additionally, we confirmed that Bud6p is phosphorylated by Ste20p *in vitro*, and that Spa2p is not. Spa2p was assigned a high posterior probability of being a Ste20p substrate and is also present in many Ste20p interactor neighbourhoods. It therefore represents a likely false positive of our predictor. It is also possible, however, that there may be requirements for Ste20p phosphorylation of Spa2p which are not present in the *in vitro* assay. Nonetheless, our predictive method resulted in the identification of two novel substrates for Ste20p phosphorylation.

Interestingly, the phosphorylation of Bni1p occurs in a C-terminal region which binds the other polarisome substrate of Ste20p, Bud6p, indicating the potential for sophisticated regulatory coordination. Coordinated regulation is supported by the observation that the combination of a *Δcla4* mutation with either *Δbud6* or a deletion of Bni1p's C-terminal region, which is phosphorylated by Ste20p, is lethal in yeast with the same terminal phenotype as the lethal *Δcla4 Δste20* mutation (123). The *in vivo* relevance of Ste20p phosphorylation and the coordination of the phosphorylation of Bni1p and Bud6p in the regulation of polarized growth remain to be determined. Nonetheless, it is

clear that a predictor based on a biochemical genomics screen for *in vitro* substrates of Ste20p kinase reveals biologically relevant avenues for further research.

Phosphorylation is the key modification involved in signal transduction, and thus serves as a cornerstone for practically all of the dynamic processes of the cell. Despite its central importance, identifying the detailed architecture of these networks has remained a fundamental challenge. Here we have described an approach which has combined biochemical genomics and bioinformatics to identify potential new substrates for the Ste20p kinase in yeast. We have confirmed experimentally that such an approach can predict true *in vitro* Ste20p substrates. Continued application of this approach should provide greater insight into Ste20p biology, while the generalization of this approach to other kinases should help in elucidating the important, but still poorly characterized global population of kinase-substrate interactions.

4.6 Acknowledgements

We gratefully thank Drs. D. Amberg and C. Boone for plasmids, and Dr. R. Wozniak for the Nup53 antibody. R.A. and A.Y.L. were the recipients of NSERC graduate student fellowships. This work was supported by the NRC and grants from the NCIC and CIHR to M.W. and D.Y.T.

This work is NRC publication XXXXX.

4.7 Materials and methods

Materials

Restriction endonucleases and DNA-modifying enzymes were obtained from New England Biolabs and GE Healthcare. The enhanced chemiluminescence (ECL) assay system, protease inhibitor tablets, and reduced glutathione were obtained from Roche. Nitrocellulose membranes were purchased from Bio-Rad. Glutathione Sepharose 4B beads and Prescission Protease were purchased from GE Healthcare. Radioisotopes were purchased from GE Healthcare and Perkin Elmer, and film for autoradiography was BioMax MS from Kodak. Acid-washed glass beads (450-600um), protease inhibitors, sorbitol, and trypsin were purchased from Sigma. Horseradish peroxidase conjugated secondary antibodies were purchased from Santa Cruz Biotechnology; the antibody against GST was described previously (444). Ste20p was detected with the polyclonal antibodies described previously (447) and Nup53 rabbit polyclonal antibodies were from Dr. R.W. Wozniak (University of Alberta, Edmonton, Canada) laboratory. The yeast GST-6xHIS Open Reading Frame collection was purchased from Open Biosystems.

Construction of plasmids

GST-fusion proteins were obtained from Open Biosystems (464). The GST-Bni1 constructs were kindly provided by C. Boone (U Toronto).

The Bud6p fragments were expressed in *E. coli*. Relevant fragments were amplified from genomic DNA (11). pRA210 expresses full-length *BUD6* and was constructed using the oligos 5'-GAGACCCGGGGAATGAAGATGGCCGTGGAT

GACC-3’ and 5’-GAGACTCGAGTTAAGTAAACCCCGGCCCAAAATATGC-3’. pRA211 expresses *BUD6*$^{1-272}$ and was constructed using the oligos 5’-GAGACCCGGGGAATGAAGATGGCCGTGGATGACC-3’and 5’-GAGACTCGAGTTAAGCTTCTGTTGTAGACTGATTTGTC-3’. pRA212 expresses *BUD6*$^{272-519}$ and was constructed using the oligos 5’-GAGACCCGGGAGCTGCTGCGGCTGCCGGCCTCATGAC-3’ and 5’GAGACTCGAGTTACCTATTAATATTATGCACTTGTTT-3’. pRA213 expresses *BUD6*$^{519-788}$ and was constructed using the oligos 5’-GAGACCCGGGAAACAAGTGCATAATATTAATAGG-3’ and 5’-GAGACTCGAGTTAAGTAAACCCCGGCCCAAAATATGC-3’. The underlined nucleotides are *SmaI* and *XhoI* sites respectively. The resultant PCR products were inserted into the vector pGEX-5T by cutting both with *SmaI* and *XhoI* followed by ligation. The resultant plasmids were confirmed by sequencing.

Yeast strains and protein purifications

Yeast media, culture conditions, and manipulations were as described (346). Transformation of yeast with plasmid DNA was achieved with lithium acetate and standard protocols (346).

Growth and induction of yeast strains for the biochemical screen were essentially as described (464). Cell patches were inoculated in SD (2%) –ura medium, and grown overnight, washed, reinoculated in raffinose (4%) -ura, and grown to an absorbance at 600nm of 0.8. Cultures were pooled by combining 5ml of each and were then induced with 4% (final concentration) galactose for 3h. GST-fusion proteins were isolated on

glutathione-sepharose beads as previously described (444). Isolated proteins conjugated to beads were dried and kept at 4C no longer than overnight. The biochemical screen followed an iterative process with the first round pools comprised of eight fusion proteins followed by deconvolution of positive pools by halves until single positives were identified.

Expression of full-length *BUD6* and associated fragments was in *E. coli* strain BL21, which was induced with 0.4mM IPTG for three hours. Fusion proteins were obtained as described (383).

Protein Kinase Assays

The biochemical screen was designed to screen roughly 10% of the yeast proteome. We reasoned that a substrate responsible for the shared essential function of Ste20p and Cla4p might itself be essential. We thus created a library of 539 essential proteins based on their GO functional and localization annotations, reasoning that these would likely still exhibit biochemical diversity characteristic of the protein population as a whole. GO terms used for the selection included broad categories including signal transduction, protein translation or degradation, cell cycle progression, among others.

Kinase assays were as described (447). Dried beads with GST-fusion proteins bound were resuspended in kinase buffer supplemented with 2μM ATP and 1μl [γ-^{32}P]-ATP (4,500 Ci/mmol, 10 Ci/μl) and were split in two aliquots, one of which received 1ul of recombinant GST-Ste20p and the other received an equal volume of protein storage buffer. Reaction mixtures were incubated for 30 minutes and then boiled for 5 minutes

after the addition of Laemmli buffer. Samples were separated by SDS-PAGE, dried, and visualized by autoradiography.

Fractionation procedures

Crude nuclei were prepared as described (395). Cells were spheroplasted with Zymolyase 100T. Spheroplasts were washed with 1.1 M sorbitol, layered over a cushion of 7.5% Ficoll 400 in 1.1 M sorbitol and sedimented at 5,000 x g for 20 min. Spheroplasts were then resuspended in PVP medium: 0.5 mM $MgCl_2$, 20 mM KH_2PO_4, pH 6.5, supplemented with a protease inhibitor pellet (Roche) and lysed using a Polytron tissue homogenizer. The lysate was diluted with an equal volume of 0.6M sucrose in PVP and sedimented at 10,000 x g for 10 min. The crude nuclear pellet was used for further analysis. To isolate ribosome-containing fractions we used a procedure described by Baim *et al*. (17), except 5-35% sucrose gradients were used.

Microscopic analysis

Cells were examined with Nomarski optics and GFP filter set using an Aristoplan microscope (Leitz Wetzlar, Germany) and Northern Exposure image analysis software (Empix Imaging Inc.). To localize Ste20p by immunofluorescence, cells were washed in the phosphate buffer and fixed in 3.7% formaldehyde for 10 min. Fixed cells were spheroplasted in a sorbitol citrate buffer (100 mM K_2HPO4, 36.4 mM citric acid, 833 mM sorbitol) containing Zymolyase 100T (10 μg/ml), washed and spotted onto microscope slides. Cells were permeabilized by incubation with ice-cold methanol for 4 min, followed by a transfer to acetone for 30 sec. Slides were blocked with 2% milk in the pBST solution for 30 min. Incubations with primary were 1 hour and with secondary

45 min. Ste20p was detected using rabbit polyclonal sera (447). The antibodies were visualized with FITC-conjugated goat anti-rabbit antibodies. Nuclear DNA was visualized with DAPI and actin with the rhodamine phalloidin peptide (Molecular Probes, Invitrogen).

Identification of predictive motifs

All *S. cerevisiae* protein sequences were obtained from the *Saccharomyces* Genome Database in August 2008 (371). The sequence of each of the 19 known substrates (14 from the *in vitro* screen and five from the literature; the positive set) was scanned, with a six-amino acid sliding window, to identify sequence fragments where at least three of the residues are predicted to be exposed according to ACCpro 4.0 (60). The identified fragments (with overlapping fragments merged into single fragments) were then used as input to the Teiresias algorithm (337). The algorithm parameters specified that identified motifs must contain at least three literal (*i.e.* non-wildcard) residues such that any three consecutive literals span at most six amino acids.

Each motif was evaluated with respect to the positive and negative (non-substrates of the *in vitro* screen) sets by computing its selectivity ratio (s) = ($\Sigma_j w_j/N_{pos}$)/($\Sigma_k w_k/N_{neg}$) where N_{pos} = 19 is the size of the positive set, N_{neg} = 525 is the size of the negative set, w_j is the weight of the motif in substrate j for $j = 1..N_{pos}$ and w_k is the weight of the motif in non-substrate k for $k = 1..N_{neg}$. The weights were computed as shown in Figure 4.3. The multiple sequence alignments were constructed with ClustalW2 (61) together with *Saccharomyces* sequences and orthology mappings obtained from (187, 371). An alignment may include two sequences for proteins in *S. bayanus* and/or *S. mikatae* since

for each of these species, there were two different research groups that generated sequences. In such an alignment, the conservation score considers whether the motif was conserved in *any* of the sequences for a given organism and therefore does not double-count. The weights of overlapping motif occurrences were adjusted so that the overlapping region contributes to the weight of only one occurrence (Figure 4.3).

The predictor of Ste20p substrates and its cross-validation

As a naïve Bayes classifier, the predictor computes the posterior probability (*i.e.* prediction score) that a given sequence encodes a Ste20p substrate as follows:

$$score = (1 + s_1^{-w1} s_2^{-w2} \ldots s_n^{-wn} P(!S)/P(S))^{-1}$$

where

$P(S) = 14/539$ is the substrate discovery rate of the *in vitro* screen (*i.e.* the prior),

$P(!S) = 1 - P(S)$ is the non-substrate discovery rate of the *in vitro* screen,

s_i represents the selectivity ratio for motif i,

wi represents the weight of motif i in the given sequence, and

$n = 23$ is the number of motifs used by the predictor (each with $s_i \geq 10$).

The motif weights for prediction are computed as in Figure 4.3 except that the alignments are not used and consequently, the conservation score is always equal to 1.

Rather than iteratively leaving out each example in the training set, training on the remaining data, followed by testing the left-out example with the resulting predictor as in standard leave-one-out cross-validation, we only iteratively left out positive examples (*i.e.* proteins in the substrate set). A random selection of 100 proteins from the negative set (~20%) was set aside for testing the predictors resulting from the different iterations.

We cross-validated in this way due to the computationally-intensive process of deriving selectivity ratios for the thousands of motifs discovered by Teiresias during each iteration.

Gene Ontology (GO) analysis

GO slim annotations from all three ontologies were obtained from SGD in August 2008 (371). The significance of the over-representation of GO category gene sets amongst the predicted substrates was computed using the hypergeometric test in the context of all annotated, protein-coding genes. For each ontology, Benjamini and Hochberg multiple-test correction (23) was performed, across all categories exhibiting a non-zero overlap with the predicted substrates, to obtain adjusted p-values (23).

Genetic and physical interaction network analysis

All *S. cerevisiae* genetic and physical interactions were obtained from SGD (371) and they correspond to BIOGRID v2.0.40 (38). The networks were reduced to protein-coding genes and self-interactions were removed. To avoid redundancy an for reasons described in the discussion, Ste20p-substrate interactions from (313) were omitted from the physical network. The neighbourhood of a gene/protein is defined as the set of genes/proteins that interact with it in the network. The significance of the overlap between a neighbourhood and the set of predicted substrates was computed using the hypergeometric test in the context of all protein-coding genes. For each network, Benjamini and Hochberg multiple-test correction (23) was performed, across all

neighbourhoods exhibiting a non-zero overlap with the predicted substrates, to obtain adjusted p-values.

The number of times a gene/protein was used as a bait in interaction screens (*b*) was used as a measurement for how frequently the gene/protein has been studied in terms of interactions. To correct for frequent study, we considered a linear model that uses *b* to predict the multiple-test corrected p-value for overlap. The model was training using data for genes/proteins whose neighbourhoods exhibit a non-zero overlap with the set of predicted substrates. The residuals of the model were taken as p-values adjusted for frequent study (with negative residuals forced to zero).

The one-sided Wilcoxon rank sum test was used to determine whether *STE20* interactor neighbourhoods tend to have lower p-values compared to the neighbourhoods of other genes in the network. The same statistical test was performed to determine whether the negative set proteins that are predicted as Ste20p substrates tend to be in more *STE20* GINs compared to all negative set proteins.

For Figures 4.6 and 4.7, we focused on predicted substrates that are present in >1 *STE20* GIN or PIN, respectively. The overlap profiles were clustered using the Ward agglomerative method and the binary distance metric (see hclust documentation in the R statistical computing framework, (320)). The significance of branch points in the resulting dendrograms was measured using multiscale bootstrap resampling (see the documentation for the pvclust R package, (320)).

4.8 Supplementary Tables and Figures

Supplementary Table 4.1s. Prediction against yeast proteome (not included for reasons of length – will be available online)

Supplementary Table 4.2s. GO slim Cellular Component analysis of predicted Ste20p substrates

GO Slim Term	GO Slim Term Size	Overlap Size	p-value	Adjusted p-value
Cellular bud	160	47	3.71E-11	9.28E-10
Site of polarized growth	162	45	7.47E-10	9.34E-09
Cell cortex	105	33	5.04E-09	4.20E-08
Plasma membrane	265	53	3.68E-06	2.30E-05
Mitochondrion	1051	155	5.18E-06	2.59E-05
Cytoskeleton	203	43	6.92E-06	2.88E-05
Cytoplasm	2834	345	0.000476	0.001699
Vacuole	202	34	0.004684	0.014638
Nucleus	1794	221	0.005773	0.016035
Golgi apparatus	215	34	0.012190	0.030476
Other	384	54	0.020105	0.045693
Cytoplasmic membrane-bounded vesicle	103	18	0.024088	0.046322
Chromosome	249	37	0.023283	0.046322
Membrane	911	115	0.026463	0.047256

Supplementary Table 4.3s. GO slim Biological Process analysis of predicted Ste20p substrates.

GO Slim Term	GO Slim Term Size	Overlap Size	p-value	Adjusted p-value
Transcription	585	105	0.00019	0.00721
Anatomical structure morphogenesis	156	35	0.00073	0.01379
Cell budding	84	21	0.00207	0.02622
Carbohydrate metabolic process	189	38	0.00368	0.03498
Vesicle-mediated transport	340	61	0.00477	0.03626
Cytokinesis	116	25	0.00698	0.04424

Supplementary Table 4.4s. GO slim Molecular Function analysis of predicted Ste20p substrates.

GO Slim Term	GO Slim Term Size	Overlap Size	p-value	Adjusted p-value
Protein kinase activity	129	36	0.00001	0.00027
Lipid binding	53	19	0.00004	0.00042
Hydrolase activity	725	131	0.00013	0.00099

Supplementary Table 4.5s. Predicted substrates (score ≥ 0.9) in the neighbourhoods of STE20 genetic interactors. Adjusted p-values were not computed for genetic interactors with neighbourhoods that do not overlap with the predicted substrates.

STE20 Genetic Interactor	Neighbourhood Size	Overlap Size	p-value	Adjusted p-value
CDC42	84	26	8.39E-07	0.001982
SWE1	45	16	1.58E-05	0.006404
GIC2	24	10	0.000138	0.031707
BUB2	86	21	0.000423	0.042764
HSP82	1729	233	0.000507	0.042764
RAS2	136	28	0.001025	0.060549
CLA4	197	36	0.002091	0.080261
GIC1	28	9	0.002646	0.090666
SLG1	36	10	0.005113	0.118427
TAF9	141	25	0.013734	0.173212
STE4	30	8	0.015272	0.178672
KES1	25	7	0.017428	0.195614
BEM1	50	11	0.020991	0.206127
CDC28	61	12	0.037011	0.243204
STE12	44	9	0.053209	0.294332
WHI2	72	13	0.056568	0.305749
PMI40	4	2	0.065104	0.311286
BEM3	14	4	0.063669	0.311286
SEC14	61	11	0.076094	0.343404
HSL7	11	3	0.118118	0.356772
CDC34	45	8	0.127147	0.379673
SIC1	150	21	0.171830	0.442463
RGA1	13	3	0.173463	0.442463
SHO1	7	2	0.181741	0.444381
AKR1	8	2	0.225106	0.460346
KIN4	8	2	0.225106	0.460346
STE5	16	3	0.266171	0.511751
PUP3	3	1	0.301282	0.514553
CLB2	79	11	0.272907	0.514553
LTE1	269	33	0.325320	0.543426
RGA2	4	1	0.380007	0.554402
SSK1	11	2	0.356320	0.554402
STE11	45	6	0.396462	0.568879
SPO12	21	3	0.426868	0.603028
TEM1	21	3	0.426868	0.603028
NCP1	5	1	0.449874	0.603408
UBA4	13	2	0.439535	0.603408
OCH1	8	1	0.615726	0.706234
URM1	12	1	0.761898	0.805036
MSB2	7	0	1.000000	N/A
STE3	5	0	1.000000	N/A
SKM1	2	0	1.000000	N/A

Supplementary Table 4.6s. Predicted substrates (score ≥ 0.9) in the neighbourhoods of Ste20p physical interactors. Adjusted p-values were not computed for physical interactors with neighbourhoods that do not overlap with the predicted substrates.

Ste20p Physical Interactor	Neighbourhood Size	Overlap Size	p-value	Adjusted p-value
Cdc28p	241	67	4.81E-13	1.44E-09
Bem1p	26	10	0.000304	0.053593
Htb2p	81	18	0.003308	0.153509
Myo3p	30	9	0.004460	0.189745
Bmh1p	51	12	0.009550	0.258371
Cdc42p	29	8	0.012388	0.258371
Slt2p	48	11	0.015618	0.290825
Cbk1p	25	7	0.017428	0.311015
Asc1p	50	11	0.020991	0.328345
Cdc24p	23	6	0.037730	0.405232
Cbr1p	18	5	0.044005	0.448729
Hsl7p	8	3	0.051646	0.463581
Ste11p	25	6	0.054610	0.465113
Ubc6p	14	3	0.203407	0.630751
Bmh2p	67	10	0.217466	0.641066
Prp21p	42	6	0.333462	0.702544
Nup53p	26	4	0.335328	0.702638
Ste4p	26	4	0.335328	0.702638
Nbp2p	4	1	0.380007	0.705863
Htb1p	67	9	0.339866	0.705863
Ncp1p	13	2	0.439535	0.731411
Cln2p	46	6	0.417478	0.731411
Bem4p	16	2	0.552262	0.785380
Boi2p	10	1	0.697505	0.846607
Rad1p	31	3	0.694673	0.846607
Erb1p	84	8	0.744227	0.874634
Boi1p	13	1	0.788761	0.889489
Erg4p	2	0	1.000000	N/A
Bud8p	4	0	1.000000	N/A

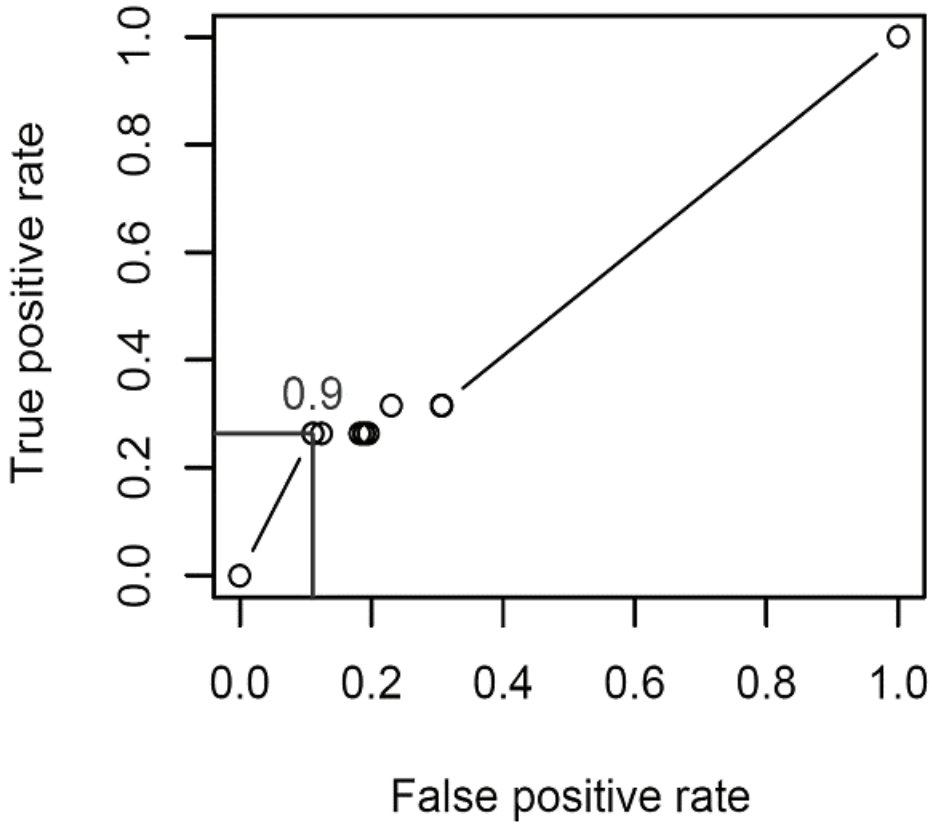

Supplementary Figure 4.1s. Receiver-Operator Characteristic (ROC) curve showing the estimated true and false positive rates of the Ste20p substrate predictor at different score thresholds. The rates associated with the threshold of 0.9 are indicated.


Height
0
1
2
3
4
5
6
SRO7
SNF2
SWI1
BOI1
MYO5
BLM10
EDE1
CHS3
KIN4
NUM1
DYN1
SHS1
DBP3
VIP1
CIN1
TEX1
HOC1
CSF1
VPS8
HIC1
HFA2
DNL4
SUT1
SAC1
SYG1
SST2
HCD1
MIH1
RAD51
MMS22
CTF18
SGS1
TOF1
PHO23
NAT1
RAD55
SPO14
PIK1
GCS1
YLR454W
MBP1
OSH3
KEX2
SEC5
ELP3
BFA1
NUP170
ECM5
CHO2
RPC40
SGO1
CDC27
SEC11
CYC8
SKG6
SSD1
MSB1
AXL2
BUD6
SPA2
BNI1
LTE1
CDC5
SPC110
STH1
RPO21
PAN1
KEM1
BUD1
MF1
HSL1
FKS1
MYO2
CDC7
PDS1
SIC1
FAB1
MSN2
BCK1
SWI4
RAD53
RIM2
RCA1
SLN1
SKN7
STE11
STE5
FAR1
RAD54
TOP3
NUP188
VAN1
RIM21
SNF5
SSN2
SPT7
MOT2
VRP1
HFI1
MSN2
MSN4
PGM1
UME6
IRA1
DPB4
BBC1
ASH1

Supplementary Figure 4.2s. Dendrogram of predicted substrates (score ≥ 0.9) clustered by their STE20 Genetic Interactor Neighbourhood (GIN) overlap profiles as in Figure 4.6A. Each branch point is labeled with an Approximately Unbiased (AU) score (see Materials and Methods) such that a score ≥ 95 corresponds to a p-value ≤ 0.05 indicating the significance of the cluster.

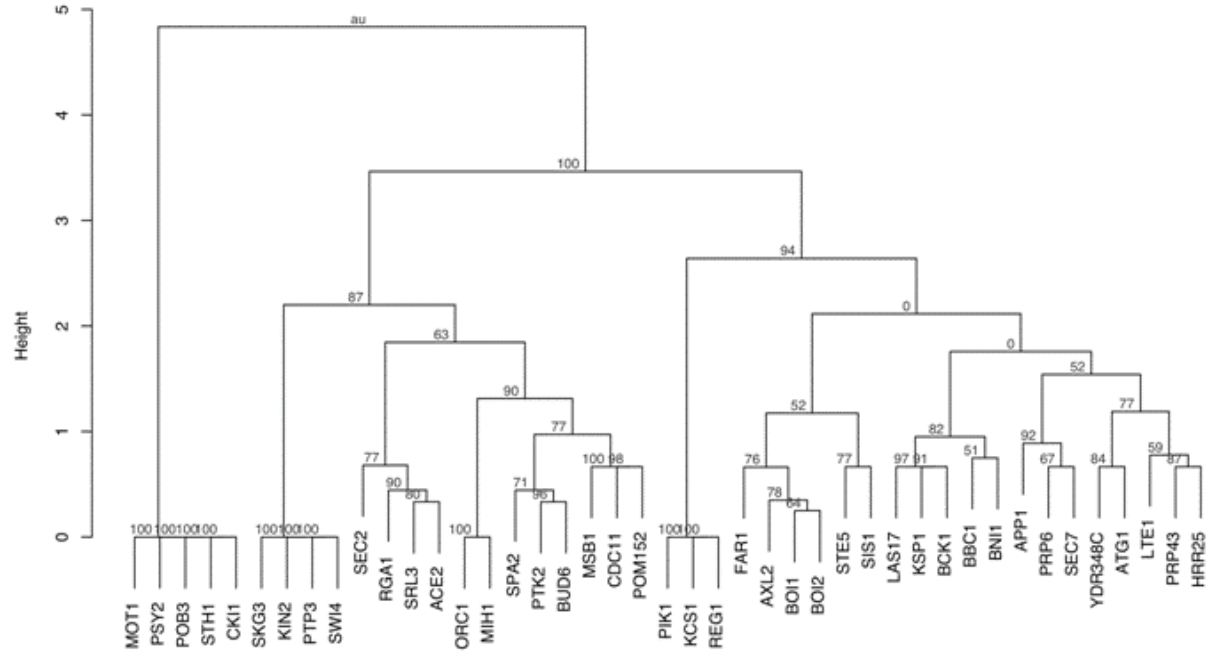

Supplementary Figure 4.3s. Dendrogram of predicted substrates (score ≥ 0.9) clustered by their Ste20p Physical Interactor Neighbourhood (PIN) overlap profiles as in Figure 4.7A. Each branch point is labeled with an Approximately Unbiased (AU) score (see Materials and Methods) such that a score ≥ 95 corresponds to a p-value ≤ 0.05 indicating the significance of the cluster.

CHAPTER FIVE

General Discussion

5.1 Summary

This study describes a novel role for the *S. cerevisiae* protein Rho5p as a regulator of cAMP-PKA signaling whose activity is controlled through regulation by phosphorylation and ubiquitination. This characterization provides a better understanding of this largely uncharacterized yeast GTPase and includes the first description of the regulation of a yeast Rho-family protein whose activity is regulated post-transcriptionally. This study also includes a biochemical genomics screen for *in vitro* substrates of the Cdc42p-effector Ste20p. The nuclear localization of Ste20p is described and a role for Ste20p in ribosomal biogenesis is suggested. The data from the screen was also used to generate a computational predictor for the identification of Ste20p substrates. This predictor employed motifs enriched in the Ste20p substrate set, and provides a significant improvement over background in the prediction of Ste20p phosphorylation. Genetic and physical interaction neighbourhoods provide biological context, and allow for the selection of potentially relevant physiological Ste20p substrates for further analysis. This analysis suggested polarisome components as likely targets for Ste20p phosphorylation; we confirmed that Bni1p and Bud6p are *in vitro* substrates for Ste20p, suggesting a link between Cdc42p activity and the polarization of polarisome-mediated actin filament assembly.

5.2 Rho5p's role and regulation in the cAMP-PKA pathway

Expression of an activated allele of *RHO5* (*RHO5*^{Q91H}) results in a number of phenotypes associated with elevated cAMP-PKA signaling, including haploid invasive growth, defects in glycogen storage, and diploid pseudohyphal growth. Additionally, the

expression of this allele exhibits synthetic growth defects with the cAMP-PKA pathway activator *RAS2*^{G19V} and rescues the lethality of a *Δras1 Δras2* mutant, suggesting its expression is sufficient to activate cAMP-PKA signaling in the absence of Ras proteins. The effects of *RHO5*^{Q91H} expression were suppressed in a *RHO5*^{Q91H} Δ*ste50* mutant by several known suppressors of hyperactive *RAS*, including *MSI1, PGM1,* and *PGM2* (161, 351). Thus, we conclude that Rho5p can regulate signaling of the Ras-associated cAMP-PKA pathway, and that this regulation is independent of Ras proteins.

The cooperation of Ras and Rho proteins in the regulation of pathways and processes has been widely observed (18). One type of cooperation involves direct interaction between the Ras and Rho proteins, where one activates the other. For instance, Ras signals through Rac in membrane ruffling in Swiss 3T3 cells (334). More commonly, Ras and Rho work in parallel to either transduce signals from common upstream targets to multiple downstream effectors, or to integrate signals from multiple upstream activators to common downstream effectors or effector pathways. For instance, signal integration between Ras and Rho proteins is observed in the activation of the transcription factor SRF, as mentioned in the Introduction. In this case, Ras and Cdc42/Rac can both activate the SRF through activation of ERK pathway signaling, and Rho proteins can also activate SRF through ERK-independent mechanisms. Ras and Rho signaling is also integrated into a variety of shared biological responses including cell-cycle progression, transformation, morphogenesis, and cell motility (18). In yeast, Ras2p and Cdc42p cooperate in the activation of the pseudohyphal growth MAPK, and expression of a dominant-negative *cdc42* allele blocks MAPK activation by activated *RAS2* (269).

The role of Rho5p in activation of cAMP-PKA signaling described here reveals another example of the integration of signaling from Ras and Rho proteins into a common pathway. cAMP-PKA signaling is controlled by two upstream pathways both of which are activated by extracellular glucose and converge on adenylyl cyclase (Cyr1p) (427). The first involves Ras2p, which is activated by its RhoGEF, Cdc25p. Ras2p, with Cdc25p and the cyclase-associated protein Srv2p, binds and activates cyclase resulting in the conversion of ATP to cAMP. The second branch upstream of cyclase consists of the heterotrimeric G-alpha subunit Gpa2p and its cognate receptor, Gpr1p. The mechanism of cyclase activation by this branch has not been described in budding yeast, but is assumed to involve direct binding between Gpa2p and cyclase, as observed in fission yeast (167). Given our observation that Rho5p associates with adenylyl cyclase in a two-hybrid assay, presumably through the Cyr1p RA domain, it is also possible that Rho5p may mediate the signaling between Gpa2p and cyclase. Indeed, G alpha subunits have previously been shown to signal through Rho GTPases in stress fiber formation and signal transduction (43, 352). Conversely, Rho5p may represent a novel third branch of input into adenylyl cyclase. Further work will be necessary to determine whether Rho5p and Gpa2p interact physically or genetically and should clarify the nature of Rho5p's participation in this pathway.

5.3 Rho5p involvement in cross-talk between cAMP-PKA and HOG signaling

The presence of a Ras-association (RA)-domain in Ste50p led to our identification of the ability of Ste50p and Rho5p to interact in an overlay assay (Chapter 2). Genetic analysis revealed that expression of an activated allele of *RHO5* (*rho5*^{Q91H}) in a *Δste50*

strain resulted in hyperosmotic sensitivity. It remains unclear whether Rho5p plays a direct role in the regulation of the hyperosmotic response. Rho5p may interact with components involved in the osmotic response in addition to Ste50p. Binding between Rho5p and Ste50p may represent one means of downregulating the pathway; the combination of *RHO5*^{Q91H} expression and *STE50* deletion thus would result in an increase in osmotic sensitivity. This would be in addition to the possible regulation by Rho5p of Ste50p's ability to participate in HOG MAPK pathway signaling; Ste50p is required for the MEKK Ste11p to signal effectively to the HOG pathway MEK Pbs2p (307). Perhaps activated Rho5p binds to Ste50p and sequesters it from participating in the signal, and thus acts to negatively regulate MAPK signaling directly. It is also possible, however, that the osmotic sensitivity of the *rho5*^{Q91H} *Δste50* strain is simply due to Rho5p-dependent activation of the cAMP-PKA pathway, and is independent of the Rho5p – Ste50p interaction. Indeed, a synthetic osmotic defect has previously been described between *Δste50* and an activated cAMP-PKA pathway due to the deletion of the high-affinity cAMP phosphodiesterase *PDE2* (306). According to this model, Rho5p's effect on the HOG response is indirect, and is solely due to the activation of cAMP-PKA signaling, and the resultant downregulation of the stress response. A third model derives from a combination of the first two: in this model, the activation of Rho5p during cAMP-PKA signaling results in an increased association between Rho5p and Ste50p, and thus inhibits the activation of the HOG pathway. In this way, the direct interaction between Rho5p and Ste50p may be involved in coordinating the two responses and ensuring that they are not coincidentally activated (Figure 5.1) Activation of the HOG pathway results in the induction of the cellular stress response, whereas

activation of the cAMP-PKA pathway results in its suppression, necessitating effective cross-talk (399).

Ste50p also participates in the Ras-activated pseudohyphal growth MAPK pathway associated with cAMP-PKA signaling. In both the HOG and pseudohyphal growth pathways, Ste50p serves to associate Ste11p to the membrane (172, 413). The selective targeting of Ste50p-Ste11p to the membrane is reported to involve either Opy2p or Cdc42p in the HOG and pseudohyphal growth pathways, respectively, though our study did not detect an interaction between Cdc42p and the Ste50p RA domain. Furthermore, Cdc42p has been implicated in HOG pathway activation (321, 393), and so is unlikely to be responsible for the selective association of Ste50p-Ste11p in one or the other pathway. Thus, given its association with Ste50 and its role in the activation of cAMP-PKA signaling, Rho5p represents a potential candidate for regulating Ste50p function *in vivo*.

5.4 Rho5p as an integrator of cAMP-PKA signaling and TOR signaling

A screen for suppressors of the osmotic sensitivity defect of the *rho5*^{Q91H} *Δste50* strain revealed several regulators of Rho5p activity. *RGD2* is a RhoGAP which has been shown to stimulate Rho5p GTPase activity *in vitro* (350). Its ability to suppress the defect associated with activated Rho5p is evidence that it is able to stimulate Rho5p GTPase activity *in vivo*. *MSI1*'s suppression of *rho5*^{Q91H} *Δste50* osmotic sensitivity suggested the

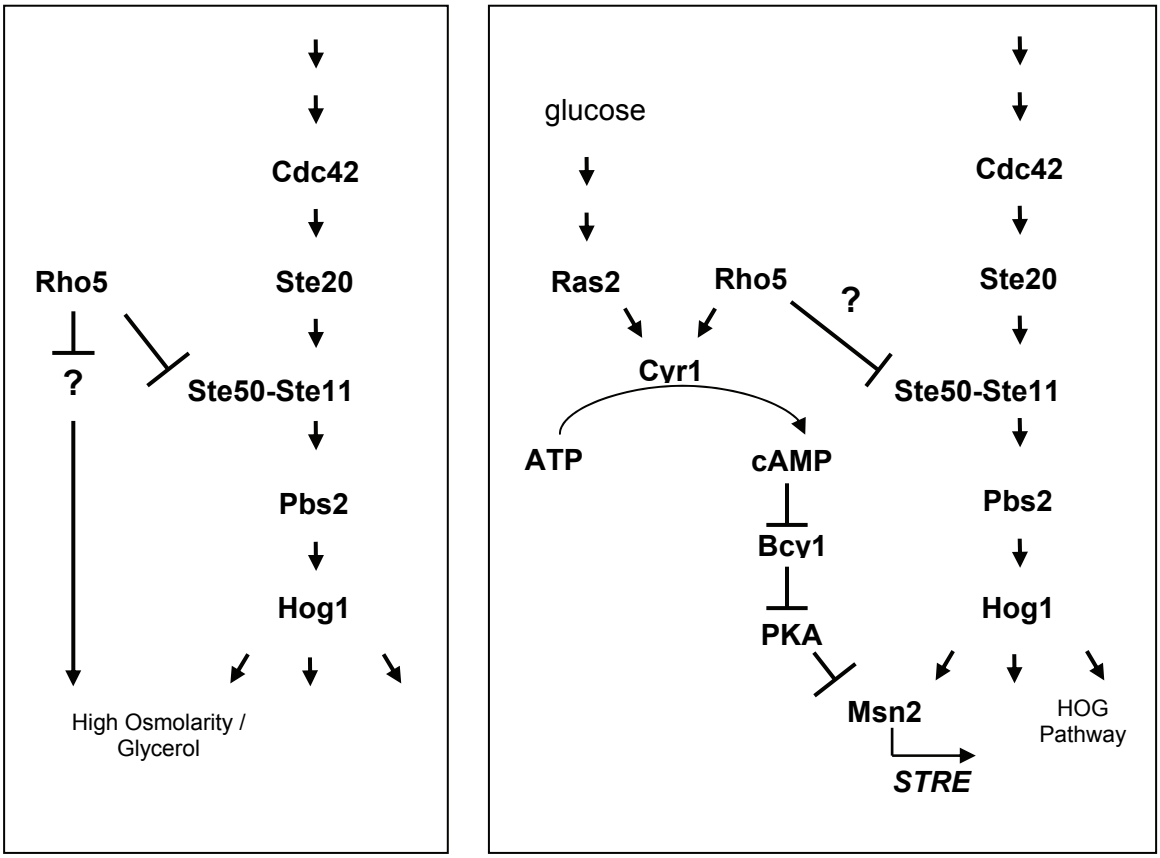

Figure 5.1. A model for Rho5p's involvement in the osmotic stress response. (*A*) Rho5p is directly involved in regulating the response to osmotic stress. Rho5p binding to Ste50p inhibits Ste50p function in the HOG MAPK pathway. Additionally, Rho5p inhibits the osmotic stress response via an unidentified cAMP-PKA-independent mechanism; (*B*) Rho5p's participation in the osmotic stress response is through the activation of cAMP-PKA signaling. Activation of PKA by Rho results in the downregulation of *STRE*-dependent transcription of genes involved in the stress response. This downregulation combined with HOG pathway inhibition in a *Δste50* mutant results in osmotic hypersensitivity. Also indicated is the possibility of the combination of the two models, wherein Rho5p activation of cAMP-PKA signaling is combined with Ste50p inhibition.

possibility of Rho5p regulation by phosphorylation and ubiquitination. Msi1p is the yeast homologue of retinoblastoma-associated protein 48 (RbAp48) and is a component of the chromatin assembly factor I (CAF-I) complex responsible for histone assembly on newly replicated DNA (186). *MSI1* was originally identified as a multicopy suppressor of *IRA1,* which encodes the RasGAP for Ras2p (351). The ability of *MSI1* overexpression to suppress the effects of Ras hyperactivity was shown to be unrelated to its function in CAF-I, but instead was due to its ability to sequester the kinase Npr1p in the nucleus (179). Npr1p is a cytoplasmic kinase whose phosphorylation antagonizes ubiquitin-mediated protein degradation of several nutrient transporters. Johnston *et al*. demonstrated that *MSI1*'s suppression of hyperactive Ras signaling involved the ubiquitination of a substrate involved in the pathway. This substrate is not Ras2p or any of its regulators; epistasis placed the regulation at or around the level of cyclase activation. Our results indicate that Rho5p activity is downregulated by *MSI1* overexpression or deletion of *NPR1* and that Rho5p is both phosphorylated by Npr1p and ubiquitinated. Genetics also suggest that ubiquitin-mediated proteasomal degradation is necessary to moderate the effects of Rho5p signaling. Combined with the observation that Rho5p can activate cAMP-PKA signaling, Rho5p thus presents a likely target for the observed *MSI1-NPR1* mediated regulation of Ras pathway signaling.

NPR1 is a nitrogen permease reactivator which encodes a kinase whose phosphorylation regulates the ubiquitin-mediated proteolysis of a number of cell permeases involved in nutrient uptake including: Tat2p, a tryptophan transporter; Mep2p an ammonium permease; Bap2p, a leucine permease; and Gap1p, the general amino acid permease (31, 79, 290, 360). Phosphorylation by Npr1p antagonizes ubiquitin-mediated

proteolysis of the high-affinity permeases Tat2p, Mep2p, and Bap2p, but promotes the ubiquitin-mediated proteolysis of the general amino-acid permease Gap1p. Npr1p activity is regulated by the target of rapamycin (TOR) signaling pathway (360), for which Npr1p represents the means of regulating amino acid permeases. TOR protein kinases (Tor1p and Tor2p) regulate protein synthesis and degradation in response to nutrient conditions (reviewed in (324)). In conditions of nutrient availability, TOR protein signaling activates protein translation and ribosome biogenesis, and inhibits autophagy and the expression of starvation-associated genes. Additionally, TOR controls the stability of amino acid permeases, and in conditions of nutrient availability results in the increased stability of high-affinity amino acid permeases and the reduced stability of general amino acid permeases. It accomplishes this by controlling the phosphorylation state of Npr1p through direct phosphorylation or dephosphorylation by type 2A phosphatases (Pph21p/22p and Sit4p) and their inhibitor Tap42p (360). Under nutrient rich conditions, activated TOR phosphorylates and inhibits Npr1p activity. Under starvation conditions, dephosphorylation of Npr1p results in its activation and the subsequent degradation of high-affinity permeases responsible for transporting amino acids essential for protein synthesis, but also the stabilization of the general amino acid permease which promotes the recruitment of amino acids which can be used as a nitrogen source (see (324)). Thus, Npr1p is a central component in the TOR signaling response to starvation.

As an activator of cAMP-PKA signaling, Rho5p participates in the regulation of the pathway responsible for regulating yeast carbon metabolism (342). As a target for Npr1p regulation, Rho5p thus represents a candidate target for mediating cross-talk

between the two metabolic pathways. Our results demonstrate that deletion of *NPR1* suppresses the effects of activated Rho5p signaling, suggesting that Npr1p phosphorylation likely inhibits Rho5p inactivation. According to a model wherein Npr1p phosphorylation of Rho5p represents a point of cross-talk between the pathways, nutrient-rich conditions result in TOR phosphorylation and inhibition of Npr1p, resulting in the inhibition of Rho5p and subsequent cAMP-PKA pathway downregulation (Figure 5.2). Under starvation conditions, Tap42-mediated dephosphorylation of Npr1p would result in the phosphorylation and subsequent stabilization of Rho5p thus allowing it to participate in cAMP-PKA pathway activation. Both pathways activate the expression of stress-response genes via Msn2p/4p-mediated transcription from *STRE* elements, and are implicated in growth under nutrient-rich conditions, so it is not obvious why an active TOR pathway should seek to downregulate the cAMP-PKA pathway. One explanation is that the negative regulation of Rho5p by TOR prevents hyperactivity of the cAMP-PKA pathway, which has been shown to result in phenotypic defects as described in Chapter III. Under nutrient-rich conditions, cAMP-PKA activity can still be stimulated by Ras proteins, and Rho5p activation of the cAMP-PKA pathway may be limited to conditions where the TOR pathway is inactivated, for instance in response to a spike in glucose levels after starvation. Further investigation will be required to better understand the Npr1p-Rho5p role in the cross-talk between the cAMP-PKA TOR pathways.

It is also possible that Rho5p may play a role in mediating cross-talk between other pathways as well. Rho5p has also been implicated in the regulation of the protein kinase C (PKC) cell integrity MAPK cascade (364). The PKC, cAMP-PKA, and TOR pathways have been shown to exhibit crosstalk in the response to caffeine (203). Rho5p

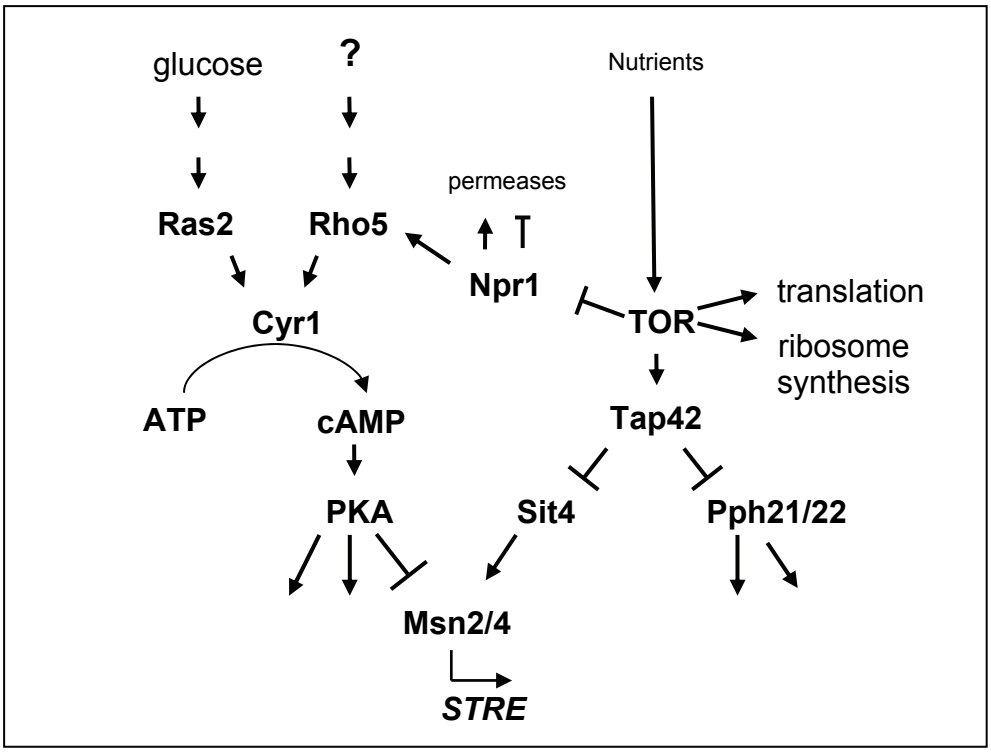

Figure 5.2. A model describing potential cross-talk between the cAMP-PKA and TOR pathways. The interaction between Rho5p and Npr1p represents an upstream link between the two pathways, which activate distinct downstream targets, but also converge on Msn2p/4p-regulated transcription of *STRE*-element promoters. The model suggests that activation of TOR pathway signaling results in the downregulation of Rho5p-mediated activation of cAMP-PKA signaling.

has also been implicated in the response to oxidative stress (380). As Rho proteins often serve as activators of multiple pathways and coordinators of cellular responses, it is clear that much remains to be determined about the ways in which Rho5p participates in these various pathways.

5.5 Computational Prediction of Ste20p substrates

The biochemical screen for *in vitro* substrates of Ste20p provided sufficient data for the creation of a computational predictor of substrates from the rest of the yeast proteome. The resultant predictor identified 22 motifs which exhibit at least a ten-fold enrichment compared to the proteome as a whole. Statistical analysis reveals that the predictor enriches substrates significantly above background level. By combining the predictor with Ste20's genetic and physical interaction neighbourhoods, it is possible to identify potentially biologically relevant Ste20p substrates. This analysis led to the identification of Bni1p and Bud6p as candidate Ste20p substrates, which were confirmed by *in vitro* kinase assays.

Consensus sites are usually used to identify potential sites of phosphorylation on proteins where phosphorylation has already been observed (416). Few kinases exhibit a strict enough consensus site to allow for the *a priori* identification of substrates. The cyclin-dependent kinase (CDK) in yeast (Cdc28p) exhibits a very strict consensus site requirement for phosphorylation, being an obligatory proline-directed kinase (276). A computational approach to the identification of CDK substrates in yeast found that the occurrence of a consensus site in a protein was insufficient to identify candidate substrates, given that roughly 1/3 of yeast proteins contains relevant sites (55). The

authors found, however, that considering global sequence characteristics, primarily the clustering of multiple CDK sites, made the prediction of CDK substrates possible. Thus, even when a strict and well-described consensus sequence exists, it is insufficient to predict novel substrates from primary sequence without consideration of global sequence characteristics. More dauntingly, few kinases meet the requisite requirement of a strict consensus site. A recent proteomic screen of kinases and substrates identified consensus sequences for only 13% of kinases (11 of 82); no consensus site has been described for Ste20p. The predictor described here uses bioinformatic techniques to discover the global sequence characteristics of Ste20p substrates, and employs multiple motifs in order to identify substrates computationally. While the predictor already improves the substrate identification capabilities above background levels, it is possible that employing an iterative process whereby a subset of high-scoring proteins is tested and the predictor is retrained may well provide increasing sensitivity. Such an approach may also provide greater insight into how the motifs interact to provide predictive power, which could result in a deeper appreciation of the biochemistry of Ste20p phosphorylation.

While this approach has proven valuable for the identification of novel substrates for Ste20p kinase, we believe the approach can be generalized for application with other kinases, including kinases from higher eukaryotes. One potential generalization of the approach takes advantage of the evolutionary conservation within kinase families. Related kinases from different species usually exhibit a conservation of substrate specificity. This has been demonstrated by the conservation of consensus sequences, where they exist, between members of kinase families in different species, for instance PKA or CDK (73). We thus hypothesized that the motifs employed by the predictor may

be conserved across eukaryotes, and that the Ste20p predictor may therefore identify potential substrates of Ste20p-related kinases in other organisms. As a brief test, we used the Ste20p predictor to rank the proteomes of various other organisms with posterior probabilities of being Ste20p substrates. The predictor scored 12% of *C. elegans* proteins as potential Ste20p substrates, similar to the 11% of proteins in the *S. cerevisiae* proteome. In other organisms, however, a much higher proportion of the proteome are designated as predicted substrates, with roughly 20% of proteins in *C. albicans, Drosophila,* mice, and humans scoring above 0.9. It is unclear why such differences exist. One explanation suggests that while the general motif corresponding to a consensus site in Ste20p substrates may be conserved, the motifs employed by the predictor designate localization signals or docking sites for proteins which are not widely conserved, and so may be present in greater quantities where they don't necessarily correlate with function. For instance, the Cdc42p GEF Cdc24p possesses similarity with related proteins in other species in the DH and PH domains, but otherwise exhibits considerable sequence divergence, and thus may not interact with PAKs in other organisms through exactly the same mechanisms as in yeast. Besides docking sites on Ste20p, predicted motifs may describe interactions with Ste20p-related scaffolds which may be yeast specific. For instance, the MAPK scaffold Ste5p does not seem to be conserved in higher eukaryotes. While the reasons remain unclear, it seems that despite the conservation of kinase families across eukaryotes, they retain species-specific elements of substrate identification.

It should, however, be possible to generalize this approach experimentally, by screening similar sets of yeast proteins with exogenous kinases directly. The availability

of reagents, especially libraries of fusion-tagged proteins makes the expression and purification of yeast proteins a straightforward process. Since the reactions are *in vitro*, any kinase which can be expressed in sufficient quantity and whose activity can be confirmed can be assayed. Yeast substrates represent the biochemical preferences of the particular kinase, and enriched motifs among the substrate set can then be used to scan relevant proteomes for potentially relevant targets.

5.6 Ste20p as a Cdc42p effector

Ste20p is a primary effector of Cdc42p in the control of actin cytoskeleton dynamics and in MAPK signaling. The combination of the biochemical predictor and genetic and physical interaction neighbourhoods suggest a number of possible Ste20p targets that may be involved in Cdc42p-related processes. These are genes which, like *STE20*, share a genetic interaction with *CDC42*, and are also predicted to be substrates of Ste20p.

Two such Cdc42p-related proteins were confirmed to be Ste20p substrates, as described in Chapter 4. *BNI1* and *BUD6* both interact genetically with *CDC42* (198). Additionally, Bni1p and Cdc42p interact physically through Bni1p's GBD (99). The binding of Cdc42p is thought to activate Bni1p activity by relieving autoinhibition, though the abrogation of this binding does not inhibit actin filament formation but results in depolarized actin cables (85). Given that *STE20* has been shown to be required for the activity of Bni1p (123), Ste20p represents a likely candidate to link Cdc42p and Bni1p activation. Indeed, a deletion of the region of *BNI1* phosphorylated by Ste20p results in deregulated supernumerary actin filament formation suggesting that this region is

essential for the control of Bni1p function *in vivo* (123). Furthermore, the combination of this *BNI1* C-terminal deletion allele with a *CLA4* deletion results in a phenotype similar to the *Δste20 Δcla4* terminal phenotype. Given that Bud6p activates Bni1p function by binding to this region, the coordinated phosphorylation of Bud6p and Bni1p represents a potentially sophisticated means of regulating actin assembly. Through its interaction with Ste20p, Cdc42p thus is able to control Bni1p-mediated actin filament formation and coordinate this process with other Cdc42-related processes at appropriate sites on the cell cortex.

Several other predicted substrates of Ste20p exhibit genetic and physical interactions with Cdc42p, and thus represent candidates for downstream targets of Cdc42p-Ste20p mediated processes. These include proteins which have been already implicated in Cdc42p-Ste20p-related processes such as polarity (Iqg1, Boi1p and Boi2p), budding, (Bem2p, Axl2p), and mitotic exit (Lte1p). Given that the mechanisms by which Cdc42p regulates these processes remain to be fully described, Cdc42p-mediated Ste20p phosphorylation of these substrates present potential targets for further examination. Additionally, novel roles for Cdc42p-Ste20p are suggested by other predicted substrates. For instance, several substrates (Elm1p, Hsl1p, Min1p) involved in mediating cell-cycle checkpoint control were identified as potential Ste20p substrates. While no role for Ste20p has been described in checkpoint regulation, Cdc42p has been shown to play a role in mediating the G2/M checkpoint, though the mechanism remains unclear (331). Ste20p phosphorylation of one or more of these predicted substrates thus represents a possible mechanism linking Cdc42p and checkpoint control. Thus, the predictor provides

suggestions into possible mechanisms of known pathways involving Cdc42p, and further work should provide more detail into how these mechanisms interact.

5.7 Conclusions

This study expands our understanding of the roles and regulation of the yeast GTPases Rho5p and Cdc42p. It describes a novel role and regulatory mechanism of the Rho-type GTPase Rho5p and provides insight into signaling downstream of Cdc42p by describing a biochemical genomics screen using the Cdc42p-effector Ste20p, with the subsequent generation of a computational predictor of Ste20p substrates. Rho GTPases in yeast are central to numerous processes, and yet they remain largely uncharacterized. Equally, though many Rho GTPases have been identified across higher eukaryotes, a detailed understanding of their roles and regulation exists for only a few. Ongoing work will continue to expand our understanding of this large family and its diverse cellular roles.

References

1. **Abo, A., M. R. Webb, A. Grogan, and A. W. Segal.** 1994. Activation of NADPH oxidase involves the dissociation of p21rac from its inhibitory GDP/GTP exchange protein (rhoGDI) followed by its translocation to the plasma membrane. Biochem J **298 Pt 3:**585-91.

2. **Adamo, J. E., J. J. Moskow, A. S. Gladfelter, D. Viterbo, D. J. Lew, and P. J. Brennwald.** 2001. Yeast Cdc42 functions at a late step in exocytosis, specifically during polarized growth of the emerging bud. J Cell Biol **155:**581-92.

3. **Adamo, J. E., G. Rossi, and P. Brennwald.** 1999. The Rho GTPase Rho3 has a direct role in exocytosis that is distinct from its role in actin polarity. Mol Biol Cell **10:**4121-33.

4. **Adams, A. E., D. I. Johnson, R. M. Longnecker, B. F. Sloat, and J. R. Pringle.** 1990. CDC42 and CDC43, two additional genes involved in budding and the establishment of cell polarity in the yeast Saccharomyces cerevisiae. J Cell Biol **111:**131-42.

5. **Aepfelbacher, M., C. Trasak, G. Wilharm, A. Wiedemann, K. Trulzsch, K. Krauss, P. Gierschik, and J. Heesemann.** 2003. Characterization of YopT effects on Rho GTPases in Yersinia enterocolitica-infected cells. J Biol Chem **278:**33217-23.

6. **Ahn, S. H., W. L. Cheung, J. Y. Hsu, R. L. Diaz, M. M. Smith, and C. D. Allis.** 2005. Sterile 20 kinase phosphorylates histone H2B at serine 10 during hydrogen peroxide-induced apoptosis in S. cerevisiae. Cell **120:**25-36.

7. **Aktories, K., C. Mohr, and G. Koch.** 1992. Clostridium botulinum C3 ADP-ribosyltransferase. Curr Top Microbiol Immunol **175:**115-31.

8. **Allal, C., A. Pradines, A. D. Hamilton, S. M. Sebti, and G. Favre.** 2002. Farnesylated RhoB prevents cell cycle arrest and actin cytoskeleton disruption caused by the geranylgeranyltransferase I inhibitor GGTI-298. Cell Cycle **1:**430-7.

9. **Allen, W. E., D. Zicha, A. J. Ridley, and G. E. Jones.** 1998. A role for Cdc42 in macrophage chemotaxis. J Cell Biol **141:**1147-57.

10. **Alonso-Monge, R., E. Real, I. Wojda, J. P. Bebelman, W. H. Mager, and M. Siderius.** 2001. Hyperosmotic stress response and regulation of cell wall integrity in Saccharomyces cerevisiae share common functional aspects. Mol Microbiol **41:**717-30.

11. **Amberg, D. C., J. E. Zahner, J. W. Mulholland, J. R. Pringle, and D. Botstein.** 1997. Aip3p/Bud6p, a yeast actin-interacting protein that is involved in morphogenesis and the selection of bipolar budding sites. Mol Biol Cell **8:**729-53.

12. **Annan, R. B., C. Wu, D. D. Waller, M. Whiteway, and D. Y. Thomas.** 2008. Rho5p is involved in mediating the osmotic stress response in Saccharomyces cerevisiae, and its activity is regulated via Msi1p and Npr1p by phosphorylation and ubiquitination. Eukaryot Cell **7:**1441-9.

13. **Ash, J., C. Wu, R. Larocque, M. Jamal, W. Stevens, M. Osborne, D. Y. Thomas, and M. Whiteway.** 2003. Genetic analysis of the interface between Cdc42p and the CRIB domain of Ste20p in Saccharomyces cerevisiae. Genetics **163:**9-20.

14. **Ashburner, M., C. A. Ball, J. A. Blake, D. Botstein, H. Butler, J. M. Cherry, A. P. Davis, K. Dolinski, S. S. Dwight, J. T. Eppig, M. A. Harris, D. P. Hill, L. Issel-Tarver, A. Kasarskis, S. Lewis, J. C. Matese, J. E. Richardson, M. Ringwald, G. M. Rubin, and G. Sherlock.** 2000. Gene ontology: tool for the unification of biology. The Gene Ontology Consortium. Nat Genet **25:**25-9.

15. **Askham, J. M., P. Moncur, A. F. Markham, and E. E. Morrison.** 2000. Regulation and function of the interaction between the APC tumour suppressor protein and EB1. Oncogene **19:**1950-8.

16. **Bagrodia, S., B. Derijard, R. J. Davis, and R. A. Cerione.** 1995. Cdc42 and PAK-mediated signaling leads to Jun kinase and p38 mitogen-activated protein kinase activation. J Biol Chem **270:**27995-8.

17. **Baim, S. B., D. F. Pietras, D. C. Eustice, and F. Sherman.** 1985. A mutation allowing an mRNA secondary structure diminishes translation of Saccharomyces cerevisiae iso-1-cytochrome c. Mol Cell Biol **5:**1839-46.

18. **Bar-Sagi, D., and A. Hall.** 2000. Ras and Rho GTPases: a family reunion. Cell **103:**227-38.

19. **Baroni, M. D., E. Martegani, P. Monti, and L. Alberghina.** 1989. Cell size modulation by CDC25 and RAS2 genes in Saccharomyces cerevisiae. Mol Cell Biol **9:**2715-23.

20. **Barry, D. M., and S. R. Wente.** 2000. Nuclear transport: never-ending cycles of signals and receptors. Essays Biochem **36:**89-103.

21. **Bender, A., and J. R. Pringle.** 1989. Multicopy suppression of the cdc24 budding defect in yeast by CDC42 and three newly identified genes including the ras-related gene RSR1. Proc Natl Acad Sci U S A **86:**9976-80.

22. **Bender, L., H. S. Lo, H. Lee, V. Kokojan, V. Peterson, and A. Bender.** 1996. Associations among PH and SH3 domain-containing proteins and Rho-type GTPases in Yeast. J Cell Biol **133:**879-94.

23. **Benjamini, Y., Hochberg, Yosef.** 1995. Controlling the False Discovery Rate: A Practical and Powerful Approach to Multiple Testing. Journal of the Royal Statistical Society. Series B (Methodological) **57:**289-300.

24. **Berzat, A. C., J. E. Buss, E. J. Chenette, C. A. Weinbaum, A. Shutes, C. J. Der, A. Minden, and A. D. Cox.** 2005. Transforming activity of the Rho family GTPase, Wrch-1, a Wnt-regulated Cdc42 homolog, is dependent on a novel carboxyl-terminal palmitoylation motif. J Biol Chem **280:**33055-65.

25. **Bhattacharyya, R. P., A. Remenyi, B. J. Yeh, and W. A. Lim.** 2006. Domains, Motifs, and Scaffolds: The Role of Modular Interactions in the Evolution and Wiring of Cell Signaling Circuits. Annu Rev Biochem.

26. **Bi, E., J. B. Chiavetta, H. Chen, G. C. Chen, C. S. Chan, and J. R. Pringle.** 2000. Identification of novel, evolutionarily conserved Cdc42p-interacting proteins and of redundant pathways linking Cdc24p and Cdc42p to actin polarization in yeast. Mol Biol Cell **11:**773-93.

27. **Bishop, A. L., and A. Hall.** 2000. Rho GTPases and their effector proteins. Biochem J **348 Pt 2:**241-55.

28. **Blom, N., S. Gammeltoft, and S. Brunak.** 1999. Sequence and structure-based prediction of eukaryotic protein phosphorylation sites. J Mol Biol **294:**1351-62.

29. **Blondel, M., P. M. Alepuz, L. S. Huang, S. Shaham, G. Ammerer, and M. Peter.** 1999. Nuclear export of Far1p in response to pheromones requires the export receptor Msn5p/Ste21p. Genes Dev **13:**2284-300.

30. **Blondel, M., J. M. Galan, Y. Chi, C. Lafourcade, C. Longaretti, R. J. Deshaies, and M. Peter.** 2000. Nuclear-specific degradation of Far1 is controlled by the localization of the F-box protein Cdc4. Embo J **19:**6085-97.

31. **Boeckstaens, M., B. Andre, and A. M. Marini.** 2007. The yeast ammonium transport protein Mep2 and its positive regulator, the Npr1 kinase, play an important role in normal and pseudohyphal growth on various nitrogen media through retrieval of excreted ammonium. Mol Microbiol **64:**534-46.

32. **Bokoch, G. M.** 2003. Biology of the p21-activated kinases. Annu Rev Biochem **72:**743-81.

33. **Bokoch, G. M., Y. Wang, B. P. Bohl, M. A. Sells, L. A. Quilliam, and U. G. Knaus.** 1996. Interaction of the Nck adapter protein with p21-activated kinase (PAK1). J Biol Chem **271:**25746-9.

34. **Bolis, A., S. Corbetta, A. Cioce, and I. de Curtis.** 2003. Differential distribution of Rac1 and Rac3 GTPases in the developing mouse brain: implications for a role of Rac3 in Purkinje cell differentiation. Eur J Neurosci **18:**2417-24.

35. **Bos, J. L.** 1989. ras oncogenes in human cancer: a review. Cancer Res **49:**4682-9.

36. **Bose, I., J. E. Irazoqui, J. J. Moskow, E. S. Bardes, T. R. Zyla, and D. J. Lew.** 2001. Assembly of scaffold-mediated complexes containing Cdc42p, the exchange factor Cdc24p, and the effector Cla4p required for cell cycle-regulated phosphorylation of Cdc24p. J Biol Chem **276:**7176-86.

37. **Bourmeyster, N., and P. V. Vignais.** 1996. Phosphorylation of Rho GDI stabilizes the Rho A-Rho GDI complex in neutrophil cytosol. Biochem Biophys Res Commun **218:**54-60.

38. **Breitkreutz, B. J., C. Stark, T. Reguly, L. Boucher, A. Breitkreutz, M. Livstone, R. Oughtred, D. H. Lackner, J. Bahler, V. Wood, K. Dolinski, and M. Tyers.** 2008. The BioGRID Interaction Database: 2008 update. Nucleic Acids Res **36:**D637-40.

39. **Brennwald, P., B. Kearns, K. Champion, S. Keranen, V. Bankaitis, and P. Novick.** 1994. Sec9 is a SNAP-25-like component of a yeast SNARE complex that may be the effector of Sec4 function in exocytosis. Cell **79:**245-58.

40. **Brinkworth, R. I., R. A. Breinl, and B. Kobe.** 2003. Structural basis and prediction of substrate specificity in protein serine/threonine kinases. Proc Natl Acad Sci U S A **100:**74-9.

41. **Broach, J. R.** 1991. RAS genes in Saccharomyces cerevisiae: signal transduction in search of a pathway. Trends Genet **7:**28-33.

42. **Brouns, M. R., S. F. Matheson, and J. Settleman.** 2001. p190 RhoGAP is the principal Src substrate in brain and regulates axon outgrowth, guidance and fasciculation. Nat Cell Biol **3:**361-7.

43. **Buhl, A. M., N. L. Johnson, N. Dhanasekaran, and G. L. Johnson.** 1995. G alpha 12 and G alpha 13 stimulate Rho-dependent stress fiber formation and focal adhesion assembly. J Biol Chem **270:**24631-4.

44. **Burbelo, P. D., D. Drechsel, and A. Hall.** 1995. A conserved binding motif defines numerous candidate target proteins for both Cdc42 and Rac GTPases. J Biol Chem **270:**29071-4.

45. **Bustelo, X. R., V. Sauzeau, and I. M. Berenjeno.** 2007. GTP-binding proteins of the Rho/Rac family: regulation, effectors and functions in vivo. Bioessays **29:**356-70.

46. **Butty, A. C., N. Perrinjaquet, A. Petit, M. Jaquenoud, J. E. Segall, K. Hofmann, C. Zwahlen, and M. Peter.** 2002. A positive feedback loop stabilizes the guanine-nucleotide exchange factor Cdc24 at sites of polarization. Embo J **21:**1565-76.

47. **Butty, A. C., P. M. Pryciak, L. S. Huang, I. Herskowitz, and M. Peter.** 1998. The role of Far1p in linking the heterotrimeric G protein to polarity establishment proteins during yeast mating. Science **282:**1511-6.

48. **Cahill, M. A., R. Janknecht, and A. Nordheim.** 1996. Signalling pathways: jack of all cascades. Curr Biol **6:**16-9.

49. **Caloca, M. J., M. L. Garcia-Bermejo, P. M. Blumberg, N. E. Lewin, E. Kremmer, H. Mischak, S. Wang, K. Nacro, B. Bienfait, V. E. Marquez, and M. G. Kazanietz.** 1999. beta2-chimaerin is a novel target for diacylglycerol: binding properties and changes in subcellular localization mediated by ligand binding to its C1 domain. Proc Natl Acad Sci U S A **96:**11854-9.

50. **Cannon, J. F., J. R. Pringle, A. Fiechter, and M. Khalil.** 1994. Characterization of glycogen-deficient glc mutants of Saccharomyces cerevisiae. Genetics **136:**485-503.

51. **Cau, J., and A. Hall.** 2005. Cdc42 controls the polarity of the actin and microtubule cytoskeletons through two distinct signal transduction pathways. J Cell Sci **118:**2579-87.

52. **Caviston, J. P., M. Longtine, J. R. Pringle, and E. Bi.** 2003. The role of Cdc42p GTPase-activating proteins in assembly of the septin ring in yeast. Mol Biol Cell **14:**4051-66.

53. **Caviston, J. P., S. E. Tcheperegine, and E. Bi.** 2002. Singularity in budding: a role for the evolutionarily conserved small GTPase Cdc42p. Proc Natl Acad Sci U S A **99:**12185-90.

54. **Chan, P. M., L. Lim, and E. Manser.** 2008. PAK is regulated by PI3K, PIX, Cdc42 and PP2Calpha and mediates focal adhesion turnover in the hyperosmotic stress-induced P38 pathway. J Biol Chem.

55. **Chang, E. J., R. Begum, B. T. Chait, and T. Gaasterland.** 2007. Prediction of cyclin-dependent kinase phosphorylation substrates. PLoS ONE **2:**e656.

56. **Charizanis, C., H. Juhnke, B. Krems, and K. D. Entian.** 1999. The oxidative stress response mediated via Pos9/Skn7 is negatively regulated by the Ras/PKA pathway in Saccharomyces cerevisiae. Mol Gen Genet **261:**740-52.

57. **Chaudhary, A., W. G. King, M. D. Mattaliano, J. A. Frost, B. Diaz, D. K. Morrison, M. H. Cobb, M. S. Marshall, and J. S. Brugge.** 2000. Phosphatidylinositol 3-kinase regulates Raf1 through Pak phosphorylation of serine 338. Curr Biol **10:**551-4.

58. **Chen, R. E., and J. Thorner.** 2007. Function and regulation in MAPK signaling pathways: lessons learned from the yeast Saccharomyces cerevisiae. Biochim Biophys Acta **1773:**1311-40.

59. **Chen, Z. J.** 2005. Ubiquitin signalling in the NF-kappaB pathway. Nat Cell Biol **7:**758-65.

60. **Cheng, J., A. Z. Randall, M. J. Sweredoski, and P. Baldi.** 2005. SCRATCH: a protein structure and structural feature prediction server. Nucleic Acids Res **33:**W72-6.

61. **Chenna, R., H. Sugawara, T. Koike, R. Lopez, T. J. Gibson, D. G. Higgins, and J. D. Thompson.** 2003. Multiple sequence alignment with the Clustal series of programs. Nucleic Acids Res **31:**3497-500.

62. **Chester, V. E.** 1968. Heritable glycogen-storage deficiency in yeast and its induction by ultra-violet light. J Gen Microbiol **51:**49-56.

63. **Cheung, W. L., K. Ajiro, K. Samejima, M. Kloc, P. Cheung, C. A. Mizzen, A. Beeser, L. D. Etkin, J. Chernoff, W. C. Earnshaw, and C. D. Allis.** 2003. Apoptotic phosphorylation of histone H2B is mediated by mammalian sterile twenty kinase. Cell **113:**507-17.

64. **Chew, T. L., R. A. Masaracchia, Z. M. Goeckeler, and R. B. Wysolmerski.** 1998. Phosphorylation of non-muscle myosin II regulatory light chain by p21-activated kinase (gamma-PAK). J Muscle Res Cell Motil **19:**839-54.

65. **Chhabra, E. S., and H. N. Higgs.** 2007. The many faces of actin: matching assembly factors with cellular structures. Nat Cell Biol **9:**1110-21.

66. **Chiroli, E., R. Fraschini, A. Beretta, M. Tonelli, G. Lucchini, and S. Piatti.** 2003. Budding yeast PAK kinases regulate mitotic exit by two different mechanisms. J Cell Biol **160:**857-74.

67. **Chow, T. Y., E. L. Perkins, and M. A. Resnick.** 1992. Yeast RNC1 encodes a chimeric protein, RhoNUC, with a human rho motif and deoxyribonuclease activity. Nucleic Acids Res **20:**5215-21.

68. **Chuang, T. H., X. Xu, U. G. Knaus, M. J. Hart, and G. M. Bokoch.** 1993. GDP dissociation inhibitor prevents intrinsic and GTPase activating protein-stimulated GTP hydrolysis by the Rac GTP-binding protein. J Biol Chem **268:**775-8.

69. **Cohen, P.** 2000. The regulation of protein function by multisite phosphorylation--a 25 year update. Trends Biochem Sci **25:**596-601.

70. **Coles, L. C., and P. E. Shaw.** 2002. PAK1 primes MEK1 for phosphorylation by Raf-1 kinase during cross-cascade activation of the ERK pathway. Oncogene **21:**2236-44.

71. **Coso, O. A., M. Chiariello, J. C. Yu, H. Teramoto, P. Crespo, N. Xu, T. Miki, and J. S. Gutkind.** 1995. The small GTP-binding proteins Rac1 and Cdc42 regulate the activity of the JNK/SAPK signaling pathway. Cell **81:**1137-46.

72. **Cotteret, S., Z. M. Jaffer, A. Beeser, and J. Chernoff.** 2003. p21-Activated kinase 5 (Pak5) localizes to mitochondria and inhibits apoptosis by phosphorylating BAD. Mol Cell Biol **23:**5526-39.

73. **Cribbs, J. T., and S. Strack.** 2007. Reversible phosphorylation of Drp1 by cyclic AMP-dependent protein kinase and calcineurin regulates mitochondrial fission and cell death. EMBO Rep **8:**939-44.

74. **Cullen, B. R.** 1996. HIV-1: is Nef a PAK animal? Curr Biol **6:**1557-9.

75. **Cullen, P. J., and G. F. Sprague, Jr.** 2000. Glucose depletion causes haploid invasive growth in yeast. Proc Natl Acad Sci U S A **97:**13619-24.

76. **Cvrckova, F., C. De Virgilio, E. Manser, J. R. Pringle, and K. Nasmyth.** 1995. Ste20-like protein kinases are required for normal localization of cell growth and for cytokinesis in budding yeast. Genes Dev **9:**1817-30.

77. **Dan, I., N. M. Watanabe, and A. Kusumi.** 2001. The Ste20 group kinases as regulators of MAP kinase cascades. Trends Cell Biol **11:**220-30.

78. **Daub, H., K. Gevaert, J. Vandekerckhove, A. Sobel, and A. Hall.** 2001. Rac/Cdc42 and p65PAK regulate the microtubule-destabilizing protein stathmin through phosphorylation at serine 16. J Biol Chem **276:**1677-80.

79. **De Craene, J. O., O. Soetens, and B. Andre.** 2001. The Npr1 kinase controls biosynthetic and endocytic sorting of the yeast Gap1 permease. J Biol Chem **276:**43939-48.

80. **Delley, P. A., and M. N. Hall.** 1999. Cell wall stress depolarizes cell growth via hyperactivation of RHO1. J Cell Biol **147:**163-74.

81. **DerMardirossian, C., A. Schnelzer, and G. M. Bokoch.** 2004. Phosphorylation of RhoGDI by Pak1 mediates dissociation of Rac GTPase. Mol Cell **15:**117-27.

82. **Dharmawardhane, S., and G. M. Bokoch.** 1997. Rho GTPases and leukocyte cytoskeletal regulation. Curr Opin Hematol **4:**12-8.

83. **Dharmawardhane, S., A. Schurmann, M. A. Sells, J. Chernoff, S. L. Schmid, and G. M. Bokoch.** 2000. Regulation of macropinocytosis by p21-activated kinase-1. Mol Biol Cell **11:**3341-52.

84. **Diekmann, D., A. Abo, C. Johnston, A. W. Segal, and A. Hall.** 1994. Interaction of Rac with p67phox and regulation of phagocytic NADPH oxidase activity. Science **265:**531-3.

85. **Dong, Y., D. Pruyne, and A. Bretscher.** 2003. Formin-dependent actin assembly is regulated by distinct modes of Rho signaling in yeast. J Cell Biol **161:**1081-92.

86. **Doye, A., A. Mettouchi, G. Bossis, R. Clement, C. Buisson-Touati, G. Flatau, L. Gagnoux, M. Piechaczyk, P. Boquet, and E. Lemichez.** 2002. CNF1 exploits the ubiquitin-proteasome machinery to restrict Rho GTPase activation for bacterial host cell invasion. Cell **111:**553-64.

87. **Drechsel, D. N., A. A. Hyman, A. Hall, and M. Glotzer.** 1997. A requirement for Rho and Cdc42 during cytokinesis in Xenopus embryos. Curr Biol **7:**12-23.

88. **Drgonova, J., T. Drgon, D. H. Roh, and E. Cabib.** 1999. The GTP-binding protein Rho1p is required for cell cycle progression and polarization of the yeast cell. J Cell Biol **146:**373-87.

89. **Drgonova, J., T. Drgon, K. Tanaka, R. Kollar, G. C. Chen, R. A. Ford, C. S. Chan, Y. Takai, and E. Cabib.** 1996. Rho1p, a yeast protein at the interface between cell polarization and morphogenesis. Science **272:**277-9.

90. **Drogen, F., S. M. O'Rourke, V. M. Stucke, M. Jaquenoud, A. M. Neiman, and M. Peter.** 2000. Phosphorylation of the MEKK Ste11p by the PAK-like kinase Ste20p is required for MAP kinase signaling in vivo. Curr Biol **10:**630-9.

91. **Du, W., P. F. Lebowitz, and G. C. Prendergast.** 1999. Cell growth inhibition by farnesyltransferase inhibitors is mediated by gain of geranylgeranylated RhoB. Mol Cell Biol **19:**1831-40.

92. **Eby, J. J., S. P. Holly, F. van Drogen, A. V. Grishin, M. Peter, D. G. Drubin, and K. J. Blumer.** 1998. Actin cytoskeleton organization regulated by the PAK family of protein kinases. Curr Biol **8:**967-70.

93. **Ellenbroek, S. I., and J. G. Collard.** 2007. Rho GTPases: functions and association with cancer. Clin Exp Metastasis **24:**657-72.

94. **Ellerbroek, S. M., K. Wennerberg, and K. Burridge.** 2003. Serine phosphorylation negatively regulates RhoA in vivo. J Biol Chem **278:**19023-31.

95. **Ellison, M. J., and M. Hochstrasser.** 1991. Epitope-tagged ubiquitin. A new probe for analyzing ubiquitin function. J Biol Chem **266:**21150-7.

96. **Estruch, F., and M. Carlson.** 1993. Two homologous zinc finger genes identified by multicopy suppression in a SNF1 protein kinase mutant of Saccharomyces cerevisiae. Mol Cell Biol **13:**3872-81.

97. **Etienne-Manneville, S., and A. Hall.** 2003. Cdc42 regulates GSK-3beta and adenomatous polyposis coli to control cell polarity. Nature **421:**753-6.

98. **Etienne-Manneville, S., and A. Hall.** 2002. Rho GTPases in cell biology. Nature **420:**629-35.

99. **Evangelista, M., K. Blundell, M. S. Longtine, C. J. Chow, N. Adames, J. R. Pringle, M. Peter, and C. Boone.** 1997. Bni1p, a yeast formin linking cdc42p and the actin cytoskeleton during polarized morphogenesis. Science **276:**118-22.

100. **Falbo, V., T. Pace, L. Picci, E. Pizzi, and A. Caprioli.** 1993. Isolation and nucleotide sequence of the gene encoding cytotoxic necrotizing factor 1 of Escherichia coli. Infect Immun **61:**4909-14.

101. **Faux, M. C., and J. D. Scott.** 1996. More on target with protein phosphorylation: conferring specificity by location. Trends Biochem Sci **21:**312-5.

102. **Feramisco, J. R., M. Gross, T. Kamata, M. Rosenberg, and R. W. Sweet.** 1984. Microinjection of the oncogene form of the human H-ras (T-24) protein results in rapid proliferation of quiescent cells. Cell **38:**109-17.

103. **Fievet, B. T., A. Gautreau, C. Roy, L. Del Maestro, P. Mangeat, D. Louvard, and M. Arpin.** 2004. Phosphoinositide binding and phosphorylation act sequentially in the activation mechanism of ezrin. J Cell Biol **164:**653-9.

104. **Filippi, M. D., C. E. Harris, J. Meller, Y. Gu, Y. Zheng, and D. A. Williams.** 2004. Localization of Rac2 via the C terminus and aspartic acid 150 specifies superoxide generation, actin polarity and chemotaxis in neutrophils. Nat Immunol **5:**744-51.

105. **Finger, F. P., T. E. Hughes, and P. Novick.** 1998. Sec3p is a spatial landmark for polarized secretion in budding yeast. Cell **92:**559-71.

106. **Flatau, G., E. Lemichez, M. Gauthier, P. Chardin, S. Paris, C. Fiorentini, and P. Boquet.** 1997. Toxin-induced activation of the G protein p21 Rho by deamidation of glutamine. Nature **387:**729-33.

107. **Forget, M. A., R. R. Desrosiers, D. Gingras, and R. Beliveau.** 2002. Phosphorylation states of Cdc42 and RhoA regulate their interactions with Rho GDP dissociation inhibitor and their extraction from biological membranes. Biochem J **361:**243-54.

108. **Frost, J. A., A. Khokhlatchev, S. Stippec, M. A. White, and M. H. Cobb.** 1998. Differential effects of PAK1-activating mutations reveal activity-dependent and -independent effects on cytoskeletal regulation. J Biol Chem **273:**28191-8.

109. **Frost, J. A., H. Steen, P. Shapiro, T. Lewis, N. Ahn, P. E. Shaw, and M. H. Cobb.** 1997. Cross-cascade activation of ERKs and ternary complex factors by Rho family proteins. Embo J **16:**6426-38.

110. **Fukumoto, Y., K. Kaibuchi, Y. Hori, H. Fujioka, S. Araki, T. Ueda, A. Kikuchi, and Y. Takai.** 1990. Molecular cloning and characterization of a novel type of regulatory protein (GDI) for the rho proteins, ras p21-like small GTP-binding proteins. Oncogene **5:**1321-8.

111. **Fukunaga, R., and T. Hunter.** 1997. MNK1, a new MAP kinase-activated protein kinase, isolated by a novel expression screening method for identifying protein kinase substrates. Embo J **16:**1921-33.

112. **Gallagher, E. D., S. Xu, C. Moomaw, C. A. Slaughter, and M. H. Cobb.** 2002. Binding of JNK/SAPK to MEKK1 is regulated by phosphorylation. J Biol Chem **277:**45785-92.

113. **Garcia-Ranea, J. A., and A. Valencia.** 1998. Distribution and functional diversification of the ras superfamily in Saccharomyces cerevisiae. FEBS Lett **434:**219-25.

114. **Gardiner, E. M., K. N. Pestonjamasp, B. P. Bohl, C. Chamberlain, K. M. Hahn, and G. M. Bokoch.** 2002. Spatial and temporal analysis of Rac activation during live neutrophil chemotaxis. Curr Biol **12:**2029-34.

115. **Garrett, M. D., G. N. Major, N. Totty, and A. Hall.** 1991. Purification and N-terminal sequence of the p21rho GTPase-activating protein, rho GAP. Biochem J **276 (Pt 3):**833-6.

116. **Ghomashchi, F., X. Zhang, L. Liu, and M. H. Gelb.** 1995. Binding of prenylated and polybasic peptides to membranes: affinities and intervesicle exchange. Biochemistry **34:**11910-8.

117. **Gideon, P., J. John, M. Frech, A. Lautwein, R. Clark, J. E. Scheffler, and A. Wittinghofer.** 1992. Mutational and kinetic analyses of the GTPase-activating protein (GAP)-p21 interaction: the C-terminal domain of GAP is not sufficient for full activity. Mol Cell Biol **12:**2050-6.

118. **Gimeno, C. J., P. O. Ljungdahl, C. A. Styles, and G. R. Fink.** 1992. Unipolar cell divisions in the yeast S. cerevisiae lead to filamentous growth: regulation by starvation and RAS. Cell **68:**1077-90.

119. **Gladfelter, A. S., I. Bose, T. R. Zyla, E. S. Bardes, and D. J. Lew.** 2002. Septin ring assembly involves cycles of GTP loading and hydrolysis by Cdc42p. J Cell Biol **156:**315-26.

120. **Gladfelter, A. S., J. J. Moskow, T. R. Zyla, and D. J. Lew.** 2001. Isolation and characterization of effector-loop mutants of CDC42 in yeast. Mol Biol Cell **12:**1239-55.

121. **Gladfelter, A. S., J. R. Pringle, and D. J. Lew.** 2001. The septin cortex at the yeast mother-bud neck. Curr Opin Microbiol **4:**681-9.

122. **Glotzer, M.** 2005. The molecular requirements for cytokinesis. Science **307:**1735-9.

123. **Goehring, A. S., D. A. Mitchell, A. H. Tong, M. E. Keniry, C. Boone, and G. F. Sprague, Jr.** 2003. Synthetic lethal analysis implicates Ste20p, a p21-activated potein kinase, in polarisome activation. Mol Biol Cell **14:**1501-16.

124. **Gopinath, S. D., S. Narumiya, and J. Dhawan.** 2007. The RhoA effector mDiaphanous regulates MyoD expression and cell cycle progression via SRF-dependent and SRF-independent pathways. J Cell Sci **120:**3086-98.

125. **Gorner, W., E. Durchschlag, M. T. Martinez-Pastor, F. Estruch, G. Ammerer, B. Hamilton, H. Ruis, and C. Schuller.** 1998. Nuclear localization of the C2H2 zinc finger protein Msn2p is regulated by stress and protein kinase A activity. Genes Dev **12:**586-97.

126. **Gotta, M., M. C. Abraham, and J. Ahringer.** 2001. CDC-42 controls early cell polarity and spindle orientation in C. elegans. Curr Biol **11:**482-8.

127. **Gourlay, C. W., and K. R. Ayscough.** 2005. Identification of an upstream regulatory pathway controlling actin-mediated apoptosis in yeast. J Cell Sci **118:**2119-32.

128. **Gruhler, A., J. V. Olsen, S. Mohammed, P. Mortensen, N. J. Faergeman, M. Mann, and O. N. Jensen.** 2005. Quantitative phosphoproteomics applied to the yeast pheromone signaling pathway. Mol Cell Proteomics **4:**310-27.

129. **Gulli, M. P., M. Jaquenoud, Y. Shimada, G. Niederhauser, P. Wiget, and M. Peter.** 2000. Phosphorylation of the Cdc42 exchange factor Cdc24 by the PAK-like kinase Cla4 may regulate polarized growth in yeast. Mol Cell **6:**1155-67.

130. **Gulli, M. P., and M. Peter.** 2001. Temporal and spatial regulation of Rho-type guanine-nucleotide exchange factors: the yeast perspective. Genes Dev **15:**365-79.

131. **Guo, W., F. Tamanoi, and P. Novick.** 2001. Spatial regulation of the exocyst complex by Rho1 GTPase. Nat Cell Biol **3:**353-60.

132. **Gururaj, A., C. J. Barnes, R. K. Vadlamudi, and R. Kumar.** 2004. Regulation of phosphoglucomutase 1 phosphorylation and activity by a signaling kinase. Oncogene **23:**8118-27.

133. **Gustin, M. C., J. Albertyn, M. Alexander, and K. Davenport.** 1998. MAP kinase pathways in the yeast Saccharomyces cerevisiae. Microbiol Mol Biol Rev **62:**1264-300.

134. **Haarer, B. K., S. H. Lillie, A. E. Adams, V. Magdolen, W. Bandlow, and S. S. Brown.** 1990. Purification of profilin from Saccharomyces cerevisiae and analysis of profilin-deficient cells. J Cell Biol **110:**105-14.

135. **Hamburger, Z. A., A. E. Hamburger, A. P. West, Jr., and W. I. Weis.** 2006. Crystal structure of the S.cerevisiae exocyst component Exo70p. J Mol Biol **356:**9-21.

136. **Haney, S. A., and J. R. Broach.** 1994. Cdc25p, the guanine nucleotide exchange factor for the Ras proteins of Saccharomyces cerevisiae, promotes exchange by stabilizing Ras in a nucleotide-free state. J Biol Chem **269:**16541-8.

137. **Hanks, S. K.** 2003. Genomic analysis of the eukaryotic protein kinase superfamily: a perspective. Genome Biol **4:**111.

138. **Hansen, S. H., M. M. Zegers, M. Woodrow, P. Rodriguez-Viciana, P. Chardin, K. E. Mostov, and M. McMahon.** 2000. Induced expression of Rnd3 is associated with transformation of polarized epithelial cells by the Raf-MEK-extracellular signal-regulated kinase pathway. Mol Cell Biol **20:**9364-75.

139. **Harrison, J. C., E. S. Bardes, Y. Ohya, and D. J. Lew.** 2001. A role for the Pkc1p/Mpk1p kinase cascade in the morphogenesis checkpoint. Nat Cell Biol **3:**417-20.

140. **Hart, M. J., A. Eva, T. Evans, S. A. Aaronson, and R. A. Cerione.** 1991. Catalysis of guanine nucleotide exchange on the CDC42Hs protein by the dbl oncogene product. Nature **354:**311-4.

141. **Hart, M. J., Y. Maru, D. Leonard, O. N. Witte, T. Evans, and R. A. Cerione.** 1992. A GDP dissociation inhibitor that serves as a GTPase inhibitor for the Ras-like protein CDC42Hs. Science **258:**812-5.

142. **Hart, M. J., K. Shinjo, A. Hall, T. Evans, and R. A. Cerione.** 1991. Identification of the human platelet GTPase activating protein for the CDC42Hs protein. J Biol Chem **266:**20840-8.

143. **Hartman, J. L. t., B. Garvik, and L. Hartwell.** 2001. Principles for the buffering of genetic variation. Science **291:**1001-4.

144. **Haskell, M. D., A. L. Nickles, J. M. Agati, L. Su, B. D. Dukes, and S. J. Parsons.** 2001. Phosphorylation of p190 on Tyr1105 by c-Src is necessary but not sufficient for EGF-induced actin disassembly in C3H10T1/2 fibroblasts. J Cell Sci **114:**1699-708.

145. **Heinemeyer, W., A. Gruhler, V. Mohrle, Y. Mahe, and D. H. Wolf.** 1993. PRE2, highly homologous to the human major histocompatibility complex-linked RING10 gene, codes for a yeast proteasome subunit necessary for chrymotryptic activity and degradation of ubiquitinated proteins. J Biol Chem **268:**5115-20.

146. **Heinemeyer, W., J. A. Kleinschmidt, J. Saidowsky, C. Escher, and D. H. Wolf.** 1991. Proteinase yscE, the yeast proteasome/multicatalytic-multifunctional proteinase: mutants unravel its function in stress induced proteolysis and uncover its necessity for cell survival. Embo J **10:**555-62.

147. **Henchoz, S., Y. Chi, B. Catarin, I. Herskowitz, R. J. Deshaies, and M. Peter.** 1997. Phosphorylation- and ubiquitin-dependent degradation of the cyclin-dependent kinase inhibitor Far1p in budding yeast. Genes Dev **11:**3046-60.

148. **Hershko, A., and A. Ciechanover.** 1998. The ubiquitin system. Annu Rev Biochem **67:**425-79.

149. **Hicke, L.** 2001. Protein regulation by monoubiquitin. Nat Rev Mol Cell Biol **2:**195-201.

150. **Hirata, D., S. Harada, H. Namba, and T. Miyakawa.** 1995. Adaptation to high-salt stress in Saccharomyces cerevisiae is regulated by Ca2+/calmodulin-dependent phosphoprotein phosphatase (calcineurin) and cAMP-dependent protein kinase. Mol Gen Genet **249:**257-64.

151. **Ho, J., and A. Bretscher.** 2001. Ras regulates the polarity of the yeast actin cytoskeleton through the stress response pathway. Mol Biol Cell **12:**1541-55.

152. **Hochstrasser, M., M. J. Ellison, V. Chau, and A. Varshavsky.** 1991. The short-lived MAT alpha 2 transcriptional regulator is ubiquitinated in vivo. Proc Natl Acad Sci U S A **88:**4606-10.

153. **Hofken, T., and E. Schiebel.** 2002. A role for cell polarity proteins in mitotic exit. Embo J **21:**4851-62.

154. **Hohmann, S.** 2002. Osmotic stress signaling and osmoadaptation in yeasts. Microbiol Mol Biol Rev **66:**300-72.

155. **Hollenberg, S. M., R. Sternglanz, P. F. Cheng, and H. Weintraub.** 1995. Identification of a new family of tissue-specific basic helix-loop-helix proteins with a two-hybrid system. Mol Cell Biol **15:**3813-22.

156. **Holly, S. P., and K. J. Blumer.** 1999. PAK-family kinases regulate cell and actin polarization throughout the cell cycle of Saccharomyces cerevisiae. J Cell Biol **147:**845-56.

157. **Holm, C., S. Rayala, K. Jirstrom, O. Stal, R. Kumar, and G. Landberg.** 2006. Association between Pak1 expression and subcellular localization and tamoxifen resistance in breast cancer patients. J Natl Cancer Inst **98:**671-80.

158. **Hopkins, A. M., S. V. Walsh, P. Verkade, P. Boquet, and A. Nusrat.** 2003. Constitutive activation of Rho proteins by CNF-1 influences tight junction structure and epithelial barrier function. J Cell Sci **116:**725-42.

159. **Hordijk, P. L., J. P. ten Klooster, R. A. van der Kammen, F. Michiels, L. C. Oomen, and J. G. Collard.** 1997. Inhibition of invasion of epithelial cells by Tiam1-Rac signaling. Science **278:**1464-6.

160. **Howard, S. C., Y. V. Budovskaya, Y. W. Chang, and P. K. Herman.** 2002. The C-terminal domain of the largest subunit of RNA polymerase II is required for stationary phase entry and functionally interacts with the Ras/PKA signaling pathway. J Biol Chem **277:**19488-97.

161. **Howard, S. C., S. J. Deminoff, and P. K. Herman.** 2006. Increased phosphoglucomutase activity suppresses the galactose growth defect associated with elevated levels of Ras signaling in S. cerevisiae. Curr Genet **49:**1-6.

162. **Huang, H. D., T. Y. Lee, S. W. Tzeng, L. C. Wu, J. T. Horng, A. P. Tsou, and K. T. Huang.** 2005. Incorporating hidden Markov models for identifying protein kinase-specific phosphorylation sites. J Comput Chem **26:**1032-41.

163. **Hulo, N., A. Bairoch, V. Bulliard, L. Cerutti, B. A. Cuche, E. de Castro, C. Lachaize, P. S. Langendijk-Genevaux, and C. J. Sigrist.** 2008. The 20 years of PROSITE. Nucleic Acids Res **36:**D245-9.

164. **Imai, J., A. Toh-e, and Y. Matsui.** 1996. Genetic analysis of the Saccharomyces cerevisiae RHO3 gene, encoding a rho-type small GTPase, provides evidence for a role in bud formation. Genetics **142:**359-69.

165. **Inouye, C., N. Dhillon, T. Durfee, P. C. Zambryski, and J. Thorner.** 1997. Mutational analysis of STE5 in the yeast Saccharomyces cerevisiae: application of a differential interaction trap assay for examining protein-protein interactions. Genetics **147:**479-92.

166. **Ishikawa, Y., H. Katoh, and M. Negishi.** 2003. A role of Rnd1 GTPase in dendritic spine formation in hippocampal neurons. J Neurosci **23:**11065-72.

167. **Ivey, F. D., and C. S. Hoffman.** 2005. Direct activation of fission yeast adenylate cyclase by the Gpa2 Galpha of the glucose signaling pathway. Proc Natl Acad Sci U S A **102:**6108-13.

168. **Jaffe, A. B., and A. Hall.** 2005. Rho GTPases: biochemistry and biology. Annu Rev Cell Dev Biol **21:**247-69.

169. **Jaffer, Z. M., and J. Chernoff.** 2002. p21-activated kinases: three more join the Pak. Int J Biochem Cell Biol **34:**713-7.

170. **Jakobi, R., C. C. McCarthy, M. A. Koeppel, and D. K. Stringer.** 2003. Caspase-activated PAK-2 is regulated by subcellular targeting and proteasomal degradation. J Biol Chem **278:**38675-85.

171. **Janmey, P. A., and U. Lindberg.** 2004. Cytoskeletal regulation: rich in lipids. Nat Rev Mol Cell Biol **5:**658-66.

172. **Jansen, G., F. Buhring, C. P. Hollenberg, and M. Ramezani Rad.** 2001. Mutations in the SAM domain of STE50 differentially influence the MAPK-mediated pathways for mating, filamentous growth and osmotolerance in Saccharomyces cerevisiae. Mol Genet Genomics **265:**102-17.

173. **Jaquenoud, M., and M. Peter.** 2000. Gic2p may link activated Cdc42p to components involved in actin polarization, including Bni1p and Bud6p (Aip3p). Mol Cell Biol **20:**6244-58.

174. **Jenna, S., N. K. Hussain, E. I. Danek, I. Triki, S. Wasiak, P. S. McPherson, and N. Lamarche-Vane.** 2002. The activity of the GTPase-activating protein CdGAP is regulated by the endocytic protein intersectin. J Biol Chem **277:**6366-73.

175. **Jin, H., and D. C. Amberg.** 2000. The secretory pathway mediates localization of the cell polarity regulator Aip3p/Bud6p. Mol Biol Cell **11:**647-61.

176. **Joberty, G., C. Petersen, L. Gao, and I. G. Macara.** 2000. The cell-polarity protein Par6 links Par3 and atypical protein kinase C to Cdc42. Nat Cell Biol **2:**531-9.

177. **Johnson, D. I.** 1999. Cdc42: An essential Rho-type GTPase controlling eukaryotic cell polarity. Microbiol Mol Biol Rev **63:**54-105.

178. **Johnson, D. I., and J. R. Pringle.** 1990. Molecular characterization of CDC42, a Saccharomyces cerevisiae gene involved in the development of cell polarity. J Cell Biol **111:**143-52.

179. **Johnston, S. D., S. Enomoto, L. Schneper, M. C. McClellan, F. Twu, N. D. Montgomery, S. A. Haney, J. R. Broach, and J. Berman.** 2001. CAC3(MSI1) suppression of RAS2(G19V) is independent of chromatin assembly factor I and mediated by NPR1. Mol Cell Biol **21:**1784-94.

180. **Jones, D. L., J. Petty, D. C. Hoyle, A. Hayes, E. Ragni, L. Popolo, S. G. Oliver, and L. I. Stateva.** 2003. Transcriptome profiling of a Saccharomyces cerevisiae mutant with a constitutively activated Ras/cAMP pathway. Physiol Genomics **16:**107-18.

181. **Joneson, T., M. A. White, M. H. Wigler, and D. Bar-Sagi.** 1996. Stimulation of membrane ruffling and MAP kinase activation by distinct effectors of RAS. Science **271:**810-2.

182. **Joyce, P. L., and A. D. Cox.** 2003. Rac1 and Rac3 are targets for geranylgeranyltransferase I inhibitor-mediated inhibition of signaling, transformation, and membrane ruffling. Cancer Res **63:**7959-67.

183. **Kadota, J., T. Yamamoto, S. Yoshiuchi, E. Bi, and K. Tanaka.** 2004. Septin ring assembly requires concerted action of polarisome components, a PAK kinase Cla4p, and the actin cytoskeleton in Saccharomyces cerevisiae. Mol Biol Cell **15:**5329-45.

184. **Kamada, Y., H. Qadota, C. P. Python, Y. Anraku, Y. Ohya, and D. E. Levin.** 1996. Activation of yeast protein kinase C by Rho1 GTPase. J Biol Chem **271:**9193-6.

185. **Kataoka, T., S. Powers, C. McGill, O. Fasano, J. Strathern, J. Broach, and M. Wigler.** 1984. Genetic analysis of yeast RAS1 and RAS2 genes. Cell **37:**437-45.

186. **Kaufman, P. D., R. Kobayashi, and B. Stillman.** 1997. Ultraviolet radiation sensitivity and reduction of telomeric silencing in Saccharomyces cerevisiae cells lacking chromatin assembly factor-I. Genes Dev **11:**345-57.

187. **Kellis, M., N. Patterson, M. Endrizzi, B. Birren, and E. S. Lander.** 2003. Sequencing and comparison of yeast species to identify genes and regulatory elements. Nature **423:**241-54.

188. **Kemp, B. E., and R. B. Pearson.** 1990. Protein kinase recognition sequence motifs. Trends Biochem Sci **15:**342-6.

189. **Kido, M., F. Shima, T. Satoh, T. Asato, K. Kariya, and T. Kataoka.** 2002. Critical function of the Ras-associating domain as a primary Ras-binding site for regulation of Saccharomyces cerevisiae adenylyl cyclase. J Biol Chem **277:**3117-23.

190. **Kikuchi, Y., E. Mizuuchi, S. Nogami, S. Morishita, and Y. Ohya.** 2007. Involvement of Rho-type GTPase in control of cell size in Saccharomyces cerevisiae. FEMS Yeast Res **7:**569-78.

191. **King, A. J., H. Sun, B. Diaz, D. Barnard, W. Miao, S. Bagrodia, and M. S. Marshall.** 1998. The protein kinase Pak3 positively regulates Raf-1 activity through phosphorylation of serine 338. Nature **396:**180-3.

192. **Kjoller, L., and A. Hall.** 1999. Signaling to Rho GTPases. Exp Cell Res **253:**166-79.

193. **Knaus, M., M. P. Pelli-Gulli, F. van Drogen, S. Springer, M. Jaquenoud, and M. Peter.** 2007. Phosphorylation of Bem2p and Bem3p may contribute to local activation of Cdc42p at bud emergence. Embo J **26:**4501-13.

194. **Knebel, A., N. Morrice, and P. Cohen.** 2001. A novel method to identify protein kinase substrates: eEF2 kinase is phosphorylated and inhibited by SAPK4/p38delta. Embo J **20:**4360-9.

195. **Kobe, B., T. Kampmann, J. K. Forwood, P. Listwan, and R. I. Brinkworth.** 2005. Substrate specificity of protein kinases and computational prediction of substrates. Biochim Biophys Acta **1754:**200-9.

196. **Koch, G., K. Tanaka, T. Masuda, W. Yamochi, H. Nonaka, and Y. Takai.** 1997. Association of the Rho family small GTP-binding proteins with Rho GDP dissociation inhibitor (Rho GDI) in Saccharomyces cerevisiae. Oncogene **15:**417-22.

197. **Kozma, R., S. Ahmed, A. Best, and L. Lim.** 1995. The Ras-related protein Cdc42Hs and bradykinin promote formation of peripheral actin microspikes and filopodia in Swiss 3T3 fibroblasts. Mol Cell Biol **15:**1942-52.

198. **Kozminski, K. G., L. Beven, E. Angerman, A. H. Tong, C. Boone, and H. O. Park.** 2003. Interaction between a Ras and a Rho GTPase couples selection of a growth site to the development of cell polarity in yeast. Mol Biol Cell **14:**4958-70.

199. **Kraakman, L., K. Lemaire, P. Ma, A. W. Teunissen, M. C. Donaton, P. Van Dijck, J. Winderickx, J. H. de Winde, and J. M. Thevelein.** 1999. A Saccharomyces cerevisiae G-protein coupled receptor, Gpr1, is specifically required for glucose activation of the cAMP pathway during the transition to growth on glucose. Mol Microbiol **32:**1002-12.

200. **Krengel, U., I. Schlichting, A. Scherer, R. Schumann, M. Frech, J. John, W. Kabsch, E. F. Pai, and A. Wittinghofer.** 1990. Three-dimensional structures of H-ras p21 mutants: molecular basis for their inability to function as signal switch molecules. Cell **62:**539-48.

201. **Kroschewski, R., A. Hall, and I. Mellman.** 1999. Cdc42 controls secretory and endocytic transport to the basolateral plasma membrane of MDCK cells. Nat Cell Biol **1:**8-13.

202. **Kumar, R., A. E. Gururaj, and C. J. Barnes.** 2006. p21-activated kinases in cancer. Nat Rev Cancer **6:**459-71.

203. **Kuranda, K., V. Leberre, S. Sokol, G. Palamarczyk, and J. Francois.** 2006. Investigating the caffeine effects in the yeast Saccharomyces cerevisiae brings new insights into the connection between TOR, PKC and Ras/cAMP signalling pathways. Mol Microbiol **61:**1147-66.

204. **Kwon, T., D. Y. Kwon, J. Chun, J. H. Kim, and S. S. Kang.** 2000. Akt protein kinase inhibits Rac1-GTP binding through phosphorylation at serine 71 of Rac1. J Biol Chem **275:**423-8.

205. **Labbe, J. C., P. S. Maddox, E. D. Salmon, and B. Goldstein.** 2003. PAR proteins regulate microtubule dynamics at the cell cortex in C. elegans. Curr Biol **13:**707-14.

206. **Lamarche, N., N. Tapon, L. Stowers, P. D. Burbelo, P. Aspenstrom, T. Bridges, J. Chant, and A. Hall.** 1996. Rac and Cdc42 induce actin polymerization and G1 cell cycle progression independently of p65PAK and the JNK/SAPK MAP kinase cascade. Cell **87:**519-29.

207. **Lamson, R. E., M. J. Winters, and P. M. Pryciak.** 2002. Cdc42 regulation of kinase activity and signaling by the yeast p21-activated kinase Ste20. Mol Cell Biol **22:**2939-51.

208. **Lang, P., F. Gesbert, M. Delespine-Carmagnat, R. Stancou, M. Pouchelet, and J. Bertoglio.** 1996. Protein kinase A phosphorylation of RhoA mediates the morphological and functional effects of cyclic AMP in cytotoxic lymphocytes. Embo J **15:**510-9.

209. **Lanker, S., M. H. Valdivieso, and C. Wittenberg.** 1996. Rapid degradation of the G1 cyclin Cln2 induced by CDK-dependent phosphorylation. Science **271:**1597-601.

210. **Lartey, J., A. Gampel, J. Pawade, H. Mellor, and A. L. Bernal.** 2006. Expression of RND proteins in human myometrium. Biol Reprod **75:**452-61.

211. **Leberer, E., D. Dignard, D. Harcus, D. Y. Thomas, and M. Whiteway.** 1992. The protein kinase homologue Ste20p is required to link the yeast pheromone response G-protein beta gamma subunits to downstream signalling components. Embo J **11:**4815-24.

212. **Leberer, E., D. Y. Thomas, and M. Whiteway.** 1997. Pheromone signalling and polarized morphogenesis in yeast. Curr Opin Genet Dev **7:**59-66.

213. **Leberer, E., C. Wu, T. Leeuw, A. Fourest-Lieuvin, J. E. Segall, and D. Y. Thomas.** 1997. Functional characterization of the Cdc42p binding domain of yeast Ste20p protein kinase. Embo J **16:**83-97.

214. **Lebowitz, P. F., J. P. Davide, and G. C. Prendergast.** 1995. Evidence that farnesyltransferase inhibitors suppress Ras transformation by interfering with Rho activity. Mol Cell Biol **15:**6613-22.

215. **Lechler, T., G. A. Jonsdottir, S. K. Klee, D. Pellman, and R. Li.** 2001. A two-tiered mechanism by which Cdc42 controls the localization and activation of an Arp2/3-activating motor complex in yeast. J Cell Biol **155:**261-70.

216. **Lechler, T., A. Shevchenko, and R. Li.** 2000. Direct involvement of yeast type I myosins in Cdc42-dependent actin polymerization. J Cell Biol **148:**363-73.

217. **Leeuw, T., A. Fourest-Lieuvin, C. Wu, J. Chenevert, K. Clark, M. Whiteway, D. Y. Thomas, and E. Leberer.** 1995. Pheromone response in yeast: association of Bem1p with proteins of the MAP kinase cascade and actin. Science **270:**1210-3.

218. **Lei, M., W. Lu, W. Meng, M. C. Parrini, M. J. Eck, B. J. Mayer, and S. C. Harrison.** 2000. Structure of PAK1 in an autoinhibited conformation reveals a multistage activation switch. Cell **102:**387-97.

219. **Leonard, D., M. J. Hart, J. V. Platko, A. Eva, W. Henzel, T. Evans, and R. A. Cerione.** 1992. The identification and characterization of a GDP-dissociation inhibitor (GDI) for the CDC42Hs protein. J Biol Chem **267:**22860-8.

220. **Lerm, M., M. Pop, G. Fritz, K. Aktories, and G. Schmidt.** 2002. Proteasomal degradation of cytotoxic necrotizing factor 1-activated rac. Infect Immun **70:**4053-8.

221. **Lerm, M., J. Selzer, A. Hoffmeyer, U. R. Rapp, K. Aktories, and G. Schmidt.** 1999. Deamidation of Cdc42 and Rac by Escherichia coli cytotoxic necrotizing factor 1: activation of c-Jun N-terminal kinase in HeLa cells. Infect Immun **67:**496-503.

222. **Leuther, K. K., and S. A. Johnston.** 1992. Nondissociation of GAL4 and GAL80 in vivo after galactose induction. Science **256:**1333-5.

223. **Li, F., L. Adam, R. K. Vadlamudi, H. Zhou, S. Sen, J. Chernoff, M. Mandal, and R. Kumar.** 2002. p21-activated kinase 1 interacts with and phosphorylates histone H3 in breast cancer cells. EMBO Rep **3:**767-73.

224. **Li, X., S. A. Gerber, A. D. Rudner, S. A. Beausoleil, W. Haas, J. Villen, J. E. Elias, and S. P. Gygi.** 2007. Large-scale phosphorylation analysis of alpha-factor-arrested Saccharomyces cerevisiae. J Proteome Res **6:**1190-7.

225. **Lin, D., A. S. Edwards, J. P. Fawcett, G. Mbamalu, J. D. Scott, and T. Pawson.** 2000. A mammalian PAR-3-PAR-6 complex implicated in Cdc42/Rac1 and aPKC signalling and cell polarity. Nat Cell Biol **2:**540-7.

226. **Lin, S. J., and V. C. Culotta.** 1995. The ATX1 gene of Saccharomyces cerevisiae encodes a small metal homeostasis factor that protects cells against reactive oxygen toxicity. Proc Natl Acad Sci U S A **92:**3784-8.

227. **Linding, R., L. J. Jensen, G. J. Ostheimer, M. A. van Vugt, C. Jorgensen, I. M. Miron, F. Diella, K. Colwill, L. Taylor, K. Elder, P. Metalnikov, V. Nguyen, A. Pasculescu, J. Jin, J. G. Park, L. D. Samson, J. R. Woodgett, R. B. Russell, P. Bork, M. B. Yaffe, and T. Pawson.** 2007. Systematic discovery of in vivo phosphorylation networks. Cell **129:**1415-26.

228. **Liu, A., W. Du, J. P. Liu, T. M. Jessell, and G. C. Prendergast.** 2000. RhoB alteration is necessary for apoptotic and antineoplastic responses to farnesyltransferase inhibitors. Mol Cell Biol **20:**6105-13.

229. **Loirand, G., C. Cario-Toumaniantz, P. Chardin, and P. Pacaud.** 1999. The Rho-related protein Rnd1 inhibits Ca2+ sensitization of rat smooth muscle. J Physiol **516 (Pt 3):**825-34.

230. **Lorenz, M. C., and J. Heitman.** 1998. The MEP2 ammonium permease regulates pseudohyphal differentiation in Saccharomyces cerevisiae. Embo J **17:**1236-47.

231. **Lorenz, M. C., and J. Heitman.** 1997. Yeast pseudohyphal growth is regulated by GPA2, a G protein alpha homolog. Embo J **16:**7008-18.

232. **Lorenz, M. C., X. Pan, T. Harashima, M. E. Cardenas, Y. Xue, J. P. Hirsch, and J. Heitman.** 2000. The G protein-coupled receptor gpr1 is a nutrient sensor that regulates pseudohyphal differentiation in Saccharomyces cerevisiae. Genetics **154:**609-22.

233. **Loyet, K. M., J. T. Stults, and D. Arnott.** 2005. Mass spectrometric contributions to the practice of phosphorylation site mapping through 2003: a literature review. Mol Cell Proteomics **4:**235-45.

234. **Lu, W., S. Katz, R. Gupta, and B. J. Mayer.** 1997. Activation of Pak by membrane localization mediated by an SH3 domain from the adaptor protein Nck. Curr Biol **7:**85-94.

235. **Madaule, P., and R. Axel.** 1985. A novel ras-related gene family. Cell **41:**31-40.

236. **Madaule, P., R. Axel, and A. M. Myers.** 1987. Characterization of two members of the rho gene family from the yeast Saccharomyces cerevisiae. Proc Natl Acad Sci U S A **84:**779-83.

237. **Madden, K., and M. Snyder.** 1998. Cell polarity and morphogenesis in budding yeast. Annu Rev Microbiol **52:**687-744.

238. **Madeo, F., E. Frohlich, M. Ligr, M. Grey, S. J. Sigrist, D. H. Wolf, and K. U. Frohlich.** 1999. Oxygen stress: a regulator of apoptosis in yeast. J Cell Biol **145:**757-67.

239. **Maeda, T., M. Takekawa, and H. Saito.** 1995. Activation of yeast PBS2 MAPKK by MAPKKKs or by binding of an SH3-containing osmosensor. Science **269:**554-8.

240. **Malliri, A., R. A. van der Kammen, K. Clark, M. van der Valk, F. Michiels, and J. G. Collard.** 2002. Mice deficient in the Rac activator Tiam1 are resistant to Ras-induced skin tumours. Nature **417:**867-71.

241. **Manke, I. A., A. Nguyen, D. Lim, M. Q. Stewart, A. E. Elia, and M. B. Yaffe.** 2005. MAPKAP kinase-2 is a cell cycle checkpoint kinase that regulates the

G2/M transition and S phase progression in response to UV irradiation. Mol Cell **17:**37-48.

242. **Manning, B. D., R. Padmanabha, and M. Snyder.** 1997. The Rho-GEF Rom2p localizes to sites of polarized cell growth and participates in cytoskeletal functions in Saccharomyces cerevisiae. Mol Biol Cell **8:**1829-44.

243. **Manning, G., G. D. Plowman, T. Hunter, and S. Sudarsanam.** 2002. Evolution of protein kinase signaling from yeast to man. Trends Biochem Sci **27:**514-20.

244. **Manning, G., D. B. Whyte, R. Martinez, T. Hunter, and S. Sudarsanam.** 2002. The protein kinase complement of the human genome. Science **298:**1912-34.

245. **Manser, E., H. Y. Huang, T. H. Loo, X. Q. Chen, J. M. Dong, T. Leung, and L. Lim.** 1997. Expression of constitutively active alpha-PAK reveals effects of the kinase on actin and focal complexes. Mol Cell Biol **17:**1129-43.

246. **Manser, E., T. Leung, H. Salihuddin, Z. S. Zhao, and L. Lim.** 1994. A brain serine/threonine protein kinase activated by Cdc42 and Rac1. Nature **367:**40-6.

247. **Marchal, C., R. Haguenauer-Tsapis, and D. Urban-Grimal.** 1998. A PEST-like sequence mediates phosphorylation and efficient ubiquitination of yeast uracil permease. Mol Cell Biol **18:**314-21.

248. **Martin, H., A. Mendoza, J. M. Rodriguez-Pachon, M. Molina, and C. Nombela.** 1997. Characterization of SKM1, a Saccharomyces cerevisiae gene encoding a novel Ste20/PAK-like protein kinase. Mol Microbiol **23:**431-44.

249. **Martinez-Pastor, M. T., G. Marchler, C. Schuller, A. Marchler-Bauer, H. Ruis, and F. Estruch.** 1996. The Saccharomyces cerevisiae zinc finger proteins Msn2p and Msn4p are required for transcriptional induction through the stress response element (STRE). Embo J **15:**2227-35.

250. **Martzen, M. R., S. M. McCraith, S. L. Spinelli, F. M. Torres, S. Fields, E. J. Grayhack, and E. M. Phizicky.** 1999. A biochemical genomics approach for identifying genes by the activity of their products. Science **286:**1153-5.

251. **Masuda, T., K. Tanaka, H. Nonaka, W. Yamochi, A. Maeda, and Y. Takai.** 1994. Molecular cloning and characterization of yeast rho GDP dissociation inhibitor. J Biol Chem **269:**19713-8.

252. **Matsui, Y., R. Matsui, R. Akada, and A. Toh-e.** 1996. Yeast src homology region 3 domain-binding proteins involved in bud formation. J Cell Biol **133:**865-78.

253. **Matsui, Y., and E. A. Toh.** 1992. Yeast RHO3 and RHO4 ras superfamily genes are necessary for bud growth, and their defect is suppressed by a high dose of bud formation genes CDC42 and BEM1. Mol Cell Biol **12:**5690-9.

254. **Matsumoto, K., I. Uno, and T. Ishikawa.** 1983. Control of cell division in Saccharomyces cerevisiae mutants defective in adenylate cyclase and cAMP-dependent protein kinase. Exp Cell Res **146:**151-61.

255. **Matsumura, F.** 2005. Regulation of myosin II during cytokinesis in higher eukaryotes. Trends Cell Biol **15:**371-7.

256. **Mazur, P., and W. Baginsky.** 1996. In vitro activity of 1,3-beta-D-glucan synthase requires the GTP-binding protein Rho1. J Biol Chem **271:**14604-9.

257. **McGrath, J. P., D. J. Capon, D. V. Goeddel, and A. D. Levinson.** 1984. Comparative biochemical properties of normal and activated human ras p21 protein. Nature **310:**644-9.

258. **Mehta, D., A. Rahman, and A. B. Malik.** 2001. Protein kinase C-alpha signals rho-guanine nucleotide dissociation inhibitor phosphorylation and rho activation and regulates the endothelial cell barrier function. J Biol Chem **276:**22614-20.

259. **Mettouchi, A., S. Klein, W. Guo, M. Lopez-Lago, E. Lemichez, J. K. Westwick, and F. G. Giancotti.** 2001. Integrin-specific activation of Rac controls progression through the G(1) phase of the cell cycle. Mol Cell **8:**115-27.

260. **Michaelson, D., J. Silletti, G. Murphy, P. D'Eustachio, M. Rush, and M. R. Philips.** 2001. Differential localization of Rho GTPases in live cells: regulation by hypervariable regions and RhoGDI binding. J Cell Biol **152:**111-26.

261. **Minden, A., A. Lin, F. X. Claret, A. Abo, and M. Karin.** 1995. Selective activation of the JNK signaling cascade and c-Jun transcriptional activity by the small GTPases Rac and Cdc42Hs. Cell **81:**1147-57.

262. **Mitsuzawa, H., I. Uno, T. Oshima, and T. Ishikawa.** 1989. Isolation and characterization of temperature-sensitive mutations in the RAS2 and CYR1 genes of Saccharomyces cerevisiae. Genetics **123:**739-48.

263. **Mizunuma, M., D. Hirata, and T. Miyakawa.** 2005. Implication of Pkc1p protein kinase C in sustaining Cln2p level and polarized bud growth in response to calcium signaling in Saccharomyces cerevisiae. J Cell Sci **118:**4219-29.

264. **Mol, P. C., H. M. Park, J. T. Mullins, and E. Cabib.** 1994. A GTP-binding protein regulates the activity of (1-->3)-beta-glucan synthase, an enzyme directly involved in yeast cell wall morphogenesis. J Biol Chem **269:**31267-74.

265. **Moon, S. Y., and Y. Zheng.** 2003. Rho GTPase-activating proteins in cell regulation. Trends Cell Biol **13:**13-22.

266. **Morandell, S., T. Stasyk, K. Grosstessner-Hain, E. Roitinger, K. Mechtler, G. K. Bonn, and L. A. Huber.** 2006. Phosphoproteomics strategies for the functional analysis of signal transduction. Proteomics **6:**4047-56.

267. **Morrison, D. K., and R. J. Davis.** 2003. Regulation of MAP kinase signaling modules by scaffold proteins in mammals. Annu Rev Cell Dev Biol **19:**91-118.

268. **Mosch, H. U., E. Kubler, S. Krappmann, G. R. Fink, and G. H. Braus.** 1999. Crosstalk between the Ras2p-controlled mitogen-activated protein kinase and cAMP pathways during invasive growth of Saccharomyces cerevisiae. Mol Biol Cell **10:**1325-35.

269. **Mosch, H. U., R. L. Roberts, and G. R. Fink.** 1996. Ras2 signals via the Cdc42/Ste20/mitogen-activated protein kinase module to induce filamentous growth in Saccharomyces cerevisiae. Proc Natl Acad Sci U S A **93:**5352-6.

270. **Moskow, J. J., A. S. Gladfelter, R. E. Lamson, P. M. Pryciak, and D. J. Lew.** 2000. Role of Cdc42p in pheromone-stimulated signal transduction in Saccharomyces cerevisiae. Mol Cell Biol **20:**7559-71.

271. **Munemitsu, S., M. A. Innis, R. Clark, F. McCormick, A. Ullrich, and P. Polakis.** 1990. Molecular cloning and expression of a G25K cDNA, the human homolog of the yeast cell cycle gene CDC42. Mol Cell Biol **10:**5977-82.

272. **Munro, P., G. Flatau, A. Doye, L. Boyer, O. Oregioni, J. L. Mege, L. Landraud, and E. Lemichez.** 2004. Activation and proteasomal degradation of rho GTPases by cytotoxic necrotizing factor-1 elicit a controlled inflammatory response. J Biol Chem **279:**35849-57.

273. **Musacchio, A., T. Gibson, P. Rice, J. Thompson, and M. Saraste.** 1993. The PH domain: a common piece in the structural patchwork of signalling proteins. Trends Biochem Sci **18:**343-8.

274. **Nern, A., and R. A. Arkowitz.** 1998. A GTP-exchange factor required for cell orientation. Nature **391:**195-8.

275. **Nern, A., and R. A. Arkowitz.** 2000. Nucleocytoplasmic shuttling of the Cdc42p exchange factor Cdc24p. J Cell Biol **148:**1115-22.

276. **Nigg, E. A.** 1993. Cellular substrates of p34(cdc2) and its companion cyclin-dependent kinases. Trends Cell Biol **3:**296-301.

277. **Nobes, C. D., and A. Hall.** 1995. Rho, rac, and cdc42 GTPases regulate the assembly of multimolecular focal complexes associated with actin stress fibers, lamellipodia, and filopodia. Cell **81:**53-62.

278. **Nonaka, H., K. Tanaka, H. Hirano, T. Fujiwara, H. Kohno, M. Umikawa, A. Mino, and Y. Takai.** 1995. A downstream target of RHO1 small GTP-binding

protein is PKC1, a homolog of protein kinase C, which leads to activation of the MAP kinase cascade in Saccharomyces cerevisiae. Embo J **14:**5931-8.

279. **Norbeck, J., and A. Blomberg.** 2000. The level of cAMP-dependent protein kinase A activity strongly affects osmotolerance and osmo-instigated gene expression changes in Saccharomyces cerevisiae. Yeast **16:**121-37.

280. **Novick, P., and P. Brennwald.** 1993. Friends and family: the role of the Rab GTPases in vesicular traffic. Cell **75:**597-601.

281. **Novick, P., B. C. Osmond, and D. Botstein.** 1989. Suppressors of yeast actin mutations. Genetics **121:**659-74.

282. **O'Rourke, S. M., I. Herskowitz, and E. K. O'Shea.** 2002. Yeast go the whole HOG for the hyperosmotic response. Trends Genet **18:**405-12.

283. **Obenauer, J. C., L. C. Cantley, and M. B. Yaffe.** 2003. Scansite 2.0: Proteome-wide prediction of cell signaling interactions using short sequence motifs. Nucleic Acids Res **31:**3635-41.

284. **Oehlen, L. J., and F. R. Cross.** 1998. Potential regulation of Ste20 function by the Cln1-Cdc28 and Cln2-Cdc28 cyclin-dependent protein kinases. J Biol Chem **273:**25089-97.

285. **Ogita, H., and Y. Takai.** 2006. Activation of Rap1, Cdc42, and rac by nectin adhesion system. Methods Enzymol **406:**415-24.

286. **Ohno, S.** 2001. Intercellular junctions and cellular polarity: the PAR-aPKC complex, a conserved core cassette playing fundamental roles in cell polarity. Curr Opin Cell Biol **13:**641-8.

287. **Olofsson, B.** 1999. Rho guanine dissociation inhibitors: pivotal molecules in cellular signalling. Cell Signal **11:**545-54.

288. **Olson, M. F., A. Ashworth, and A. Hall.** 1995. An essential role for Rho, Rac, and Cdc42 GTPases in cell cycle progression through G1. Science **269:**1270-2.

289. **Olson, M. F., H. F. Paterson, and C. J. Marshall.** 1998. Signals from Ras and Rho GTPases interact to regulate expression of p21Waf1/Cip1. Nature **394:**295-9.

290. **Omura, F., and Y. Kodama.** 2004. The N-terminal domain of yeast Bap2 permease is phosphorylated dependently on the Npr1 kinase in response to starvation. FEMS Microbiol Lett **230:**227-34.

291. **Ooi, S. L., X. Pan, B. D. Peyser, P. Ye, P. B. Meluh, D. S. Yuan, R. A. Irizarry, J. S. Bader, F. A. Spencer, and J. D. Boeke.** 2006. Global synthetic-lethality analysis and yeast functional profiling. Trends Genet **22:**56-63.

292. **Osman, M. A., and R. A. Cerione.** 1998. Iqg1p, a yeast homologue of the mammalian IQGAPs, mediates cdc42p effects on the actin cytoskeleton. J Cell Biol **142:**443-55.

293. **Ozaki-Kuroda, K., Y. Yamamoto, H. Nohara, M. Kinoshita, T. Fujiwara, K. Irie, and Y. Takai.** 2001. Dynamic localization and function of Bni1p at the sites of directed growth in Saccharomyces cerevisiae. Mol Cell Biol **21:**827-39.

294. **Pan, X., and J. Heitman.** 1999. Cyclic AMP-dependent protein kinase regulates pseudohyphal differentiation in Saccharomyces cerevisiae. Mol Cell Biol **19:**4874-87.

295. **Pasqualucci, L., P. Neumeister, T. Goossens, G. Nanjangud, R. S. Chaganti, R. Kuppers, and R. Dalla-Favera.** 2001. Hypermutation of multiple proto-oncogenes in B-cell diffuse large-cell lymphomas. Nature **412:**341-6.

296. **Patalano, S., G. Pruliere, F. Prodon, A. Paix, P. Dru, C. Sardet, and J. Chenevert.** 2006. The aPKC-PAR-6-PAR-3 cell polarity complex localizes to the centrosome attracting body, a macroscopic cortical structure responsible for asymmetric divisions in the early ascidian embryo. J Cell Sci **119:**1592-603.

297. **Paterson, H. F., A. J. Self, M. D. Garrett, I. Just, K. Aktories, and A. Hall.** 1990. Microinjection of recombinant p21rho induces rapid changes in cell morphology. J Cell Biol **111:**1001-7.

298. **Payne, W. E., and J. I. Garrels.** 1997. Yeast Protein database (YPD): a database for the complete proteome of Saccharomyces cerevisiae. Nucleic Acids Res **25:**57-62.

299. **Pearson, R. B., and B. E. Kemp.** 1991. Protein kinase phosphorylation site sequences and consensus specificity motifs: tabulations. Methods Enzymol **200:**62-81.

300. **Pellicena, P., and J. Kuriyan.** 2006. Protein-protein interactions in the allosteric regulation of protein kinases. Curr Opin Struct Biol **16:**702-9.

301. **Perkins, D. N., D. J. Pappin, D. M. Creasy, and J. S. Cottrell.** 1999. Probability-based protein identification by searching sequence databases using mass spectrometry data. Electrophoresis **20:**3551-67.

302. **Peter, M., A. M. Neiman, H. O. Park, M. van Lohuizen, and I. Herskowitz.** 1996. Functional analysis of the interaction between the small GTP binding protein Cdc42 and the Ste20 protein kinase in yeast. Embo J **15:**7046-59.

303. **Pintard, L., D. Kressler, and B. Lapeyre.** 2000. Spb1p is a yeast nucleolar protein associated with Nop1p and Nop58p that is able to bind S-adenosyl-L-methionine in vitro. Mol Cell Biol **20:**1370-81.

304. **Pollard, T. D.** 2007. Regulation of actin filament assembly by Arp2/3 complex and formins. Annu Rev Biophys Biomol Struct **36:**451-77.

305. **Ponting, C. P., and D. R. Benjamin.** 1996. A novel family of Ras-binding domains. Trends Biochem Sci **21:**422-5.

306. **Poplinski, A., C. Hopp, and M. Ramezani-Rad.** 2007. Ste50 adaptor protein influences Ras/cAMP-driven stress-response and cell survival in Saccharomyces cerevisiae. Curr Genet **51:**257-68.

307. **Posas, F., E. A. Witten, and H. Saito.** 1998. Requirement of STE50 for osmostress-induced activation of the STE11 mitogen-activated protein kinase kinase kinase in the high-osmolarity glycerol response pathway. Mol Cell Biol **18:**5788-96.

308. **Powers, S., K. O'Neill, and M. Wigler.** 1989. Dominant yeast and mammalian RAS mutants that interfere with the CDC25-dependent activation of wild-type RAS in Saccharomyces cerevisiae. Mol Cell Biol **9:**390-5.

309. **Preudhomme, C., C. Roumier, M. P. Hildebrand, E. Dallery-Prudhomme, D. Lantoine, J. L. Lai, A. Daudignon, C. Adenis, F. Bauters, P. Fenaux, J. P. Kerckaert, and S. Galiegue-Zouitina.** 2000. Nonrandom 4p13 rearrangements of the RhoH/TTF gene, encoding a GTP-binding protein, in non-Hodgkin's lymphoma and multiple myeloma. Oncogene **19:**2023-32.

310. **Price, L. S., M. Langeslag, J. P. ten Klooster, P. L. Hordijk, K. Jalink, and J. G. Collard.** 2003. Calcium signaling regulates translocation and activation of Rac. J Biol Chem **278:**39413-21.

311. **Prieto-Sanchez, R. M., and X. R. Bustelo.** 2003. Structural basis for the signaling specificity of RhoG and Rac1 GTPases. J Biol Chem **278:**37916-25.

312. **Pruyne, D., and A. Bretscher.** 2000. Polarization of cell growth in yeast. J Cell Sci **113 (Pt 4):**571-85.

313. **Ptacek, J., G. Devgan, G. Michaud, H. Zhu, X. Zhu, J. Fasolo, H. Guo, G. Jona, A. Breitkreutz, R. Sopko, R. R. McCartney, M. C. Schmidt, N. Rachidi, S. J. Lee, A. S. Mah, L. Meng, M. J. Stark, D. F. Stern, C. De Virgilio, M. Tyers, B. Andrews, M. Gerstein, B. Schweitzer, P. F. Predki, and M. Snyder.** 2005. Global analysis of protein phosphorylation in yeast. Nature **438:**679-84.

314. **Puntervoll, P., R. Linding, C. Gemund, S. Chabanis-Davidson, M. Mattingsdal, S. Cameron, D. M. Martin, G. Ausiello, B. Brannetti, A. Costantini, F. Ferre, V. Maselli, A. Via, G. Cesareni, F. Diella, G. Superti-Furga, L. Wyrwicz, C. Ramu, C. McGuigan, R. Gudavalli, I. Letunic, P. Bork, L. Rychlewski, B. Kuster, M. Helmer-Citterich, W. N. Hunter, R. Aasland, and T. J. Gibson.** 2003. ELM server: A new resource for investigating

short functional sites in modular eukaryotic proteins. Nucleic Acids Res **31:**3625-30.

315. **Qadota, H., Y. Anraku, D. Botstein, and Y. Ohya.** 1994. Conditional lethality of a yeast strain expressing human RHOA in place of RHO1. Proc Natl Acad Sci U S A **91:**9317-21.

316. **Qadota, H., C. P. Python, S. B. Inoue, M. Arisawa, Y. Anraku, Y. Zheng, T. Watanabe, D. E. Levin, and Y. Ohya.** 1996. Identification of yeast Rho1p GTPase as a regulatory subunit of 1,3-beta-glucan synthase. Science **272:**279-81.

317. **Qiu, R. G., A. Abo, and G. Steven Martin.** 2000. A human homolog of the C. elegans polarity determinant Par-6 links Rac and Cdc42 to PKCzeta signaling and cell transformation. Curr Biol **10:**697-707.

318. **Qiu, R. G., J. Chen, D. Kirn, F. McCormick, and M. Symons.** 1995. An essential role for Rac in Ras transformation. Nature **374:**457-9.

319. **Qiu, R. G., J. Chen, F. McCormick, and M. Symons.** 1995. A role for Rho in Ras transformation. Proc Natl Acad Sci U S A **92:**11781-5.

320. **R Development Core Team.** 2007. R: A Language and Environment for Statistical Computing. R Foundation for Statistical Computing, Vienna, Austria.

321. **Raitt, D. C., F. Posas, and H. Saito.** 2000. Yeast Cdc42 GTPase and Ste20 PAK-like kinase regulate Sho1-dependent activation of the Hog1 MAPK pathway. Embo J **19:**4623-31.

322. **Ramer, S. W., and R. W. Davis.** 1993. A dominant truncation allele identifies a gene, STE20, that encodes a putative protein kinase necessary for mating in Saccharomyces cerevisiae. Proc Natl Acad Sci U S A **90:**452-6.

323. **Ramezani-Rad, M.** 2003. The role of adaptor protein Ste50-dependent regulation of the MAPKKK Ste11 in multiple signalling pathways of yeast. Curr Genet **43:**161-70.

324. **Raught, B., A. C. Gingras, and N. Sonenberg.** 2001. The target of rapamycin (TOR) proteins. Proc Natl Acad Sci U S A **98:**7037-44.

325. **Rayala, S. K., P. R. Molli, and R. Kumar.** 2006. Nuclear p21-activated kinase 1 in breast cancer packs off tamoxifen sensitivity. Cancer Res **66:**5985-8.

326. **Rayala, S. K., A. H. Talukder, S. Balasenthil, R. Tharakan, C. J. Barnes, R. A. Wang, M. Aldaz, S. Khan, and R. Kumar.** 2006. P21-activated kinase 1 regulation of estrogen receptor-alpha activation involves serine 305 activation linked with serine 118 phosphorylation. Cancer Res **66:**1694-701.

327. **Remenyi, A., M. C. Good, R. P. Bhattacharyya, and W. A. Lim.** 2005. The role of docking interactions in mediating signaling input, output, and discrimination in the yeast MAPK network. Mol Cell **20:**951-62.

328. **Remenyi, A., M. C. Good, and W. A. Lim.** 2006. Docking interactions in protein kinase and phosphatase networks. Curr Opin Struct Biol **16:**676-85.

329. **Rennefahrt, U. E., S. W. Deacon, S. A. Parker, K. Devarajan, A. Beeser, J. Chernoff, S. Knapp, B. E. Turk, and J. R. Peterson.** 2007. Specificity profiling of Pak kinases allows identification of novel phosphorylation sites. J Biol Chem **282:**15667-78.

330. **Richman, T. J., and D. I. Johnson.** 2000. Saccharomyces cerevisiae cdc42p GTPase is involved in preventing the recurrence of bud emergence during the cell cycle. Mol Cell Biol **20:**8548-59.

331. **Richman, T. J., M. M. Sawyer, and D. I. Johnson.** 1999. The Cdc42p GTPase is involved in a G2/M morphogenetic checkpoint regulating the apical-isotropic switch and nuclear division in yeast. J Biol Chem **274:**16861-70.

332. **Richman, T. J., K. A. Toenjes, S. E. Morales, K. C. Cole, B. T. Wasserman, C. M. Taylor, J. A. Koster, M. F. Whelihan, and D. I. Johnson.** 2004. Analysis of cell-cycle specific localization of the Rdi1p RhoGDI and the structural determinants required for Cdc42p membrane localization and clustering at sites of polarized growth. Curr Genet **45:**339-49.

333. **Ridley, A. J.** 2001. Rho family proteins: coordinating cell responses. Trends Cell Biol **11:**471-7.

334. **Ridley, A. J., H. F. Paterson, C. L. Johnston, D. Diekmann, and A. Hall.** 1992. The small GTP-binding protein rac regulates growth factor-induced membrane ruffling. Cell **70:**401-10.

335. **Riento, K., and A. J. Ridley.** 2003. Rocks: multifunctional kinases in cell behaviour. Nat Rev Mol Cell Biol **4:**446-56.

336. **Rigaut, G., A. Shevchenko, B. Rutz, M. Wilm, M. Mann, and B. Seraphin.** 1999. A generic protein purification method for protein complex characterization and proteome exploration. Nat Biotechnol **17:**1030-2.

337. **Rigoutsos, I., and A. Floratos.** 1998. Combinatorial pattern discovery in biological sequences: The TEIRESIAS algorithm. Bioinformatics **14:**55-67.

338. **Roberts, A. W., C. Kim, L. Zhen, J. B. Lowe, R. Kapur, B. Petryniak, A. Spaetti, J. D. Pollock, J. B. Borneo, G. B. Bradford, S. J. Atkinson, M. C. Dinauer, and D. A. Williams.** 1999. Deficiency of the hematopoietic cell-specific Rho family GTPase Rac2 is characterized by abnormalities in neutrophil function and host defense. Immunity **10:**183-96.

339. **Roberts, R. L., and G. R. Fink.** 1994. Elements of a single MAP kinase cascade in Saccharomyces cerevisiae mediate two developmental programs in the same cell type: mating and invasive growth. Genes Dev **8:**2974-85.

340. **Robinson, N. G., L. Guo, J. Imai, E. A. Toh, Y. Matsui, and F. Tamanoi.** 1999. Rho3 of Saccharomyces cerevisiae, which regulates the actin cytoskeleton and exocytosis, is a GTPase which interacts with Myo2 and Exo70. Mol Cell Biol **19:**3580-7.

341. **Rogers, S., R. Wells, and M. Rechsteiner.** 1986. Amino acid sequences common to rapidly degraded proteins: the PEST hypothesis. Science **234:**364-8.

342. **Rolland, F., J. Winderickx, and J. M. Thevelein.** 2002. Glucose-sensing and -signalling mechanisms in yeast. FEMS Yeast Res **2:**183-201.

343. **Rolli-Derkinderen, M., V. Sauzeau, L. Boyer, E. Lemichez, C. Baron, D. Henrion, G. Loirand, and P. Pacaud.** 2005. Phosphorylation of serine 188 protects RhoA from ubiquitin/proteasome-mediated degradation in vascular smooth muscle cells. Circ Res **96:**1152-60.

344. **Ron, D., M. Zannini, M. Lewis, R. B. Wickner, L. T. Hunt, G. Graziani, S. R. Tronick, S. A. Aaronson, and A. Eva.** 1991. A region of proto-dbl essential for its transforming activity shows sequence similarity to a yeast cell cycle gene, CDC24, and the human breakpoint cluster gene, bcr. New Biol **3:**372-9.

345. **Roof, R. W., B. D. Dukes, J. H. Chang, and S. J. Parsons.** 2000. Phosphorylation of the p190 RhoGAP N-terminal domain by c-Src results in a loss of GTP binding activity. FEBS Lett **472:**117-21.

346. **Rose, M. D., F. M. Winston, P. Hieter, F. Sherman, G. R. Fink, J. Hicks, and Cold Spring Harbor Laboratory.** 1990. Methods in yeast genetics : a laboratory course manual. Cold Spring Harbor Laboratory, Cold Spring Harbor.

347. **Rosenblatt, J., L. P. Cramer, B. Baum, and K. M. McGee.** 2004. Myosin II-dependent cortical movement is required for centrosome separation and positioning during mitotic spindle assembly. Cell **117:**361-72.

348. **Rossman, K. L., C. J. Der, and J. Sondek.** 2005. GEF means go: turning on RHO GTPases with guanine nucleotide-exchange factors. Nat Rev Mol Cell Biol **6:**167-80.

349. **Roth, A. F., and N. G. Davis.** 2000. Ubiquitination of the PEST-like endocytosis signal of the yeast a-factor receptor. J Biol Chem **275:**8143-53.

350. **Roumanie, O., C. Weinachter, I. Larrieu, M. Crouzet, and F. Doignon.** 2001. Functional characterization of the Bag7, Lrg1 and Rgd2 RhoGAP proteins from Saccharomyces cerevisiae. FEBS Lett **506:**149-56.

351. **Ruggieri, R., K. Tanaka, M. Nakafuku, Y. Kaziro, A. Toh-e, and K. Matsumoto.** 1989. MSI1, a negative regulator of the RAS-cAMP pathway in Saccharomyces cerevisiae. Proc Natl Acad Sci U S A **86:**8778-82.

352. **Sah, V. P., M. Hoshijima, K. R. Chien, and J. H. Brown.** 1996. Rho is required for Galphaq and alpha1-adrenergic receptor signaling in cardiomyocytes. Dissociation of Ras and Rho pathways. J Biol Chem **271:**31185-90.

353. **Saka, A., M. Abe, H. Okano, M. Minemura, H. Qadota, T. Utsugi, A. Mino, K. Tanaka, Y. Takai, and Y. Ohya.** 2001. Complementing yeast rho1 mutation groups with distinct functional defects. J Biol Chem **276:**46165-71.

354. **Sanders, L. C., F. Matsumura, G. M. Bokoch, and P. de Lanerolle.** 1999. Inhibition of myosin light chain kinase by p21-activated kinase. Science **283:**2083-5.

355. **Saraste, M., and M. Hyvonen.** 1995. Pleckstrin homology domains: a fact file. Curr Opin Struct Biol **5:**403-8.

356. **Sarner, S., R. Kozma, S. Ahmed, and L. Lim.** 2000. Phosphatidylinositol 3-kinase, Cdc42, and Rac1 act downstream of Ras in integrin-dependent neurite outgrowth in N1E-115 neuroblastoma cells. Mol Cell Biol **20:**158-72.

357. **Saunders, N. F., R. I. Brinkworth, T. Huber, B. E. Kemp, and B. Kobe.** 2008. Predikin and PredikinDB: a computational framework for the prediction of protein kinase peptide specificity and an associated database of phosphorylation sites. BMC Bioinformatics **9:**245.

358. **Sauzeau, V., H. Le Jeune, C. Cario-Toumaniantz, A. Smolenski, S. M. Lohmann, J. Bertoglio, P. Chardin, P. Pacaud, and G. Loirand.** 2000. Cyclic GMP-dependent protein kinase signaling pathway inhibits RhoA-induced Ca2+ sensitization of contraction in vascular smooth muscle. J Biol Chem **275:**21722-9.

359. **Saveanu, C., J. C. Rousselle, P. Lenormand, A. Namane, A. Jacquier, and M. Fromont-Racine.** 2007. The p21-activated protein kinase inhibitor Skb15 and its budding yeast homologue are 60S ribosome assembly factors. Mol Cell Biol **27:**2897-909.

360. **Schmidt, A., T. Beck, A. Koller, J. Kunz, and M. N. Hall.** 1998. The TOR nutrient signalling pathway phosphorylates NPR1 and inhibits turnover of the tryptophan permease. Embo J **17:**6924-31.

361. **Schmidt, A., and A. Hall.** 2002. Guanine nucleotide exchange factors for Rho GTPases: turning on the switch. Genes Dev **16:**1587-609.

362. **Schmidt, G., P. Sehr, M. Wilm, J. Selzer, M. Mann, and K. Aktories.** 1997. Gln 63 of Rho is deamidated by Escherichia coli cytotoxic necrotizing factor-1. Nature **387:**725-9.

363. **Schmidt, M., A. Varma, T. Drgon, B. Bowers, and E. Cabib.** 2003. Septins, under Cla4p regulation, and the chitin ring are required for neck integrity in budding yeast. Mol Biol Cell **14:**2128-41.

364. **Schmitz, H. P., S. Huppert, A. Lorberg, and J. J. Heinisch.** 2002. Rho5p downregulates the yeast cell integrity pathway. J Cell Sci **115:**3139-48.

365. **Schubbert, S., K. Shannon, and G. Bollag.** 2007. Hyperactive Ras in developmental disorders and cancer. Nat Rev Cancer **7:**295-308.

366. **Schurmann, A., A. F. Mooney, L. C. Sanders, M. A. Sells, H. G. Wang, J. C. Reed, and G. M. Bokoch.** 2000. p21-activated kinase 1 phosphorylates the death agonist bad and protects cells from apoptosis. Mol Cell Biol **20:**453-61.

367. **Sells, M. A., and J. Chernoff.** 1997. Emerging from the Pak: the p21-activated protein kinase family. Trends Cell Biol **7:**162-7.

368. **Senawongse, P., A. R. Dalby, and Z. R. Yang.** 2005. Predicting the phosphorylation sites using hidden Markov models and machine learning methods. J Chem Inf Model **45:**1147-52.

369. **Seshan, A., A. J. Bardin, and A. Amon.** 2002. Control of Lte1 localization by cell polarity determinants and Cdc14. Curr Biol **12:**2098-110.

370. **Severson, A. F., and B. Bowerman.** 2003. Myosin and the PAR proteins polarize microfilament-dependent forces that shape and position mitotic spindles in Caenorhabditis elegans. J Cell Biol **161:**21-6.

371. **SGD.** Saccharomyces Genome Database.

372. **Shah, K., Y. Liu, C. Deirmengian, and K. M. Shokat.** 1997. Engineering unnatural nucleotide specificity for Rous sarcoma virus tyrosine kinase to uniquely label its direct substrates. Proc Natl Acad Sci U S A **94:**3565-70.

373. **Shah, K., and K. M. Shokat.** 2003. A chemical genetic approach for the identification of direct substrates of protein kinases. Methods Mol Biol **233:**253-71.

374. **Sheu, Y. J., B. Santos, N. Fortin, C. Costigan, and M. Snyder.** 1998. Spa2p interacts with cell polarity proteins and signaling components involved in yeast cell morphogenesis. Mol Cell Biol **18:**4053-69.

375. **Shimada, Y., M. P. Gulli, and M. Peter.** 2000. Nuclear sequestration of the exchange factor Cdc24 by Far1 regulates cell polarity during yeast mating. Nat Cell Biol **2:**117-24.

376. **Shimada, Y., P. Wiget, M. P. Gulli, E. Bi, and M. Peter.** 2004. The nucleotide exchange factor Cdc24p may be regulated by auto-inhibition. Embo J **23:**1051-62.

377. **Shin, D. Y., K. Matsumoto, H. Iida, I. Uno, and T. Ishikawa.** 1987. Heat shock response of Saccharomyces cerevisiae mutants altered in cyclic AMP-dependent protein phosphorylation. Mol Cell Biol **7:**244-50.

378. **Silvius, J. R., and F. l'Heureux.** 1994. Fluorimetric evaluation of the affinities of isoprenylated peptides for lipid bilayers. Biochemistry **33:**3014-22.

379. **Simon, M. N., C. De Virgilio, B. Souza, J. R. Pringle, A. Abo, and S. I. Reed.** 1995. Role for the Rho-family GTPase Cdc42 in yeast mating-pheromone signal pathway. Nature **376:**702-5.

380. **Singh, K., P. J. Kang, and H. O. Park.** 2008. The Rho5 GTPase is necessary for oxidant-induced cell death in budding yeast. Proc Natl Acad Sci U S A **105:**1522-7.

381. **Singh, R. R., C. Song, Z. Yang, and R. Kumar.** 2005. Nuclear localization and chromatin targets of p21-activated kinase 1. J Biol Chem **280:**18130-7.

382. **Sirri, V., D. Hernandez-Verdun, and P. Roussel.** 2002. Cyclin-dependent kinases govern formation and maintenance of the nucleolus. J Cell Biol **156:**969-81.

383. **Smith, D. B., and K. S. Johnson.** 1988. Single-step purification of polypeptides expressed in Escherichia coli as fusions with glutathione S-transferase. Gene **67:**31-40.

384. **Solski, P. A., K. Abe, and C. J. Der.** 2000. Analyses of transforming activity of Rho family activators. Methods Enzymol **325:**425-41.

385. **Somlyo, A. P.** 1999. Kinases, myosin phosphatase and Rho proteins: curiouser and curiouser. J Physiol **516 (Pt 3):**630.

386. **Stanbrough, M., and B. Magasanik.** 1995. Transcriptional and posttranslational regulation of the general amino acid permease of Saccharomyces cerevisiae. J Bacteriol **177:**94-102.

387. **Stanhill, A., N. Schick, and D. Engelberg.** 1999. The yeast ras/cyclic AMP pathway induces invasive growth by suppressing the cellular stress response. Mol Cell Biol **19:**7529-38.

388. **Symons, M.** 1996. Rho family GTPases: the cytoskeleton and beyond. Trends Biochem Sci **21:**178-81.

389. **Symons, M., and J. Settleman.** 2000. Rho family GTPases: more than simple switches. Trends Cell Biol **10:**415-9.

390. **Takahashi, K., T. Sasaki, A. Mammoto, K. Takaishi, T. Kameyama, S. Tsukita, and Y. Takai.** 1997. Direct interaction of the Rho GDP dissociation

inhibitor with ezrin/radixin/moesin initiates the activation of the Rho small G protein. J Biol Chem **272:**23371-5.

391. **Takai, Y., K. Kaibuchi, A. Kikuchi, and T. Sasaki.** 1995. Effects of prenyl modifications on interactions of small G proteins with regulators. Methods Enzymol **250:**122-33.

392. **Tamaki, H.** 2007. Glucose-stimulated cAMP-protein kinase A pathway in yeast Saccharomyces cerevisiae. J Biosci Bioeng **104:**245-50.

393. **Tatebayashi, K., K. Yamamoto, K. Tanaka, T. Tomida, T. Maruoka, E. Kasukawa, and H. Saito.** 2006. Adaptor functions of Cdc42, Ste50, and Sho1 in the yeast osmoregulatory HOG MAPK pathway. Embo J **25:**3033-44.

394. **Tcheperegine, S. E., X. D. Gao, and E. Bi.** 2005. Regulation of cell polarity by interactions of Msb3 and Msb4 with Cdc42 and polarisome components. Mol Cell Biol **25:**8567-80.

395. **Tcheperegine, S. E., M. Marelli, and R. W. Wozniak.** 1999. Topology and functional domains of the yeast pore membrane protein Pom152p. J Biol Chem **274:**5252-8.

396. **Tcherkezian, J., and N. Lamarche-Vane.** 2007. Current knowledge of the large RhoGAP family of proteins. Biol Cell **99:**67-86.

397. **ten Klooster, J. P., Z. M. Jaffer, J. Chernoff, and P. L. Hordijk.** 2006. Targeting and activation of Rac1 are mediated by the exchange factor beta-Pix. J Cell Biol **172:**759-69.

398. **Thevelein, J. M.** 1992. The RAS-adenylate cyclase pathway and cell cycle control in Saccharomyces cerevisiae. Antonie Van Leeuwenhoek **62:**109-30.

399. **Thevelein, J. M.** 1994. Signal transduction in yeast. Yeast **10:**1753-90.

400. **Thevelein, J. M., and J. H. de Winde.** 1999. Novel sensing mechanisms and targets for the cAMP-protein kinase A pathway in the yeast Saccharomyces cerevisiae. Mol Microbiol **33:**904-18.

401. **Thompson, G., D. Owen, P. A. Chalk, and P. N. Lowe.** 1998. Delineation of the Cdc42/Rac-binding domain of p21-activated kinase. Biochemistry **37:**7885-91.

402. **Tiedje, C., D. G. Holland, U. Just, and T. Hofken.** 2007. Proteins involved in sterol synthesis interact with Ste20 and regulate cell polarity. J Cell Sci **120:**3613-24.

403. **Tillement, V., I. Lajoie-Mazenc, A. Casanova, C. Froment, M. Penary, D. Tovar, R. Marquez, B. Monsarrat, G. Favre, and A. Pradines.** 2008.

Phosphorylation of RhoB by CK1 impedes actin stress fiber organization and epidermal growth factor receptor stabilization. Exp Cell Res.

404. **Toda, T., S. Cameron, P. Sass, M. Zoller, J. D. Scott, B. McMullen, M. Hurwitz, E. G. Krebs, and M. Wigler.** 1987. Cloning and characterization of BCY1, a locus encoding a regulatory subunit of the cyclic AMP-dependent protein kinase in Saccharomyces cerevisiae. Mol Cell Biol **7:**1371-7.

405. **Toda, T., S. Cameron, P. Sass, M. Zoller, and M. Wigler.** 1987. Three different genes in S. cerevisiae encode the catalytic subunits of the cAMP-dependent protein kinase. Cell **50:**277-87.

406. **Toda, T., I. Uno, T. Ishikawa, S. Powers, T. Kataoka, D. Broek, S. Cameron, J. Broach, K. Matsumoto, and M. Wigler.** 1985. In yeast, RAS proteins are controlling elements of adenylate cyclase. Cell **40:**27-36.

407. **Toenjes, K. A., M. M. Sawyer, and D. I. Johnson.** 1999. The guanine-nucleotide-exchange factor Cdc24p is targeted to the nucleus and polarized growth sites. Curr Biol **9:**1183-6.

408. **Togawa, A., J. Miyoshi, H. Ishizaki, M. Tanaka, A. Takakura, H. Nishioka, H. Yoshida, T. Doi, A. Mizoguchi, N. Matsuura, Y. Niho, Y. Nishimune, S. Nishikawa, and Y. Takai.** 1999. Progressive impairment of kidneys and reproductive organs in mice lacking Rho GDIalpha. Oncogene **18:**5373-80.

409. **Tolliday, N., L. VerPlank, and R. Li.** 2002. Rho1 directs formin-mediated actin ring assembly during budding yeast cytokinesis. Curr Biol **12:**1864-70.

410. **Tong, A. H., M. Evangelista, A. B. Parsons, H. Xu, G. D. Bader, N. Page, M. Robinson, S. Raghibizadeh, C. W. Hogue, H. Bussey, B. Andrews, M. Tyers, and C. Boone.** 2001. Systematic genetic analysis with ordered arrays of yeast deletion mutants. Science **294:**2364-8.

411. **Totsukawa, G., Y. Yamakita, S. Yamashiro, D. J. Hartshorne, Y. Sasaki, and F. Matsumura.** 2000. Distinct roles of ROCK (Rho-kinase) and MLCK in spatial regulation of MLC phosphorylation for assembly of stress fibers and focal adhesions in 3T3 fibroblasts. J Cell Biol **150:**797-806.

412. **Trono, D., and J. K. Wang.** 1997. Nef and PAK: virulence factor and cellular accomplice. Chem Biol **4:**13-5.

413. **Truckses, D. M., J. E. Bloomekatz, and J. Thorner.** 2006. The RA domain of Ste50 adaptor protein is required for delivery of Ste11 to the plasma membrane in the filamentous growth signaling pathway of the yeast Saccharomyces cerevisiae. Mol Cell Biol **26:**912-28.

414. **Tu, S., and R. A. Cerione.** 2001. Cdc42 is a substrate for caspases and influences Fas-induced apoptosis. J Biol Chem **276:**19656-63.

415. **Tu, S., W. J. Wu, J. Wang, and R. A. Cerione.** 2003. Epidermal growth factor-dependent regulation of Cdc42 is mediated by the Src tyrosine kinase. J Biol Chem **278:**49293-300.

416. **Ubersax, J. A., E. L. Woodbury, P. N. Quang, M. Paraz, J. D. Blethrow, K. Shah, K. M. Shokat, and D. O. Morgan.** 2003. Targets of the cyclin-dependent kinase Cdk1. Nature **425:**859-64.

417. **Ueda, T., A. Kikuchi, N. Ohga, J. Yamamoto, and Y. Takai.** 1990. Purification and characterization from bovine brain cytosol of a novel regulatory protein inhibiting the dissociation of GDP from and the subsequent binding of GTP to rhoB p20, a ras p21-like GTP-binding protein. J Biol Chem **265:**9373-80.

418. **Unwin, R. D., D. W. Sternberg, Y. Lu, A. Pierce, D. G. Gilliland, and A. D. Whetton.** 2005. Global effects of BCR/ABL and TEL/PDGFRbeta expression on the proteome and phosphoproteome: identification of the Rho pathway as a target of BCR/ABL. J Biol Chem **280:**6316-26.

419. **Urich, M., M. Senften, P. E. Shaw, and K. Ballmer-Hofer.** 1997. A role for the small GTPase Rac in polyomavirus middle-T antigen-mediated activation of the serum response element and in cell transformation. Oncogene **14:**1235-41.

420. **Versele, M., and J. Thorner.** 2004. Septin collar formation in budding yeast requires GTP binding and direct phosphorylation by the PAK, Cla4. J Cell Biol **164:**701-15.

421. **Vincent, S., P. Jeanteur, and P. Fort.** 1992. Growth-regulated expression of rhoG, a new member of the ras homolog gene family. Mol Cell Biol **12:**3138-48.

422. **von Mering, C., R. Krause, B. Snel, M. Cornell, S. G. Oliver, S. Fields, and P. Bork.** 2002. Comparative assessment of large-scale data sets of protein-protein interactions. Nature **417:**399-403.

423. **Wallar, B. J., and A. S. Alberts.** 2003. The formins: active scaffolds that remodel the cytoskeleton. Trends Cell Biol **13:**435-46.

424. **Wang, H. R., A. A. Ogunjimi, Y. Zhang, B. Ozdamar, R. Bose, and J. L. Wrana.** 2006. Degradation of RhoA by Smurf1 ubiquitin ligase. Methods Enzymol **406:**437-47.

425. **Wang, H. R., Y. Zhang, B. Ozdamar, A. A. Ogunjimi, E. Alexandrova, G. H. Thomsen, and J. L. Wrana.** 2003. Regulation of cell polarity and protrusion formation by targeting RhoA for degradation. Science **302:**1775-9.

426. **Wang, R. A., A. Mazumdar, R. K. Vadlamudi, and R. Kumar.** 2002. P21-activated kinase-1 phosphorylates and transactivates estrogen receptor-alpha and promotes hyperplasia in mammary epithelium. Embo J **21:**5437-47.

427. **Wang, Y., M. Pierce, L. Schneper, C. G. Guldal, X. Zhang, S. Tavazoie, and J. R. Broach.** 2004. Ras and Gpa2 mediate one branch of a redundant glucose signaling pathway in yeast. PLoS Biol **2:**E128.

428. **Watanabe, T., S. Wang, J. Noritake, K. Sato, M. Fukata, M. Takefuji, M. Nakagawa, N. Izumi, T. Akiyama, and K. Kaibuchi.** 2004. Interaction with IQGAP1 links APC to Rac1, Cdc42, and actin filaments during cell polarization and migration. Dev Cell **7:**871-83.

429. **Welsh, C. F., K. Roovers, J. Villanueva, Y. Liu, M. A. Schwartz, and R. K. Assoian.** 2001. Timing of cyclin D1 expression within G1 phase is controlled by Rho. Nat Cell Biol **3:**950-7.

430. **Wennerberg, K., and C. J. Der.** 2004. Rho-family GTPases: it's not only Rac and Rho (and I like it). J Cell Sci **117:**1301-12.

431. **Werner-Washburne, M., E. L. Braun, M. E. Crawford, and V. M. Peck.** 1996. Stationary phase in Saccharomyces cerevisiae. Mol Microbiol **19:**1159-66.

432. **Wherlock, M., A. Gampel, C. Futter, and H. Mellor.** 2004. Farnesyltransferase inhibitors disrupt EGF receptor traffic through modulation of the RhoB GTPase. J Cell Sci **117:**3221-31.

433. **Whitehead, I. P., S. Campbell, K. L. Rossman, and C. J. Der.** 1997. Dbl family proteins. Biochim Biophys Acta **1332:**F1-23.

434. **Wild, A. C., J. W. Yu, M. A. Lemmon, and K. J. Blumer.** 2004. The p21-activated protein kinase-related kinase Cla4 is a coincidence detector of signaling by Cdc42 and phosphatidylinositol 4-phosphate. J Biol Chem **279:**17101-10.

435. **Wilkins, A., Q. Ping, and C. L. Carpenter.** 2004. RhoBTB2 is a substrate of the mammalian Cul3 ubiquitin ligase complex. Genes Dev **18:**856-61.

436. **Willems, A. R., S. Lanker, E. E. Patton, K. L. Craig, T. F. Nason, N. Mathias, R. Kobayashi, C. Wittenberg, and M. Tyers.** 1996. Cdc53 targets phosphorylated G1 cyclins for degradation by the ubiquitin proteolytic pathway. Cell **86:**453-63.

437. **Wilson, B. A., M. Khalil, F. Tamanoi, and J. F. Cannon.** 1993. New activated RAS2 mutations identified in Saccharomyces cerevisiae. Oncogene **8:**3441-5.

438. **Winters, M. J., R. E. Lamson, H. Nakanishi, A. M. Neiman, and P. M. Pryciak.** 2005. A membrane binding domain in the ste5 scaffold synergizes with gbetagamma binding to control localization and signaling in pheromone response. Mol Cell **20:**21-32.

439. **Wodarz, A.** 2002. Establishing cell polarity in development. Nat Cell Biol **4:**E39-44.

440. **Won, K. A., and S. I. Reed.** 1996. Activation of cyclin E/CDK2 is coupled to site-specific autophosphorylation and ubiquitin-dependent degradation of cyclin E. Embo J **15:**4182-93.

441. **Wong, Y. H., T. Y. Lee, H. K. Liang, C. M. Huang, T. Y. Wang, Y. H. Yang, C. H. Chu, H. D. Huang, M. T. Ko, and J. K. Hwang.** 2007. KinasePhos 2.0: a web server for identifying protein kinase-specific phosphorylation sites based on sequences and coupling patterns. Nucleic Acids Res **35:**W588-94.

442. **Worthylake, R. A., and K. Burridge.** 2003. RhoA and ROCK promote migration by limiting membrane protrusions. J Biol Chem **278:**13578-84.

443. **Wu, C., G. Jansen, J. Zhang, D. Y. Thomas, and M. Whiteway.** 2006. Adaptor protein Ste50p links the Ste11p MEKK to the HOG pathway through plasma membrane association. Genes Dev **20:**734-46.

444. **Wu, C., E. Leberer, D. Y. Thomas, and M. Whiteway.** 1999. Functional characterization of the interaction of Ste50p with Ste11p MAPKKK in Saccharomyces cerevisiae. Mol Biol Cell **10:**2425-40.

445. **Wu, C., T. Leeuw, E. Leberer, D. Y. Thomas, and M. Whiteway.** 1998. Cell cycle- and Cln2p-Cdc28p-dependent phosphorylation of the yeast Ste20p protein kinase. J Biol Chem **273:**28107-15.

446. **Wu, C., V. Lytvyn, D. Y. Thomas, and E. Leberer.** 1997. The phosphorylation site for Ste20p-like protein kinases is essential for the function of myosin-I in yeast. J Biol Chem **272:**30623-6.

447. **Wu, C., M. Whiteway, D. Y. Thomas, and E. Leberer.** 1995. Molecular characterization of Ste20p, a potential mitogen-activated protein or extracellular signal-regulated kinase kinase (MEK) kinase kinase from Saccharomyces cerevisiae. J Biol Chem **270:**15984-92.

448. **Yaffe, M. B., G. G. Leparc, J. Lai, T. Obata, S. Volinia, and L. C. Cantley.** 2001. A motif-based profile scanning approach for genome-wide prediction of signaling pathways. Nat Biotechnol **19:**348-53.

449. **Yaglom, J., M. H. Linskens, S. Sadis, D. M. Rubin, B. Futcher, and D. Finley.** 1995. p34Cdc28-mediated control of Cln3 cyclin degradation. Mol Cell Biol **15:**731-41.

450. **Yamaguchi, Y., K. Ota, and T. Ito.** 2007. A novel Cdc42-interacting domain of the yeast polarity establishment protein Bem1. Implications for modulation of mating pheromone signaling. J Biol Chem **282:**29-38.

451. **Yamamoto, M., N. Marui, T. Sakai, N. Morii, S. Kozaki, K. Ikai, S. Imamura, and S. Narumiya.** 1993. ADP-ribosylation of the rhoA gene product

by botulinum C3 exoenzyme causes Swiss 3T3 cells to accumulate in the G1 phase of the cell cycle. Oncogene **8:**1449-55.

452. **Yamochi, W., K. Tanaka, H. Nonaka, A. Maeda, T. Musha, and Y. Takai.** 1994. Growth site localization of Rho1 small GTP-binding protein and its involvement in bud formation in Saccharomyces cerevisiae. J Cell Biol **125:**1077-93.

453. **Yang, F., X. Li, M. Sharma, M. Zarnegar, B. Lim, and Z. Sun.** 2001. Androgen receptor specifically interacts with a novel p21-activated kinase, PAK6. J Biol Chem **276:**15345-53.

454. **Yasuda, S., F. Oceguera-Yanez, T. Kato, M. Okamoto, S. Yonemura, Y. Terada, T. Ishizaki, and S. Narumiya.** 2004. Cdc42 and mDia3 regulate microtubule attachment to kinetochores. Nature **428:**767-71.

455. **Yonemura, S., T. Matsui, S. Tsukita, and S. Tsukita.** 2002. Rho-dependent and -independent activation mechanisms of ezrin/radixin/moesin proteins: an essential role for polyphosphoinositides in vivo. J Cell Sci **115:**2569-80.

456. **Yoshida, S., K. Kono, D. M. Lowery, S. Bartolini, M. B. Yaffe, Y. Ohya, and D. Pellman.** 2006. Polo-like kinase Cdc5 controls the local activation of Rho1 to promote cytokinesis. Science **313:**108-11.

457. **Yoshioka, K., S. Nakamori, and K. Itoh.** 1999. Overexpression of small GTP-binding protein RhoA promotes invasion of tumor cells. Cancer Res **59:**2004-10.

458. **Zalcman, G., V. Closson, G. Linares-Cruz, F. Lerebours, N. Honore, A. Tavitian, and B. Olofsson.** 1995. Regulation of Ras-related RhoB protein expression during the cell cycle. Oncogene **10:**1935-45.

459. **Zhang, S., J. Han, M. A. Sells, J. Chernoff, U. G. Knaus, R. J. Ulevitch, and G. M. Bokoch.** 1995. Rho family GTPases regulate p38 mitogen-activated protein kinase through the downstream mediator Pak1. J Biol Chem **270:**23934-6.

460. **Zhang, X., E. Bi, P. Novick, L. Du, K. G. Kozminski, J. H. Lipschutz, and W. Guo.** 2001. Cdc42 interacts with the exocyst and regulates polarized secretion. J Biol Chem **276:**46745-50.

461. **Zhang, X., K. Orlando, B. He, F. Xi, J. Zhang, A. Zajac, and W. Guo.** 2008. Membrane association and functional regulation of Sec3 by phospholipids and Cdc42. J Cell Biol **180:**145-58.

462. **Zhao, Z. S., T. Leung, E. Manser, and L. Lim.** 1995. Pheromone signalling in Saccharomyces cerevisiae requires the small GTP-binding protein Cdc42p and its activator CDC24. Mol Cell Biol **15:**5246-57.

463. **Zhu, G., Y. Liu, and S. Shaw.** 2005. Protein kinase specificity. A strategic collaboration between kinase peptide specificity and substrate recruitment. Cell Cycle **4:**52-6.

464. **Zhu, H., M. Bilgin, R. Bangham, D. Hall, A. Casamayor, P. Bertone, N. Lan, R. Jansen, S. Bidlingmaier, T. Houfek, T. Mitchell, P. Miller, R. A. Dean, M. Gerstein, and M. Snyder.** 2001. Global analysis of protein activities using proteome chips. Science **293:**2101-5.

465. **Zhu, H., J. F. Klemic, S. Chang, P. Bertone, A. Casamayor, K. G. Klemic, D. Smith, M. Gerstein, M. A. Reed, and M. Snyder.** 2000. Analysis of yeast protein kinases using protein chips. Nat Genet **26:**283-9.

466. **Ziman, M., J. M. O'Brien, L. A. Ouellette, W. R. Church, and D. I. Johnson.** 1991. Mutational analysis of CDC42Sc, a Saccharomyces cerevisiae gene that encodes a putative GTP-binding protein involved in the control of cell polarity. Mol Cell Biol **11:**3537-44.

467. **Zohn, I. E., M. Symons, M. Chrzanowska-Wodnicka, J. K. Westwick, and C. J. Der.** 1998. Mas oncogene signaling and transformation require the small GTP-binding protein Rac. Mol Cell Biol **18:**1225-35.

468. **Zolnierowicz, S., and M. Bollen.** 2000. Protein phosphorylation and protein phosphatases. De Panne, Belgium, September 19-24, 1999. Embo J **19:**483-8.

469. **Zumbihl, R., M. Aepfelbacher, A. Andor, C. A. Jacobi, K. Ruckdeschel, B. Rouot, and J. Heesemann.** 1999. The cytotoxin YopT of Yersinia enterocolitica induces modification and cellular redistribution of the small GTP-binding protein RhoA. J Biol Chem **274:**29289-93.

APPENDIX